“Anti-inflammatory and anticancer activities of natural products and their derivatives”

Kumulative Dissertation zur Erlangung des Grades

“Doktor der Naturwissenschaften’’

im Promotionsfach Pharmazie

Johannes Gutenberg Universität-Mainz

Vorgelegt von Assia Imene Drif

Mainz, Juni 2025

“Anti-inflammatory and anticancer activities of natural products and their derivatives”

Kumulative Dissertation zur Erlangung des Grades

“Doktor der Naturwissenschaften’’

im Promotionsfach Pharmazie

Am Fachbereich Chemie, Pharmazie, Geographie und Geowissenschaften der Johannes Gutenberg Universität-Mainz

Vorgelegt von Assia Imene Drif

Geboren am 25.10.1993 in Algier, Algerien

Mainz, Juni 2025

Betreuer:

Prof. Dr. Thomas Efferth

Gutachter der Arbeit:

Prof. Dr. Thomas Efferth

Prof. Dr. Kristina Friedland

Datum der mündlichen Prüfung

28/08/2025

Prüfungskommission:

Prof. Dr. Peter Langguth (Vorsitzender)

Prof. Dr. Thomas Efferth

Prof. Dr. Kristina Friedland

Dr. Mona Dawood (Protokoll)

D77 (Dissertation Universität Mainz

Publications

Original articles as first author

1. ***Assia I. Drif**, Bharati Avula, Ikhlas A. Khan, and Thomas Efferth. COX2-inhibitory and cytotoxic activities of phytoconstituents of *Matricaria chamomilla* L. *Appl. Sci.* 2023;*13*(15):8935 **(IF = 2.5)**
2. ***Assia I. Drif**, Rümeysa Yücer, Roxana Damiescu, Nadeen T. Ali, Tobias H. Abu Hagar, Bharati Avula, Ikhlas A. Khan and Thomas Efferth. Anti-Inflammatory and Cancer-Preventive Potential of Chamomile (*Matricaria chamomilla* L.): A Comprehensive in Silico and In Vitro Study. *Biomedicines* 2024;12(7):1484 **(IF = 4.7)**

Original articles as co-author

1. *Mohamed E. M. Saeed, Rümeysa Yücer, Mona Dawood, Mohamed-Elamir F. Hegazy, **Assia Drif**, Edna Ooko, Onat Kadioglu, Ean-Jeong Seo, Fadhil S. Kamounah, Salam J. Titinchi, Beatrice Bachmeier and Thomas Efferth. In Silico and In Vitro Screening of 50 Curcumin Compounds as EGFR and NF-κB Inhibitors. *Int J Mol Sci.* 2022;23(7):3966. **(IF = 5.6)**
2. Mohamed E.M. Saeed, **Assia I. Drif** and Thomas Efferth. Biomarker Profiling Revealed Carcinoembryonic Antigen as a Target of Artesunate in a Ductal Breast Cancer Patient. *Anticancer Res.* 2022;42(7):3483-3494. **(IF = 1.6)**
3. Grace Gar-Lee Yue, Adele Joyce Gomes, Mohamed E.M. Saeed, Kei-Yin Tsui, Mona Dawood**, Assia I. Drif**, Eric Chun-Wai Wong, Wai-Fung Lee, Wenjing Liu, Philip Wai-Yan Chiu, Thomas Efferth, Clara Bik-San Lau. Identification of active components in Andrographis paniculata targeting on CD81 in esophageal cancer in vitro and in vivo. *Phytomedicine* 2022;102:154183 **(IF = 6.7)**
4. Sami A. Khalid, Mona Dawood, Joelle C. Boulos, Monica Wasfi, **Assia Drif**, Faranak Bahramimehr, Nasim Shahhamzehei, Letian Shan and Thomas Efferth. Identification of gedunin from a phytochemical depository as a novel multidrug resistance-bypassing tubulin inhibitor of cancer cells. *Molecules* 2022;27(18):5858 **(IF = 4.2)**

Conference papers

1. Young presenter at the 6th Cancer World Congress 2022: COX2-inhibitory and cytotoxic activities of phytoconstituents of Matricaria chamomilla L.

* *These publications are included in this dissertation.*

Contribution to articles included in the dissertation

1. **Title:** COX2-inhibitory and cytotoxic activities of phytoconstituents of *Matricaria chamomilla* L.

Authorship contribution: A.I.D. performed the experiments and analyses; B.A. performed the phytochemical analysis; I.A.K. edited the manuscript; and T.E. supervised the project and wrote the manuscript. All authors have read and agreed to the published version of the manuscript.

2. **Title:** Anti-Inflammatory and Cancer-Preventive Potential of Chamomile (*Matricaria chamomilla* L.): A Comprehensive in Silico and In Vitro Study

Authorship contribution: A.I.D. performed the experiments and analyses, R.Y. assisted in conducting experiments and analysis. R.D. performed the microscale thermophoresis experiment, N.T.A. Wrote the methodology for the cell cycle and annexin-v apoptosis experiment in the material and methods section, T.H.A.H. performed the docking analysis of the protein tubulin, B.A. performed the phytochemical analysis, I.A.K. edited the manuscript, and T.E. supervised the project and wrote the manuscript. All authors have read and agreed to the published version of the manuscript.

3. **Title:** In Silico and In Vitro Screening of 50 Curcumin Compounds as EGFR and NF-κB Inhibitors

Authorship contribution: T.E. and B.B. designed the study. R.Y., A.D. and M.D. performed molecular docking experiments and calculations. M.E.M.S., E.O., R.Y., E.-J.S., A.D., M.D. and O.K. carried out the experiments. S.J.T. and F.S.K. synthesized the compounds. M.-E.F.H. optimized the compounds and revised the structures for molecular docking. T.E. supervised the work and provided the facilities for the study. M.E.M.S. and T.E. wrote the manuscript. All authors have read and agreed to the published version of the manuscript.

5. Erklärung

Hiermit erkläre ich an Eides statt, dass ich diese Arbeit selbstständig verfasst und keine anderen als die angegebenen Quellen und Hilfsmittel verwendet habe.

Ort, Datum

Assia Drif

Acknowledgment

First and foremost, I would like to express my sincere gratitude to my supervisor, Prof. Dr. Efferth. I am truly grateful that he gave me the opportunity to pursue my Ph.D. within his renowned group. He allowed me to learn and grow in our field, which I am most passionate about. Namely, inflammation and cancer treatment with phytomedicines. I also grew personally during this time. I learned that in science, it is most important to never give up. It is okay to make mistakes and learn from them and working as a team gives us strength. Professor Efferth is known for his strong scientific background and outstanding academic performance, and I am lucky to be his student. I can't thank him enough for his support and immense patience.

My thanks goes to my collaborator Dr. Avula and Professor Khan for performing the chamomile compounds extractions and delivering it to us. Besides, my thanks go to my co-authors for their efforts and engagement in the research work. "If I have seen further, it is by standing on the shoulders of giants." Isaac Newton, Letter to Robert Hooke, 1675

I would like to thank Prof. Dr. Freedland, Prof. Dr. Thomas Efferth, Prof. Dr. Peter Langguth for taking part in the dissertation committee, and Dr. Rümeysa Yücer for being the secretary in the oral examination.

I would like to express my warmest gratitude to my father Dr. Boualem Drif, my mother Dr. Nawal Drif, my husband Maximilian Hornstein, my sister Assila, my brother Sido, my father-in-low Dr. Hornstein, and my mother-in-low Doris Hornstein. I am grateful for my family for standing with me and supporting me in sickness and health throughout this whole journey. I must thank my parents and my husband for their unconditional love and support.

Last but not least, I have special thanks to my friends in Germany who have always been a major source of support when things would get discouraging, Dr. Xiaohua Lu, Dr. Yücer Rümeysa, Nasim Shahhamzehei, Kaushik Iyer, Ejlal Omer, Dr. Joelle C Boulos, Dr. Min Zhou, Dr. Mona Dawood, Varol Ayşegül, Mohamed Elbadawi, and so forth.

Special gratitude to Latifa, Ghalia, Bota, Thomas, Amir, Melissa, Roberto, Raphaella. "There is nothing I would not do for those who are really my friends. I have no notion of loving people by halves; it is not my nature." Jane Austin, Northanger Abbey.

Abstract

Natural products have shown great potential due to their biological properties and their bioactive components, which demonstrate multiple mechanisms of action and lower cytotoxicity compared to conventional synthetic drugs. This dissertation focuses on the therapeutic potential of chamomile molecules (*Matricaria chamomilla* L.) and curcumin analogues (from *Curcuma longa* L.), as anti-inflammatory and cancer preventive agents.

In our investigations, an *in silico* virtual drug screening by molecular docking of 212 phytochemicals from chamomile revealed potential COX2 and NF-κB inhibitors, including β-amyrin, β-sitosterol, myricetin, lupeol, and quercetin. The *in silico* findings were validated through microscale thermophoresis and biochemical assays. The use of the various -omics facilitate the profiling of the bioactivity of these compounds. Furthermore, the bioinformatic analysis were then further verified through cytotoxicity assays using various cancer cell lines, and flow cytometric assays. These experiments allowed to demonstrate the potential to overcome resistance mechanisms associated with established anticancer drugs. In addition to evaluate their effect on modulating the reactive oxygen species generation and mitochondrial membrane potential. Moreover, the immunofluorescence microscopy of α-tubulin revealed significant correlations between the chamomile compounds myricetin, lupeol, and quercetin and vincristine, a well-established microtubule inhibitor. Notably, lupeol and quercetin induced G2/M cell cycle arrest and apoptosis. Further, western blot and RT-PCR assays were performed to highlights the involvement of the chamomile compounds in the regulation of immune response during inflammation.

Similarly, an extensive analysis of 50 curcumin derivatives demonstrated their binding affinity to key cancer-related target proteins, including EGFR and NF-κB. The study indicated that several curcumin analogues had a stronger binding affinity than curcumin itself, suggesting that their derivatization could lead to improved target specificity and enhanced efficacy as anticancer agents. This was supported by a variety of bioactivity assays, including resazurin cell viability, assessment of oxidative stress and lactate dehydrogenase assays.

In conclusion, our research highlights the ability of chamomile and curcumin derivatives to influence various biological processes within the cell and their therapeutic potential in treating inflammation and preventing cancer. Given the promising attributes of these natural products, it seems promising to further investigate them in vitro and in vivo studies, as well as in clinical trials.

Zusammenfassung

Naturarzneimittel haben ein großes Potenzial aufgrund ihrer biologischen Eigenschaften und bioaktiven Inhaltsstoffe, die mehrere Wirkmechanismen und eine geringere Zytotoxizität als herkömmliche synthetische Arzneimittel aufweisen. Diese Dissertation befasst sich mit dem therapeutischen Potential von Molekülen der Kamille (*Matricaria chamomilla* L.) und von Curcumin-Analoga (aus *Curcuma longa* L.) als entzündungshemmende und krebsvorbeugende Wirkstoffe.

In unseren Untersuchungen wurden durch ein virtuelles *in silico* Wirkstoffscreening mittels molekularen Dockings von 212 Phytochemikalien der Kamille potenzielle COX2- und NF-κB-Inhibitoren identifiziert, darunter β-Amyrin, β-Sitosterol, Myricetin, Lupeol und Quercetin. Die *in silico* gewonnenen Erkenntnisse wurden durch mikroskalige Thermophorese und biochemische Assays validiert. Die Anwendung verschiedener -omics ermöglicht die Erstellung von Bioaktivitätsprofilen dieser Verbindungen. Darüber hinaus wurden die bioinformatischen Analysen durch Zytotoxizitätstests mit verschiedenen Krebszelllinien und durchflusszytometrische Assays weiter verifiziert. Mit diesen Experimenten konnte das Potenzial zur Überwindung von Resistenzmechanismen gegenüber etablierten Krebsmedikamenten nachgewiesen werden. Des Weiteren wurde ihr Effekt auf die Modulation der Bildung reaktiver Sauerstoffspezies und des mitochondrialen Membranpotenzials evaluiert. Die Immunfluoreszenzmikroskopie von α-Tubulin zeigte darüber hinaus signifikante Korrelationen zwischen den Kamilleninhaltsstoffen Myricetin, Lupeol, Quercetin und dem bekannten Mikrotubuli-Inhibitor Vincristin. Insbesondere Lupeol und Quercetin induzierten eine Verlangsamung des G2/M-Zellzyklus und Apoptose. Zusätzlich wurden Western Blot- und RT-PCR-Assays durchgeführt, um die Beteiligung von Kamilleninhaltsstoffen an der Regulation der Immunantwort bei Entzündungen zu untersuchen.

Eine umfassende Analyse von 50 Curcumin-Derivaten zeigte deren Bindungsaffinität zu wichtigen krebsrelevanten Zielproteinen, darunter EGFR und NF-κB. Die Studie zeigte, dass mehrere Curcumin-Analoga eine höhere Bindungsaffinität aufwiesen als Curcumin selbst, was darauf hindeutet, dass ihre Derivatisierung zu einer verbesserten Zielspezifität und Wirksamkeit als Krebsmedikament führen könnte. Diese Beobachtung wurde durch eine Reihe von Bioaktivitätstests bestätigt, einschließlich Resazurin-Zellviabilität, oxidativer Stressbewertung und Laktatdehydrogenasetests.

Zusammenfassend unterstreichen unsere Untersuchungen die Fähigkeit von Kamille- und Curcumin-Derivaten, verschiedene biologische Prozesse in der Zelle zu beeinflussen, sowie ihr therapeutisches Potenzial bei der Behandlung von Entzündungen und der Prävention von Krebs. Angesichts der vielversprechenden Eigenschaften dieser Naturkomponenten erscheint es vielversprechend, sie in *in vitro* und *in vivo* Studien sowie in klinischen Versuchen weiter zu untersuchen.

1. Introduction

Inflammation and cancer are interconnected through complex molecular pathways, and NF-κB plays a major role in both these processes. In inflammation, NF-κB is a key activator of inflammation, orchestrating the expression of proinflammatory genes. Simultaneously, one downstream effect of this is the upregulation of cyclooxygenase-2 (COX-2), a mediator of inflammation, which, in turn, sustains NF-κB activation, creating a feedback loop. In cancer, this continuous expression of NF-κB becomes particularly consequential, especially when coupled with oncogenic pathways such as the epidermal growth factor receptor (EGFR) signaling. Together, these mechanisms lead to constitutive NF-κB activation, enhancing cancer cell resistance to apoptosis and supporting tumor survival. This intricate interplay between inflammation and cancer, mediated by NF-κB, presents both challenges and opportunities in understanding and treating inflammation and malignancies. Therefore, our research focuses on natural, compound-based treatments targeting NF-κB, COX_2, and EGFR, specifically examining the bioactive compounds in chamomile and turmeric, both known for their anti-inflammatory properties. This approach offers a promising direction for therapies that could amplify the role of natural products in both inflammation and cancer.

1.1. Inflammation

Inflammation, derived from Latin term *Inflammatio*, means flame or to set on fire. Hippocrates in the 5th century BCE was the first to identify inflammation a healing response after injury. It took till the 1st century CE for Aulus Celsus to define the four-cardinal signs of inflammation. Ten centuries later, Ibn Sina (Avicenna) recorded in his encyclopaedia "The canon of medicines" (al-Qanun fi al-tib) all 5 signs of inflammation and suggested various plants, such as garlic, chamomile, and saffron, to treat acute inflammation, among other diseases. Building on previous discoveries, J. Hunter in the 18th century CE categorized inflammation into three types: adhesive inflammation, referring to the formation of the fibrous adhesions between tissues; suppurative inflammation, characterize by pus formation, an outcome of a severe inflammation; and ulcerative inflammation, related to the observed open sores due to the tissue loss. In the 19th century CE, a deeper knowledge of inflammation started to be established histologically with the development of microscopy and thanks to Rudolph Virchow. During this era, the role of polymorphonuclear leukocytes in the immune response to inflammation was introduced, and inflammation was then differentiated into 4 types: exudative, infiltrative, parenchymatous and proliferative. (1–5)

Inflammation is a biological response of the body tissue to a harmful stimulus, aimed at repairing tissues and restoring the internal homeostatic state. There are two types of inflammation: acute and chronic. Acute inflammation is a short-lived (days to weeks) response usually activated through injuries or infections. Chronic inflammation is a prolonged and sustained response (months to years) to persistent infections, autoimmune diseases, neurological conditions, exposure to toxins or pollutants, and cancer. (4,6,7) (Figure 1)

The stimuli that trigger these responses are divided in two major categories: external and internal factors. External factors can be non-microbial, such as allergens, irritants, and toxic compounds, or microbial. The microbial factors include the virulence factor that helps pathogens colonize and infect tissues, and the pathogens associated molecular patterns (PAMPs), which are small molecules with conserved patterns e.g., peptidoglycan, lipopolysaccharide, lipoteichoic acid, manner, and viral RNA/DNA. Internal factors, commonly known as DAMPs or damaged associated molecular patterns, these are intracellular proteins released from an injured tissue or dying cells. (8,9) (Figure 1)

Moreover, when these patterns (PAMPs and DAMPs) are recognized by pattern recognition receptors (PRRs), they activate leukocytes, which in turn induce two types of immune responses: innate and adaptive. The innate response is the first line of defense; it is non-specific, does not involve immunological memory and lasts few minutes to hours. In contrast, the adaptive response is antigen-specific, comes second in the line of defense, takes weeks or months to develop after the initial exposure and creates immunological memory involving T and B cells. (10,11) (Figure 1)

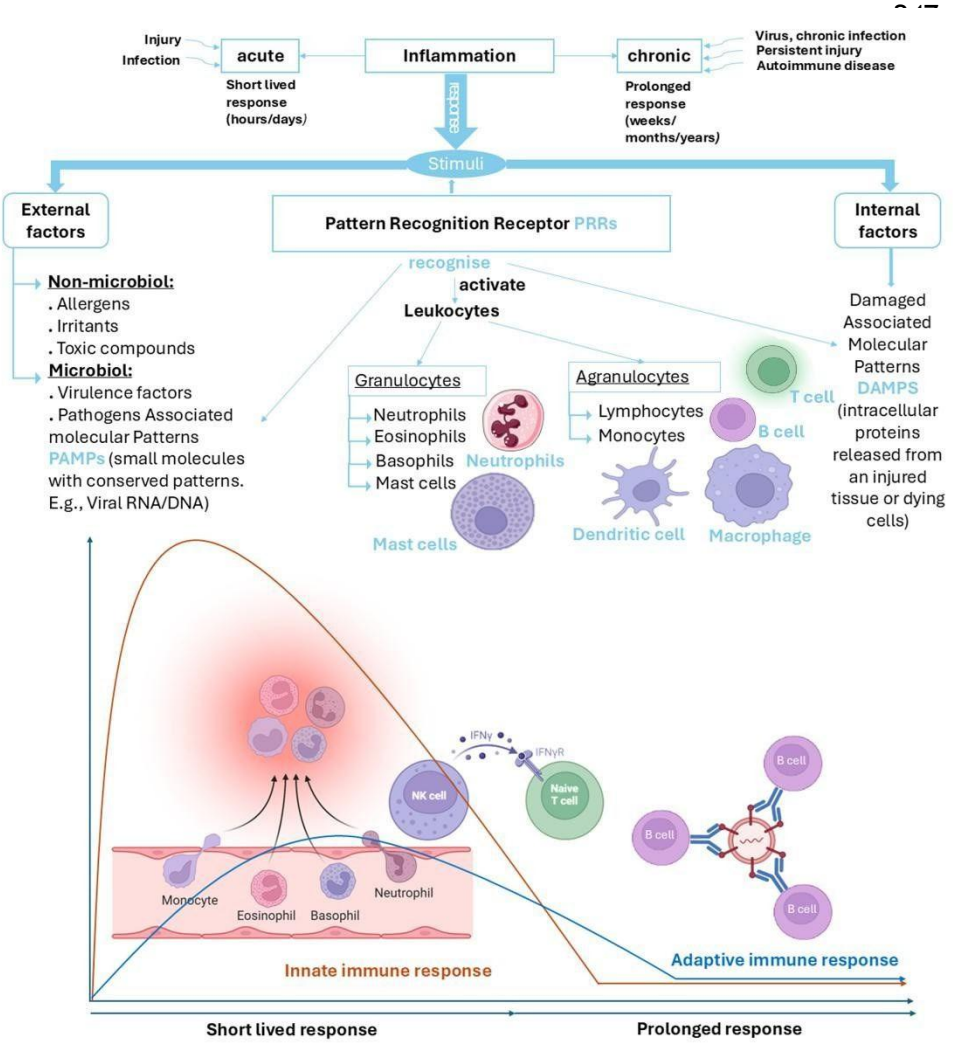

Figure 1. Scheme illustrating inflammation. This figure was created with Biorender.com.

Leukocytes (Greek; white cells) are the primary cellular components of the immune system, involved in both innate and adaptive response. They originate from the stem cells in bone marrow and differentiate into myeloblasts and monoblasts, also known as granulocytes and agranulocytes. The monoblasts include lymphocytes (T cells and B cells) and monocytes, which differentiate into macrophages and dendritic cells. The granulocytes, or myeloblasts are characterized with small granules containing proteins. This group includes neutrophils that are most abundant in the blood and are the first to act during acute inflammation. Eosinophils are less present in the blood but have a crucial role in eliminating parasites, asthma, and allergic reactions, in some cases their level increases during an autoimmune disease. Basophils are the least found in the blood and mostly activated when allergic reaction occurs. (Figure 1)

Mast cells are granulated cells found predominantly in the connective tissues beneath the epithelium of the skin, gastrointestinal tract, respiratory tract, and surrounded by blood vessels

and lymphatic vessels. These cells play a crucial role in the immune system, particularly during inflammation. Unlike other granulocytes, mast cells have an important role in both innate and adaptive immune responses. Their primary function is in mediating allergic responses, but they also exhibit antibacterial, antiparasitic, and antiviral activities. Notably, during adaptive immune responses, mast cells contribute to the activation of cytotoxic T cells through the release of TNF-alpha and the activation of NF-κB. Additionally, mast cells regulate a variety of physiological functions, such as vasodilation, angiogenesis, and the function of various organs and tissues. They achieve this by generating and releasing a range of multipotent molecules, including histamine, proteases, proteoglycans, leukotrienes, heparin, cytokines, chemokines, prostaglandins, and growth factors. These molecules enable mast cells to regulate the function of different cells, including dendritic cells, macrophages, T cells, B cells, fibroblasts, eosinophils, endothelial cells, and epithelial cells. (12–21) (Figure 2)

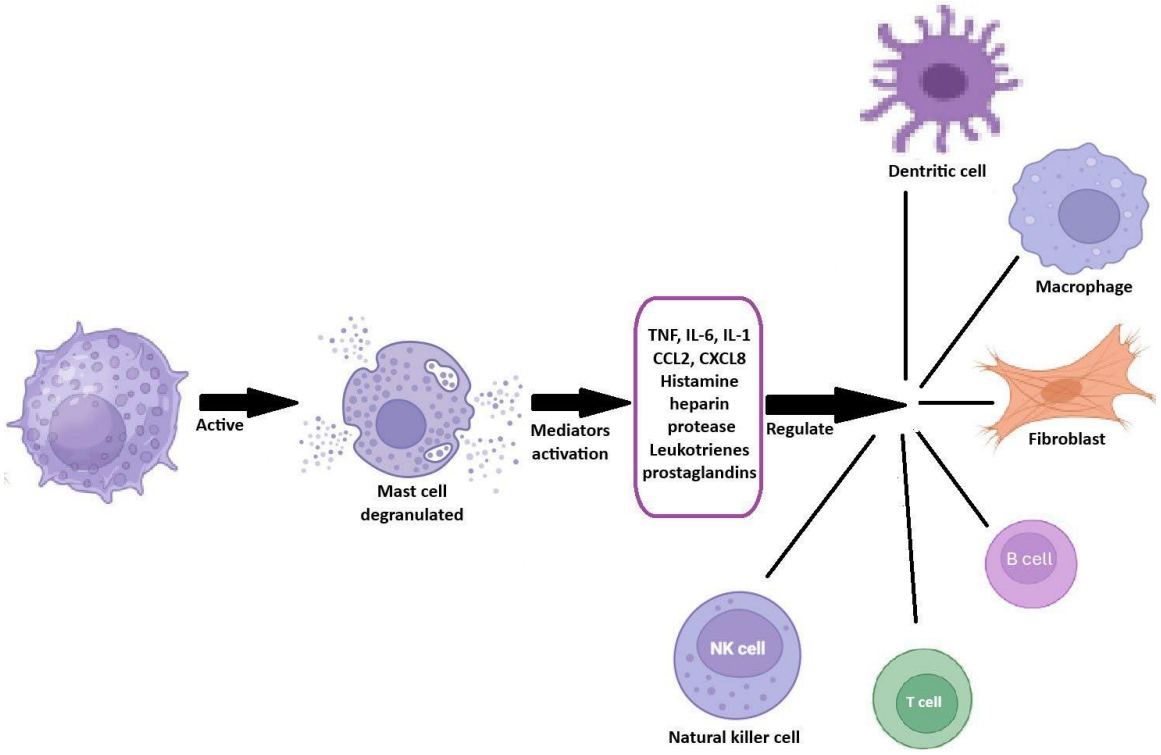

Figure 2. The function of mast cells in response to inflammation. This figure was created with Biorender.com.

1.1.1 Cyclooxygenase 2

Prostaglandin Endoperoxide H Synthase 2 or COX2 is an enzyme isoform of the cyclooxygenase from the myeloperoxidase family. It is overexpressed especially during inflammation,

carcinogenesis, and tumorigenesis through various factors: cytokines, growth factors, oncogenes, and tumor promoters. Usually in a stable state it is absent or found at a very low level. (22–24)

COX2 is a homodimer enzyme composed of 604 amino acids, constructed of two major domains: N-terminal domain and C-terminal domain. The N-terminal domain also known as the catalytic domain, is formed by five key components: a hydrophobic signal peptide directs COX-2 polypeptide into the endoplasmic reticulum (ER) lumen, a 17-amino-acid signal recognition peptide, dimerization domain containing the epidermal growth factor EGF-like modules the formation of the COX2 homodimer, membrane binding domain that anchors COX2 to the lipid bilayer of the ER and nuclear envelope, and the globular catalytic domain features two critical sites: the COX active site, extending from the membrane binding domain to the hydrophobic dead-end catalytic domain that contributes to COX2's drug selectivity and substrate binding flexibility. The peroxidase active site features a cleft that is pivotal for the activation of COX-2. The C-terminal domain, in contrast, contains 27 amino acids pivotal for the degradation of COX-2, ending with a small peptide of four amino acids enabling the signal to keep the enzyme in the ER. (25–29) (Figure 3)

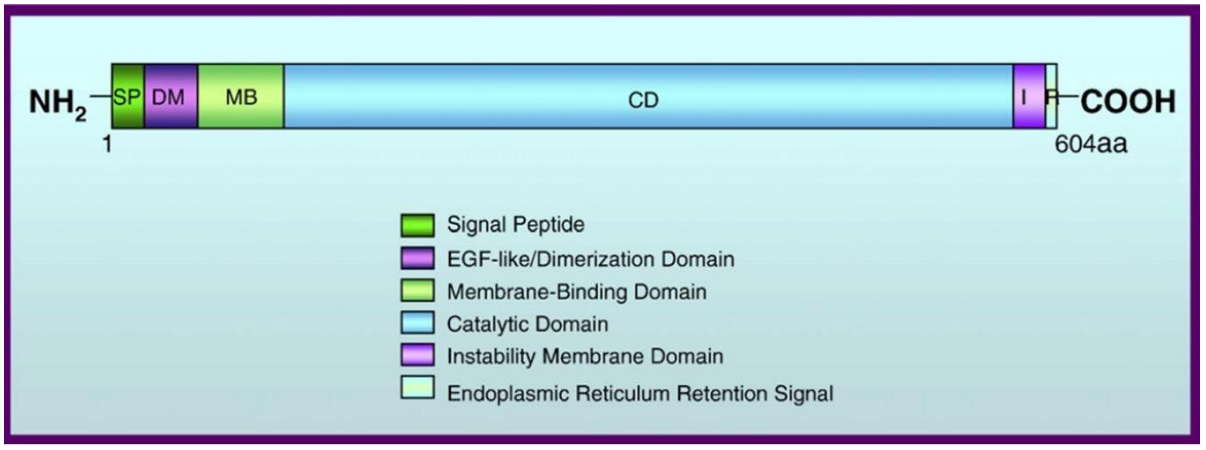

Figure 3. Illustration of the structure of the human primary protein cyclooxygenase 2. (30) (Taken from: Rizzo MT. Cyclooxygenase-2 in oncogenesis. Clinica Chimica Acta. 2011;412(9-10):671-87). (With permission from Elsevier, and Creative Commons. This work is licensed under non-commercial License Number: CC BY-NC 4.0. To view a copy this license, visit https://creativecommons.org/licenses/by-nc/4.0/)

Role of Prostaglandin Endoperoxide H Synthase 2

Cyclooxygenase 2 is a key enzyme responsible for the synthesis of prostaglandins, which play crucial roles in inflammation, pain, fever and cancer. Once expressed in the endoplasmic reticulum or in the nuclear envelope membranes, COX2 catalyzes the conversion of arachidonic

acid into Prostaglandin G2 (PGG2) through a process of oxidation. In this reaction, COX2 removes hydrogen from the carbon at position 13 (C13) of arachidonic acid and adds two oxygen molecules (O_2), forming the hydroperoxy endoperoxide PGG2. Subsequently, COX2 further reduces PGG2 by two electrons, converting it into Prostaglandin H2 (PGH2), a stable intermediate also known as hydroxy endoperoxide. PGH2 is then processed in the cytosol by specific synthases to produce various biologically active prostaglandins, including Prostacyclin (PGI2) and Prostaglandin E2 (PGE2), both of which are important mediators of inflammation and are implicated in cancer progression. Notably, COX2 differs from its isomer COX1 in its ability to metabolize a broader range of arachidonic acid derivatives, among them Endocannabinoid contributing significantly to carcinogenesis and other pathological conditions. (22,27,31–38) (Figure 4).

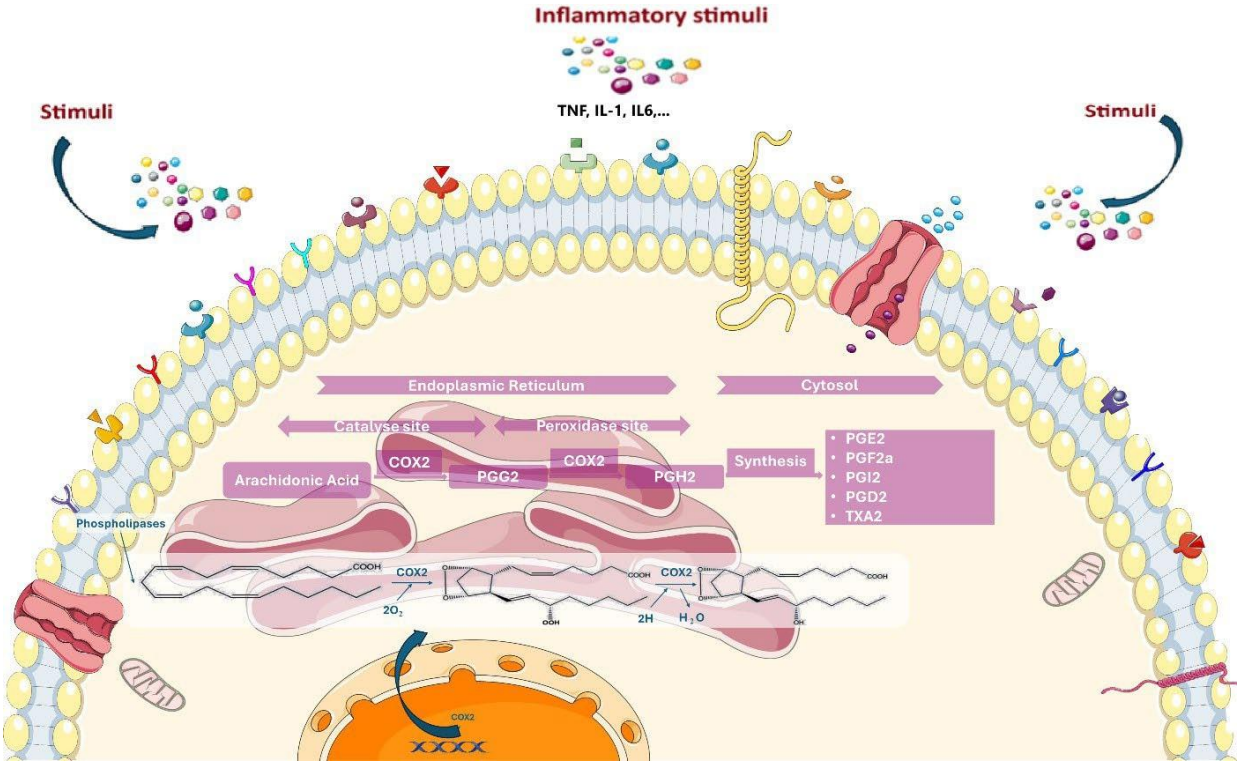

Figure 4. Cyclooxygenase 2 pathway in the synthesis of prostaglandins. This figure was created with Biorender.com and Smart Servier Medical Art under the license CC BY 4.0. To view a copy of the license, visit https://creativecommons.org/licenses/by/4.0/

1.1.2 Nuclear Factor kappa-B (NF-κB)

NF-κB is a family of transcription factors. It includes diverse homodimers and heterodimers proteins originated from five genes: NF-κB 1 (p50/p105), NF-κB 2 (p52/p100), RelA (p65), RelB, cRel (39). The original name of NF-κB is the Nuclear Factor kappa-light-chain-enhancer of activated B cells, referring to how it was first discovered in 1986 while investigating the

regulation and maturation of B cells essential for the adaptive immune response (40–42). Subsequently, NF-κB was found to be involved in diverse biological processes beyond the development of B cells such as cell survival and proliferation. Under normal conditions, NF-κB dimers are retained in the cytoplasm in an inactive form bound to its inhibitors known as IκBs (Inhibitors of κB). Activation of NF-κB occurs through two primary signaling pathways: the canonical pathway, triggered by cytokines such as tumor necrosis factor-alpha (TNF-α), and the non-canonical pathway, mediated by NF-κB-inducing kinase (NIK). Both pathways converge on the IκB kinase (IKK) complex, consisting of IKKα, IKKβ, and IKKγ (NEMO), which phosphorylates and induces the degradation of IκB proteins. This degradation releases NF-κB dimers, allowing them to translocate to the nucleus where they activate the transcription of genes involved in inflammation, immune regulation, cell growth, and survival. Dysregulation of NF-κB signaling is implicated in chronic inflammation and various cancers, highlighting its critical role in maintaining cellular and immune homeostasis. (43–49) (Figure 5)

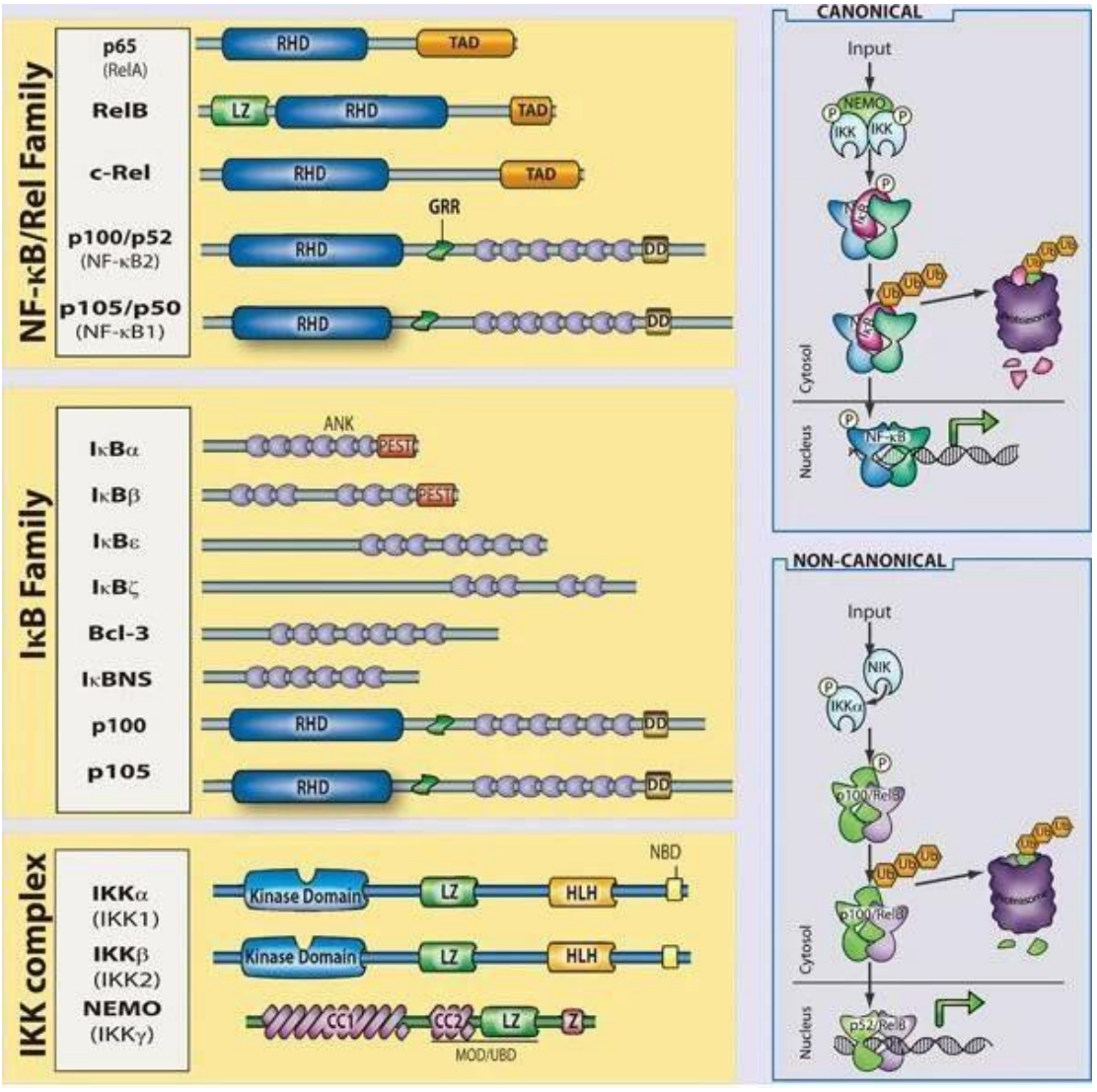

Figure 5. Schematic representation the canonical and non-canonical pathways of NF-κB´s activation, and the three protein families: NF-κB, IκB, and IKK. (50) (Take from: Hayden MS, Ghosh S. NF-κB in immunobiology. Cell Res. 2011;21(2):223-44. (With the permission of Springer Nature, and Copyright Clearance Center's RightsLink® service. This work is licensed under the license number: 5875950938719)

1.2 From Inflammation to Carcinogenesis

The link between inflammation and cancer was discovered long time ago. In the 19th century, the German physician Rudolf Virchow was the first to hypothesize a connection between inflammation and cancer, observing the presence of leukocytes in tumors and suggesting they originated from sites of chronic inflammation (51,52). Since then, scientific advancements have identified the primary components of the tumor microenvironment (TME), which consist of stromal cells and inflammatory immune cells. This understanding has highlighted the dual role of the immune system in carcinogenesis, functioning both as a tumor suppressor and a promoter of tumor growth. The immune system's anti-tumor activity helps limit tumor heterogeneity, while pro-tumor inflammation supports cancer progression by suppressing anti-tumor immunity through signaling molecules such as cytokines, interleukins, and chemokines. Key examples include tumor necrosis factor-alpha (TNF-α) and interleukin-6 (IL-6) (53,54). Moreover, inflammatory immune cells, such as tumor-associated macrophages and T-cells within the TME, have been shown to contribute to cancer growth, invasion, and metastasis (55,56). Notably today, it is widely accepted that inflammation not only plays a role in carcinogenesis and tumorigenesis but also aids in the growth and spread of cancer (57–59). This understanding was significantly advanced by the discovery of the link between the nuclear factor-kappa B (NF-κB) signaling pathway and tumor cell survival and proliferation. NF-κB is now recognized as a key mediator in the relationship between chronic inflammation and cancer progression (54,60–63). Additionally, the role of cyclooxygenase-2 (COX-2) in carcinogenesis was uncovered through research on non-steroidal anti-inflammatory drugs (NSAIDs). There are clinical studies that showed the prolonged use of NSAIDs revealed their cancer-preventive and chemopreventive effects, as they inhibit COX-2, which plays a crucial role in promoting inflammation linked to tumor development. This finding marked a major advancement in cancer research and prevention strategies (57,64–69).

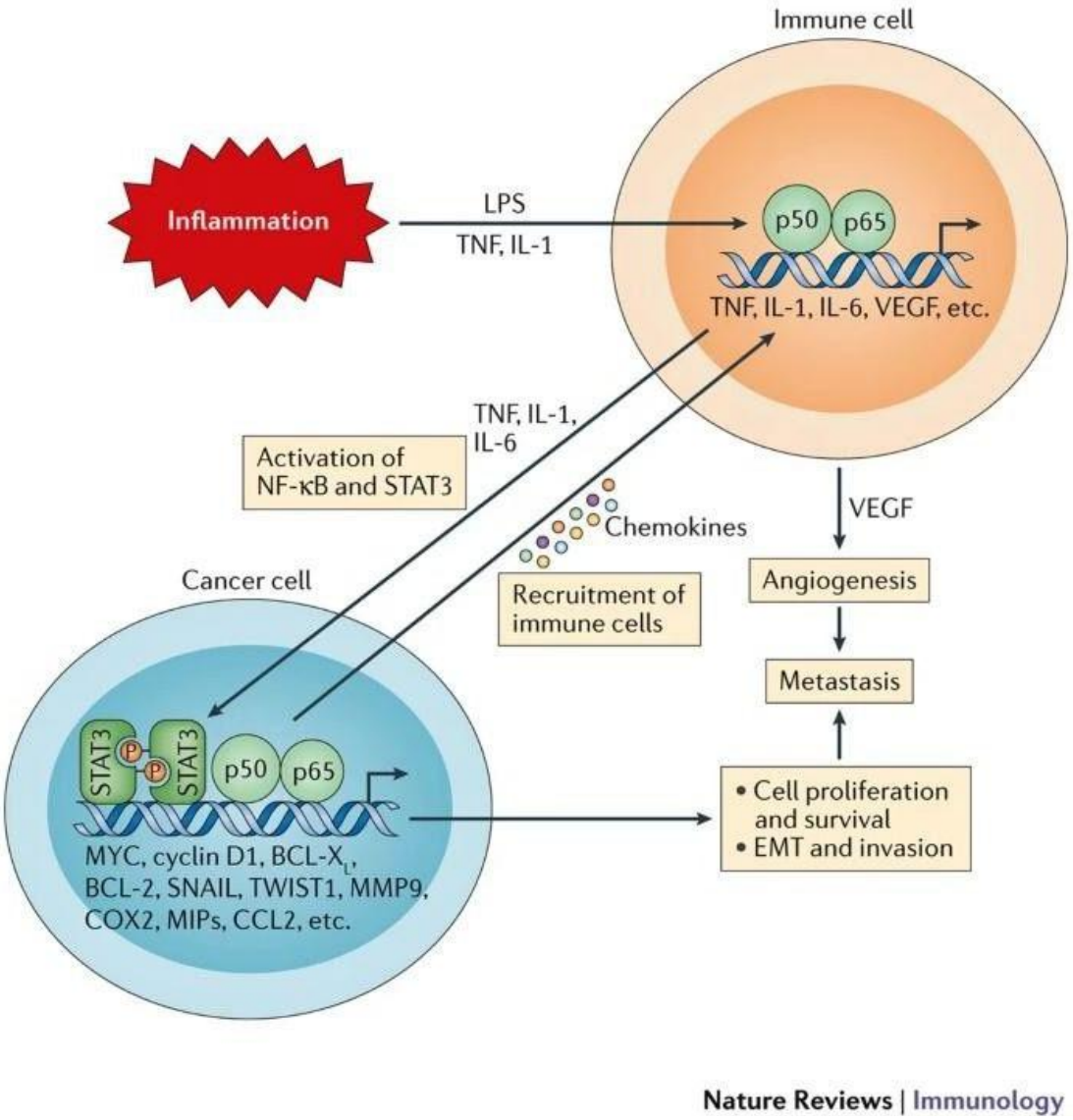

Figure 6. Chronic inflammation initiating cancer-immune cells interaction within tumor environment. The illustration highlights the involvement of NF-κB activation and COX2 overexpression in promoting cell proliferation. (70) (Taken from: Taniguchi K, Karin M. NF-κB, inflammation, immunity and cancer: coming of age. Nature Reviews Immunology. 2018;18(5):309-24). (With the permission of Nature Reviews Immunology, and Copyright Clearance Center's RightsLink® service. This work is licensed under the license number: 5875961439978)

1.3 Alpha/Beta-Tubulin

Microtubules are structural proteins composed of α-tubulin and β-tubulin dimers, forming a key component of the cytoskeleton along with microfilaments and intermediate filaments (71,72). These three cytoskeletal elements provide structural support to the cell, maintaining its shape, adhesion, and motility. Microtubules also play a critical role in intracellular trafficking and facilitate cell signaling (73,74). Microtubule assembly is guided by microtubule organizing

centers (MTOCs) and γ-tubulin. There are two main types of MTOCs: centrosomes, located near the nucleus, and basal bodies, found at the base of cilia and flagella on the cell membrane. MTOCs are essential for organizing microtubules during processes such as chromosome segregation during cell division, regulation of the cell cycle, and cell proliferation—factors that are crucial in cancer therapy (75–78). During inflammation, microtubules are essential for the formation and activation of immune cells, such as T-cells, as they regulate cell signaling pathways necessary for an effective immune response. Additionally, states of hyperinflammation and chronic inflammation have been linked to tubulin dysfunction, which have been seen to contribute to the progression of inflammation into carcinogenesis (79–83).

1.3.1 The Interaction Between Tubulin with NF-κB Signaling

Both NF-κB and COX-2 are well-established to play significant roles in both inflammation and cancer. Studies have also demonstrated a connection between microtubules and inflammatory proteins. Additionally, research has shown that NF-κB activation enhances signaling in various inflammatory pathways, including the cGAS-STING (cyclic GMP-AMP synthase-Stimulator of Interferon Genes) pathway, which is critical for innate and adaptive immune responses. When a DNA virus enters the cytoplasm, the cGAS enzyme recognizes it and, using ATP and GTP, synthesizes cyclic GMP-AMP (cGAMP). cGAMP then activates the STING molecule located in the endoplasmic reticulum (ER). STING translocates to the Golgi apparatus with the help of microtubules, interacting with COPII vesicles during transport. Once there, STING activates the IκB kinase (IKK) complex, which phosphorylates IκB, leading to NF-κB activation. NF-κB then migrates to the nucleus, where it triggers the expression of pro-inflammatory cytokines. Simultaneously, transcription factor IRF3 (interferon regulatory factor 3) is activated, allowing for the expression of type I interferons (IFN-I) (84–87). However, in chronic inflammatory conditions, the overexpression of NF-κB can induce microtubule depolymerization. This inhibits the proper trafficking of STING to lysosomes for degradation, resulting in prolonged STING activation and elevated secretion, contributing to sustained inflammation (88–90). (Figure 7)

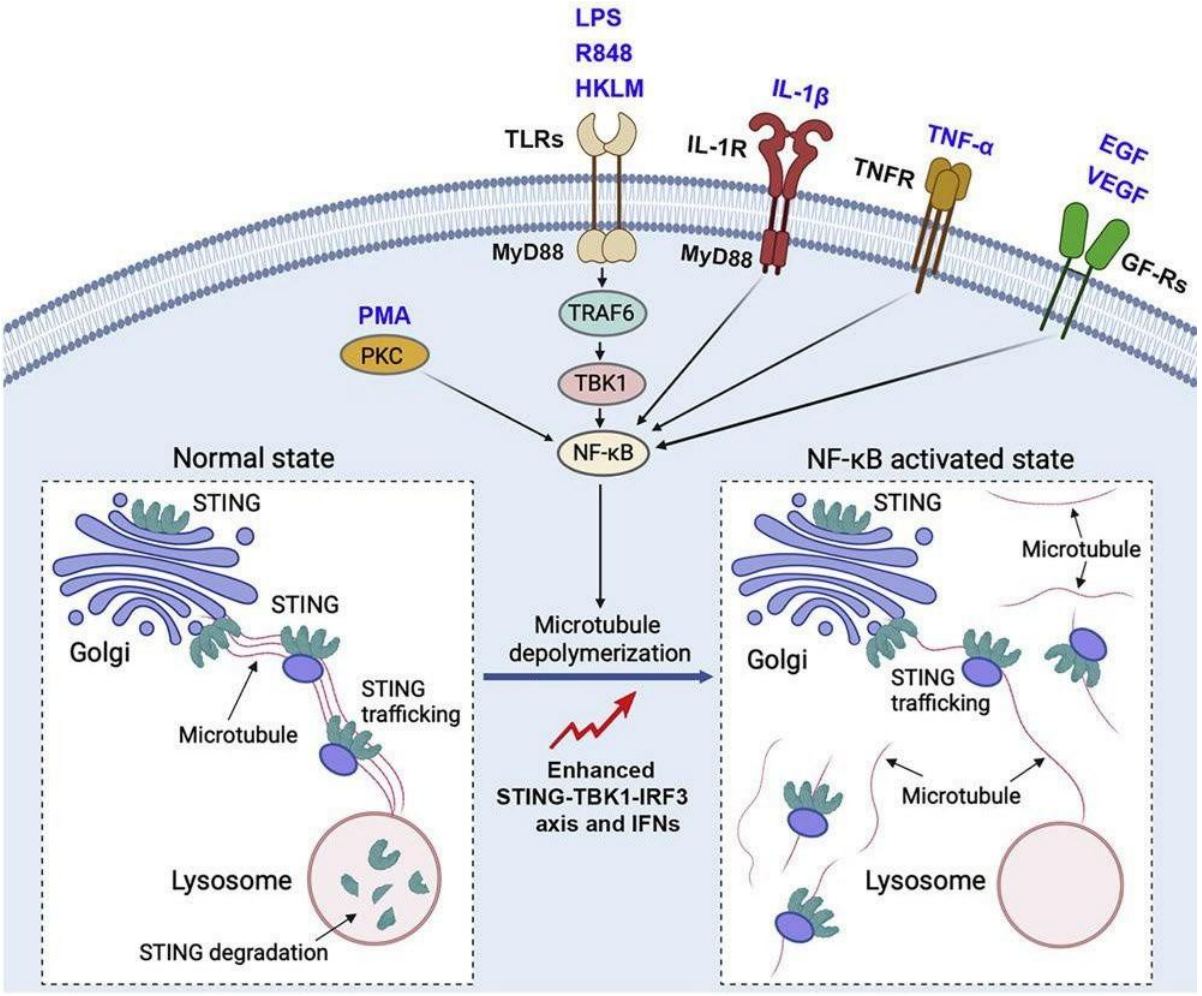

Figure 7. The interaction between microtubules and NF-κB during inflammation. (88) (Taken from: Zhang L, Wei X, Wang Z, Liu P, Hou Y, Xu Y, Su H, Koci MD, Yin H, Zhang C. NF-κB activation enhances STING signaling by altering microtubule-mediated STING trafficking. Cell Reports. 2023;42(3)). (With the permission Elsevier, and Copyright RightsLink® service. This work is licensed under the Creative Commons CC-BY-NC-ND license)

1.3.2 The Link Between Tubulin and COX2

The relationship between COX-2 and microtubules represents an intriguing area of research with potential implications for cancer therapy and cellular biology. Throughout years of research, some interesting connections between COX2 and microtubules. Over the years, several studies have uncovered intriguing connections between COX-2 and microtubules. Given that microtubules regulate cell signaling and molecular trafficking, there is evidence suggesting that microtubule dynamics may influence the regulation and localization of COX-2 within the cell.

(91–93)

Chronic inflammation leads to elevated levels of prostaglandin E2 (PGE2), which acts in an autocrine manner by binding to and activating EP receptors. This signaling, particularly through EP2 and EP4 receptors, triggers intracellular cascades that primarily increase cyclic AMP (cAMP) production, leading to the overexpression of COX-2. This creates positive feedback loop that amplifies the inflammatory response, eventually contributing to carcinogenesis. Notably, it has been shown that microtubule disruption interferes with PGE2-induced cAMP elevation, as microtubules are involved in the trafficking and organization of EP receptors. (94–100)

Research has explored the synergistic effects of combining COX-2 inhibitors with microtubule-disrupting agents to enhance anti-cancer efficacy. Some studies have even led to the development of hybrid molecules designed to simultaneously inhibit COX-2 and disrupt microtubules, potentially offering a novel therapeutic approach. (101–103)

1.4 Mitochondria and ROS Generation

Mitochondria, a membrane-bound organelle, were discovered in the early 1960s and revolutionized biology not only because they are considered the "powerhouse" of the cell, but also because they contain their own mitochondrial DNA (mtDNA), which replicates independently within the cell. These two features make mitochondria essential for various cellular functions, particularly in energy production, cell differentiation, and apoptosis (104,105). One of the by-products of mitochondrial activity is reactive oxygen species (ROS), highly reactive molecules that play dual roles in cellular processes (106). At physiological levels, mitochondrial ROS (mtROS) act as important signaling molecules, regulating cellular processes like the adaptive immune response and maintaining cellular homeostasis. However, during acute or chronic inflammation, excessive ROS production can lead to oxidative stress, damaging cellular components such as proteins, lipids, and DNA (including mtDNA). This oxidative damage can result in mitochondrial dysfunction and trigger cell death via apoptosis. (107–113)

The last two decades, Mitochondria have become a central focus in cancer research due to their role in regulating apoptosis (114). Cancer cells often develop mechanisms to evade mitochondrial apoptosis, giving them a resistance (115–117). One of the key mechanisms involves altering the balance between pro-apoptotic and anti-apoptotic proteins in the Bcl-2 family. These proteins regulate mitochondrial outer membrane permeabilization (MOMP), which changes in mitochondrial dynamics and morphology. Normally, mitochondria undergo continuous cycles of fusion and fission, which coordinate their size, shape, and function. When the anti-apoptotic

proteins like Bcl-2, Bcl-xL, and Mcl-1 are overexpressed mitochondria tend to stay in a fused state, which helps them evade degradation by immune cells like macrophages and dendritic cells, contributing to cancer cell survival. (118–123)

Moreover, ROS also play a complex role in cancer. The overproduction of ROS mediate to the continuous expression of transcription factors like NF-κB and upregulation enzymes like COX-2. Interestingly, both NF-κB and COX-2 have been associated to the anti-apoptotic pathways that support cancer cell survival and proliferation, which make them indirectly associated to regulation of mitochondria's dynamic. (124–131)

1.5 Multidrug Resistance

The resistance of cancer cells is not only linked to mitochondrial dynamics but also to their resistance to cancer treatments. One of the major challenges in cancer therapy occurs when patients have a resistance to one, or multiple drugs also referred as the Multidrug resistance (MDR). MDR can be driven by two major categories: intrinsic factors and extrinsic factors. (132,133) (Figure 8).

Intrinsic factors pre-existing within cancer cells before treatment begins. These include genetic mutations in genes regulating cell death including epidermal growth factor receptor (EGFR) and p53 gene expressing tumor suppressor protein, drug metabolism, and DNA repair mechanisms. Such mutations can lead to the sustained production of anti-apoptotic proteins such as Bcl-2, Bcl-xL, and Mcl-1, as well as an overexpression of membrane transporters like P-glycoprotein (P-gp) and ATP-binding cassette (ABC) transporters. These transporters are particularly problematic, as they enhance the efflux of chemotherapeutic compounds, reducing their intracellular concentrations below effective levels (134–139).

Extrinsic factors, on the other hand, emerge during treatment. These may include acquired resistance after repeated rounds of chemotherapy, changes in the tumor microenvironment (TME), and conditions like hypoxia (low oxygen levels) or interactions with surrounding stromal cells (140,141). Inflammation also plays a critical role in extrinsic resistance. Research has shown that when cancer cells detect chemotherapeutic agents, they activate survival pathways often associated with inflammatory signaling, where the two proteins NF-κB and COX2 are found to be consistently overexpressed (142–146). (Figure 9)

To overcome multidrug resistance (MDR) in cancer therapy, one of goals is to identify drug additives, or chemosensitizers, that can be combined with existing chemotherapeutic agents to enhance their effectiveness. These additives, particularly natural products and their derivatives,

are highly preferable due to their ability to target and reverse the mechanisms driving MDR while offering the advantage of low cytotoxicity. This makes cancer cells more susceptible to chemotherapy with fewer adverse effects on healthy tissues. (147–149)

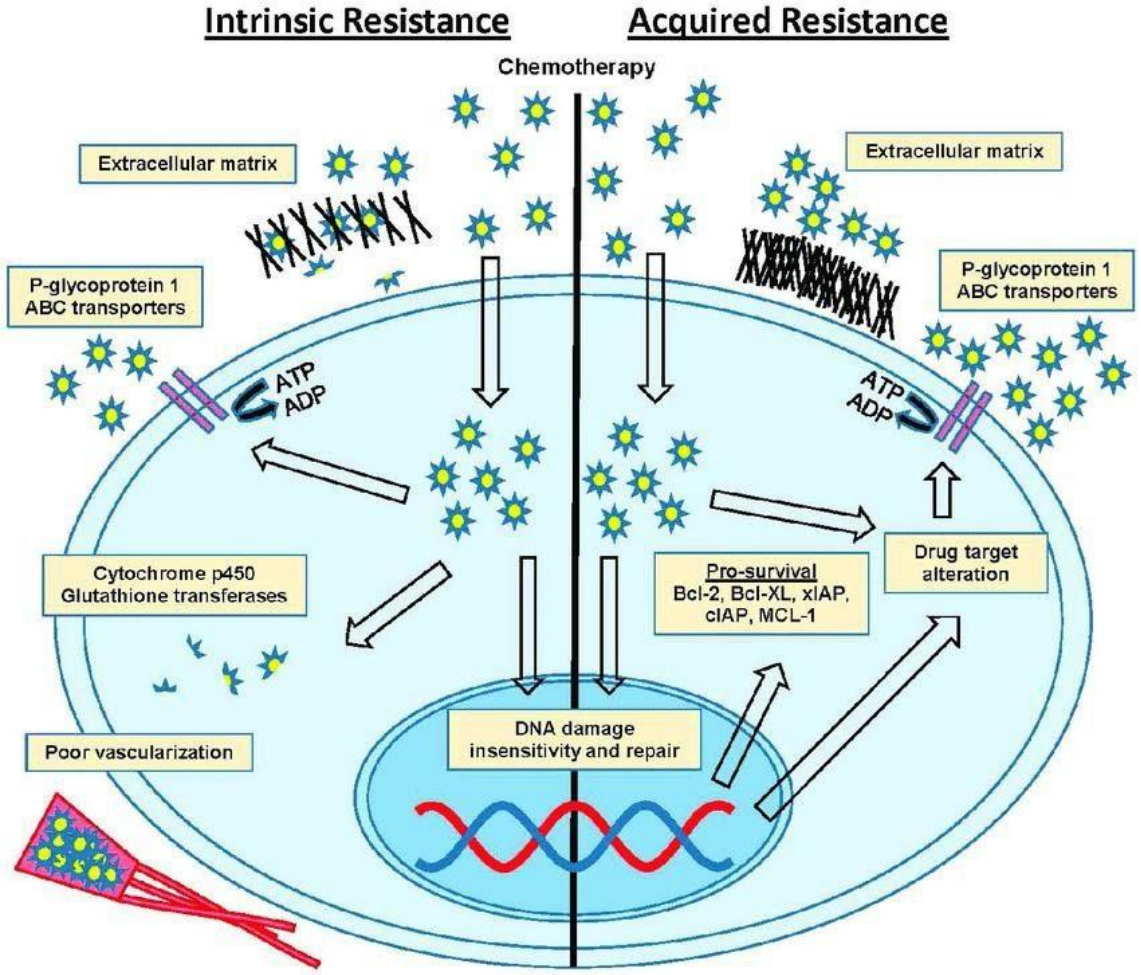

Figure 8. Multidrug resistance mechanism under the intrinsic/extrinsic factors. (150) (Taken from: Cornelison R, Llaneza DC, Landen CN. Emerging therapeutics to overcome chemoresistance in epithelial ovarian cancer: a mini-review. International journal of molecular sciences. 2017;18(10):2171). (With the permission from Frontier. This work is licensed under the Creative Commons Attribution 4.0 International License. To view a copy of this license, visit http://creativecommons.org/licenses/by/4.0/ of Creative Commons CC BY 4.0 license)

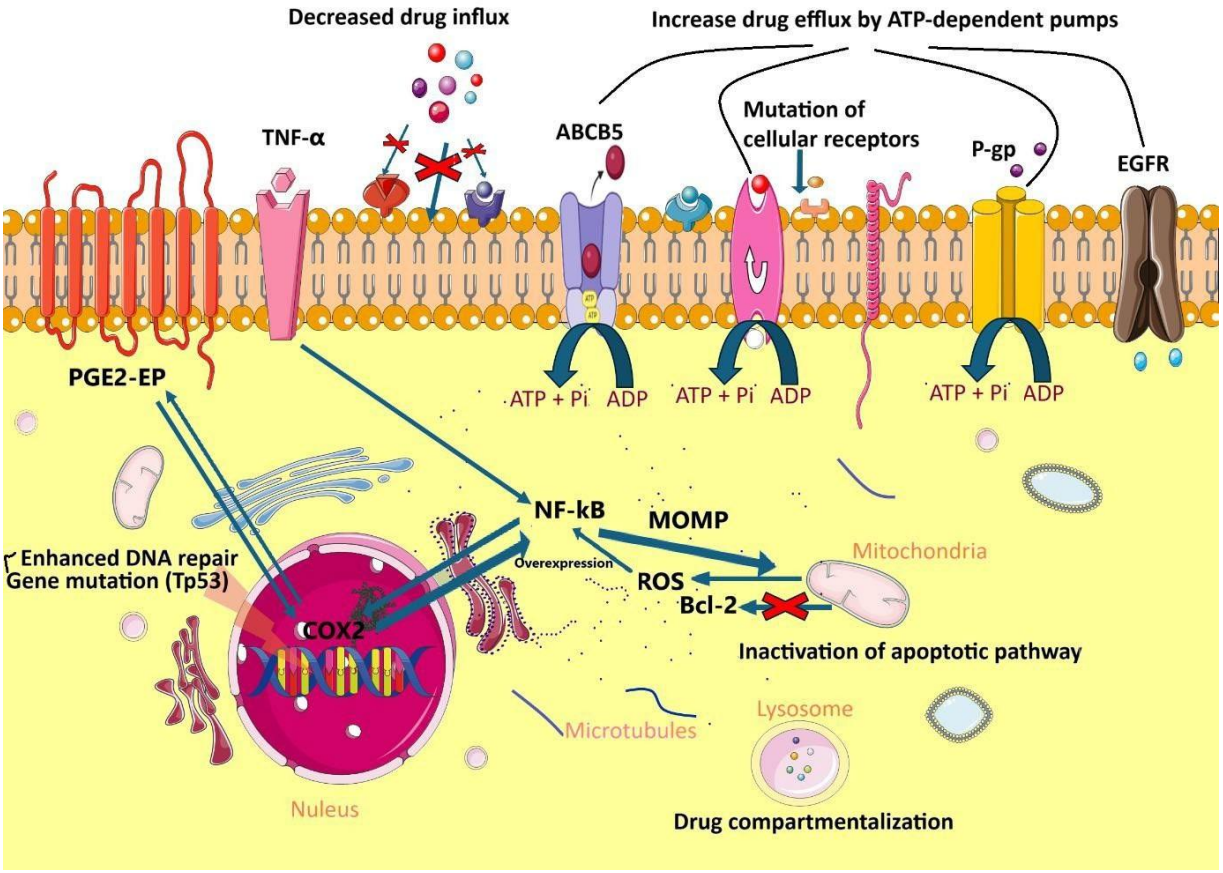

Figure 9. Mechanisms of anticancer drug resistance: efflux pump-mediated mechanisms of MDR, DNA repair and gene mutation. Highlighting the overexpression of NF-κB and COX2 pathways linked to the increase of ROS and the alteration of the membrane potential of mitochondria. This figure was created with Biorender.com and Smart Servier Medical Art under the license CC BY 4.0. To view a copy of the license, visit https://creativecommons.org/licenses/by/4.0/

1.6 Chamomile

Chamomile has been known for thousands of years, for its various health benefits and therefore has been used in the treatment of several conditions thanks to its antioxidant and antimicrobial properties (151–153). This plant is considered safe for consumption by the U.S. Food and Drug Administration (FDA), which classifies it as generally accepted as safe (GRAS) (154–156). Aside from this, chamomile has shown to be very useful in treating muscle spasms, rheumatism, and metabolic disorders (157,158). Further, chamomile tea preparations, especially those made of German chamomile (*Matricaria chamomilla* L.) have been rich in studies investigating the possibility of antidepressant, anti-stress, anti-inflammatory, and anticancer activity (159–163). In clinical research studies, chamomile tea extracts have been proven to be effective against

inflammation such as inflammatory bowel disease, eczema and mucositis caused by chemotherapy and radiotherapy (164–166). Additionally, chamomile has shown promise in alleviating peripheral neuropathic pain, a common side effect of chemotherapy. These anti-inflammatory and analgesic effects are attributed to chamomile's bioactive compounds, precisely to its secondary metabolites such as apigenin and α-bisabolol which have been shown to modulate inflammatory pathways such as inhibiting the activity of COX2 and NF-κB and promote healing during both inflammation and cancer (167–174).

1.6.1 Chemical constituents and biological activity of *Matricaria chamomilla* L.

German Chamomile (*Matricaria recutita* L.) belongs to the family Asteraceae, native to Europe and west Asia. is rich in terpenoids (α-bisabolol, farnesol, chamazulene, lupeol), flavonoids (apigenin, luteolin, quercetin, myricetin), coumarins (herniarin, umbelliferon), organic acid (caffeic acid, chlorogenic acid), sterols (stigmasterol, taraxasterol), phenolics (apigenin-7-glucoside, luteolin-7-glucoside), polysaccharides, volatile oils, polyacetylenes, and mineral. (152,175–177) (Table 1)

These diverse chemical components give the plant a wide range of biological activities. Studies have demonstrated that flavonoids such as apigenin, luteolin, and chamazulene exhibit anti-inflammatory effects by inhibiting pro-inflammatory enzymes like cyclooxygenase (COX) and lipoxygenase, which in turn reduces the production of inflammatory mediators. Free radicals have been associated with cardiovascular disease and cancer. The high amount of phenolics and flavonoids like quercetin gave the plant its antioxidant activity that helps neutralize free radicals, protecting cells from oxidative damage. In addition, the terpenoids in chamomile, particularly α-bisabolol, have been shown to have antimicrobial properties, effective against various bacterial and fungal pathogens. Furthermore, polysaccharide-polyphenolic conjugates isolated from M. chamomilla have demonstrated the ability to reduce platelet aggregation in a dose-dependent manner, without toxic effects on blood cells, suggesting potential applications in treating blood coagulation disorders In vitro studies have also shown that chamomile flower extract exhibits cytotoxic activity against cancer cells, including human hepatoma cells (HepG-2) and colorectal cancer cells (HT-29), by inhibiting nitric oxide (NO) production. Among its many biological properties. (178–183)

Notably, Chamomile poses a long list of biological properties and is renowned for its anti-inflammatory effects. However, its potential anti-cancer properties have garnered increasing interest in recent years. Over the past decade, research has demonstrated chamomile's ability to inhibit cancer cell growth and induce apoptosis (programmed cell death) by regulating key

proteins such as COX-2 and NF-κB. These findings raise the potential of chamomile to be used as an adjuvant to chemotherapy or to help overcome multidrug resistance in cancer treatment. (Figure 10)

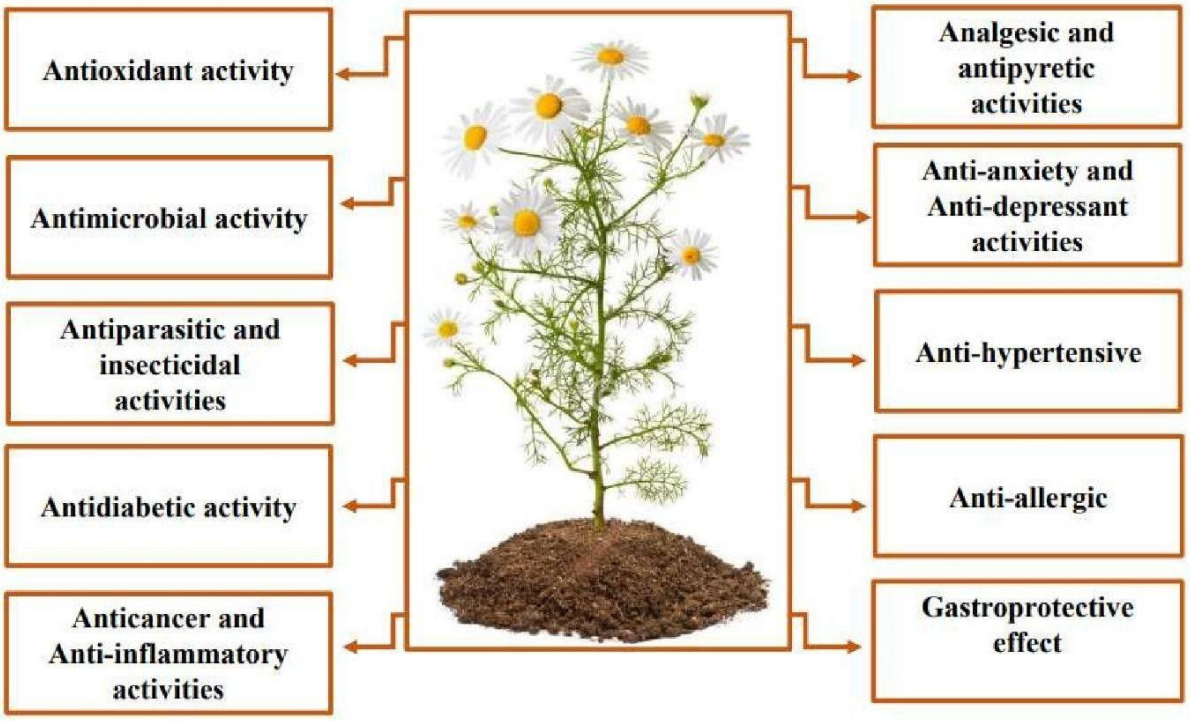

Figure 10. The biological virtues of *Matricaria chamomilla* L. (184) (Taken from: El Mihyaoui A, Esteves da Silva JC, Charfi S, Candela Castillo ME, Lamarti A, Arnao MB. Chamomile (Matricaria chamomilla L.): a review of ethnomedicinal use, phytochemistry and pharmacological uses. Life. 2022;12(4):479). (With the permission from mdpi. This work is licensed under the Creative Commons Attribution 4.0 International License. To view a copy of this license, visit http://creativecommons.org/licenses/by/4.0/ of Creative Commons CC BY 4.0 license).

1.7 Curcumin

Curcumin is a natural compound derived from the Turmeric rhizomes of (*Curcuma longa* L). It is used as spice for cooking but has also a variety of medicinal virtues, it can be found as a powder, tea, cream, and even capsule. Similar to chamomile, curcumin has many biological properties including antiviral, antioxidant, anti-bacterial, anti-inflammatory, and anti-cancer. These properties have intrigued numerous researchers, it has been tested in clinical trials. In cancer research deep investigations have been led to understand the mechanism of action of this molecule in cancer cells. Interestingly, curcumin have been found to inhibit cell proliferation,

metastasis process and overcome some multidrug resistance mechanisms. Furthermore, it has been demonstrated that curcumin was positively effective in inhibiting the NF-κB and EGFR pathways in many cancer types. (185–188)

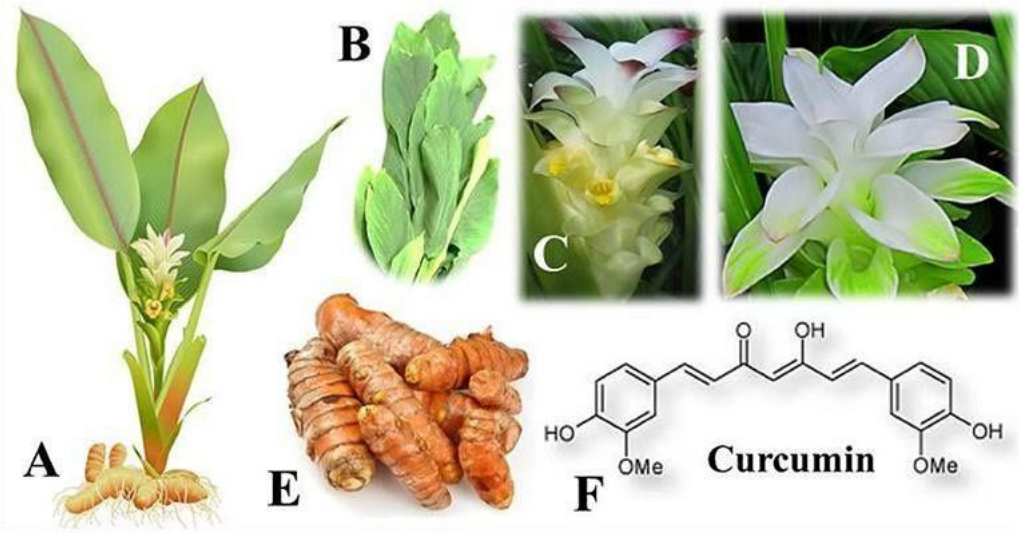

Figure 11. The Turmeric plant *Curcuma longa* L. A) Planta. B) Folium. C, D) Flos. E) Rhizoma. F) 2D structure of curcumin. (189) (Taken from: Tripathy S, Verma DK, Thakur M, Patel AR, Srivastav PP, Singh S, Gupta AK, Chavez-Gonzalez ML, Aguilar CN, Chakravorty N, Verma HK. Curcumin extraction, isolation, quantification and its application in functional foods: a review with a focus on immune enhancement activities and COVID-19. Frontiers in Nutrition. 2021;8:747956). (With the permission from Frontier. This work is licensed under the Creative Commons Attribution 4.0 International License. To view a copy of this license, visit http://creativecommons.org/licenses/by/4.0/ of Creative Commons CC BY 4.0 license).

Table 1. The classification, CAS number, molecular, name, and 2D structures of molecules extracted from German chamomile *Matricaria chamomilla* L used in this dissertation. (Molecular structures were downloaded from PubChem accessed 30 September 2024)

	CAS number	Molecular Formula	Name	2D structure
	Flavonoids			
1	520-36-5	C15H10O5	Apigenin	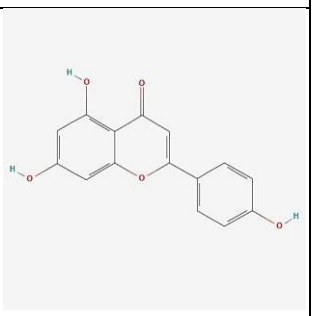
2	529-44-2	C15H10O8	Myricetin	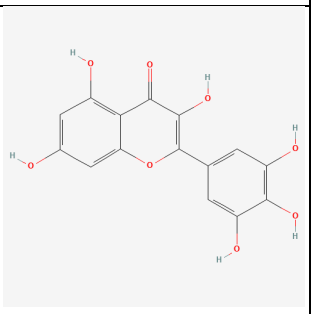
3	117-39-5	C15H10O7	Quercetin	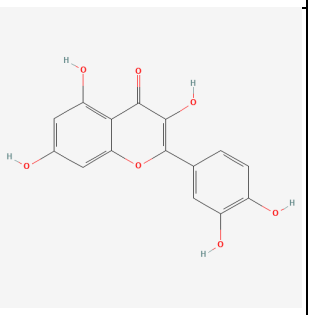
	Terpenoids			
4	559-70-6	C30H52O	β-Amyrin	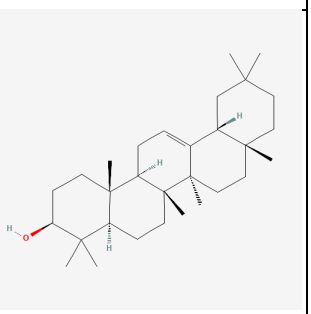

5	473-15-4	C15H26O	β-Eudesmol	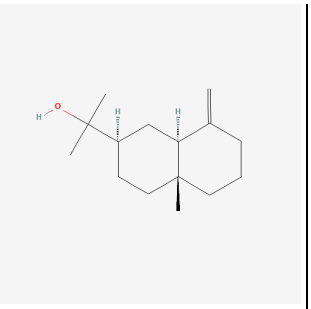
6	106-28-5	C15H26O	Farnesol	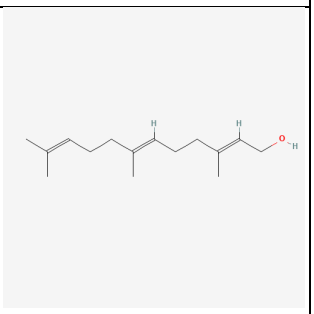
7	545-47-1	C30H50O	Lupeol	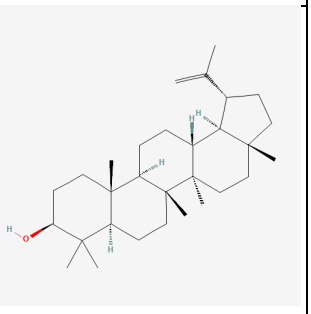
	Sterols			
8	474-58-8	C35H60O6	Daucosterol	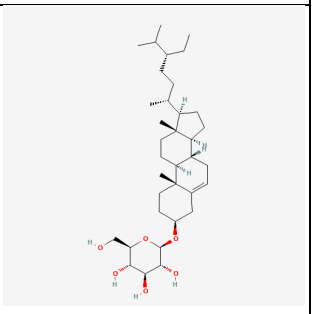
9	83-46-5	C29H50O	β-Sitosterol	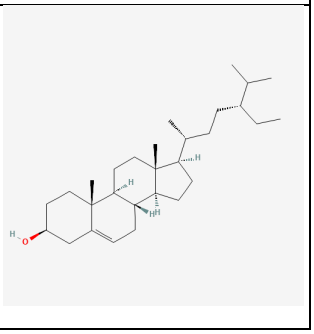

596

2. Objective of the thesis

In this study, we focused on inflammation and its link to cancer. In human history, we have come from far, we have made many achievements in the development of technology and medicine. Nevertheless, there are still millions of people suffering from chronic inflammatory diseases and millions that are still dying from cancer. In fact, billions of dollars are gained in the industry of pharma in anti-inflammatory and anti-cancer treatments but still people´s suffering is still ongoing.

In that purpose, our focus is on finding alternative treatments that can help overcome these pharmacological obstacles by using Phyto-pharmaceuticals. Today, natural products have again gained their place in the market race, over 60% of natural derivates drugs including the synthetic compounds that are based on natural pharmacophores, are used as an anti-cancer drugs, e.g., artemisinin and taxol.

Since, chamomile is well known champion used for thousands of years against inflammation. We wanted to investigate deeper in its effect against cancer and what role can it have in the cancer therapy. Many chamomile compounds have already been investigated, we wanted to explore the effect of other compounds that we extracted from the flower of the German chamomile such as quercetin, lupeol, beta-amyrin, myricetin.

Initially, we aimed to investigate the effects of chamomile compounds against COX2, a well-known anti-inflammatory protein that is primarily induced during inflammation and is often overexpressed in cancers such as colorectal cancer. Seven chamomile compounds were selected for testing based on their affinity for COX2, determined through in silico molecular docking studies.

Afterwards, we concentrated on myricetin as it stood out from the other six when its cytotoxicity was analyzed through the NCI60 cell line panel. By performing a cross-resistance profiling of myricetin from the NCI60 database, we found that myricetin correlated mostly with tubulin inhibitors such as vincristine. Subsequently, we validated the effect of this molecule on alpha-tubulin using immunofluorescence microscopy.

Moreover, we wanted to know if myricetin was also involved in classical drug resistance. Consequently, after profiling myricetin in drug resistance mechanisms using the NCI60 cell line panel, we verified in vitro that it was not involved in multidrug resistance mechanisms.

Finally, we wanted to emphasize the utility of finding a potential COX2 inhibitor like myricetin by demonstrating that COX2 plays an important role in cancer. We found that its high expression

is associated with worse survival prognosis of renal clear cell carcinoma patients, utilizing Kaplan-Meier survival time analysis.

Lastly, NF-κB is a renowned anti-inflammatory and anti-apoptotic protein, which has long been researched for its involvement in the survival and proliferation of cancer cells. In a similar pattern as mentioned above, we tested the affinity of chamomile compounds with the NF-κB (p65/RelA) protein and selected six of them to confirm their inhibitory effect against the protein using an NF-κB inhibitor assay. Since mitochondria and ROS generation have been demonstrated to be involved in cancer and linked to NF-κB, we were curious if our top compound, β-amyrin, had any effect on them.

After performing various -omics analyses using the NCI60, we chose lupeol and quercetin to verify the findings in vitro by performing immunofluorescence microscopy of α-tubulin, resazurin assay, apoptosis, and cell cycle analysis.

Furthermore, the role of NF-κB in promoting the expression of genes during inflammation and/or carcinogenesis, such as the production of cytokines and interleukins, was investigated. Therefore, we performed a real-time PCR assay to prove that the three selected compounds could indeed inhibit IL-6 and IL-1β during inflammation. Additionally, we wanted to test that the three molecules do inhibit NF-κB by conducting a western blot using total cellular NF-κB extracted from the induced inflammatory cells, HEK-Blue Null 1.

Finally, we explored if NF-κB overexpression would have an impact on the survival of patients afflicted with renal clear carcinoma using the KMPlotter database.

As supplementary project related to the above-mentioned NF-κB study. We focused on curcumin and its 50 derivatives, exploring their effects on NF-κB and EGFR *in silico* and *in vitro*. In addition to their bioactivity within cancer cells, through resazurin assays, lactate dehydrogenase assay, flow cytometric measurement of reactive oxygen species, and annexin V/propidium iodide assay.

3. Results and Discussion

More than 200 chamomile compounds were extracted from the flower of the German chamomile and were analysed using liquid chromatography diode array detector-quadrupole time-of-flight mass spectrometry (LC-DAD-QToF). These compounds were then studied with two prompt anti-inflammatory proteins Cyclooxygenase2 and the Nuclear transcription factor kappa B.

3.1 COX2-Inhibitory and Cytotoxic Activities of Phytoconstituents of *Matricaria chamomilla* L.

A total of 212 ligands found in chamomile were virtually screened against the enzyme COX2. Among these, β-sitosterol exhibited the highest binding affinity, with a docking score of -11.73 (± 0.44) kcal/mol. This result was consistent with the COX2 inhibition screening assay, confirming the strong interaction between the selected compounds and COX2.

The resazurin assays demonstrated that chamomile extract effectively inhibited hematopoietic cancer cell lines CCRF-CEM and AMO-1, with IC_{50} values 3.7 ± 4.7 µg/ml to 28.0 ± 2.2 µg/ml, respectively. However, the extract was not effective against the resistance of the colon cancer cell line HCT116 p53-/- knockout, with an IC_{50} of 74.3 ± 0.4 µg/ml, indicating a resistance 2.65 times greater than that of the wild-type HCT116 p53+/+ (IC_{50} of 28.0 ± 2.2 µg/ml).

Further analysis of the NCI60 cancer cell line panel identified apigenin, farnesol, and myricetin as the most active compounds. Given that apigenin and farnesol had already been studied by our group, we focused on myricetin. Oncobiogram analysis revealed that myricetin's bioactivity significantly correlated with 5 of 10 tubulin inhibitors and 2 of 14 tyrosine kinase inhibitors. Immunofluorescence microscopy of GFP-tagged α-tubulin confirmed that myricetin inhibits microtubules in a manner similar to vincristine.

The number one issue in cancer therapy is multidrug resistance. Through drug resistance profiling using NCI60 data, myricetin demonstrated cross-resistance only with classical anticancer drugs linked to glutathione S-transferase P (GSTP) activity and cellular proliferation rates. This finding suggests that other chamomile components, rather than myricetin, might be responsible for the resistance observed in HCT116 p53-/- knockout cells when treated with the plant extract. Additionally, proteomics analysis identified several proteins responsive to myricetin that may be involved in its mode of action and multidrug resistance mechanisms. These proteins include those involved in mRNA metabolism (e.g., DDX39B, CSNK2A), programmed cell death (e.g., TP53I3, PDCD5), and genome stability (e.g., CDK2, BLM).

Finally, Kaplan-Meier survival analysis using the KMPlotter database revealed that COX2 overexpression correlates with poorer survival in patients with renal clear cell carcinoma. This

688 finding accentuates the potential therapeutic value of identifying a strong COX2 inhibitor to
689 improve patient outcomes.

690

Further reading: Appendix I

COX2-inhibitory and cytotoxic activities of phytoconstituents of Matricaria chamomilla L.

Assia I. Drif, Bharati Avula, Ikhlas A. Khan, and Thomas Efferth

3.2 Anti-Inflammatory and Cancer-Preventive Potential of Chamomile (*Matricaria chamomilla* L.): A Comprehensive *in Silico* and In Vitro Study

The molecular docking of 212 phytochemicals found in chamomile against NF-κB revealed that β-amyrin had the highest affinity for the protein (−8.70 ± <0.01 kcal/mol, pKi 0.42 ± < 0.01 μM). These molecular docking results were further confirmed using microscale thermophoresis, which demonstrated that β-amyrin binds to NF-κB with a K_D value of 943 ± 113 nM. The results also significantly correlated with the NF-κB reporter assay, showing that β-amyrin was the most potent inhibitor of NF-κB , achieving 61.1% (±7.3) inhibition at 10 μM.

Additionally, an oxidative stress assay revealed that β-amyrin was effective in reducing ROS generation in an inflammatory state with elevated oxidative stress, with reductions of 12.30% ($p = 0.1$), 10.83% ($p = 0.05$), and 8.80% ($p = 0.01$) at concentrations of 0.1 μM, 1 μM, and 10 μM, respectively. To assess its effect on mitochondrial membrane potential, we used HEK-Blue Null1 cells under induced inflammation. β-amyrin led to apoptosis in 52.6% of the cell population, while 47.6% of the cells remained viable. Conversely, the resazurin assay showed that β-amyrin was not cytotoxic to CCRF-CEM leukemia cells. Interestingly, β-amyrin was not included in the NCI60 database. Therefore, following the cytotoxicity analysis, we selected lupeol and quercetin, the next most cytotoxic chamomile compounds identified in the NCI60 panel. Moreover, the oncobiogram analysis revealed that both compounds correlated with microtubule inhibitors. This was confirmed by immunofluorescence microscopy, which showed that both lupeol and quercetin inhibited the polymerization of α-tubulin at 10 μM. *In silico* docking studies further supported these findings, showing that lupeol and quercetin had a higher affinity for α-tubulin when docked in the vincristine pocket (−8.62 ± 0.04 kcal/mol for lupeol and −6.77 ± 0.06 kcal/mol for quercetin) compared to paclitaxel and colchicine. Both compounds' impact on microtubules was also reflected in their ability to arrest the U2OS cell cycle at the G2/M phase after 72 hours of treatment at 4x IC50. The cytotoxicity of lupeol and quercetin was further tested *in vitro* using the resazurin assay, which demonstrated toxic activity against leukemia, glioblastoma, and colorectal cancer cell lines. However, osteosarcoma cells were more resistant to these compounds. Notably, knockout cells of P-glycoprotein, EGFR, and TP53 showed reduced or no resistance to lupeol and quercetin compared to conventional cancer drugs. This finding substantiated our bioinformatic analyses, suggesting that neither compound is associated with cross-resistance mechanisms. An apoptosis assay on CCRF-CEM and U2OS cells reaffirmed that lupeol and quercetin induced apoptosis in hematopoietic cells but had no effect on osteosarcoma cells.

Lastly, RT-PCR analysis showed that β-amyrin, quercetin, and lupeol significantly

725 downregulated the expression of inflammatory genes. While western blot analysis revealed that
726 only β-amyrin and quercetin inhibited NF-κB activity.
727 In light of these findings, Kaplan-Meier analysis emphasized the correlation between NF-κB
728 overexpression and the short survival time of patients with renal clear cell carcinoma,
729 highlighting the importance of discovering novel NF-κB inhibitors.

730

Further reading: Appendix II

Anti-Inflammatory and Cancer-Preventive Potential of Chamomile (Matricaria chamomilla L.): A Comprehensive in Silico and In Vitro Study

Assia I. Drif, Rümeysa Yücer, Roxana Damiescu, Nadeen T. Ali 1, Tobias H. Abu Hagar, Bharati Avula, Ikhlas A. Khan 2 and Thomas Efferth

3.3 Side project:

In Silico and In Vitro Screening of 50 Curcumin Compounds as EGFR and NF-κB Inhibitors

The 50 curcumin analogues were screened in silico to calculate their binding affinity with NF-κB and EGFR using molecular docking. The binding affinities of the ligands to EGFR and NF-κB proteins were found to be similar. For EGFR, the binding energy values ranged from −12.12 (±0.21) to −7.34 (±0.07) kcal/mol, with pKi values between 0.00013 (±0.00006) and 3.45 (±0.10) µM. For NF-κB, the binding energies ranged from −12.97 (±0.47) to −6.24 (±0.06) kcal/mol, with pKi values from 0.0004 (±0.0003) to 10.05 (±4.03) µM. Interestingly, 20 of these compounds showed better affinity for both targets than curcumin, indicating that these derivatives may be better candidates than curcumin as anticancer drug agents. These results were further validated using microscale thermophoresis. The bioactivity of curcumin, N-(3-nitrophenyl pyrazole), and 1A9 was then explored, revealing that the cytotoxicity of the two analogue candidates was higher than that of curcumin. Notably, the N-(3-nitrophenylpyrazole) derivative induced higher ROS generation but did not activate apoptosis, unlike curcumin and 1A9. This suggests that N-(3-nitrophenylpyrazole) and other curcumin derivatives may provoke cell death through different downstream and ROS-dependent mechanisms. Insightfully, compounds such as N-(3-nitrophenylpyrazole) could be promising cancer treatments due to their ability to bypass apoptosis and target apoptosis-resistant tumors.

Overall, this study presents an optimistic outlook for curcumin derivatives in cancer therapy.

Further reading: Appendix III
In Silico and In Vitro Screening of 50 Curcumin Compounds as EGFR and NF-κB Inhibitors

Mohamed E. M. Saeed, Rümeysa Yücer, Mona Dawood, Mohamed-Elamir F. Hegazy, Assia Drif, Edna Ooko, Onat Kadioglu, Ean-Jeong Seo, Fadhil S. Kamounah, Salam J. Titinchi, Beatrice Bachmeier and Thomas Efferth

4. Conclusion

The need to discover novel therapeutic drugs to treat inflammation and cancer has become more urgent than ever. The natural products play a crucial role in the treatment and prevention of these conditions due to their bioactive compounds. Importantly, they are known to exhibit lower cytotoxicity and fewer side effects than the conventional synthetic drugs. In this research, we demonstrated the ability of chamomile compounds and curcumin analogues to act through multiple mechanisms, such as inducing apoptosis, reducing oxidative stress, regulating mitochondrial membrane potential, modulating immune responses, and even overcoming multidrug resistance. This highlights their versatility and their potential as anti-inflammatory and cancer preventive agents.

Continued research into these compounds may lead to novel, effective treatments, offering hope as alternatives to conventional therapies.

5. References

1. Institute for Molecular Bioscience. The University of Queensland. [cited 2024 Jul 11]. Timeline of inflammation. Available from: https://stories.uq.edu.au/imb/the-edge/inflammation/timeline-of-inflammation/index.html
2. Hosseinzadeh H, Nassiri-Asl M. Avicenna's (Ibn Sina) the canon of medicine and saffron (Crocus sativus): a review. Phytotherapy Research. 2013;27(4):475-83.
3. Turk JL. Inflammation: John Hunter's" A treatise on the blood, inflammation and gun-shot wounds". International journal of experimental pathology. 1994;75(6):385.
4. Antonelli M, Kushner I. It's time to redefine inflammation. FASEB Journal. 2017;31(5):1787–91.
5. Mahdizadeh S, Ghadiri MK, Gorji A. Avicenna's Canon of Medicine: a review of analgesics and anti-inflammatory substances. Avicenna journal of phytomedicine. 2015;5(3):182.
6. Punchard NA, Whelan CJ, Adcock I. The journal of inflammation. Journal of inflammation. 2004;1:1-4.
7. Roe K. An inflammation classification system using cytokine parameters. Scandinavian journal of immunology. 2021;93(2):e12970.
8. Tang D, Kang R, Coyne CB, Zeh HJ, Lotze MT. PAMP s and DAMP s: Signal 0s that spur autophagy and immunity. Immunological reviews. 2012;249(1):158-75.
9. Chen L, Deng H, Cui H, Fang J, Zuo Z, Deng J, Li Y, Wang X, Zhao L. Inflammatory responses and inflammation-associated diseases in organs. Oncotarget. 2018 Jan 1;9(6):7204.
10. Dempsey PW, Vaidya SA, Cheng G. The art of war: Innate and adaptive immune responses. Cellular and Molecular Life Sciences CMLS. 2003;60:2604-21.
11. Medzhitov R. Recognition of microorganisms and activation of the immune response. Nature. 2007;449(7164):819-26.
12. Tigner A, Ibrahim SA, Murray I V. Histology, White Blood Cell. StatPearls [Internet]. 2022 Nov 14 [cited 2024 Jul 29]; Available from: https://www.ncbi.nlm.nih.gov/books/NBK563148/
13. Granulocyte: MedlinePlus Medical Encyclopedia [Internet]. [cited 2024 Jul 29]. Available from: https://medlineplus.gov/ency/article/003440.htm
14. Di Benedetto P, Ruscitti P, Vadasz Z, Toubi E, Giacomelli R. Macrophages with regulatory functions, a possible new therapeutic perspective in autoimmune diseases. Autoimmun Rev. 2019;18(10).
15. Mank V, Azhar W, Brown K. Leukocytosis. StatPearls [Internet]. 2024 Apr 21 [cited 2024 Jul 30]; Available from: https://www.ncbi.nlm.nih.gov/books/NBK560882/
16. Janeway Jr CA, Travers P, Walport M, Shlomchik MJ. The components of the immune system. InImmunobiology: The Immune System in Health and Disease. 5th edition 2001. Garland Science.

17. Siemińska I, Poljańska E, Baran J. Granulocytes and cells of granulocyte origin—the relevant players in colorectal cancer. International Journal of Molecular Sciences. 2021;22(7):3801.

18. Krystel-Whittemore M, Dileepan KN, Wood JG. Mast cell: a multi-functional master cell. Frontiers in immunology. 2016;6:620.

19. DD M. Mast cells. Physiol Rev. 1997;77:1033-79.

20. Yong LCJ. The mast cell: origin, morphology, distribution, and function. Experimental and Toxicologic Pathology. 1997;49(6):409–24.

21. Grabauskas G, Wu X, Gao J, Li JY, Turgeon DK, Owyang C. Prostaglandin E2, produced by mast cells in colon tissues from patients with irritable bowel syndrome, contributes to visceral hypersensitivity in mice. Gastroenterology. 2020;158(8):2195-207.

22. Greenhough A, Smartt HJ, Moore AE, Roberts HR, Williams AC, Paraskeva C, Kaidi A. The COX-2/PGE 2 pathway: key roles in the hallmarks of cancer and adaptation to the tumour microenvironment. Carcinogenesis. 2009;30(3):377-86.

23. Hidalgo-Estévez AM, Stamatakis K, Jiménez-Martínez M, López-Pérez R, Fresno M. Cyclooxygenase 2-regulated genes an alternative avenue to the development of new therapeutic drugs for colorectal cancer. Frontiers in Pharmacology. 2020;11:533.

24. Kuete V, Efferth T. Biodiversity, natural products and cancer treatment. Biodiversity, Natural Products and Cancer Treatment. World Scientific Publishing Co.; 2014;1–412.

25. Rizzo MT. Cyclooxygenase-2 in oncogenesis. Clinica Chimica Acta. 2011;412:671–87.

26. Zarghi A, Arfaei S. Selective COX-2 inhibitors: a review of their structure-activity relationships. Iranian journal of pharmaceutical research: IJPR. 2011;10(4):655.

27. Rouzer CA, Marnett LJ. Cyclooxygenases: structural and functional insights. Journal of lipid research. 2009;50:S29-34.

28. Lucido MJ, Orlando BJ, Vecchio AJ, Malkowski MG. Crystal Structure of Aspirin-Acetylated Human Cyclooxygenase-2: Insight into the Formation of Products with Reversed Stereochemistry. Biochemistry. 2016;55(8):1226–38.

29. Jain P, Satija J, Sudandiradoss C. Discovery of andrographolide hit analog as a potent cyclooxygenase-2 inhibitor through consensus MD-simulation, electrostatic potential energy simulation and ligand efficiency metrics. Scientific Reports. 2023;13(1):8147.

30. Rizzo MT. Cyclooxygenase-2 in oncogenesis. Clinica Chimica Acta. 2011;412(9–10):671–87.

31. Simon LS. Role and regulation of cyclooxygenase-2 during inflammation. The American journal of medicine. 1999;106(5):37S-42S.

32. Rouzer CA, Marnett LJ. Structural and chemical biology of the interaction of cyclooxygenase with substrates and non-steroidal anti-inflammatory drugs. Chemical Reviews. 2020;120(15):7592-641.

33. Rouzer CA, Marnett LJ. Non-redundant functions of cyclooxygenases: oxygenation of endocannabinoids. Journal of Biological Chemistry. 2008;283(13):8065-9.

34. Rouzer CA, Marnett LJ. Endocannabinoid oxygenation by cyclooxygenases, lipoxygenases, and cytochromes P450: cross-talk between the eicosanoid and endocannabinoid signaling pathways. Chemical reviews. 2011;111(10):5899-921.

35. Kraemer SA, Arthur KA, Denison MS, Smith WL, DeWitt DL. Regulation of prostaglandin endoperoxide H synthase-2 expression by 2, 3, 7, 8-tetrachlorodibenzo-p-dioxin. Archives of biochemistry and biophysics. 1996;330(2):319-28.

36. Alhouayek M, Muccioli GG. COX-2-derived endocannabinoid metabolites as novel inflammatory mediators. Trends in pharmacological sciences. 2014;35(6):284-92.

37. Ricciotti E, FitzGerald GA. Prostaglandins and inflammation. Arteriosclerosis, thrombosis, and vascular biology. 2011;31(5):986-1000.

38. Aoki T, Narumiya S. Prostaglandins and chronic inflammation. Trends Pharmacol Sci. 2012;33(6):304–11.

39. Ghosh G, Wang VYF, Huang D Bin, Fusco A. NF-κB regulation: Lessons from structures. Immunol Rev. 2012;246(1):36–58.

40. Singh H, Sen R, Baltimore D, Sharp PA. A nuclear factor that binds to a conserved sequence motif in transcriptional control elements of immunoglobulin genes. Nature. 1986;319(6049):154-8.

41. Baltimore D. Discovering NF-κB. Cold Spring Harbor perspectives in biology. 2009;1(1):a000026.

42. Celebrating 25 years of NF-κB. Nat Immunol. 2011;12(8):681.

43. Lawrence T. The nuclear factor NF-κB pathway in inflammation. Cold Spring Harbor perspectives in biology. 2009;1(6):a001651.

44. Cile Hellin AC, Calmant P, Gielen J, Bours V, Merville MP. Nuclear factor ± kB-dependent regulation of p53 gene expression induced by daunomycin genotoxic drug. Oncogene. 1998;16(9):1187–95.

45. Shrum CK, Defrancisco D, Meffert MK. Stimulated nuclear translocation of NF-κB and shuttling differentially depend on dynein and the dynactin complex. Proceedings of the National Academy of Sciences. 2009;106(8):2647-52.

46. Dong QM, Ling C, Chen X, Zhao LI. Inhibition of tumor necrosis factor-α enhances apoptosis induced by nuclear factor-κB inhibition in leukemia cells. Oncology letters. 2015;10(6):3793-8.

47. Magnani M, Crinelli R, Bianchi M, Antonelli A. The ubiquitin-dependent proteolytic system and other potential targets for the modulation of nuclear factor-kB (NF-kB). Current drug targets. 2000;1(4):387-99.

48. Jacobs MD, Harrison SC. Structure of an IκBα/NF-κB complex. Cell. 1998;95(6):749-58.

902 49. Chen FE, Ghosh G. Regulation of DNA binding by Rel/NF-κB transcription factors:
903 structural views. Oncogene. 1999;18(49):6845-52.

904 50. Hayden MS, Ghosh S. NF-κB in immunobiology. Cell Res. 2011;21(2):223–44.

905 51. Wen Y, Zhu Y, Zhang C, Yang X, Gao Y, Li M, et al. Chronic inflammation, cancer
906 development and immunotherapy. Front Pharmacol. 2022;13:1040163.

907 52. David H. Rudolf Virchow and Modern Aspects of Tumor Pathology. Pathol Res Pract.
908 1988;183(3):356–64.

909 53. Chen FE, Ghosh G. Regulation of DNA binding by Rel/NF-κB transcription factors:
910 structural views. Oncogene. 1999;18(49):6845-52.

911 54. Omiyale O, Awolade R, Oyetade O, Onuh K, Chiemela D, Odunlade G, Shodipe O,
912 Demola M, Agbanobi M, Edema A, Ayeni O. Inflammation and Cancer: The Most
913 Recent Findings. Journal of Health Science and Medical Research. 2024;3:20241082.

914 55. Grivennikov SI, Greten FR, Karin M. Immunity, inflammation, and cancer. Cell.
915 2010;140(6):883-99.

916 56. Nowacki MP, Janik P, Nowacki PM. Inflammation and metastases. Med Hypotheses.
917 1996;47(3):193–6.

918 57. B. Vendramini-Costa D, E. Carvalho J. Molecular Link Mechanisms between
919 Inflammation and Cancer. Curr Pharm Des. 2012;18(26):3831–52.

920 58. Coussens LM, Werb Z. Inflammation and cancer. Nature. 2002;420(6917):860-7.

921 59. Zhao H, Wu L, Yan G, Chen Y, Zhou M, Wu Y, Li Y. Inflammation and tumor progression:
922 signaling pathways and targeted intervention. Signal transduction and targeted
923 therapy. 2021;6(1):263.

924 60. Karin M. Nuclear factor-κB in cancer development and progression. Nature.
925 2006;441(7092):431-6.

926 61. Yu H, Lin L, Zhang Z, Zhang H, Hu H. Targeting NF-κB pathway for the therapy of
927 diseases: mechanism and clinical study. Signal transduction and targeted therapy.
928 2020;5(1):209.

929 62. Serasanambati M, Chilakapati SR. Function of nuclear factor kappa B (NF-kB) in
930 human diseases-a review. South Indian Journal of Biological Sciences. 2016;2(4):368-
931 87.

932 63. Ben-Neriah Y, Karin M. Inflammation meets cancer, with NF-κB as the matchmaker.
933 Nature immunology. 2011;12(8):715-23.

934 64. Li S, Jiang M, Wang L, Yu S. Combined chemotherapy with cyclooxygenase-2 (COX-2)
935 inhibitors in treating human cancers: Recent advancement. Biomedicine C
936 Pharmacotherapy. 2020;129:110389.

937 65. Hida T, Yatabe Y, Achiwa H, Muramatsu H, Kozaki KI, Nakamura S, Ogawa M,
938 Mitsudomi T, Sugiura T, Takahashi T. Increased expression of cyclooxygenase 2 occurs
939 frequently in human lung cancers, specifically in adenocarcinomas. Cancer research.
940 1998;58(17):3761-4.

66. Hashemi Goradel N, Najafi M, Salehi E, Farhood B, Mortezaee K. Cyclooxygenase-2 in cancer: a review. Journal of cellular physiology. 2019;234(5):5683-99.

67. Castelao JE, Bart RD, DiPerna CA, Sievers EM, Bremner RM. Lung cancer and cyclooxygenase-2. Annals of Thoracic Surgery. 2003;76(4):1327–35.

68. Chadwick Derek, Goode Jamie, Novartis Foundation. Cancer and inflammation. John Wiley C Sons; 2004;280.

69. Williams CS, Mann M, DuBois RN. The role of cyclooxygenases in inflammation, cancer, and development. Oncogene. 1999;18(55):7908-16.

70. Taniguchi K, Karin M. NF-κB, inflammation, immunity and cancer: coming of age. Nature Reviews Immunology. 2018;18(5):309-24.

71. Luduena RF, Shooter EM, Wilson L. Structure of the tubulin dimer. Journal of Biological Chemistry. 1977;252(20):7006–14.

72. Erickson HP, Stoffler D. Protofilaments and rings, two conformations of the tubulin family conserved from bacterial FtsZ to alpha/beta and gamma tubulin. The Journal of cell biology. 1996;135(1):5-8.

73. Binarová P, Tuszynski J. Tubulin: structure, functions and roles in disease. Cells. 2019;8(10):1294.

74. Adrian M, Weber M, Tsai MC, Glock C, Kahn OI, Phu L, Cheung TK, Meilandt WJ, Rose CM, Hoogenraad CC. Polarized microtubule remodeling transforms the morphology of reactive microglia and drives cytokine release. Nature communications. 2023;14(1):6322.

75. Wu J, Akhmanova A. Microtubule-organizing centers. Annual review of cell and developmental biology. 2017;33(1):51-75.

76. Tucker JB. Spatial organization of microtubule-organizing centers and microtubules. The Journal of cell biology. 1984;99(1 Pt 2):55s.

77. Hall A. The cytoskeleton and cancer. Cancer and Metastasis Reviews. 2009;28:5-14.

78. Honore S, Pasquier E, Braguer D. Understanding microtubule dynamics for improved cancer therapy. Cellular and Molecular Life Sciences CMLS. 2005;62:3039-56.

79. Endres T, Duesler L, Corey DA, Kelley TJ. In vivo impact of tubulin polymerization promoting protein (Tppp) knockout to the airway inflammatory response. Scientific Reports. 2023;13(1):12272.

80. Karki P, Birukova AA. Microtubules as major regulators of endothelial function: implication for lung injury. Frontiers in Physiology. 2021;12:758313.

81. Herreros L, Rodrıguez-Fernández JL, Brown MC, Alonso-Lebrero JL, Cabanas C, Sánchez-Madrid F, Longo N, Turner CE, Sánchez-Mateos P. Paxillin localizes to the lymphocyte microtubule organizing center and associates with the microtubule cytoskeleton. Journal of Biological Chemistry. 2000;275(34):26436-40.

82. Maliekal TT, Dharmapal D, Sengupta S. Tubulin isotypes: emerging roles in defining cancer stem cell niche. Frontiers in Immunology. 2022;13:876278.

83. Ritter A, Kreis NN. Microtubule Dynamics and Cancer. Cancers. 2022;14(18):4368.

84. Decout A, Katz JD, Venkatraman S, Ablasser A. The cGAS–STING pathway as a therapeutic target in inflammatory diseases. Nature Reviews Immunology. 2021;21(9):548-69.

85. Chen Q, Sun L, Chen ZJ. Regulation and function of the cGAS–STING pathway of cytosolic DNA sensing. Nature immunology. 2016;17(10):1142-9.

86. Pan J, Fei CJ, Hu Y, Wu XY, Nie L, Chen J. Current understanding of the cGAS-STING signaling pathway: Structure, regulatory mechanisms, and related diseases. Zoological Research. 2023;44(1):183.

87. Han J, Wang Z, Han F, Peng B, Du J, Zhang C. Microtubule disruption synergizes with STING signaling to show potent and broad-spectrum antiviral activity. Plos Pathogens. 2024;20(2):e1012048.

88. Zhang L, Wei X, Wang Z, Liu P, Hou Y, Xu Y, Su H, Koci MD, Yin H, Zhang C. NF-κB activation enhances STING signaling by altering microtubule-mediated STING trafficking. Cell Reports. 2023;42(3).

89. Rosette C, Karin M. Cytoskeletal control of gene expression: depolymerization of microtubules activates NF-kappa B. Journal of Cell Biology. 1995;128(6):1111–9.

90. Kuchitsu Y, Mukai K, Uematsu R, Takaada Y, Shinojima A, Shindo R, Shoji T, Hamano S, Ogawa E, Sato R, Miyake K. STING signalling is terminated through ESCRT-dependent microautophagy of vesicles originating from recycling endosomes. Nature Cell Biology. 2023;25(3):453-66.

91. Tyagi A, Kamal MA, Poddar NK. Integrated pathways of COX-2 and mTOR: roles in cell sensing and Alzheimer's disease. Frontiers in Neuroscience. 2020;14:693.

92. Eligini S, Songia P, Cavalca V, Crisci M, Tremoli E, Colli S. Cytoskeletal architecture regulates cyclooxygenase-2 in human endothelial cells: Autocrine modulation by prostacyclin. Journal of Cellular Physiology. 2012;227(12):3847-56.

93. Eligini S, Cavalca V, Songia P, Crisci M, Tremoli E, Colli S. Cytoskeletal architecture regulates cyclooxygenase-2 in human endothelial cells. BLOOD TRANSFUSION. 2010;8(suppl. 4):s55-.

94. Venza I, Giordano L, Piraino G, Medici N, Ceci G, Teti D. Prostaglandin E2 signalling pathway in human T lymphocytes from healthy and conjunctiva basal cell carcinoma-bearing subjects. Immunol Cell Biol. 2001;79(5):482–9.

95. Shehzad A, Lee J, Lee YS. Autocrine prostaglandin E2 signaling promotes promonocytic leukemia cell survival via COX-2 expression and MAPK pathway. BMB reports. 2015;48(2):109.

96. Santiso A, Heinemann A, Kargl J. Prostaglandin E2 in the tumor microenvironment, a convoluted affair mediated by EP receptors 2 and 4. Pharmacological Reviews. 2024;76(3):388-413.

97. Milne SA, Perchick GB, Boddy SC, Jabbour HN. Expression, localization, and signaling of PGE2 and EP2/EP4 receptors in human nonpregnant endometrium across the menstrual cycle. The Journal of Clinical Endocrinology C Metabolism. 2001;86(9):4453-9.

98. Vleeshouwers W, Van den Dries K, De Keijzer S, Joosten B, Lidke DS, Cambi A. Characterization of the signaling modalities of prostaglandin E2 receptors EP2 and EP4 reveals crosstalk and a role for microtubules. Frontiers in Immunology. 2021;11:613286.

99. Vidensky S, Zhang Y, Hand T, Goellner J, Shaffer A, Isakson P, Andreasson K. Neuronal overexpression of COX-2 results in dominant production of PGE 2 and altered fever response. Neuromolecular medicine. 2003;3:15-27.

100. Diaz-Munoz MD, Osma-Garcia IC, Fresno M, Iniguez MA. Involvement of PGE2 and the cAMP signalling pathway in the up-regulation of COX-2 and mPGES-1 expression in LPS-activated macrophages. Biochemical Journal. 2012;443(2):451-61.

101. Punganuru SR, Madala HR, Mikelis C, Srivenugopal KS. Design of a Rofecoxib-Combretastatin hybrid drug that exerts highly potent antimicrotubule, anti-angiogenesis properties and Cox-2 inhibition both in cell culture and xenograft models. Cancer Research. 2016;76(14_Supplement):4839-.

102. Punganuru SR, Madala HR, Mikelis CM, Dixit A, Arutla V, Srivenugopal KS. Conception, synthesis, and characterization of a rofecoxib-combretastatin hybrid drug with potent cyclooxygenase-2 (COX-2) inhibiting and microtubule disrupting activities in colon cancer cell culture and xenograft models. Oncotarget. 2018;9(40):26109.

103. Weber GF. Drugs that Suppress Proliferation. Molecular Therapies of Cancer. 2015:113–62.

104. Chinnery PF, Schon EA. Mitochondria. Journal of Neurology, Neurosurgery C Psychiatry. 2003;74(9):1188-99.

105. McBride HM, Neuspiel M, Wasiak S. Mitochondria: more than just a powerhouse. Current biology. 2006;16(14):R551-60.

106. Li R, Jia Z, Trush MA. Defining ROS in biology and medicine. Reactive oxygen species (Apex, NC). 2016;1(1):9.

107. Martín Giménez VM, de Las Heras N, Ferder L, Lahera V, Reiter RJ, Manucha W. Potential effects of melatonin and micronutrients on mitochondrial dysfunction during a cytokine storm typical of oxidative/inflammatory diseases. Diseases. 2021;9(2):30.

108. Mitochondrial dysfunction and Inflammatory Responses | Encyclopedia MDPI [Internet]. [cited 2023 Oct 13]. Available from: https://encyclopedia.pub/entry/8923

109. O'Malley J, Kumar R, Inigo J, Yadava N, Chandra D. Mitochondrial stress response and cancer. Trends in cancer. 2020;6(8):688-701.

110. Ko EY, Cho SH, Kwon SH, Eom CY, Jeong MS, Lee W, Kim SY, Heo SJ, Ahn G, Lee KP, Jeon YJ. The roles of NF-κB and ROS in regulation of pro-inflammatory mediators of

inflammation induction in LPS-stimulated zebrafish embryos. Fish C shellfish immunology. 2017;68:525-9.

111. Wallace DC. Mitochondria and cancer. Nature Reviews Cancer. 2012;12(10):685-98.

112. Huang Z, Chen Y, Zhang Y. Mitochondrial reactive oxygen species cause major oxidative mitochondrial DNA damages and repair pathways. Journal of biosciences. 2020;45(1):84.

113. Murphy MP. Understanding and preventing mitochondrial oxidative damage. Biochemical Society Transactions. 2016;44(5):1219-26.

114. Denisenko TV, Gorbunova AS, Zhivotovsky B. Mitochondrial involvement in migration, invasion and metastasis. Frontiers in cell and developmental biology. 2019;7:355.

115. Jin P, Jiang J, Zhou L, Huang Z, Nice EC, Huang C, Fu L. Mitochondrial adaptation in cancer drug resistance: prevalence, mechanisms, and management. Journal of Hematology C Oncology. 2022;15(1):97.

116. Bodaar K, Yamagata N, Barthe A, Landrigan J, Chonghaile TN, Burns M, Stevenson KE, Devidas M, Loh ML, Hunger SP, Wood B. JAK3 mutations and mitochondrial apoptosis resistance in T-cell acute lymphoblastic leukemia. Leukemia. 2022;36(6):1499-507.

117. Ngoi NY, Choong C, Lee J, Bellot G, Wong AL, Goh BC, Pervaiz S. Targeting mitochondrial apoptosis to overcome treatment resistance in cancer. Cancers. 2020;12(3):574.

118. Sessions DT, Kashatus DF. Mitochondrial dynamics in cancer stem cells. Cellular and Molecular Life Sciences. 2021;78:3803-16.

119. Karbowski M. Mitochondria on guard: role of mitochondrial fusion and fission in the regulation of apoptosis. BCL-2 Protein Family: Essential Regulators of Cell Death. 2010:131-42.

120. Perfettini JL, Roumier T, Kroemer G. Mitochondrial fusion and fission in the control of apoptosis. Trends in cell biology. 2005;15(4):179-83.

121. Dai H, Meng W, Kaufmann S. BCL2 Family, Mitochondrial Apoptosis, and Beyond. Cancer Transl Med. 2016;2(1):7.

122. Czabotar PE, Garcia-Saez AJ. Mechanisms of BCL-2 family proteins in mitochondrial apoptosis. Nature reviews Molecular cell biology. 2023;24(10):732-48.

123. Autret A, Martin SJ. Bcl-2 family proteins and mitochondrial fission/fusion dynamics. Cellular and molecular life sciences. 2010;67:1599-606.

124. Zhong Z, Umemura A, Sanchez-Lopez E, Liang S, Shalapour S, Wong J, He F, Boassa D, Perkins G, Ali SR, McGeough MD. NF-κB restricts inflammasome activation via elimination of damaged mitochondria. Cell. 2016;164(5):896-910.

125. Albensi BC. What is nuclear factor kappa B (NF-κB) doing in and to the mitochondrion?. Frontiers in cell and developmental biology. 2019;7:154.

126. Lin F, Luo J, Gao W, Wu J, Shao Z, Wang Z, Meng J, Ou Z, Yang G. COX-2 promotes breast cancer cell radioresistance via p38/MAPK-mediated cellular anti-apoptosis and invasiveness. Tumor Biology. 2013;34:2817-26.

127. Liu B, Qu L, Yan S. Cyclooxygenase-2 promotes tumor growth and suppresses tumor immunity. Cancer cell international. 2015;15:1-6.

128. Singh B, Berry JA, Shoher A, Lucci A. COX-2 induces IL-11 production in human breast cancer cells. Journal of Surgical Research. 2006;131(2):267–75.

129. Ivanova D, Zhelev Z, Aoki I, Bakalova R, Higashi T. Overproduction of reactive oxygen species-obligatory or not for induction of apoptosis by anticancer drugs. Chinese Journal of Cancer Research. 2016;28(4):383.

130. Singh R, Manna PP. Reactive oxygen species in cancer progression and its role in therapeutics. Exploration of Medicine. 2022;3(1):43-57.

131. Liou JY, Aleksic N, Chen SF, Han TJ, Shyue SK, Wu KK. Mitochondrial localization of cyclooxygenase-2 and calcium-independent phospholipase A2 in human cancer cells: Implication in apoptosis resistance. Exp Cell Res. 2005;306(1):75–84.

132. Frączek N, Bronisz I, Pietryka M, Kępińska D, Strzała P, Mielnicka K, Korga A, Dudka J. An outline of main factors of drug resistance influencing cancer therapy. Journal of Chemotherapy. 2016;28(6):457-64.

133. Baguley BC. Multiple drug resistance mechanisms in cancer. Molecular biotechnology. 2010;46:308-16.

134. Gillet JP, Gottesman MM. Mechanisms of multidrug resistance in cancer. Multi-drug resistance in cancer. 2010:47-76.

135. Goebel J, Chmielewski J, Hrycyna CA. The roles of the human ATP-binding cassette transporters P-glycoprotein and ABCG2 in multidrug resistance in cancer and at endogenous sites: Future opportunities for structure-based drug design of inhibitors. Cancer Drug Resistance. 2021;4(4):784.

136. Khan SU, Fatima K, Aisha S, Malik F. Unveiling the mechanisms and challenges of cancer drug resistance. Cell Communication and Signaling. 2024;22(1):109.

137. Goebel J, Chmielewski J, Hrycyna CA. The roles of the human ATP-binding cassette transporters P-glycoprotein and ABCG2 in multidrug resistance in cancer and at endogenous sites: Future opportunities for structure-based drug design of inhibitors. Cancer Drug Resistance. 2021;4(4):784.

138. Emran TB, Shahriar A, Mahmud AR, Rahman T, Abir MH, Siddiquee MF, Ahmed H, Rahman N, Nainu F, Wahyudin E, Mitra S. Multidrug resistance in cancer: understanding molecular mechanisms, immunoprevention and therapeutic approaches. Frontiers in Oncology. 2022;12:891652.

139. Wang H, Guo M, Wei H, Chen Y. Targeting p53 pathways: mechanisms, structures, and advances in therapy. Signal transduction and targeted therapy. 2023;8(1):92.

140. Kadkol HA, Jain VI, Patil AB. Multi drug resistance in cancer therapy-an overview. J. Crit. Rev. 2019;6(6):1-6.

141. Pritchard JR, Lee MJ, Peyton SR. Materials-driven approaches to understand extrinsic drug resistance in cancer. Soft matter. 2022;18(18):3465-72.

142. Vaidya FU, Sufiyan Chhipa A, Mishra V, Gupta VK, Rawat SG, Kumar A, Pathak C. Molecular and cellular paradigms of multidrug resistance in cancer. Cancer reports. 2022;5(12):e1291.

143. Labbozzetta M, Notarbartolo M, Poma P. Can NF-κB be considered a valid drug target in neoplastic diseases? Our point of view. International journal of molecular sciences. 2020;21(9):3070.

144. Hoesel B, Schmid JA. The complexity of NF-κB signaling in inflammation and cancer. Molecular cancer. 2013;12:1-5.

145. Bell CR, Pelly VS, Moeini A, Chiang SC, Flanagan E, Bromley CP, Clark C, Earnshaw CH, Koufaki MA, Bonavita E, Zelenay S. Chemotherapy-induced COX-2 upregulation by cancer cells defines their inflammatory properties and limits the efficacy of chemoimmunotherapy combinations. Nature communications. 2022;13(1):2063.

146. Bell CR, Zelenay S. COX-2 upregulation by tumour cells post-chemotherapy fuels the immune evasive dark side of cancer inflammation. Cell Stress. 2022;6(9):76.

147. Sailo BL, Chauhan S, Hegde M, Girisa S, Alqahtani MS, Abbas M, Goel A, Sethi G, Kunnumakkara AB. Therapeutic potential of tocotrienols as chemosensitizers in cancer therapy. Phytother Res. 2024 Feb 14.

148. Pharmaceuticals | Special Issue: Chemosensitizers for Cancer Chemotherapy [Internet]. [cited 2024 Sep 15]. Available from: https://www.mdpi.com/journal/pharmaceuticals/special_issues/cancer_chemotherapy

149. Roy NK, Tewari D, Esposito MT. Editorial: Chemosensitizing effect of natural products against cancers: Applications in enhancing chemotherapy and immunotherapy. Front Pharmacol. 2022;13:988226.

150. Cornelison R, Llaneza DC, Landen CN. Emerging therapeutics to overcome chemoresistance in epithelial ovarian cancer: a mini-review. International journal of molecular sciences. 2017;18(10):2171.

151. Srivastava JK, Shankar E, Gupta S. Chamomile: A herbal medicine of the past with a bright future. Molecular medicine reports. 2010;3(6):895-901.

152. Dai YL, Li Y, Wang Q, Niu FJ, Li KW, Wang YY, Wang J, Zhou CZ, Gao LN. Chamomile: a review of its traditional uses, chemical constituents, pharmacological activities and quality control studies. Molecules. 2022;28(1):133.

153. Al-Dabbagh B, Elhaty IA, Elhaw M, Murali C, Al Mansoori A, Awad B, et al. Antioxidant and anticancer activities of chamomile (Matricaria recutita L.). BMC Res Notes. 2019;12(1).

154. Hassan D. Amerolative influence of chamomile (Matricaria recutita L.) on synthetic food additive induced probable toxicity in male albino rats. Journal of Food and Dairy Sciences. 2021;12(7):161-70.

155. CFR - Code of Federal Regulations Title 21 [Internet]. [cited 2024 Sep 17]. Available from: https://www.accessdata.fda.gov/scripts/cdrh/cfdocs/cfcfr/CFRSearch.cfm?fr=182.10

156. Belsito DV, Klaassen CD, Liebler DC, Hill RA. Safety assessment of Chamomilla Recutita-derived ingredients as used in cosmetics. Proceedings of the 2013 Cosmetic Ingredient Review Expert Panel. 2013 Aug 16. Available from: https://www.cir-safety.org/sites/default/files/chamom032016tent.pdf

157. Pirouzpanah S, Mahboob S, Sanayei M, Hajaliloo M, Safaeiyan A. The effect of chamomile tea consumption on inflammation among rheumatoid arthritis patients: randomized clinical trial. Progress in Nutrition. 2017;19(1-S):27-33.

158. Sándor Z, Mottaghipisheh J, Veres K, Hohmann J, Bencsik T, Horváth A, Kelemen D, Papp R, Barthó L, Csupor D. Evidence supports tradition: The in vitro effects of roman chamomile on smooth muscles. Frontiers in Pharmacology. 2018;9:323.

159. Ghamchini VM, Salami M, Mohammadi GR, Moradi Z, Kavosi A, Movahedi A, et al. The Effect of Chamomile Tea on Anxiety and Depression in Cancer Patients Treated with Chemotherapy. Journal of Young Pharmacists. 2019;11(3):309–12.

160. Chang SM, Chen CH. Effects of an intervention with drinking chamomile tea on sleep quality and depression in sleep disturbed postnatal women: A randomized controlled trial. J Adv Nurs. 2016;72(2):306–15.

161. Khan N, Kalam MA, Alam MT, Haq SA, Showket W, Dar ZA, Rafiq N, Mushtaq W, Rafeeqi TA, Dar MY, Akbar S. Drug Standardization through Pharmacognostic Approaches and estimation of anticancer potential of chamomile (Matricaria chamomilla L.) using Prostate-cancer cell lines: an in-vitro study. Journal of Cancer. 2023;14(3):490.

162. Zadam MH, Ahmida M, Djaber N, Ounacer LS, Sekiou O, Taibi F, Bencheikh R, Chouala K, Boudjema K, Tichati L, Zaafour M. In-vivo anti-inflammatory effects of Roman Chamomile (Chamaemelum nobile) aqueous extracts collected from the National Park of El-Kala (North-East, Algeria). Cellular and Molecular Biology. 2023;69(9):245-54.

163. Thalluri G, Srinu P. Role of chamomile in cancer treat-ment. J Pathol Clin Med Res. 2018;1(001).

164. Elhadad MA, El-Negoumy E, Taalab MR, Ibrahim RS, Elsaka RO. The effect of topical chamomile in the prevention of chemotherapy-induced oral mucositis: A randomized clinical trial. Oral Diseases. 2022;28(1):164-72.

165. Maleki M, Mardani A, Manoochehri M, Ashghali Farahani M, Vaismoradi M, Glarcher M. Effect of chamomile on the complications of cancer: a systematic review. Integrative Cancer Therapies. 2023;22:15347354231164600.

166. Salehi B, Jornet PL, López EP, Calina D, Sharifi-Rad M, Ramírez-Alarcón K, Forman K, Fernández M, Martorell M, Setzer WN, Martins N. Plant-derived bioactives in oral mucosal lesions: a key emphasis to curcumin, lycopene, chamomile, aloe vera, green tea and coffee properties. Biomolecules. 2019;9(3):106.

167. Vissiennon C, Hammoud D, Rodewald S, Fester K, Goos KH, Nieber K, Arnhold J. Chamomile flower, myrrh, and coffee charcoal, components of a traditional herbal medicinal product, diminish proinflammatory activation in human macrophages. Planta medica. 2017;83(10):846-54.

168. Srivastava JK, Gupta S. Antiproliferative and apoptotic effects of chamomile extract in various human cancer cells. Journal of agricultural and food chemistry. 2007;55(23):9470-8.

169. Srivastava JK, Gupta S. Extraction, characterization, stability and biological activity of flavonoids isolated from chamomile flowers. Molecular and cellular pharmacology. 2009;1(3):138.

170. Nováková L, Vildová A, Mateus JP, Gonalves T, Solich P. Development and application of UHPLC-MS/MS method for the determination of phenolic compounds in Chamomile flowers and Chamomile tea extracts. Talanta. 2010;82(4):1271–80.

171. Shukla S, Shankar E, Fu P, MacLennan GT, Gupta S. Suppression of NF-κB and NF-κB-regulated gene expression by apigenin through IκBα and IKK pathway in TRAMP mice. Plos one. 2015;10(9):e0138710.

172. Adham AN, Abdelfatah S, Naqishbandi AM, Mahmoud N, Efferth T. Cytotoxicity of apigenin toward multiple myeloma cell lines and suppression of iNOS and COX-2 expression in STAT1-transfected HEK293 cells. Phytomedicine. 2021;80:153371.

173. Venkataraman B, Almarzooqi S, Raj V, Dudeja PK, Bhongade BA, Patil RB, Ojha SK, Attoub S, Adrian TE, Subramanya SB. α-Bisabolol Mitigates Colon Inflammation by Stimulating Colon PPAR-γ Transcription Factor: In Vivo and In Vitro Study. PPAR research. 2022;2022(1):5498115.

174. Najafi B, Mojab F, Ghaderi L, Farhadifar F, Roshani D, Seidi J. The Effect of Chamomile Flower Essence on Pain Severity after Elective Caesarean Section under Spinal Anaesthesia: A Randomized Clinical Trial. Journal of Clinical C Diagnostic Research. 2017;11(11).

175. Singh O, Khanam Z, Misra N, Srivastava MK. Chamomile (Matricaria chamomilla L.): an overview. Pharmacognosy reviews. 2011;5(9):82.

176. Chauhan R, Singh S, Kumar V, Kumar A, Kumari A, Rathore S, Kumar R, Singh S. A comprehensive review on biology, genetic improvement, agro and process technology of German chamomile (Matricaria chamomilla L.). Plants. 2021;11(1):29.

177. Satyal P, Shrestha S, Setzer WN. Composition and Bioactivities of an (E)-β-Farnesene Chemotype of Chamomile (Matricaria chamomilla) Essential Oil from Nepal. Nat Prod Commun. 2015;10(8):1453-7.

178. Al-Dabbagh B, Elhaty IA, Elhaw M, Murali C, Al Mansoori A, Awad B, Amin A. Antioxidant and anticancer activities of chamomile (Matricaria recutita L.). BMC research notes. 2019;12:1-8.

179. Danaei N, Panahi Kokhdan E, Manzouri L, Nikseresht M. TheEffect of bevacizumab and hydroalcohlic Extract of Matricaria chamomilla on cell viability and nitric oxide

production of the colorectal cancer cell line (HT-29). Armaghane Danesh. 2016;20(12):1107-18.

180. Roby MHH, Sarhan MA, Selim KAH, Khalel KI. Antioxidant and antimicrobial activities of essential oil and extracts of fennel (Foeniculum vulgare L.) and chamomile (Matricaria chamomilla L.). Ind Crops Prod. 2013;44:437–45.

181. Saeedi M, Khanavi M, Shahsavari K, Manayi A. Matricaria chamomilla: an Updated Review on Biological Activities of the Plant and Constituents. Research Journal of Pharmacognosy (RJP). 2024;11(1):109–36.

182. Dai YL, Li Y, Wang Q, Niu FJ, Li KW, Wang YY, Wang J, Zhou CZ, Gao LN. Chamomile: a review of its traditional uses, chemical constituents, pharmacological activities and quality control studies. Molecules. 2022;28(1):133.

183. Talebi S, Sharifan P, Ostad AN, Shariati SE, Ghalibaf AM, Barati M, Aghasizadeh M, Ghazizadeh H, Shabani N, Ferns G, Rahimi HR. The Antioxidant and Anti-inflammatory Properties of Chamomile and Its Constituents. Reviews in Clinical Medicine. 2022;9(3).

184. El Mihyaoui A, Esteves da Silva JC, Charfi S, Candela Castillo ME, Lamarti A, Arnao MB. Chamomile (Matricaria chamomilla L.): a review of ethnomedicinal use, phytochemistry and pharmacological uses. Life. 2022;12(4):479.

185. Aggarwal BB, Surh YJ, Shishodia S, editors. The Molecular Targets and Therapeutic Uses of Curcumin in Health and Disease. 2007; 595.

186. Wan Mohd Tajuddin WN, Lajis NH, Abas F, Othman I, Naidu R. Mechanistic understanding of curcumin's therapeutic effects in lung cancer. Nutrients. 2019;11(12):2989.

187. Zorofchian Moghadamtousi S, Abdul Kadir H, Hassandarvish P, Tajik H, Abubakar S, Zandi K. A review on antibacterial, antiviral, and antifungal activity of curcumin. BioMed research international. 2014;2014(1):186864.

188. Zhang T, He Q, Liu Y, Chen Z, Hu H. Efficacy and Safety of Curcumin Supplement on Improvement of Insulin Resistance in People with Type 2 Diabetes Mellitus: A Systematic Review and Meta-Analysis of Randomized Controlled Trials. Evidence-Based Complementary and Alternative Medicine. 2021;2021(1):4471944.

189. Tripathy S, Verma DK, Thakur M, Patel AR, Srivastav PP, Singh S, Gupta AK, Chavez-Gonzalez ML, Aguilar CN, Chakravorty N, Verma HK. Curcumin extraction, isolation, quantification and its application in functional foods: a review with a focus on immune enhancement activities and COVID-19. Frontiers in Nutrition. 2021;8:747956.

6. Appendices (Published Articles)

7. Curriculum Vitae

applied sciences

MDPI

Article

COX2-Inhibitory and Cytotoxic Activities of Phytoconstituents of *Matricaria chamomilla* L.

Assia I. Drif [1], Bharathi Avula [2], Ikhlas A. Khan [2] and Thomas Efferth [1,*]

[1] Department of Pharmaceutical Biology, Institute of Pharmaceutical and Biomedical Sciences, Johannes Gutenberg University, Staudinger Weg 5, 55128 Mainz, Germany; adrif@uni-mainz.de
[2] National Center for Natural Products Research (NCNPR), School of Pharmacy, University of Mississippi, Oxford, MS 38677, USA; bavula@olemiss.edu (B.A.)
* Correspondence: efferth@uni-mainz.de; Tel.: +49-6131-3925751

Abstract: Chamomile tea is a popular beverage and herbal remedy with various health benefits, including antioxidant and antimicrobial activities and beneficial effects on metabolism. In this study, we investigated the inhibitory activities of secondary metabolites from *Matricaria chamomile* L. against COX2, an enzyme involved in inflammation and linked to cancer development. The cytotoxicity of the compounds was also evaluated on a panel of 60 cancer cell lines. Myricetin, one of the COX2-inhibiting and cytotoxic compounds in chamomile tea, was further studied to determine a proteomic expression profile that predicts the sensitivity or resistance of tumor cell lines to this compound. The expression of classical mechanisms of anticancer drug resistance did not affect the responsiveness of cancer cells to myricetin, e.g., ATP-binding cassette (ABC) transporters (ABCB, ABCB5, ABCC1, ABCG2), tumor suppressors (p53, WT1), and oncogenes (EGFR, RAS), whereas significant correlations between myricetin responsiveness and GSTP expression and cellular proliferation rates were observed. Additionally, Kaplan–Meier survival time analyses revealed that high COX2 expression is associated with a worse survival prognosis in renal clear cell carcinoma patients, suggesting a potential utility for COX2 inhibition by myricetin in this tumor type. Overall, this study provides insight into the molecular modes of action of chamomile secondary metabolites and their potential as cancer-preventive or therapeutic agents.

Keywords: anti-inflammatory activity; beverages; cancer; chemoprevention; proteomics; tea

Citation: Drif, A.I.; Avula, B.; Khan, I.A.; Efferth, T. COX2-Inhibitory and Cytotoxic Activities of Phytoconstituents of *Matricaria chamomilla* L. *Appl. Sci.* **2023**, *13*, 8935. https://doi.org/10.3390/app13158935

Academic Editor: Lidia Feliu

Received: 9 April 2023
Revised: 24 July 2023
Accepted: 29 July 2023
Published: 3 August 2023

1. Introduction

Chamomile tea is widely known for its medicinal properties and is commonly used in traditional medicine for its antioxidant and antimicrobial activities [1,2]. In addition, Chamomile tea is also recognized for its value as a food due to its beneficial effect on metabolism, especially in the kidneys and liver. The safe use of chamomile was approved by the U.S. Food and Drug Administration (FDA's GRAS) [3,4]. Several studies have shown the effect of chamomile against muscle spasms, rheumatism, and gastrointestinal disorders [5,6]. Furthermore, extensive literature promotes the effect of chamomile tea, such as the German chamomile *Matricaria chamomilla* L., against obesity, depression, stress, inflammation, and cancer [7–12]. Moreover, different clinical trials demonstrated not only the anti-inflammatory effect against eczema as well as chemo-and radiotherapy-induced mucositis by a chamomile tea extract and its bioactive secondary metabolites, apigenin and α-bisabolol [13,14]. Furthermore, analgesic effects have been shown against peripheral neuropathic pain, a side effect from chemotherapy, and apoptotic activity by inhibiting COX2 and NF-κB [15,16].

The German chamomile (*M. chamomilla* L., syn. *Matricaria recutita* L.) and Roman chamomile (*Chamaemelum nobile* L. (All)) are the most known chamomile species. They are both rich in flavonoids, phenolic acids, and terpenoids. The German chamomile contains more terpenoids and is more resistant to pathogens [17]. Furthermore, its flower extract

contained more of these components than tea and essential oil [18]. Apigenin was one of the first compounds extracted from chamomile [19], which has been studied in the past for its anti-carcinogenic and anti-apoptotic effects [20–22]. The compounds inhibit cancer cell proliferation by blocking the activity of numerous proteins, including RelA/p65 and COX2 [23,24].

COX2 is an important enzyme that plays a key role in inflammation. It is involved in the production of prostaglandins, which promote inflammation. Inflammation is a necessary process for the body's immune response against infection or injury, but if it becomes chronic, it can lead to a range of health problems, including cancer [25–28].

Our aim in this study was to investigate the molecular modes of action of secondary metabolites extracted from *M. chamomile* in terms of their inhibitory activity against COX2 and their cytotoxicity towards a panel of 60 cell lines from the National Cancer Institute. Then, we focused on myricetin, one of the COX2-inhibiting and cytotoxic chemical constituents of chamomile tea, to determine a proteomic expression profile that predicts the sensitivity or resistance of tumor cell lines to this compound. Finally, we mined the KM Plotter database to identify tumor types where high COX2 expression is associated with a worse Kaplan–Meier survival prognosis in cancer patients in an endeavor to envision a clinical situation where COX2 inhibition by myricetin might exert preventive or therapeutic potential.

2. Materials and Methods

2.1. Phytochemical Analysis

Chemicals

Nine standards were used as reference compounds. The compounds were *cis*-GMCA [(*Z*)-2-β-D-glucopyranosyloxy-4-methoxycinnamicacid] (**2**), *trans*-GMCA [(*E*)-2-β-D-glucopyranosyloxy-4-methoxycinnamic acid] (**4**), quercetagetin-7-*O*-β-D-glucopyranoside (**3**), apigenin-7-*O*-β-D-glucoside (**6**), apigenin 7-*O*-(6″-*O*-acetyl-β-D-glucopyranoside) (**7**), tonghosu [2-(2′,4′-hexadiynylidene)-1,6-dioxaspiro [4,4]-non-3-ene] (**9**) were isolated at the National Center for Natural Products Research (NCNPR), University of Mississippi, Oxford, MS, USA. The identity and purity of these compounds are confirmed by chromatographic (TLC, HPLC) methods, and the analysis of the spectral data (IR, 1D- and 2D-NMR, ESI-HRMS) in comparison with published spectral data is also confirmed. The purity of these isolated compounds was found to be greater than 95%. Chlorogenic acid (**1**) and apigenin (**8**) were purchased from Chromadex (Santa Ana, CA, USA, purity greater than 97%). Luteolin-7-*O*-β-D-glucoside (**5**) was purchased from Indofine Chemical Company, Inc. (Hillsborough, NJ, USA, purity greater than 97%). Acetonitrile and formic acid were of HPLC grade and purchased from Fisher Scientific (Fair Lawn, NJ, USA). Water for the HPLC mobile phase was purified using a Milli-Q system (Millipore) [29].

2.2. Instrumentation and Chromatographic Conditions of Liquid Chromatography with a Diode Array Detector–Quadrupole Time-of-Flight Mass Spectrometry (LC–DAD–QToF)

The phytochemical analysis using liquid chromatography–diode array detector–quadrupole time-of-flight mass spectrometry (LC–DAD–QToF) was performed according to recently published protocols [29,30]. An Agilent 1290 Series liquid chromatographic system was used (Agilent Technologies, Santa Clara, CA, USA), comprising a binary pump, a vacuum solvent degasser, an autosampler with 108-vial well-plate trays, a thermostatically controlled column compartment, and a diode array detector. The separation was achieved on an Agilent Poroshell 120 EC-C18 column (150 mm × 2.1 mm I.D., 2.7 µm). The mobile phase consisted of water with 0.1% formic acid (A) and acetonitrile with 0.1% formic acid (B) at a flow rate of 0.25 mL/min. Analysis was performed using the following gradient elution: 90% A/10% B to 60%A/40%B in 15 min; in the next 15 min to 100% B. Each run was followed by a 5-min wash with 100% B and an equilibration period of 5 min with initial conditions of 90% A/10% B. One microliter of sample was injected, and the column temperature was maintained at 40 °C. The mass spectrometric analysis was performed with

a QToF-MS (Model #G6545B, Agilent Technologies, Santa Clara, CA, USA) equipped with an ESI source using the following parameters: drying gas (N_2) flow rate, 13 L/min; drying gas temperature, 325 °C; nebulizer pressure, 35 psig; sheath gas temperature, 300 °C; sheath gas flow, 11 L/min; capillary voltage, 3500 V; nozzle voltage, 0 V; skimmer, 65 V; Oct RF V, 750 V; and fragmentor voltage, 175 V. All the operations, acquisition, and analysis of data were controlled using Agilent MassHunter Acquisition Software Ver. A.10.1 and processed with MassHunter Qualitative Analysis Software Ver. B.7.00. Each sample was analyzed in positive and negative modes over the range of m/z = 100–1700 and extended dynamic range (flight time to m/z 1700 at a 2 GHz acquisition rate). Accurate mass measurements were obtained by means of reference ion correction using reference masses at m/z 121.0509 (protonated purine) and 922.0098 [protonated hexakis (1H, 1H, 3H-tetrafluoropropoxy) phosphazine, or HP-921] in positive ion mode. The UV detection wavelength was in the range of 200–500 nm. The phytochemical analysis with UHPLC–DAD–QToF was performed according to recently published protocols [29,30].

2.3. Virtual Drug Screening and Molecular Docking

A list of more than 1000 chamomile compounds was first screened in silico against COX2 using PyRx [31,32]. The COX2 crystal structure was taken from the Protein Data Bank (PDB ID: 5F1A) [33,34]. This structure was prepared for virtual drug screening using the Chimera software [35]. We cut the crystal structure and used chain A within the catalytic domain of 5F1A. Using AutoDockTools-1.5.7rcl [34], water molecules were deleted, polar hydrogen atoms were added and merged, the missing atoms and bonds were repaired, and Kollman charges were added.

After performing the virtual screening with PyRx, 211 ligands from more than 1000 compounds were selected and subjected to molecular docking against COX2 using Autodock 4.2.6 [36–38]. A Grid-box was set based on the interaction of the known COX2 ligand salicylic acid with the amino acids of COX2-5F1A [39]. Its dimensions were 104 × 70 × 100 Å spacing 0.369 Å the Grid-center x = 45.667 Å, y = 28.779 Å and z = 232.841 Å. The Lamarckian Genetic Algorithm (LGA) was applied to seek the lowest binding energies (LBE, kcal/mol) and predicted inhibition constants (pKi, µM) with docking parameters set to 250 runs and 2,500,000 energy evaluations for each cycle. Mean values ± SD were calculated from each of the three independent dockings. BIOVIA Discovery Studio Visualizer 2021 [40] was used for the 3D visualization pictures of the interaction between the ligands and the amino acids of the crystal structure of COX2.

A total of 207 samples from chamomile was included in this present study (Supplementary Table S1).

2.4. Fluorometric COX2 Inhibitor Screening Assay

To validate the in silico results from virtual drug screening, we performed an in vitro COX2 inhibitor assay (BioVision Incorporate Berlin, Germany [41]) according to the manufacturer's instructions. The assay is based on the fluorometric detection of prostaglandin G2, which is produced by the conversion of arachidonic acid by the catalytic activity of COX2. Selected phytochemicals of chamomile tea (apigenin, β-amyrin, β-eudesmol, β-sitosterol, daucosterol, farnesol, and myricetin) were chosen based on their LBE values from virtual drug screening. These compounds were tested for their COX2 inhibition in vitro at concentrations of 0.1 µM and 1 µM.

2.5. Pharmacological Testing and Gene/Protein Expression Profiling of Tumor Cell Lines

The Developmental Therapeutics Program of the National Cancer Institute (Bethesda, MA, USA) [42] used a series of human tumor cell lines from diverse origins (leukemia, melanoma, brain tumors, and carcinoma of the lung, colon, kidney, ovary, breast, or prostate) for drug screening [43]. The data of compound screening ($\log_{10}$IC50 values obtained by a sulforhodamine 123 assay) as well as transcriptomic and proteomic expression

data were deposited at the NCI website [44]. For statistical correlation analyses, we used Pearson's correlation test (WinStat, Kalmia Inc., Cambridge, MA, USA).

2.6. Growth Inhibition Assay

Resazurin reduction assay was conducted to measure the growth inhibitory activity of *Chamomilla matricaria* L. Human CCRF-CEM leukemia and human AMO1 multiple myeloma cells were seeded at a density of 1×10^4 cells per well in 96-well plates using 100 µL of RPMI 1640 medium. These cells were then treated with the extract at 7 different concentrations, each diluted in 100 µL of medium, and incubated for 72 h. Similarly, HCT116 $p53^{+/+}$ wildtype and drug-resistant HCT $p53^{-/-}$ knockout colon cancer cells were seeded (5×10^3 cells/well) in 100 µL DMEM medium and allowed to adhere for 24 h. The next day, these cells were treated with the same series of extract concentrations and incubated for an additional 48 h [45]. On the final day of incubation, 20 µL of 0.01% resazurin solution from Promega (Mannheim, Germany) was added to each well and left to incubate for over 4 h at 37 °C. The fluorescence signal was then measured at an excitation wavelength of 544 nm and an emission wavelength of 590 nm using the Infinite M2000 Pro-plate reader from Tecan (Crailsheim, Germany). The experiment was independently replicated three times, and each concentration was tested with six replicates. The growth inhibitory effect of the treatment was represented as the percentage of cell viability and graphed as a dose–response curve. The IC_{50} value representing the concentration at which the growth was inhibited by 50% was calculated using Microsoft Excel 2021 (Version 2306 Build 16.0.16529.20164) [46].

2.7. Kaplan–Meier Survival Analysis

Data from more than 30,000 samples of 21 tumor types are deposited in the KMPlotter database [47–49]. The Kaplan–Meier statistics algorithm of this database was used to identify the prognostic value of COX2 mRNA expression for the survival time of cancer patients. We used a false discovery rate (FDR) calculation to exclude type I errors in multiple comparisons [50]. We included only Kaplan–Meier statistics with FDR rates ≤ 5%, indicating that not more than 5% of "declared" positive results were truly negative.

2.8. Immunofluorescence Microscopy of GFP Tagged α-Tubulin

Human U2OS osteosarcoma cells were left to attach for 24 h in µ-Slide 8 Well (30,000 cells/well) (ibidi, Gräfelfing, Germany). The next day, the cells were treated with myricetin (0.1, 1, 10 µM) (Sigma-Alderich Chemie GmbH, Taufkirchen, Germany) as well as paclitaxel (1 µM) and vincristine (1 µM) (both of the drugs were a gift from the pharmacy of the university hospital Johannes Gutenberg Mainz, Germany) as positive controls, along with DMSO as a negative control. After 24 h, cells were washed with PBS, fixed with 4% paraformaldehyde, and stained with 1 µg/mL of 4′6-diamidino-2-phenylindole (DAPI, Sigma Aldrich, Darmstadt, Germany) in the dark. Subsequently, the slides were immersed in Mounting Medium (ibidi, Gräfelfing, Germany). Widefield imaging was performed using a THUNDER Imager Live Cell (Leica Microsystems, Wetzlar, Germany) based on a Leica DMi8 microscope stand. Both transmission light and fluorescence images were acquired using a 63×/1.40 NA objective (HC PL APO CS2 63×/1.40 OIL UV). Fluorescence was excited with an LED light source (LED8, Leica) at 395 nm and 488 nm for imaging of DAPI and Tubulin–GFP, respectively. A quadband filter cube (DFT51010, Leica) split fluorescence excitation and emission light, and additional emission filters (460/80 for imaging of DAPI signals and 535/70 for imaging of GFP signals) were used to reduce bleed-through. The camera (Leica DFC9000 GTC) was operated in 2 × 2 binning mode, resulting in a pixel size of 206 nm measured in the object plane. Exposure times were set to 200 ms (GFP–Tubulin), 25 ms (DAPI), and 150 ms (differential interference contrast (DIC)). Images were analyzed with Image J software (National Institute of Health, Bethesda, MD, USA). The methodology of this experiment was described by us [51] and the microscopy techniques by Marton Gelléri (Institute of Molecular Biology gGmbH (IMB), Mainz, Germany).

3. Results

3.1. Phytochemical Analysis

The phytochemical analysis of chamomile extract was conducted using liquid chromatography–diode array detector–quadrupole time-of-flight mass spectrometry (LC–DAD–QToF). As shown in Figure 1, 21 phytochemicals were tentatively detected.

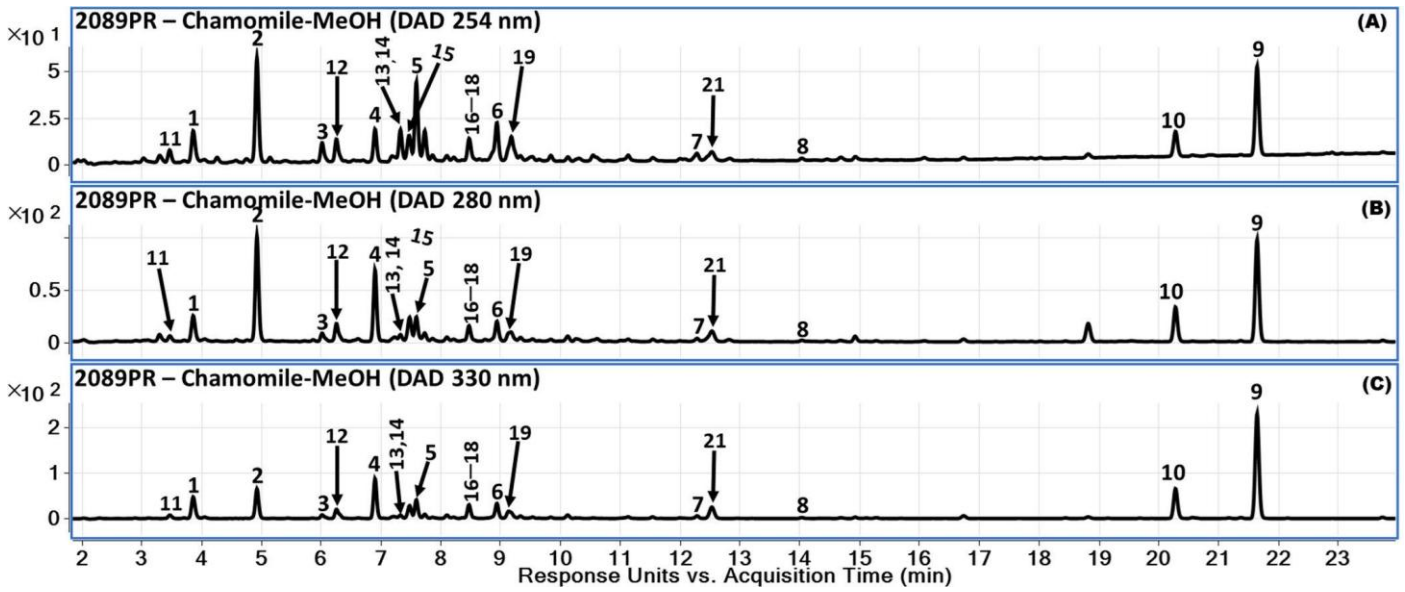

Figure 1. Typical LC–DAD chromatogram (absorbance vs. retention time) of a tea sample (*Matricaria chamomilla* L.) at 254 nm (**A**), 280 nm (**B**) and 330 nm (**C**): chlorogenic acid (**1**), *cis*-GMCA [(*Z*)-2-β-D-glucopyranosyloxy-4-methoxycinnamic acid] (**2**), quercetagetin-7-*O*-β-D-glucopyranoside (**3**), *trans*-GMCA [(*E*)-2-β-D-glucopyranosyloxy-4-methoxycinnamic acid] (**4**), luteolin-7-*O*-β-D-glucoside (**5**), apigenin-7-*O*-β-D-glucoside (**6**), apigenin 7-*O*-(6″-*O*-acetyl-β-D-glucopyranoside) (**7**), apigenin (**8**), and isomers of tonghaosu [2-(2′,4′-hexadiynylidene)-1,6-dioxaspiro [4,4]-non-3-ene] (**9**–**10**), esculin (**11**), isoquercitrin (**12**), loliolide/isololiolide (**13**–**14**), quercitrin (**15**), 3,5-di-caffeoylquinic acid (**16**–**18**), isorhamnetin 3-*O*-β-D-glucopyranoside (**19**), quercetagetin 4′-methyl ether 7-(6-(*E*)-caffeoylglucoside) (**20**), glucuronolactone (**21**), and myricetin (**22**). All compounds were assigned based on mass spectrometry.

3.2. Cytotoxicity Assay

To examine the activity of chamomile extract against cancer cell lines, we have conducted growth inhibition assays. The extract revealed cytotoxicity against different cancer types. The IC_{50} values of the two hematopoietic cell lines CCRF-CEM and AMO1 (23.7 ± 4.7 µg/mL to 28.0 ± 2.2 µg/mL) were lower than those of the colon cancer cell lines. Wildtype HCT116 $p53^{+/+}$ had an IC_{50} value of 28.0 ± 2.2 µg/mL, and HCT116 $p53^{-/-}$ knockout cells had an IC_{50} value of 74.3 ± 0.4 µg/mL. Hence, the p53 knockout cells were 2.65-fold more resistant to the chamomile extract than the p53 wild-type cells (Figure 2).

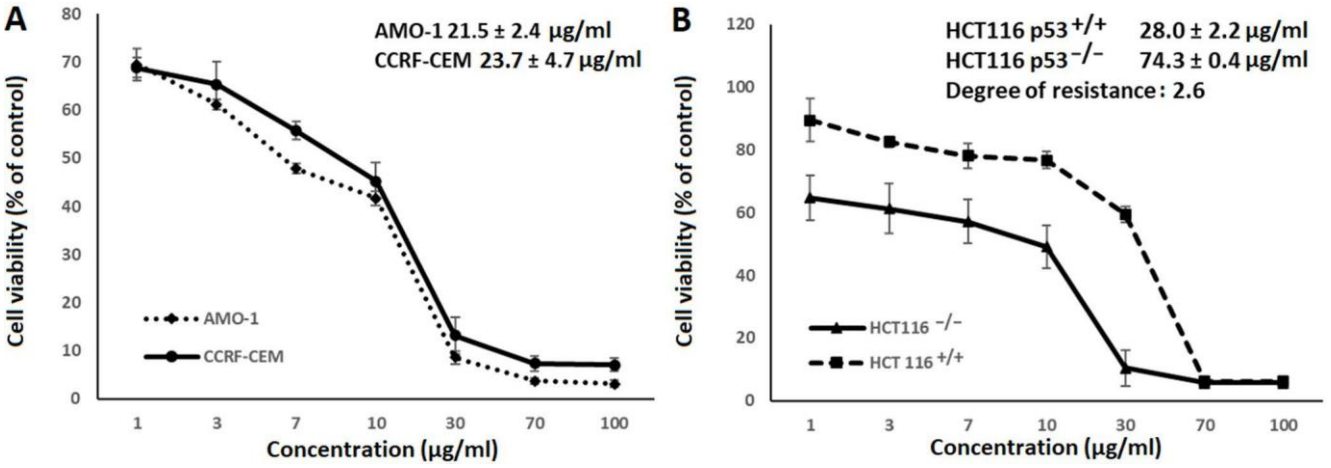

Figure 2. Dose–response curve of the extract of chamomile in hematopoietic and colon cancer cell lines determined by a resazurin assay. (**A**) Growth inhibition of CCRF-CEM leukemia cells and AMO-1 multiple myeloma cells. (**B**) Growth inhibition of HCT116 $p53^{+/+}$ wildtype and drug-resistant HCT116 $p53^{-/-}$ knockout cells. The IC_{50} values were determined from the dose–response curve, and the degree of resistance was obtained by dividing the IC_{50} value of HCT $p53^{-/-}$ by the IC_{50} value of HCT $p53^{+/+}$. The mean values ± standard deviation values are from three independent experiments.

3.3. Molecular Docking In Silico

To investigate the full potential of chamomile tea, a total of 212 chamomile compounds were docked against human COX2 (PDB: 5F1A) using the PyRx program. Thirty of these 212 compounds were selected as the most abundant for further analysis. Table 1 shows the low binding energies (LBE, kcal/mol) and the predicted inhibition constants (pKi, µM) of these 30 ligands. The LBE and pKi values of these phytochemicals correlated significantly with each other (Pearson correlation test, $p = 7.53 \times 10 - 20$; $r = 0.574$; Figure 1, 1st line left panel). The LBE values of 27 out of 30 substances were smaller than −6 kcal/mol (cut-off) and ranged from −11.73 (±0.44) kcal/mol (β-sitosterol) to −6.01 (±<0.01) kcal/mol (P-cymene). The pKi values of these 27 compounds were in a range from 0.003 (±0.002) µM to 39.57 (±<0.01) µM. Seven of the 27 compounds were selected because these substances were found in the NCI database (dtp.cancer.gov, accessed on 1 July 2023), whose data are required for further investigations. Celecoxib was used as a positive control drug since it is a well-known COX2 inhibitor. As shown in Figure 3 (1st line, middle, and right panel), the compounds were bound to three domains of COX2. Myricetin, daucosterol, and β-amyrin interacted with the first domain; β-sitosterol, apigenin, farnesol, and β-eudesmol with the second domain; and celecoxib with the third domain. Lines 2–5 of Figure 1 depict the three-dimensional binding poses of the compounds and the interacting amino acids.

Table 1. Molecular docking of 30 chamomile compounds binds to COX2 (PDB ID: 5F1A). Shown are the lowest binding energies (kcal/mol), predicted inhibition constants (µM), and the pharmacophores interacting between the ligands and COX2. Bold indicates hydrogen bonds.

No.	Compounds	LBE (kcal/mol)	pKi (µM)	Pharmacophore
1.	β-Sitosterol	−11.73 ± 0.33	0.003 ± 0.002	ALA199, ALA202, GLN203, THR206, HIS207, PHE210, THR212, HIS214, ASN382, TYR385, HIS386, TRP387, **HIS388**, LEU390, LEU391
2	Celecoxib	−10.18 ± 0.03	0.03 ± <0.01	**HIS90**, GLN192, LEU352, SER353, TYR355, LEU359, TRP387, VAL523, ALA527
3	β-Amirin	−9.59 ± 0.01	0.09 ± <0.01	LEU145, GLY225, HIS226, GLY227, **VAL228**, ASN375, ARG376, **GLY533**, **ASN537**, VAL538

Table 1. *Cont.*

No.	Compounds	LBE (kcal/mol)	pKi (μM)	Pharmacophore
4	(+)-Catechin	−9.43 ± <0.01	0.12 ± <0.01	**ALA199**, ALA202, GLN203, THR206, HIS207, PHE210, **ASN382**, HIS386, **TRP387**, HIS388, LEU390, LEU391
5	α-Bisabolol	−9.30 ± 0.03	0.15 ± 0.01	ALA199, THE206, HIS207, PHE210, ASN382, **TYR385**, HIS386, **TRP387**, HIS388, LEU390, LEU391
6	Daucosterol	−9.26 ± 0.01	0.17 ± <0.01	LEU145, LEU224, GLY225, HIS226, GLY227, VAL228, ASP229, GLY235, **GLU236**, THR237, LU238, **ARG333**, GLN374, ASN375, ARG376, ASN537, VAL538
7	β-Eudesmol	−9.18 ± 0.01	0.19 ± <0.01	**ALA199**, ALA202, GLN203, THR206, HIS207, TYR385, HIS386, TRP387, HIS388, LEU390, LEU391
8	Bisabelol oxide B	−9.02 ± 0.01	0.24 ± <9.91	**ALA199**, ALA202, GLN203, THR206, PHE210, TYR385, HIS386, TRP387, HIS388, LEU390, LEU391
9	Kaempferol	−8.93 ± 0.02	0.28 ± 0.01	ALA199, ALA202, GLN203, **THR206**, HIS205, **ASN382**, HIS386, TRP387, HIS388, LEU390, LEU391
10	Luteolin-7-*O*-glucoside	−8.92 ± 0.07	0.29 ± 0.03	PHE200, **GLN203**, HIS207, PHE210, **ASN382**, TYR385, TRP387, **HIS388**, LEU390, LEU391, TYR404, VAL444
11	(-)-Epicatechin	−8.89 ± 0.07	0.31 ± 0.04	**ALA199**, ALA202, **GLN203**, HIS207, PHE210, **ASN382**, **TYR385**, HIS386, **TRP387**, HIS388, LEU390, LEU391
12	Apigenin	−8.84 ± 0.06	0.33 ± 0.03	**ALA199**, ALA202, GLN203, **HIS207**, PHE210, **THR212**, **HIS214**, **ASN382**, TYR385, HIS386, TRP387, HIS388, LEU390
13	Quercitin hydrate	−8.82 ± 0.08	0.34 ± 0.04	**ALA199**, ALA202, GLN203, THR206, HIS207, PHE210, **ASN382**, HIS386, TRP387, HIS388, LEU390, LEU391
14	Chlorogenic acid	−8.67 ± 0.10	0.44 ± 0.08	**ALA199**, ALA202, GLN203, THR206, PHE210, TYR385, HIS386, TRP387, HIS388, LEU390, LEU391
15	Luteolin	−8.67 ± 0.12	0.45 ± 0.09	ALA202, GLN203, HIS207, PHE210, ASN382, TYR385, HIS386, TRP387, HIS388, LEU390, LEU391
16	Lupeol	−8.47 ± <0.01	0.62 ± <0.01	GLY225, HIS226, GLY227, VAL228, ASP229, ARG333, ILE337, TYR373, GLN374, ASN375, GLY536, ASN537, VAL538
17	Bisabolol oxide A	−8.38 ± <0.01	0.71 ± 0.01	ALA199, PHE200, ALA202, GLN203, **THR206**, HIS207, TYR385, TRP387, LEU390, LEU391
18	Guaiazulene	−8.33 ± <0.01	0.79 ± <0.01	ALA199, ALA202, GLN203, HIS207, PHE210, **ASN382**, TYR385, HIS386, TRP387, HIS388, LEU390, LEU391
19	Myrecitin	−8.32 ± 0.41	0.94 ± 0.71	GLY225, GLY227, VAL228, GLN374, ASN375, ARG376, GLY533, ASN537
20	Quercitrin	−8.29 ± 0.06	0.85 ± 0.08	ILE124, ASP125, **PRO128**, THR129, **THR149**, ALA151, **ASN375**, ARG376, **ALA378**, PHE529
21	Farnesol	−7.98 ± 0.10	1.42 ± 0.23	ALA202, THR206, TYR385, HIS386, TRP387, HIS388, LEU390, LEU391
22	Bisabolone oxide A	−7.92 ± <0.01	1.57 ± <0.01	ALA199, ALA202, GLN203, THR206, PHE210, TYR385, TRP387, HIS388, LEU390, LEU391
23	Chamazulene	−7.74 ± 0.01	2.10 ± 0.01	ALA199, ALA202, GLN203, THR206, **HIS207**, PHE210, **ASN382**, TYR385, HIS386, TRP387, HIS388, LEU390, LEU391
24	Caffeic acid	−7.09 ± 0.08	6.41 ± 0.87	ALA202, THR206, TYR385, HIS386, TRP387, HIS388, LEU391
25	(+)-Terpinen-4-ol	−6.92 ± <0.01	8.47 ± 0.01	ALA202, GLN203, HIS207, PHE210, **THR212**, **ASN382**, TYR385, HIS386, TRP387, LEU390

Table 1. *Cont.*

No.	Compounds	LBE (kcal/mol)	pKi (μM)	Pharmacophore
26	Citronellol	−6.01 ± 0.01	39.50 ± 6.52	ILE124, ASP125, **THR129**, **THR149**, ARG150, ASN375, ARG376, ILE377, ALA378, PHE529
27	P-Cymene	−6.01 ± <0.01	39.57 ± <0.01	ALA202, THR206, TYR385, HIS388, LEU390, LEU391, ALA199, GLN203, THR206, HIS207, PHE210, TYR385, TRP387, HIS388, LEU390, LYS97, ASN104, GLN350, TYR355, HIS356, LYS358

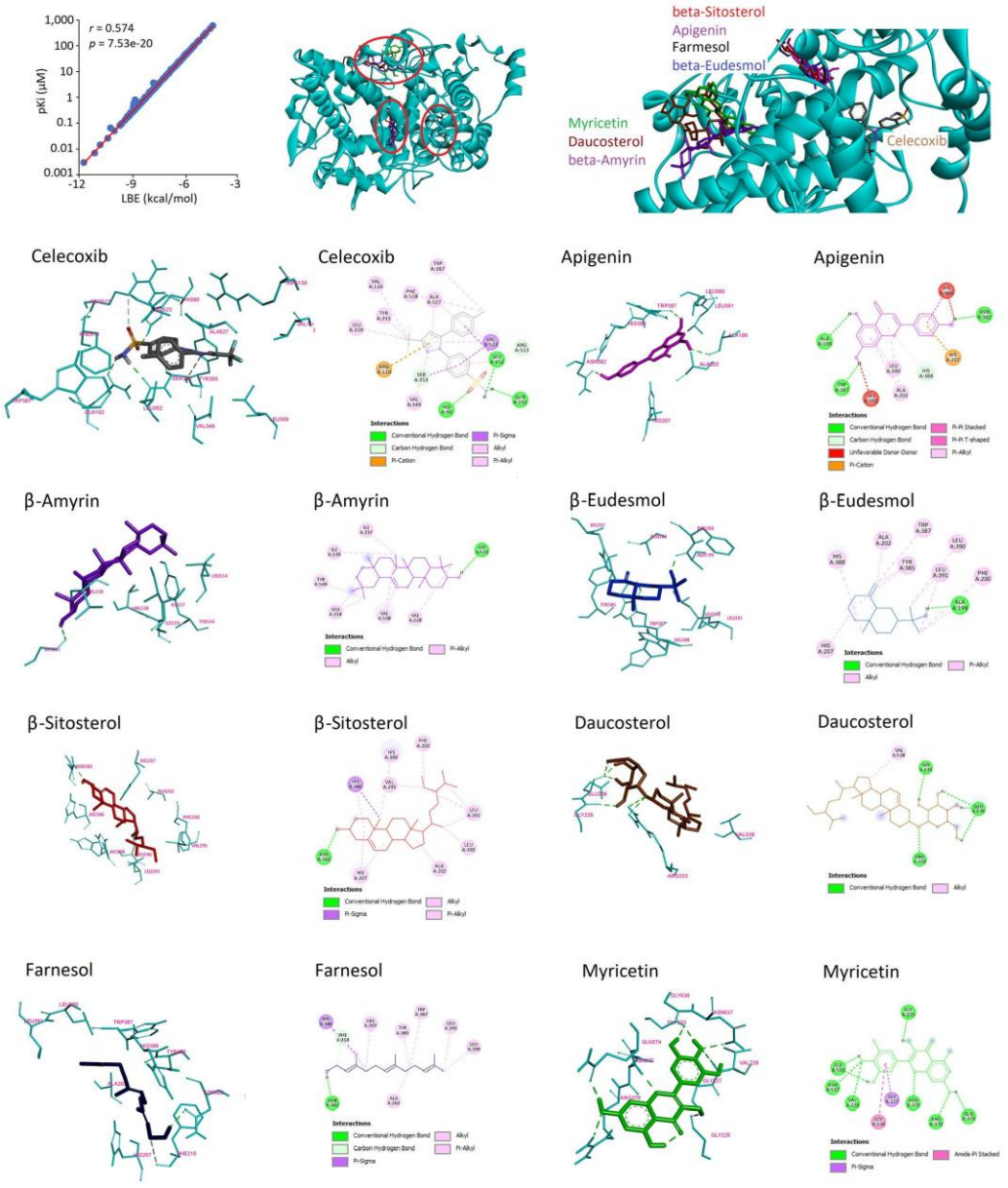

Figure 3. Molecular docking analysis of 7 compounds derived from chamomile (*Matricaria chamomilla*) and celecoxib to COX2 (5F1A). They were bound to different pockets within the same domain. The three red circles indicate the different binding sites. The low binding energy (Kcal/mol) values significantly correlate with the predicted inhibition constant pki (μM) ($r = 0.574$; $p = 7.53 \times 10^{-20}$), as shown on the left graph. The 2D and 3D illustrations (Lines 2–5) show the interaction of celecoxib, apigenin, β-amyrin, β-eudesmol, β-sitosterol, daucosterol, farnesol, and myricetin with different amino acids of COX2.

3.4. Inhibition of COX2 Enzyme Activity In Vitro

To exemplarily verify the in silico predicted interaction of the compounds with COX2, we measured the enzymatic activity upon treatment with the selected seven phytochemicals. Figure 4A illustrates the rest activity of COX2 after treatment with β-sitosterol, β-amyrin, β-eudesmol, daucosterol, apigenin, myricetin, and farnesol at concentrations of 0.1 and 1 µM. β-Sitosterol exerted the highest inhibitory effect on COX2, with percentages of 92% and 98%, respectively. By contrast, apigenin had the lowest inhibitory activity (42% and 90%, respectively). Then, we corrected the percentages of COX2 rest activity upon treatment with 0.1 µM of the compounds in vitro with the LBE values in silico and found a significant correlation (Pearson collection test, $p = 0.030$; $r = 0.736$) (Figure 4B). We also observed a significant correlation upon treatment with 1 µM ($p = 0.042$; $r = 0.692$) (Figure 4C).

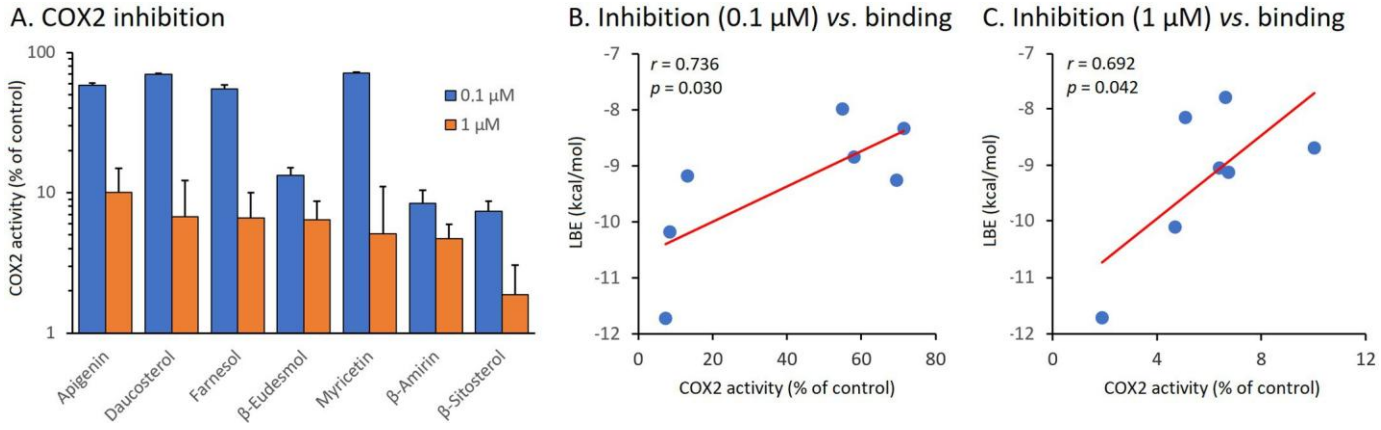

Figure 4. (**A**). The percentage of the rest activity of COX2 after treatment with apigenin, β-amyrin, β-eudesmol, β-sitosterol, daucosterol, farnesol, and myricetin at 0.1 and 1 µM. (**B**,**C**). Pearson correlation of COX2 rest activity (%) at 0.1 and 1 µM treatment, respectively, vs. low binding energy (kcal/mol). Blue points represent COX2 activity in vitro vs. lowest binding energy (LBE in silico. Red line represents linear regression of blue points.

3.5. Cytotoxicity against Tumor Cells In Vitro

Since there is a mechanistic link between inflammation and carcinogenesis [52], we were interested in exploring the COX2-inhibitory activity of the selected compounds. The cytotoxicity of the selected compounds towards 60 cell lines of different tumor origins (leukemia, melanoma, brain tumors, carcinoma of the colon, ovary, breast, kidney, lung, or prostate) determined by a sulforhodamine B assay was mined in the NCI database (dtp.cancer.gov; accessed on 1 July 2023). The responsiveness of these cell lines is plotted as mean $\log_{10}IC_{50}$ values for each tumor type in Figure 5. β-Sitosterol and daucosterol were minimally active against the tumor cell lines, while apigenin, myricetin, and farnesol were most active (Figure 5A). Celecoxib, the control drug, was the most active. β-Amyrin was not included in the NCI database. Therefore, we detected the cytotoxicity of this compound in CCRF-CEM cells which are also included in the NCI cell line panel and found that this compound did not affect these tumor cells. Since we previously investigated apigenin and farnesol in the NCI cell line panel [53–56], we focused on myricetin in the present study. The inhibitory activity of myricetin against the tumor cells shown in Figure 5B demonstrated that this compound was most active against colon and lung cancer cell lines. For comparison, celecoxib as a control drug was most active against leukemia and prostate cancer cell lines (Figure 5C).

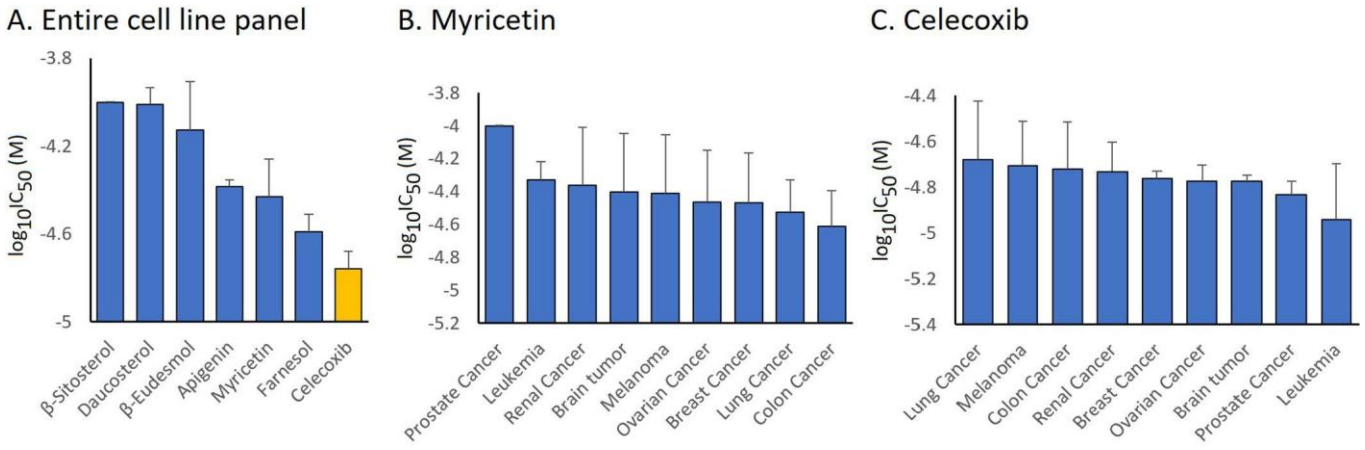

Figure 5. (**A**) Cytotoxicity of the six selected chamomile derivates with celecoxib (positive control) to 60 NCI tumor cell lines was plotted as mean $\log_{10}IC_{50}$ values for each tumor type. (**B**,**C**) the inhibitory activity of myricetin and celecoxib (control drugs), respectively, against the NCI 60 cell line panel plotted as mean $\log_{10}IC_{50}$.

3.6. Oncobiogram Analysis

It is well accepted that natural products usually exert their bioactivity through multiple rather than single mechanisms [57]. Therefore, we assumed that myricetin might not only exert COX2-inhibitory activity. For this reason, we correlated the $\log_{10}IC_{50}$ values for myricetin in 60 tumor cell lines to those of 91 standard anticancer compounds from diverse pharmacological classes. Significant correlations in cellular responsiveness were observed between myricetin and five of the ten tubulin inhibitors and two of the fourteen tyrosine kinase inhibitors. Correlations with drugs of other classes were not found (Figure 6A). A closer look at which tubulin inhibitor is correlated to myricetin is shown in Figure 6B.

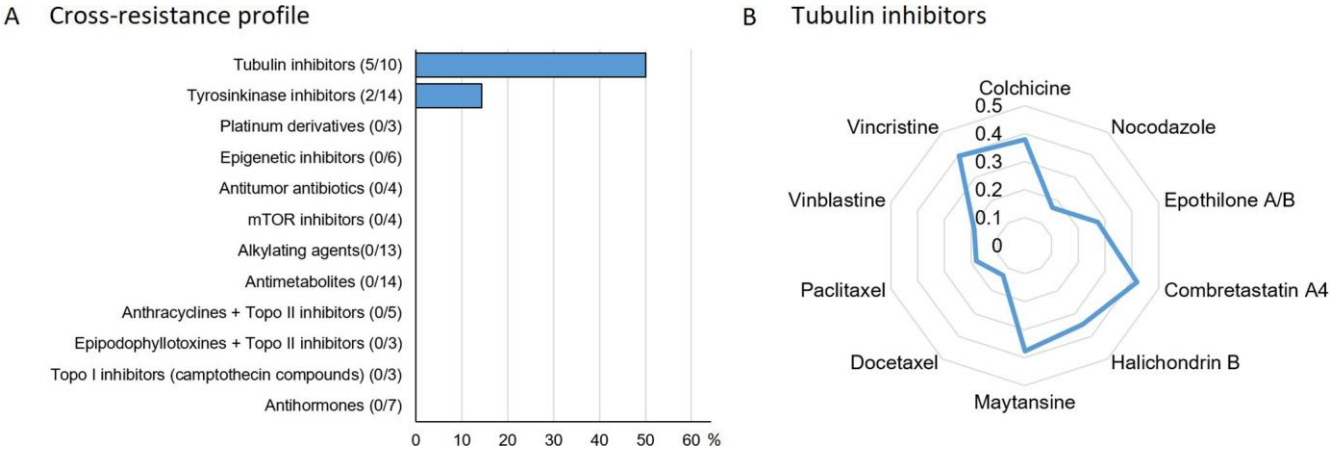

Figure 6. Cross-resistance profiling of myricetin to standard anticancer drugs. (**A**) Percentage of standard anticancer drugs from different pharmacological classes that significantly correlated to the responsiveness of NCI tumor cell lines to myricetin. It shows that 5 of the 10 tubulin inhibitors and 2 of the 14 tyrosine kinase inhibitors significantly correlate to myricetin. (**B**) The tubulin inhibitors are correlated to myricetin.

3.7. Effect of Myricetin on α-Tubulin

To validate the results obtained from the oncobiogram analysis that myricetin might interact with tubulin, U2OS cells transfected with GFP α-tubulin were subjected to myricetin treatment at concentrations of 0.1, 1, and 10 μM for 24 h. The effect of myricetin on microtubules is depicted in Figure 7. Indeed, myricetin inhibits microtubules. In contrast to the

well-organized microtubules seen in the untreated control cells, the myricetin-treated cells displayed shortened microtubule fragments that condensed around the nucleus, similar to vincristine-treated cells. Conversely, paclitaxel-treated cells exhibited extended and disorganized tubulin. Additionally, at the higher concentration of 10 µM myricetin, not only was the polymerization of microtubules significantly hindered (as evident from the reduced density of microtubules), but there were also multiple spindle poles observed in the area of the nucleus.

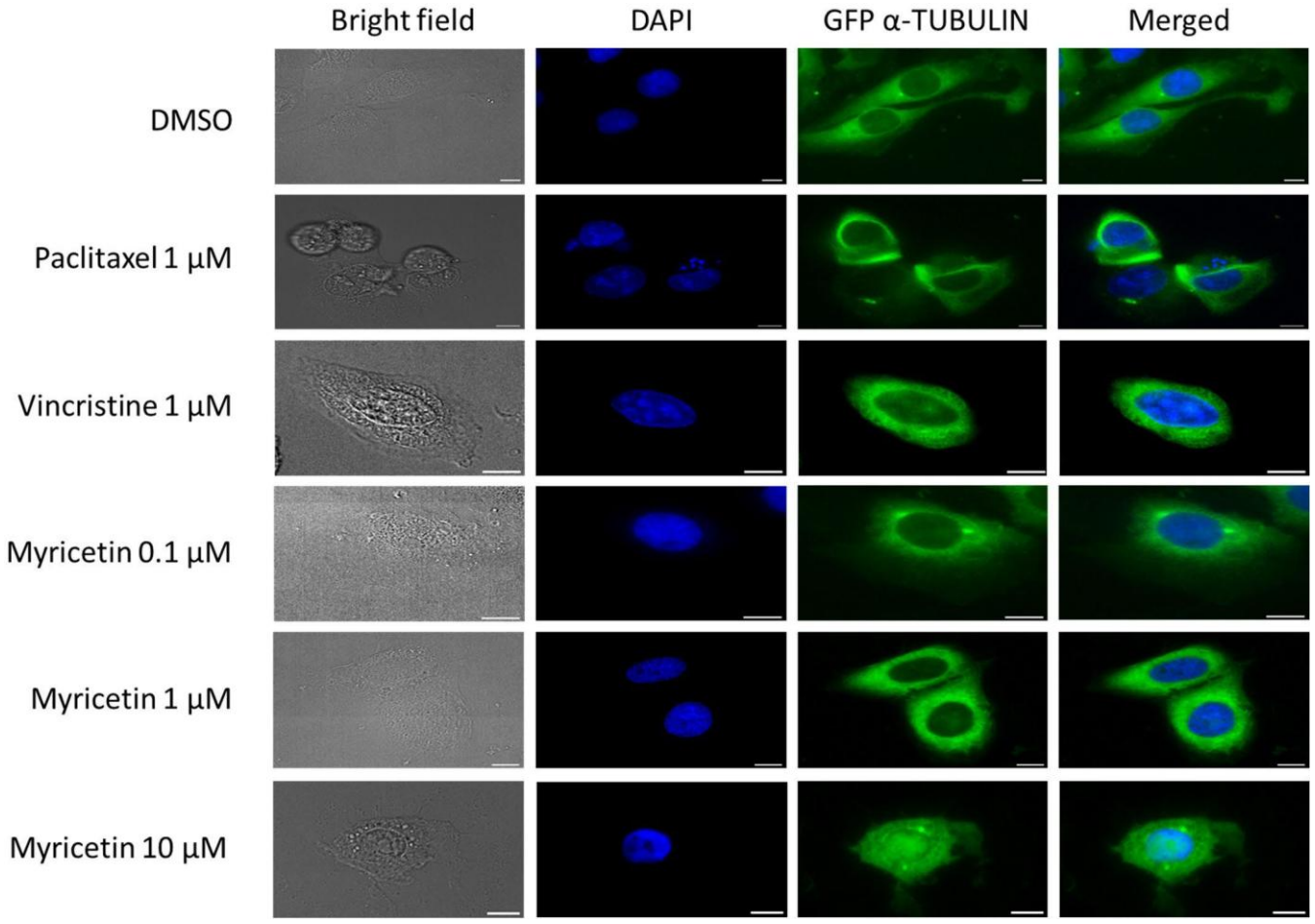

Figure 7. Disruption of the microtubule network in U2OS cells treated with myricetin. Fixed U2OS cells were treated with DMSO and various concentrations of Myricetin at 0.1, 1, 10 µM, vincristine at 1 µM, and paclitaxel at 1 µM for 24 h. Micrographs of the cells were captured at 63 × 1.40 NA objective (HC PL APO CS2 63×/1.40 OIL UV) magnification using the Thunder Imager Live Cell microscope. The microtubules were visualized with green fluorescence, and the images were merged with DAPI (blue) to represent the nucleus. Scale bars indicate 10 µm.

3.8. Proteome Analysis

To gain more insight into the determinants that define the sensitivity or resistance of cell lines to myricetin, the expression of a total of 3171 proteins in the 60 NCI cell lines deposited at the NCI database (dtp.cancer.gov accessed on 23 July 2023) was correlated to the $\log_{10}IC_{50}$ values of myricetin using COMPARE analysis. A compilation of the top 40 proteins (20 directly correlating and 20 inversely correlating with myricetin) and their biological functions is compiled in Supplementary Table S2.

As a next step, we clustered the expression profiles using the hierarchical Ward cluster method within the first dimension and the $\log_{10}IC_{50}$ values for myricetin in the second dimension. This two-dimensional clustering generated a color-coded heat map (Figure 8). Four major clusters were obtained for the 40 proteins (clusters A–D), and another three

clusters appeared for the tumor cell lines tested (clusters 1–3). The cellular responsiveness of the cell lines to myricetin was categorized by defining the cell lines as being sensitive if their individual $\log_{10}IC_{50}$ values were smaller than the median value across all cell lines and as being resistant if the individual $\log_{10}IC_{50}$ value was higher than the median. By using the χ^2 test, we calculated the statistical difference between the sensitive and resistant cell lines. Indeed, the distribution of clusters 1 and 2 (containing mainly myricetin-resistant cell lines) and cluster 3 (mainly containing sensitive cell lines) was statistically significant ($p = 4.89 \times 10^{-4}$).

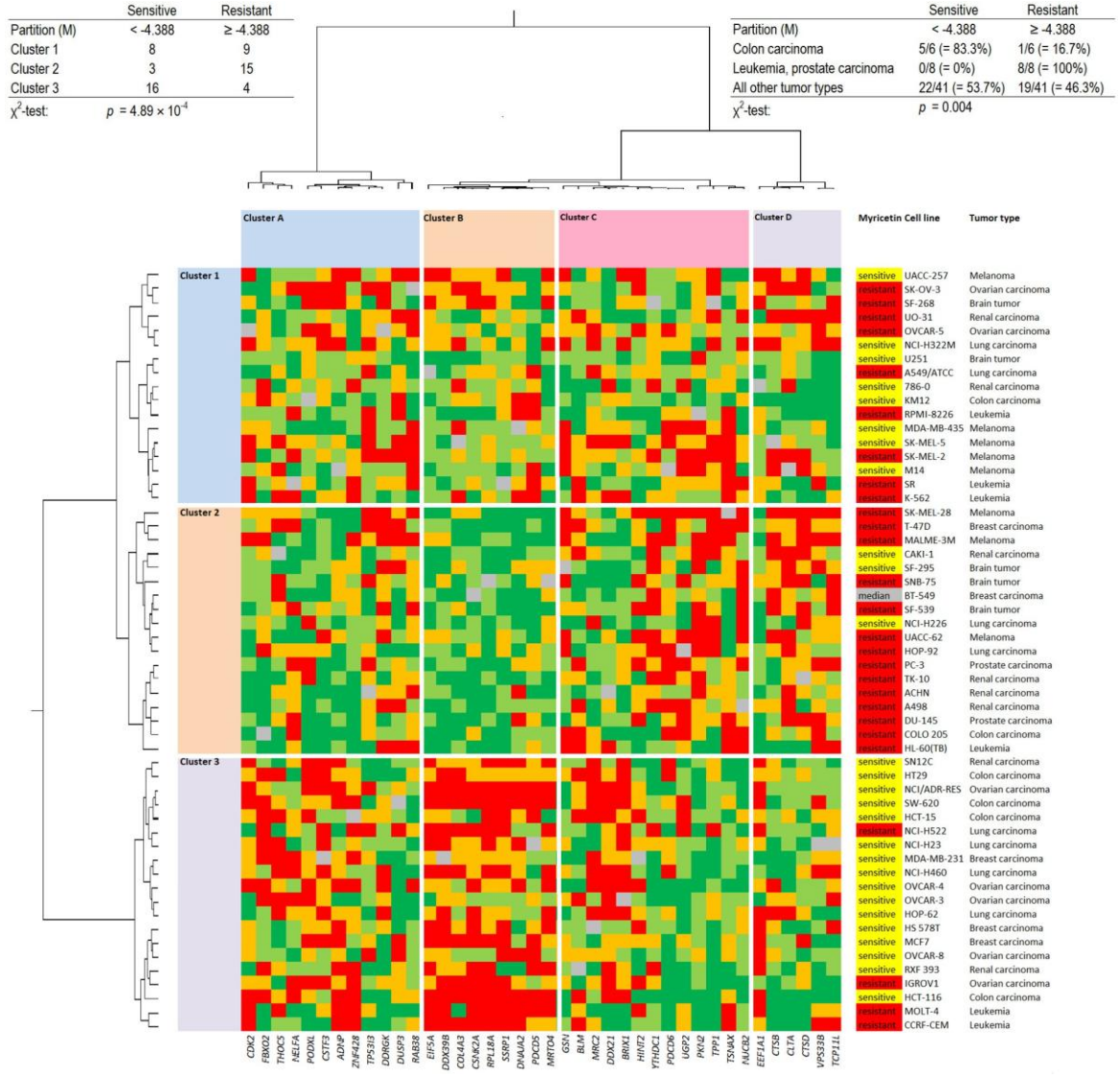

Figure 8. A 2D color-coded heat map and agglomerative cluster analysis of protein expression in the response of 60 NCI tumor cell lines to myricetin ($\log_{10}IC_{50}$). On the right side of the heat map are the responsive cell lines to myricetin and their respective tumor types. Clusters A–D represent the 40 top proteins, and on the left are the 3 major clusters appearing for the tumor cell lines. The cellular responsiveness of various cell lines to myricetin was classified based on their individual $\log_{10}IC_{50}$ values. Cell lines were classified as "sensitive" if their $\log_{10}IC_{50}$ values were lower than the median value of all cell lines and as "resistant" if their $\log_{10}IC_{50}$ values were higher than the median value. The χ^2 test shows statistical significance ($p = 4.89 \times 10^{-4}$) by comparing the three different clusters of protein expression in the cell lines, where clusters 1 and 2 contained mainly myricetin-resistant cell lines, and cluster 3 contained mainly sensitive cell lines.

3.9. Drug Resistance Profiling of Myricetin

Moreover, we addressed the question of whether myricetin is involved in classical drug resistance phenotypes of ABC-transporters (P-glycoprotein, ABCB5, ABCC1, and ABCG2), as well as oncogenes (EGFR), tumor suppressors (TP53, WT1), and others (heat shock protein HSP90, glutathione S-transferase π, and the proliferation rate of the cell lines) (Table 2). We did not observe statistically significant correlations between the $\log_{10}IC_{50}$ values for myricetin and any of the resistance parameters except for GSTP and cellular proliferation rates. This indicates that the effectiveness of myricetin may be limited by these two drug resistance mechanisms, while all other resistance mechanisms to established anticancer drugs may not be relevant for myricetin.

Table 2. Correlation between the $\log_{10}IC_{50}$ values for myricetin and various mechanisms of multidrug resistance in the NCI panel of tumor cell lines, including ABC-transporter-mediated (P-glycoprotein/ABCB1, ABCB5, ABCC1, and ABCG2), EGFR, RAS, TP53, WT1, HSP90, GST, and the proliferative rate. Bold and * $p < 0.05$ and $r > 0.3$ (or $r < -0.3$).

		Myricetin ($\log_{10}$ IC_{50}, M)	**Control Drug ($\log_{10}$ IC_{50}, M)**
ABCB1 Expression			Epirubicin
7q21 (Chromosomal	*r*-value	−0.120	**0.447** *
Locus of *ABCB1* Gene)	*p*-value	0.207	$\mathbf{3.55 \times 10^{-4}}$ *
ABCB1 Expression	*r*-value	−0.124	**0.533** *
(Microarray)	*p*-value	0.186	* $\mathbf{6.82 \times 10^{-6}}$
ABCB1 Expression	*r*-value	0.118	* **0.410**
(RT-PCR)	*p*-value	0.215	* $\mathbf{1.54 \times 10^{-3}}$
ABCB5 Expression			Maytansine
ABCB5 Expression	*r*-value	−0.040	**0.454** *
(Microarray)	*p*-value	0.384	$\mathbf{6.67 \times 10^{-4}}$ *
ABCB5 Expression	*r*-value	0.060	**0.402** *
(RT-PCR)	*p*-value	0.330	**0.0026** *
ABCC1 Expression			Vinblastine
DNA Gene	*r*-value	0.059	**0.429** *
Copy Number	*p*-value	0.333	**0.001** *
ABCC1 Expression	*r*-value	−0.035	**0.398** *
(Microarray)	*p*-value	0.402	**0.003** *
ABCC1 Expression	*r*-value	0.149	0.299
(RT-PCR)	*p*-value	0.170	**0.036** *
ABCG2 Expression			Pancratistatin
ABCG2 Expression	*r*-value	0.163	**0.329** *
(Microarray)	*p*-value	0.120	**0.006** *
ABCG2 Expression	*r*-value	−0.127	**0.346** *
(Western Blot)	*p*-value	0.177	**0.004** *
EGFR Expression			Erlotinib
EGFR Gene	*r*-value	0.135	−0.245
Copy Number	*p*-value	0.160	**0.029** *
EGFR Expression	*r*-value	0.133	**−0.458** *
(Microarray)	*p*-value	0.164	$\mathbf{1.15 \times 10^{-4}}$ *
EGFR Expression	*r*-value	0.077	**−0.379** *
(PCR Slot Blot)	*p*-value	0.291	**0.002** *
EGFR Expression	*r*-value	0.166	**−0.376** *
(Protein Array)	*p*-value	0.113	**0.001** *
***N-/K-/H-RAS* Mutations**			Melphalan
TP53 Mutation	r-value	0.052	**0.367** *
(cDNA Sequencing)	*p*-value	0.354	**0.002** *

Table 2. *Cont.*

		Myricetin (log_{10} IC_{50}, M)	Control Drug (log_{10} IC_{50}, M)
TP53 Mutation			5-Fluorouracil
TP53 Mutation	*r*-value	0.077	**−0.502 ***
(cDNA Sequencing)	*p*-value	0.290	**3.50×10^{-5} ***
TP53 Function	*r*-value	0.211	**−0.436 ***
(Yeast Functional Assay)	*p*-value	0.071	**5.49×10^{-4} ***
WT1 Expression			Ifosfamide
WT1 Expression	*r*-value	0.064	**−0.316 ***
(Microarray)	*p*-value	0.320	**0.007 ***
GSTP1 Expression			Etoposide
GSTP1 Expression	*r*-value	−0.257	**0.399**
(Microarray)	*p*-value	**0.028**	**9.58×10^{-4} ***
GST Expression	*r*-value	−0.225	**0.509**
(Northern Blot)	*p*-value	**0.048**	**2.24×10^{-5} ***
HSP90 Expression			Geldanamycin
HSP90 Expression	*r*-value	−0.172	**−0.392 ***
(Microarray)	*p*-value	0.105	**0.001 ***
Proliferation			5-Fluorouracil
Cell Doubling	*r*-value	0.258	**0.627 ***
	p-value	**0.031**	**7.14×10^{-6} ***

3.10. Survival Analysis

Finally, we explored the relevance of COX2 expression for the survival prognosis of cancer patients. We speculated that a COX2 inhibitor (e.g., myricetin) should be more effective in tumors with high COX2 expression. A second assumption was that the connection between inflammation and COX2 expression is related to cancer growth, which might imply that high expression is related to short survival. Hence, COX2 inhibitors might contribute to the prolongation of the survival prognosis. Therefore, we performed Kaplan–Meier survival analyses using the KMPlotter database. The analysis of 21 tumor types revealed that high COX2 mRNA expression significantly correlated with shorter overall survival times in patients suffering from renal clear cell carcinoma than low COX2 expression (Figure 9A; $p = 1.2 \times 10^{-4}$). Refining the analyses within this group of patients showed that female patients with renal clear cell carcinoma with high COX2 expression died significantly earlier than those with low COX2 expression (Figure 9B; $p = 3 \times 10^{-5}$). Similarly, patients with low neoantigen load and high COX2 expression in their renal clear cell tumors had a worse survival prognosis than those with high COX2 expression (Figure 9C; $p = 3 \times 10^{-5}$). This data indicates that COX2-inhibiting compounds from chamomile tea might exert beneficial effects in the prevention and treatment of this tumor type.

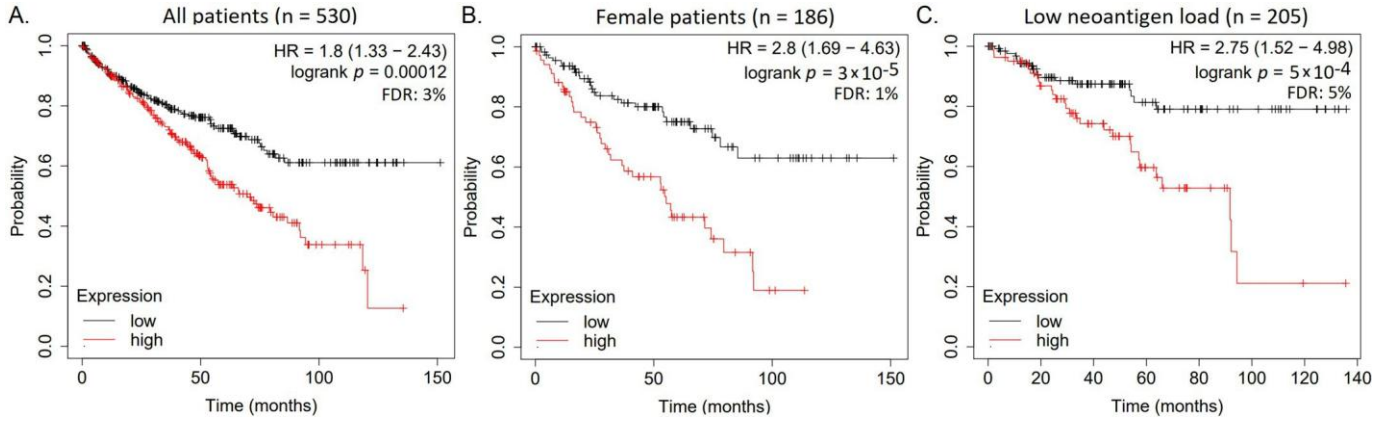

Figure 9. Kaplan–Meier statistics of overall survival time (months) for renal clear cell carcinoma correlating with the expression of *COX2* mRNA obtained from the KMPlotter database. (**A**) All patient profiles: *COX2* mRNA expression correlates significantly with overall survival time, $p = 1.2 \times 10^{-4}$. (**B**) Female patients' profile: *COX2* mRNA expression correlates significantly with overall survival time, $p = 3 \times 10^{-5}$. (**C**) Patients with low neoantigen load and high *COX2* expression in their renal clear cell tumors had a worse survival prognosis than those with high *COX2* expression, $p = 3 \times 10^{-5}$.

4. Discussion

Chamomile tea has been widely utilized as a spice for food preservation and in traditional medicine. Its phenolic and flavonoid attributes offer anti-inflammatory and antioxidant properties [58]. Extensive research has been conducted on the cellular and molecular mechanisms of chamomile tea constituents against cancer, such as apigenin [59]. Since inflammation is related to carcinogenesis [60], we focused this study on the phytochemical constituents of chamomile tea and their effects against COX2, as well as their anti-inflammatory and cytotoxic activities on cancer cells.

In understanding the beneficial effect, phytochemistry plays a crucial role in characterizing the composition of secondary plant metabolites [61]. In chamomile tea, more than 200 substances have been identified from the classes of flavonoids, terpenoids, alkaloids, tannins, and polyphenols [62]. Other teas also contain compounds of these chemical classes, with differences in the specific types and quantities of their substances. For example, chamomile tea does not contain caffeine, while black, green, pu-erh, and oolong teas contain varying high amounts of caffeine [63]. Catechin is found in a very high quantity in green tea due to its minimized antioxidant capacity compared to chamomile, black, and peppermint tea [64,65], and chamomile tea is also the richest in apigenin in contrast to peppermint tea [66]. The question is whether or not the interaction between these different substances may be synergetic or additive. We suggest that the death of cancer cells is more probable if exposed to a combination of various substances in an additive manner rather than surrendering in a synergistic way, which means that the cell has an evolutionary mechanism predisposed to it. Moreover, the concept has been explored as to whether phytochemicals may act synergistically or additively as chemopreventive agents or if combined with cancer drugs for therapeutic intervention. This has been documented in several studies [67–69].

COX2 is an enzyme that plays a major role in inflammation and carcinogenesis. Since it is produced only during inflammation to catalyze the conversion of arachidonic acid to different prostaglandins [70]. Furthermore, arachidonic acid derivatives, including endocannabinoids such as 2-arachidonyl-glycerol, are capable of selectively binding to COX2 to undergo oxygenation and catalysis, resulting in the synthesis of hydroxyl-endoperoxide analogs. The prostaglandin H analog is then converted into glyceryl prostaglandins, including prostaglandin E2 and prostaglandin I2, which have anti-inflammatory and proliferative properties [71,72].

The positive feedback loop between COX2 expression and PGE2 production is involved in multiple cellular mechanisms and pathways, which, among other functions, can contribute to the promotion of tumor growth [73]. Hence, the development of COX2 inhibitors is crucial for treating both inflammation and cancer. Unlike traditional non-steroidal anti-inflammatory drugs (NSAIDs) that can have severe gastrointestinal side effects due to the suppression of COX1, COX2 selective inhibitors celecoxib, rofecoxib, and valdecoxib have fewer side effects. Nevertheless, it has been observed clinically that COXIBs can lead to cardiovascular toxicity [74]. Considering this, we investigated the potential of chamomile tea to inhibit COX2 and its cytotoxic effects against different cancer types. For that purpose, we conducted resazurin assays to measure the growth-inhibitory effects of chamomile extract against hematopoietic tumor cell lines (leukemia, multiple myeloma) and colon cancer cells. Hematopoietic cancer cells are frequently more sensitive to cytotoxic agents than solid cancer cells. This was also observed with our chamomile extract. We used two colon cancer cell lines: a p53 wildtype and a knockout line. The tumor suppressor p53 is not only a major driver of carcinogenesis if it is mutated but also causes resistance to anticancer drugs [75]. In previous investigations, we found that HCT116 $p53^{-/-}$ cells were resistant to the standard anticancer drug doxorubicin [76]. The p53 knockout cells were also moderately but significantly resistant to the chamomile extract compared to p53 wildtype cells (2.65-fold).

We have also performed virtual screening and molecular docking. By calculating the lowest binding energies of more than 200 compounds, we were able to focus on a few promising molecules to conduct a COX2 inhibitor screening assay for testing their activity against COX2. Subsequently, we narrowed our focus on myricetin to study its effect against cancer in addition to inflammation by conducting multiple advanced analyses such as oncobiogram, proteome, and Kaplan–Meier survival analyses.

Our results from molecular docking and the COX2 inhibition screening assay were significantly correlative. Seven of our compounds (β-sitosterol, β-amyrin, dausosterol, β-eudesmol, apigenin, farnesol, and myricetin) demonstrated high affinity binding to COX2. Moreover, the 60 NCI analyses have shown that β-sitosterol, β-eudesmol, and daucosterol were less effective on cancer cells compared to apigenin, myricetin, and farnesol. As we previously worked on apigenin and farnesol [55,56], we turned our focus to myricetin in the present investigation. The latter compound was more active against colon and lung cancer than other tumor types. This correlated with previous studies revealing that colon and lung cancers, among other tumor types, exhibited excessive COX2 expression [77,78]. More importantly, cell proliferation and anti-apoptosis effects were activated in colon cancer by the binding of prostaglandin E2 to its corresponding prostaglandin E2 receptor and to its respective G-protein, which stimulated the release of epidermal growth receptor (EGR) responsible for the activation of extracellular kinase ERK and the AKT/PI3kinase pathway, and in lung cancer, the PGE2-EP1R-Gq complex triggered cell growth through the activation of phospholipase C and ERK [79].

An important aspect is that the expression of target proteins such as COX2 may not be of equal prognostic value in all cancer types. We mined the KM Plotter database to associate COX2 expression with survival times in various tumor types. This approach was recently also applied to antioxidant response genes and tumor suppressor genes [48,80].

High COX2 expression was significantly associated with a shorter survival probability in renal clear cell carcinoma patients, indicating that COX2 inhibition by myricetin might positively affect the survival times for patients suffering from this tumor type. Here, we found that high COX2 expression in renal clear cell carcinoma was associated with shorter overall survival times for patients, and female patients with high COX2 expression died significantly earlier than those with low COX2 expression. Moreover, patients with a low neoantigen load and high COX2 expression had a worse survival prognosis than those with high COX2 expression. It can be speculated that patients with low neoantigen loads might be less susceptible to immunotherapy approaches than those with high neoantigen loads and, thus, might be more immunotherapy-resistant [47].

Our findings suggest that targeting COX2 expression with compounds such as myricetin could be a promising strategy for improving the survival prognosis of patients with renal clear cell carcinoma, especially tumors with low neoantigen loads. It may be hypothesized that myricetin might be effective in this subgroup of patients.

Furthermore, we also found from the oncobiogram analysis that myricetin may also inhibit tubulin and tyrosine kinases. Substantially, this finding has been reinforced with our obtained data from immunofluorescence microscopy of the effect of myricetin on α-tubulin. Myricetin at concentrations of 0.1 and 1 µM has blocked microtubule polymerization in a comparable manner as vincristine at 1 µM. Microtubules are composed of tubulin. They are responsible for the maintenance and stabilization of endothelial cells. The discovery of novel tubulin inhibitors plays an important role in tumor vasculature-based therapies [81]. Hence, the inhibition of tubulin by myricetin may not only be linked to the inhibition of COX2 but also to the inhibition of endothelial cell responses. Interestingly, many authors suggested that COX2 and PGE2 may work together to activate receptor tyrosine kinases, which are involved in regulating cell growth and division, e.g., in colon cancer [82,83]. In addition, COX2 overexpression in cancer cells elevated PGE2 production, which in turn activated vascular endothelial growth factor (VEGF) and/or other endothelial cell responses, promoting angiogenesis [73,79,84].

Additionally, in our analysis, we found that myricetin is not related to classical anticancer drug resistance mechanisms such as ATP-binding cassette (ABC) transporters (P-glycoprotein/ABCB1, ABCB5, ABCC1, ABCG2), tumor suppressors (TP53, WT1), or oncogenes (EGFR, RAS), except for glutathione S-transferase P (GSTP) and cellular proliferation rates.

COX2 overexpression contributed to P-glycoprotein-mediated multidrug resistance via regulation of c-Jun N-terminal protein kinase (JNK), which phosphorylates the transcription factor c-Jun on its N-terminus at Ser63/73 (pc-Jun) in colorectal cancer [85]. This could be an explanation for the absence of cross-resistance of P-glycoprotein-expressing cells towards myricetin.

WT1 is a tumor suppressor that produces different transcription factors that promote cell growth and survival. While its mutation has been initially linked to childhood kidney cancer (Wilms tumor), studies have suggested that WT1 can play either a promoting or inhibitory role in tumor formation and apoptosis in many tumor types [86–88]. A combined therapy targeting COX2 and WT1 has been proposed, as the two pathways have been shown to synergistically promote tumor cell proliferation in lung cancer. The authors found that suppressing the COX2 pathway with celecoxib increased WT1 expression, which may explain why myricetin did not appear to affect cross-resistance in WT1-expressing tumors [89]. Knocking down the WT1 gene led to an upregulation of COX2, particularly in Wilms' tumors, suggesting that inhibiting COX2 in combination with other targeted treatments could be beneficial in treating cancer [90,91]. P53 is also a tumor suppressor that regulates cell growth and promotes apoptosis (controlling cell cycle arrest) but, in parallel, also plays a crucial role in the progression of many cancer types when it is mutated. The *TP53* gene is mutated in several cancer types, including lung and colon cancer, and regaining its functions is an important therapeutic approach in cancer [92–94]. Genotoxic stress-induced p53 activated the Ras/Raf/MAPK pathway that led to COX2 expression downstream [95]. Moreover, COX2 promoted tumorigenesis by inhibiting the transcriptional activity of normal functional p53 and DNA damage-induced apoptosis. Further, The COX2-inhibitor NS-398 blocked the interaction between COX2 and p53, which activated apoptosis [96]. It has been discussed that the crosstalk between COX2 and p53 happens through different pathways [97].

There is a lot of published evidence that mutant p53 contributes to multidrug resistance [94]. It has been proposed to reduce drug resistance by increasing wild-type p53 in cancer. Myricetin increases the expression of the p53 protein and alters the function of Bcl-2 proteins, resulting in increased activity of apoptotic pathways such as Bax and Bak, which are also regulated by p53 [98]. This finding is particularly relevant because previous

investigations showed that the PGE2 ligand–receptor complex induced by COX2 inhibited the activation of Bax [99]. Consequently, we hypothesize that the crosstalk between p53 and COX2 and the COX2 inhibition by myricetin may explain why p53-mutant cells were not cross-resistant to myricetin. Nevertheless, we also found HCT116p53$^{-/-}$ cells were resistant to our chamomile extract compared to HCT116p53$^{+/+}$ cells. An explanation could be that other compounds, but not myricetin, in the chamomile extract were responsible for the resistance.

The epidermal growth factor receptor (EGFR) is a key factor in cell growth and is highly expressed in various carcinoma types, with lung and colon cancers being among the most affected. The activation of EGFR is essential for many cancer pathways, making it a prime target for cancer therapy. Despite the effectiveness of EGFR tyrosine kinase inhibitors in lung cancer treatment, resistance often develops through the activation of alternative pathways such as c-Met, HGF, and AXL, as well as divergent downstream pathways such as Ras/Raf/MAPK, Akt, and STAT. The Ras family, which includes H-Ras, N-Ras, and K-Ras, is one of the earliest discovered oncogenes and plays a crucial role in cell growth and proliferation by binding to the Raf and MAPK pathways controlled by EGFR. Mutations in Ras confer resistance to cancer drugs, making them a challenge in cancer therapy [100–103]. It is now well known that Ras mutant tumors are inherently resistant to anticancer agents, necessitating the development of alternative treatment strategies, and several agents targeting signaling components in the MAPK and PI3K pathways downstream of mutant K-Ras are currently undergoing clinical trials [104].

Myricetin has been reported to interact with and alter pathways such as AKT [105–108], which are linked to COX2. Myricetin-mediated COX2 inhibition might block EGFR- and Ras-related signaling cascades, potentially making tumor cells more sensitive to drugs and more susceptible to the blockade of cancer cell survival.

In the NCI cell line panel, there was no cross-resistance of myricetin to epirubicin, maytansine, vinblastine, pancratistatin (ABC transporters control drugs), erlotinib (EGFR inhibitor), melphalan (Ras control drug), 5-fluorouracil (p53 control drug), or ifosfamine (WT1 control drug). Nevertheless, there was a significant correlation with etoposide, which was used as the control drug for GSTP1. This is an enzyme mostly known for its detoxification, cytoprotective, and anti-apoptotic activities [109]. In aberrant crypt foci (ACF) in colonic adenoma, COX2 was inactive and GSTP1 was active, allowing ACF proliferation. ACF were also resistant to deoxycholic acid-induced apoptosis through this detoxification process rather than inflammation [110]. The activity of plant polyphenols and flavonoids against both GSTP1-1 and CS-X pumps on breast cancer cell lines has been investigated. Due to its multiple hydroxyl groups, myricetin had no inhibitory effect on GSTP1-1 and only a moderate effect on CS-X compared to two strongly active flavonoids, quercetin and luteolin [111]. GSTP1 plays an active role in cancer and contributes to drug resistance through its detoxification capability, and myricetin does not affect the function of GSTP1, which may explain the missing cross-resistance of GSTP1 to myricetin in the NCI cell line panel.

The main concept of our research efforts is to find cytotoxic compounds that can be used as functional food ingredients with negative side effects and that are able to bypass multidrug resistance or even provoke collateral sensitivity in resistant tumor cells [112–115]. Myricetin is a flavonoid present in tea, wine, fruits, and vegetables [116]. For decades, myricetin has been recognized for its antioxidant, anticancer, antidiabetic, and anti-inflammatory activities [117–120]. Furthermore, it has been reported that myricetin reduces resistance to anticancer drugs and other cytotoxic agents. Among them were camptothecin and podophyllotoxin by inducing topoisomerase I/II-DNA complex, cisplatin in ovarian and colon cancer cells by inducing apoptosis through Bax/Bcl-2 proteins, resveratrol in an additive manner by inhibiting 12-*O*-tetradecanoylphorbol-13-acetate (TPA) and EGF, as well as vincristine by blocking ABCC1 (MRP1) and ABCC2 (MRP2) [98,119,121,122].

There are findings that suggest that exposure to carcinogens may not only initiate carcinogenesis but also confer resistance to the very agents used to treat tumors [123–126].

Moreover, inflammation plays a significant role in the process of carcinogenesis, particularly in prostate and colon cancer. It is common sense that chronic inflammation leads to DNA damage, tissue damage, and abnormal cell growth that can ultimately result in cancer. Chemoprevention is a promising approach to preventing cancer by using natural or synthetic compounds to inhibit the development of cancer at its earliest stages. Several studies have demonstrated that anti-inflammatory agents prevent the initiation, promotion, and progression of cancer by modulating various molecular targets. Therefore, targeting inflammation through chemoprevention may represent a promising strategy for preventing cancer development and progression [127–131].

Therefore, it is straightforward to elaborate on chamomile, which contains not only myricetin but also various other bioactive compounds, including apigenin, farnesol, quercetin, and luteolin, to act as chemopreventive agents. This notion was supported by our growth inhibition assay, where the chamomile extract demonstrated significant activity against several cancer cell lines. It could, thus, be hypothesized that chamomile tea may help to prevent cancer and also suppress cancer cell growth at the early stages of tumor development.

For this reason, we used proteome analysis to gain more insights into the molecular mechanisms underlying the sensitivity and resistance of cancer cell lines to myricetin. The expression of 3171 proteins was determined in the NCI cell line panel [42] and correlated with the $\log_{10}IC_{50}$ values of these cell lines for myricetin in the present investigation. The top 20 directly correlating proteins (indicating myricetin resistance) and the top 20 inversely correlating proteins (indicating myricetin sensitivity) were subjected to hierarchical cluster analysis. The distribution of the myricetin-resistant cell lines in clusters 1 and 2 and the myricetin-sensitive cell lines in cluster 3 was statistically significant (p = 0.00049). The 40 relevant proteins associated with cellular myricetin responsiveness are involved in a variety of multifactorial interactions.

The formation of clusters A–D has been performed to better illustrate the distribution of protein expression in clusters 1–4 (i.e., red and green fields). The assembly of proteins in clusters A–D occurred according to their degrees of protein up- or downregulation in the specific tumor cell lines. A preferential assembly of the molecular and cellular functions of these proteins was not observed in clusters A–D. However, many proteins with functions relevant to cancer were identified from this proteomic analysis (Supplementary Table S2), e.g., proteins involved in mRNA metabolism (DDX39B, CSNK2A, RPL18A, MRTO4, DDX21, BRIX1, HINT2, YTHDC1, and EEF1A1), proteins involved in programmed cell death (TP53I3, DDRGK, EIF5A, PDCD5, and PDCD6), proteins involved in cell growth, differentiation, and genome stability (CDK2, NELFA, PODXL, PKN2, THOC5, and BLM), transcription factors and signal transduction proteins (ADNP, ZNF428, SSRP1, TSNAX, DUSPP3, RAB38, and TCP1), and others (FBO2, COL4A3, DNAJA2, GSN, MRC2, UGP2, TPP1, NUCB2, CTSB, CLTA, CTSD, and VPS33B). The exact mechanisms by which these proteins influence sensitivity or resistance to myricetin are largely unknown at present but deserve further investigation in the future. Clearly, the sensitivity and resistance of cancer cells to myricetin are multi-factorially determined. The identified proteins might be used to predict, prior to treatment, the responsiveness of cancer cells to myricetin and could guide the development of new therapeutic strategies for individualized cancer treatment.

These results are in agreement with a multitude of previous observations that natural products rather act by multiple mechanisms than by single mechanisms [57]. Additionally, the pharmacological effects of phytotherapeutics may result from synergetic interactions among multiple phytochemicals. Therefore, it is important to better understand the synergistic effects of herbal mixtures to develop more effective multi-target drugs with fewer side effects [132]. The generation of expression profiles to predict the response to chemotherapy is an important step toward individualizing chemotherapy [133,134]. In this context, the role of natural products cannot be ignored. If the profiles of standard drugs are known, then we could look for phytochemicals with fundamentally different expression profiles. This could provide a rational basis to make resistant and refractory tumors responsive to therapy again [135–137]. In the past, we have mainly used transcriptomics and

epigenomics [138–143]. The significance of such profiles for cancer prevention with tea is also worth noting, as it has a different profile than cytostatic drugs. Overall, the use of expression profiles from natural products offers promising avenues for improving cancer treatment and prevention.

5. Conclusions

In conclusion, the effects of tea on cancer prevention and therapy are not solely attributed to apigenin, as previously reported [144–146], but to a combination of many other natural substances. In the present work, we focused particularly on myricetin due to its potential cancer-inhibiting bioactivity. However, the inhibitory effect of myricetin on cancer cells may be moderate and weaker than conventional anticancer drugs, making it more appropriate for cancer prevention than therapy. Nonetheless, the potential of myricetin and other natural substances in cancer prevention and treatment cannot be ignored. Therefore, our findings provide valuable insights into the potential of natural substances for cancer prevention and as an additive to cancer therapy. Ultimately, the development of effective cancer prevention strategies is critical to reducing the burden of this disease on individual cancer patients. The potential of myricetin for individualized treatment is worth further exploring in the future.

Supplementary Materials: The following supporting information can be downloaded at: https://www.mdpi.com/article/10.3390/app13158935/s1, Table S1: Phyto chemical profiling of Chamomile (*Matricaria chamomilla* L.); Table S2: Correlation of constitutive mRNA expression of genes identified by COMPARE analysis with $\log_{10}IC_{50}$ values for myricetin of the NCI tumor cell lines.

Author Contributions: A.I.D. performed the experiments and analyses; B.A. performed the phytochemical analysis; I.A.K. edited the manuscript; and T.E. supervised the project and wrote the manuscript. All authors have read and agreed to the published version of the manuscript.

Funding: This research received no external funding.

Institutional Review Board Statement: Not applicable.

Informed Consent Statement: Not applicable.

Data Availability Statement: Data are available upon reasonable request.

Acknowledgments: We thank the Microscope Core Facility at the Institute of Molecular Biology (Marton Gelléri, Institute of Molecular Biology gGmbH (IMB), Mainz, Germany) for their kind training and technical support for the microscopy-related experiment.

Conflicts of Interest: The authors declare that there are no conflict of interest.

References

1. McKay, D.L.; Blumberg, J.B. The Role of Tea in Human Health: An Update. *J. Am. Coll. Nutr.* **2013**, *21*, 1–13. [CrossRef]
2. Srivastava, J.K.; Shankar, E.; Gupta, S. Chamomile: A Herbal Medicine of the Past with a Bright Future (Review). *Mol. Med. Rep.* **2010**, *3*, 895–901.
3. Hassan, D.M.A.; Salah-Eldin, A.A. Amerolative Influence of Chamomile (*Matricaria recutita* L.) on Synthetic Food Additive Induced Probable Toxicity in Male Albino Rats. *J. Food Dairy Sci. J.* **2021**, *12*, 161–170. [CrossRef]
4. *CFR—Code of Federal Regulations Title 21*; Food and Drug Administration: Silver Spring, MD, USA, 2023; p. 3.
5. Sándor, Z.; Mottaghipisheh, J.; Veres, K.; Hohmann, J.; Bencsik, T.; Horváth, A.; Kelemen, D.; Papp, R.; Barthó, L.; Csupor, D. Evidence Supports Tradition: The in Vitro Effects of Roman Chamomile on Smooth Muscles. *Front. Pharmacol.* **2018**, *9*, 323. [CrossRef] [PubMed]
6. Pirouzpanah, S.; Mahboob, S.; Sanayei, M.; Hajaliloo, M.; Safaeiyan, A. The Effect of Chamomile Tea Consumption on Inflammation among Rheumatoid Arthritis Patients: Randomized Clinical Trial. *Prog. Nutr.* **2017**, *19*, 27–33. [CrossRef]
7. Bayliak, M.M.; Dmytriv, T.R.; Melnychuk, A.V.; Strilets, N.V.; Storey, K.B.; Lushchak, V.I. Chamomile as a Potential Remedy for Obesity and Metabolic Syndrome. *EXCLI J.* **2021**, *20*, 1261–1286. [CrossRef]
8. Srivastava, J. Antiproliferative and Apoptotic Effects of Chamomile Extract in Various Human Cancer Cells. *J. Agric. Food Chem.* **2007**, *55*, 9470–9478. [CrossRef]
9. Srivastava, J.K.; Pandey, M.; Gupta, S. Chamomile, a Novel and Selective COX-2 Inhibitor with Anti-Inflammatory Activity. *Life Sci.* **2009**, *85*, 663–669. [CrossRef]

10. Chang, S.M.; Chen, C.H. Effects of an Intervention with Drinking Chamomile Tea on Sleep Quality and Depression in Sleep Disturbed Postnatal Women: A Randomized Controlled Trial. *J. Adv. Nurs.* **2016**, *72*, 306–315. [CrossRef]
11. Gh, D.; Kermanian, S.; Mozaffari-Khosravi, H.; Dastgerdi, G.; Zavar-Reza, J.; Rahmanian, M. The Effect of Chamomile Tea versus Black Tea on Glycemic Control and Blood Lipid Profiles in Depressed Patients with Type 2 Diabetes: A Randomized Clinical Trial. *J. Nutr. Food Secur.* **2018**, *3*, 157–166.
12. Ghamchini, V.M.; Salami, M.; Mohammadi, G.R.; Moradi, Z.; Kavosi, A.; Movahedi, A.; Bidkhori, M.; Aryaeefar, M.R. The Effect of Chamomile Tea on Anxiety and Depression in Cancer Patients Treated with Chemotherapy. *J. Young Pharm.* **2019**, *11*, 309–312. [CrossRef]
13. Paula Gardiner Chamomile (Matricaria Recutita, Anthemis Nobilis). The Longwood Herbal Task Force and The Center for Holistic Pediatric Education and Research. 1999, pp. 1–21. Available online: https://tratamientocelular.com/papers/cmran.pdf (accessed on 31 March 2023).
14. El Joumaa, M.M.; Borjac, J.M. Matricaria Chamomilla: A Valuable Insight into Recent Advances in Medicinal Uses and Pharmacological Activities. *Phytochem. Rev.* **2022**, *21*, 1913–1940. [CrossRef]
15. Wu, B.Y.; Liu, C.T.; Su, Y.L.; Chen, S.Y.; Chen, Y.H.; Tsai, M.Y. A Review of Complementary Therapies with Medicinal Plants for Chemotherapy-Induced Peripheral Neuropathy. *Complement. Ther. Med.* **2019**, *42*, 226–232. [CrossRef]
16. Salehi, B.; Jornet, P.L.; López, E.P.F.; Calina, D.; Sharifi-Rad, M.; Ramírez-Alarcón, K.; Forman, K.; Fernández, M.; Martorell, M.; Setzer, W.N.; et al. Plant-Derived Bioactives in Oral Mucosal Lesions: A Key Emphasis to Curcumin, Lycopene, Chamomile, Aloe Vera, Green Tea and Coffee Properties. *Biomolecules* **2019**, *9*, 106. [CrossRef] [PubMed]
17. Tai, Y.; Ling, C.; Wang, C.; Wang, H.; Su, L.; Yang, L.; Jiang, W.; Yu, X.; Zheng, L.; Feng, Z.; et al. Analysis of Terpenoid Biosynthesis Pathways in German Chamomile (*Matricaria recutita*) and Roman Chamomile (*Chamaemelum nobile*) Based on Co-Expression Networks. *Genomics* **2020**, *112*, 1055–1064. [CrossRef] [PubMed]
18. Nováková, L.; Vildová, A.; Mateus, J.P.; Gonalves, T.; Solich, P. Development and Application of UHPLC-MS/MS Method for the Determination of Phenolic Compounds in Chamomile Flowers and Chamomile Tea Extracts. *Talanta* **2010**, *82*, 1271–1280. [CrossRef]
19. Power, F.B.; Browning, H. CCXI.—The Constituents of the Flowers of Matricaria Chamomilla. *J. Chem. Soc. Trans.* **1914**, *105*, 2280–2291. [CrossRef]
20. Lefort, É.C.; Blay, J. Apigenin and Its Impact on Gastrointestinal Cancers. *Mol. Nutr. Food Res.* **2013**, *57*, 126–144. [CrossRef]
21. Xu, Y.; Xin, Y.; Diao, Y.; Lu, C.; Fu, J.; Luo, L.; Yin, Z. Synergistic Effects of Apigenin and Paclitaxel on Apoptosis of Cancer Cells. *PLoS ONE* **2011**, *6*, e29169. [CrossRef]
22. Patel, D.; Shukla, S.; Gupta, S. Apigenin and Cancer Chemoprevention: Progress, Potential and Promise (Review). *Int. J. Oncol.* **2007**, *30*, 233–245. [CrossRef]
23. Srivastava, J.K.; Gupta, S. Extraction, Characterization, Stability and Biological Activity of Flavonoids Isolated from Cham-omile Flowers. *Mol. Cell. Pharmacol.* **2009**, *1*, 138. [CrossRef]
24. Bhaskaran, N.; Shukla, S.; Srivastava, J.K.; Gupta, S. Chamomile: An Anti-Inflammatory Agent Inhibits Inducible Nitric Oxide Synthase Expression by Blocking RelA/P65 Activity. *Int. J. Mol. Med.* **2010**, *26*, 935–940. [CrossRef] [PubMed]
25. Rajakariar, R.; Yaqoob, M.M.; Gilroy, D.W. COX-2 in Inflammation and Resolution. *Mol. Interv.* **2006**, *6*, 199. [CrossRef] [PubMed]
26. Williams, C.S.; Mann, M.; DuBois, R.N. The Role of Cyclooxygenases in Inflammation, Cancer, and Development. *Oncogene* **2000**, *18*, 7908–7916. [CrossRef] [PubMed]
27. Vardeh, D.; Wang, D.; Costigan, M.; Lazarus, M.; Saper, C.B.; Woolf, C.J.; Fitzgerald, G.A.; Samad, T.A. COX2 in CNS Neural Cells Mediates Mechanical Inflammatory Pain Hypersensitivity in Mice. *J. Clin. Investig.* **2009**, *119*, 287–294. [CrossRef]
28. Seibert, K.; Masferrer, J.L. Role of Inducible Cyclooxygenase (COX-2) in Inflammation. *Receptor* **1994**, *4*, 17–23.
29. Avula, B.; Bae, J.Y.; Wang, Y.H.; Wang, M.; Ali, Z.; Khan, I.A. Chemical Profiling and Characterization of Anthraquinones from Two Bulbine Species and Dietary Supplements Using Liquid Chromatography–High Resolution Mass Spectrometry. *J. AOAC Int.* **2021**, *104*, 1394–1407. [CrossRef] [PubMed]
30. Avula, B.; Sagi, S.; Masoodi, M.H.; Bae, J.Y.; Wali, A.F.; Khan, I.A. Quantification and Characterization of Phenolic Compounds from Northern Indian Propolis Extracts and Dietary Supplements. *J. AOAC Int.* **2020**, *103*, 1378–1393. [CrossRef] [PubMed]
31. Supianto, A.A.; Nurdiansyah, R.; Weng, C.W.; Zilvan, V.; Yuwana, R.S.; Arisal, A.; Pardede, H.F.; Lee, M.M.; Huang, C.H.; Ng, K.L. Cluster-Based Text Mining for Extracting Drug Candidates for the Prevention of COVID-19 from the Biomedical Literature. *J. Taibah Univ. Med. Sci.* **2023**, *18*, 787–801. [CrossRef]
32. PyRx (Version 0.8). Available online: https://pyrx.sourceforge.io/ (accessed on 31 March 2023).
33. Lucido, M.J.; Orlando, B.J.; Vecchio, A.J.; Malkowski, M.G. Crystal Structure of Aspirin-Acetylated Human Cyclooxygenase-2: Insight into the Formation of Products with Reversed Stereochemistry HHS Public Access. *Biochemistry* **2016**, *55*, 1226–1238. [CrossRef]
34. RCSB PDB—5F1A: The Crystal Structure of Salicylate Bound to Human Cyclooxygenase-2. Available online: https://www.rcsb.org/structure/5F1A (accessed on 31 March 2023).
35. UCSF Chimera Home Page. Available online: https://www.cgl.ucsf.edu/chimera/ (accessed on 30 March 2023).
36. Search|Scripps Research. Available online: https://www.scripps.edu/search/?s=autodocktools (accessed on 31 March 2023).

37. Morris, G.M.; Goodsell, D.S.; Pique, M.E.; Huey, R.; Forli, S.; Hart, W.E.; Halliday, S.; Belew, R.; Olson, A.J. User Guide AutoDock Version 4.2 Updated for Version 4.2.6 Automated Docking of Flexible Ligands to Flexible Receptors; 1991. Available online: http://autodock.scripps.edu/ (accessed on 30 March 2023).
38. AutoDock. Available online: https://autodock.scripps.edu/ (accessed on 31 March 2023).
39. Yadav, T.C.; Kumar, N.; Raj, U.; Goel, N.; Vardawaj, P.K.; Prasad, R.; Pruthi, V. Exploration of Interaction Mechanism of Tyrosol as a Potent Anti-Inflammatory Agent. *J. Biomol. Struct. Dyn.* **2019**, *38*, 382–397. [CrossRef] [PubMed]
40. Free Download: BIOVIA Discovery Studio Visualizer—Dassault Systèmes. Available online: https://discover.3ds.com/discovery-studio-visualizer-download (accessed on 30 March 2023).
41. *ab283401*; COX-2 Inhibitor Screening Kit (Fluorometric). Abcam plc.: Singapore, 2020.
42. About NCI—NCI. Available online: https://www.cancer.gov/about-nci (accessed on 30 March 2023).
43. Alley, M.C.; Scudiere, D.A.; Monks, A.; Hursey, M.L.; Czerwinski, M.J.; Fine, D.L.; Abbott, B.J.; Mayo, J.G.; Shoemaker, R.H.; Boyd, M.R. Feasibility of drug screening with panels of human tumor cell lines using a microculture tetrazolium assay1. *Cancer Res.* **1988**, *48*, 89–90.
44. Developmental Therapeutics Program (DTP). Available online: https://dtp.cancer.gov/ (accessed on 30 March 2023).
45. Investigations of Anticancer Compounds from Camellia Sinensis: Green, Black, and White Tea—ProQuest. Available online: https://www.proquest.com/docview/1625976354?fromopenview=true&pq-origsite=gscholar (accessed on 22 July 2023).
46. Kuete, V.; Wabo, H.K.; Eyong, K.O.; Feussi, M.T.; Wiench, B.; Krusche, B.; Tane, P.; Folefoc, G.N.; Efferth, T. Anticancer Activities of Six Selected Natural Compounds of Some Cameroonian Medicinal Plants. *PLoS ONE* **2011**, *6*, e21762. [CrossRef] [PubMed]
47. Kaplan-Meier Plotter. Available online: https://kmplot.com/analysis/ (accessed on 30 March 2023).
48. Lánczky, A.; Gyo˝rffy, B. Web-Based Survival Analysis Tool Tailored for Medical Research (KMplot): Development and Implementation. *J. Med. Internet Res.* **2021**, *23*, e27633. [CrossRef] [PubMed]
49. Nagy, Á.; Munkácsy, G.; Gyo˝rffy, B. Pancancer Survival Analysis of Cancer Hallmark Genes. *Sci. Rep.* **2021**, *11*, 6047. [CrossRef]
50. Benjamini, Y.; Hochberg, Y. Controlling the False Discovery Rate: A Practical and Powerful Approach to Multiple Testing. *J. R. Stat. Soc. Ser. B Stat. Methodol.* **1995**, *57*, 289–300. [CrossRef]
51. Zhou, M.; Boulos, J.C.; Klauck, S.M.; Efferth, T.; Zhou, M.; Boulos, J.C.; Efferth, T.; Klauck, S.M. The Cardiac Glycoside ZINC253504760 Induces Parthanatos-Type Cell Death and G2/M Arrest via Downregulation of MEK1/2 Phosphorylation in Leukemia Cells. *Cell Biol. Toxicol.* **2023**, *3*, 1–27. [CrossRef]
52. Vezzani, B.; Carinci, M.; Previati, M.; Giacovazzi, S.; Della Sala, M.; Gafà, R.; Lanza, G.; Wieckowski, M.R.; Pinton, P.; Giorgi, C. Epigenetic Regulation: A Link between Inflammation and Carcinogenesis. *Cancers* **2022**, *14*, 1221. [CrossRef]
53. Saeed, M.; Efferth, T.; Kadioglu, O.; Khalid, H.; Sugimoto, Y. Activity of the Dietary Flavonoid, Apigenin, against Multidrug-Resistant Tumor Cells as Determined by Pharmacogenomics and Molecular Docking. *J. Immunother. Cancer* **2015**, *3*, 1. [CrossRef]
54. Wei, Z.-F.; Luo, M.; Zhao, C.-J.; Li, C.-Y.; Gu, C.-B.; Wang, W.; Zu, Y.-G.; Efferth, T.; Fu, Y.-J. UV-Induced Changes of Active Components and Antioxidant Activity in Postharvest Pigeon Pea [*Cajanus cajan* (L.) Millsp.] Leaves. *J. Agric. Food Chem.* **2013**, *61*, 1165–1171. [CrossRef]
55. Adham, A.N.; Abdelfatah, S.; Naqishbandi, A.M.; Mahmoud, N.; Efferth, T. Cytotoxicity of Apigenin toward Multiple Myeloma Cell Lines and Suppression of iNOS and COX-2 Expression in STAT1-Transfected HEK293 Cells. *Phytomedicine* **2021**, *80*, 153371. [CrossRef]
56. Kuete, V.; Efferth, T. Molecular Determinants of Cancer Cell Sensitivity and Resistance towards the Sesquiterpene Farnesol. *Pharmaœuticals* **2011**, *4*, 567–580. [CrossRef]
57. Efferth, T.; Koch, E. Complex Interactions between Phytochemicals. *The Multi-Target Therapeutic Concept of Phytotherapy. Curr. Drug Targets* **2011**, *12*, 122–132. [PubMed]
58. Bhattacherjee, S.; Ray, A.; Chakraborty, K. Therapeutic and Ethnopharmacological Role of Chamomile (*Matricaria chamomilla* L.) and Its Holistic Impact on Genomics-A Comprehensive Review. *World J. Pharm. Res.* **2022**, *11*, 705. [CrossRef]
59. Shukla, S.; Gupta, S. Apigenin: A Promising Molecule for Cancer Prevention. *Pharm. Res.* **2010**, *27*, 962–978. [CrossRef]
60. Yasui, Y.; Tanaka, T. Protein Expression Analysis of Inflammation-Related Colon Carcinogenesis. *J. Carcinog.* **2009**, *8*, 10. [CrossRef] [PubMed]
61. Singh, A. (Ed.) *Herbalism, Phytochemistry and Ethnopharmacology*; CRC Press: Boca Raton, FL, USA, 2011.
62. Dai, Y.L.; Li, Y.; Wang, Q.; Niu, F.J.; Li, K.W.; Wang, Y.Y.; Wang, J.; Zhou, C.Z.; Gao, L.N. Chamomile: A Review of Its Traditional Uses, Chemical Constituents, Pharmacological Activities and Quality Control Studies. *Molecules* **2023**, *28*, 133. [CrossRef]
63. Baek, G.H.; Yang, S.W.; Yun, C.I.; Lee, J.G.; Kim, Y.J. Determination of Methylxanthine Contents and Risk Characterisation for Various Types of Tea in Korea. *Food Control* **2022**, *132*, 108543. [CrossRef]
64. Yoo, K.; Hwang, I.K.; Moon, B. Comparative Flavonoids Contents of Selected Herbs and Associations of Their Radical Scavenging Activity with Antiproliferative Actions in V79-4 Cells. *J. Food Sci.* **2009**, *74*, C419–C425. [CrossRef]
65. Cleverdon, R.; Elhalaby, Y.; McAlpine, M.D.; Gittings, W.; Ward, W.E. Total Polyphenol Content and Antioxidant Capacity of Tea Bags: Comparison of Black, Green, Red Rooibos, Chamomile and Peppermint over Different Steep Times. *Beverages* **2018**, *4*, 15. [CrossRef]
66. McKay, D.L.; Blumberg, J.B.; Research Labora-tory, A.; Mayer, J. A Review of the Bioactivity and Potential Health Benefits of Chamomile Tea (*Matricaria recutita* L.). *Phytother. Res.* **2006**, *20*, 519–530. [CrossRef] [PubMed]

67. Rizeq, B.; Gupta, I.; Ilesanmi, J.; AlSafran, M.; Rahman, M.D.M.; Ouhtit, A. The Power of Phytochemicals Combination in Cancer Chemoprevention. *J. Cancer* **2020**, *11*, 4521–4533. [CrossRef] [PubMed]
68. Tanos, V.; Brzezinski, A.; Drize, O.; Strauss, N.; Peretz, T. Synergistic Inhibitory Effects of Genistein and Tamoxifen on Human Dysplastic and Malignant Epithelial Breast Cells In Vitro. *Eur. J. Obstet. Gynecol. Reprod. Biol.* **2002**, *102*, 188–194. [CrossRef]
69. Hemalswarya, S.; Doble, M. Potential Synergism of Natural Products in the Treatment of Cancer. *Phytother. Res.* **2006**, *20*, 239–249. [CrossRef] [PubMed]
70. Chadwick, D.; Goode, J. *Novartis Foundation. Cancer and Inflammation*; John Wiley & Sons: Chichester, UK, 2004; ISBN 047085510X.
71. Alhouayek, M.; Muccioli, G.G. COX-2-Derived Endocannabinoid Metabolites as Novel Inflammatory Mediators. *Trends Pharmacol. Sci.* **2014**, *35*, 284–292. [CrossRef]
72. Rouzer, C.A.; Marnett, L.J. Non-Redundant Functions of Cyclooxygenases: Oxygenation of Endocannabinoids. *J. Biol. Chem.* **2008**, *283*, 8065–8069. [CrossRef]
73. Hashemi Goradel, N.; Najafi, M.; Salehi, E.; Farhood, B.; Mortezaee, K. Cyclooxygenase-2 in Cancer: A Review. *J. Cell Physiol.* **2019**, *234*, 5683–5699. [CrossRef]
74. Rouzer, C.A.; Marnett, L.J. Endocannabinoid Oxygenation by Cyclooxygenases, Lipoxygenases, and Cytochromes P450: Cross-Talk between the Eicosanoid and Endocannabinoid Signaling Pathways. *Chem. Rev.* **2011**, *111*, 5899–5921. [CrossRef]
75. Hientz, K.; Mohr, A.; Bhakta-Guha, D.; Efferth, T. The Role of P53 in Cancer Drug Resistance and Targeted Chemotherapy. *Oncotarget* **2017**, *8*, 8921. [CrossRef]
76. Mbaveng, A.T.; Damen, F.; Guefack, M.G.F.; Tankeo, S.B.; Abdelfatah, S.; Bitchagno, G.T.M.; Çelik, I˙.; Kuete, V.; Efferth, T. 8,8-Bis-(Dihydroconiferyl)-Diferulate Displayed Impressive Cytotoxicity towards a Panel of Human and Animal Cancer Cells. *Phytomedicine* **2020**, *70*, 153215. [CrossRef]
77. Eberhart, C.E.; Coffey, R.J.; Radhika, A.; Giardiello, F.M.; Ferrenbach, S.; Dubois, R.N. Up-Regulation of Cyclooxygenase 2 Gene Expression in Human Colorectal Adenomas and Adenocarcinomas. *Gastroenterology* **1994**, *107*, 1183–1188. [CrossRef] [PubMed]
78. Hida, T.; Yatabe, Y.; Achiwa, H.; Muramatsu, H.; Kozaki, K.-I.; Nakamura, S.; Ogawa, M.; Mitsudomi, T.; Sugiura, T.; Takahashi, T. Increased Expression of Cyclooxygenase 2 Occurs Frequently in Human Lung Cancers, Specifically in Adenocarcinomas. *Cancer Res.* **1998**, *58*, 1761–3764.
79. Rizzo, M.T. Cyclooxygenase-2 in Oncogenesis. *Clin. Chim. Acta* **2011**, *412*, 671–687. [CrossRef] [PubMed]
80. Gyo˝rffy, B. Discovery and Ranking of the Most Robust Prognostic Biomarkers in Serous Ovarian Cancer. *Geroscience* 2023, *submitted*. [CrossRef]
81. Banerjee, S.; Hwang, D.-J.; Li, W.; Miller, D.D. Molecules Current Advances of Tubulin Inhibitors in Nanoparticle Drug Delivery and Vascular Disruption/Angiogenesis. *Molecules* **2016**, *21*, 1468. [CrossRef]
82. Shao, J.; Evers, B.M.; Sheng, H. Prostaglandin E2 Synergistically Enhances Receptor Tyrosine Kinase-Dependent Signaling System in Colon Cancer Cells. *J. Biol. Chem.* **2004**, *279*, 14287–14293. [CrossRef]
83. Han, C.; Michalopoulos, G.K.; Wu, T. Prostaglandin E2 Receptor EP1 Transactivates EGFR/MET Receptor Tyrosine Kinases and Enhances Invasiveness in Human Hepatocellular Carcinoma Cells. *J. Cell Physiol.* **2006**, *207*, 261–270. [CrossRef]
84. Brecht, K.; Weigert, A.; Hu, J.; Popp, R.; Fisslthaler, B.; Korff, T.; Fleming, I.; Geisslinger, G.; Brüne, B. Macrophages Programmed by Apoptotic Cells Promote Angiogenesis via Prostaglandin E2. *FASEB J.* **2011**, *25*, 2408–2417. [CrossRef]
85. Sui, H.; Zhou, S.; Wang, Y.; Liu, X.; Zhou, L.; Yin, P.; Fan, Z.; Li, Q. COX-2 Contributes to P-Glycoprotein-Mediated Multidrug Resistance via Phosphorylation of c-Jun at Ser63/73 in Colorectal Cancer. *Carcinogenesis* **2011**, *32*, 667–675. [CrossRef]
86. Yang, L.; Han, Y.; Saiz, S.; Minden, M.D. A Tumor Suppressor and Oncogene: The WT1 Story. *Leukemia* **2007**, *21*, 868–876. [CrossRef]
87. Scharnhorst, V.; van der Eb, A.J.; Jochemsen, A.G. WT1 Proteins: Functions in Growth and Differentiation. *Gene* **2001**, *273*, 141–161. [CrossRef]
88. Simpson, L.A.; Burwell, E.A.; Thompson, K.A.; Shahnaz, S.; Chen, A.R.; Loeb, D.M. The Antiapoptotic Gene A1/BFL1 Is a WT1 Target Gene That Mediates Granulocytic Differentiation and Resistance to Chemotherapy. *Blood* **2006**, *107*, 4695–4702. [CrossRef] [PubMed]
89. Wu, C.; Li, X.; Zhang, D.; Xu, B.; Hu, W.; Zheng, X.; Zhu, D.; Zhou, Q.; Jiang, J.; Wu, C.; et al. IL-1β-Mediated Up-Regulation of WT1D via MiR-144-3p and Their Synergistic Effect with NF-KB/COX-2/HIF-1α Pathway on Cell Proliferation in LUAD. *Cell. Physiol. Biochem.* **2018**, *48*, 2493–2502. [CrossRef]
90. Fridman, E.; Pinthus, J.H.; Kopolovic, J.; Ramon, J.; Mor, O.; Mor, Y. Expression of Cyclooxygenase-2 in Wilms Tumor: Immunohistochemical Study Using Tissue Microarray Methodology. *J. Urol.* **2006**, *176*, 1747–1750. [CrossRef] [PubMed]
91. Maturu, P.; Jones, D.; Ruteshouser, E.C.; Hu, Q.; Reynolds, J.M.; Hicks, J.; Putluri, N.; Ekmekcioglu, S.; Grimm, E.A.; Dong, C.; et al. Role of Cyclooxygenase-2 Pathway in Creating an Immunosuppressive Microenvironment and in Initiation and Progression of Wilms' Tumor. *Neoplasia* **2017**, *19*, 237–249. [CrossRef] [PubMed]
92. George, D.P. P53 how crucial is its role in cancer? *Int. J. Curr. Pharm. Res.* **2011**, *3*, 19–25.
93. Tomicic, M.T.; Dawood, M.; Efferth, T. Epigenetic alterations upstream and downstream of p53 signaling in colorectal carcinoma. *Cancers* **2021**, *13*, 4072. [CrossRef]
94. Leber, M.F.; Efferth, T. Molecular Principles of Cancer Invasion and Metastasis (Review). *Int. J. Oncol.* **2009**, *34*, 881–895.
95. Han, J.A.; Kim, J.I.; Ongusaha, P.P.; Hwang, D.H.; Ballou, L.R.; Mahale, A.; Aaronson, S.A.; Lee, S.W. p53-mediated induction of Cox-2 counteracts p53- or genotoxic stress-induced apoptosis. *EMBO J.* **2002**, *21*, 5635–5644. [CrossRef]

96. Choi, E.M.; Heo, J.I.; Oh, J.Y.; Kim, Y.M.; Ha, K.S.; Kim, J.I.; Han, J.A. COX-2 regulates p53 activity and inhibits DNA damage-induced apoptosis. *Biochem. Biophys. Res. Commun.* **2005**, *328*, 1107–1112. [CrossRef]
97. de Moraes, E.; Dar, N.A.; Gallo, C.V.D.M.; Hainaut, P. Cross-talks between cyclooxygenase-2 and tumor suppressor protein p53: Balancing life and death during inflammatory stress and carcinogenesis. *Int. J. Cancer* **2007**, *121*, 929–937. [CrossRef] [PubMed]
98. Huang, H.; Chen, A.Y.; Ye, X.; Li, B.; Rojanasakul, Y.; Rankin, G.O.; Chen, Y.C. Myricetin inhibits proliferation of cisplatin-resistant cancer cells through a p53-dependent apoptotic pathway. *Int. J. Oncol.* **2015**, *47*, 1494–1502. [CrossRef] [PubMed]
99. Greenhough, A.; Wallam, C.A.; Hicks, D.J.; Moorghen, M.; Williams, A.C.; Paraskeva, C. The proapoptotic BH3-only protein Bim is downregulated in a subset of colorectal cancers and is repressed by antiapoptotic COX-2/PGE2 signaling in colorectal adenoma cells. *Oncogene* **2010**, *29*, 3398–3410. [CrossRef] [PubMed]
100. Normanno, N.; de Luca, A.; Bianco, C.; Strizzi, L.; Mancino, M.; Maiello, M.R.; Carotenuto, A.; de Feo, G.; Caponigro, F.; Salomon, D.S. Epidermal growth factor receptor (EGFR) signaling in cancer. *Gene* **2006**, *366*, 2–16. [CrossRef]
101. Huang, L.; Fu, L. Mechanisms of resistance to EGFR tyrosine kinase inhibitors. *Acta Pharm. Sin. B* **2015**, *5*, 390–401. [CrossRef]
102. Healy, F.M.; Prior, I.A.; MacEwan, D.J.; David MacEwan, C.J. The importance of Ras in drug resistance in cancer. *Br. J. Pharmacol.* **2022**, *179*, 2334–2355. [CrossRef]
103. Fernández-Medarde, A.; Santos, E. Ras in cancer and developmental diseases. *Genes Cancer* **2011**, *2*, 344–358. [CrossRef]
104. Weickhardt, A.J.; Tebbutt, N.C.; Mariadason, J.M. Strategies for overcoming inherent and acquired resistance to EGFR inhibitors by targeting downstream effectors in the RAS/PI3K pathway. *Curr. Cancer Drug Targets* **2010**, *10*, 824–833. [CrossRef]
105. Lee, K.W.; Kang, N.J.; Rogozin, E.A.; Kim, H.G.; Cho, Y.Y.; Bode, A.M.; Lee, H.J.; Surh, Y.J.; Bowden, G.T.; Dong, Z. Myricetin is a novel natural inhibitor of neoplastic cell transformation and MEK1. *Carcinogenesis* **2007**, *28*, 1918–1927. [CrossRef]
106. Jung, S.K.; Lee, K.W.; Kim, H.Y.; Oh, M.H.; Byun, S.; Lim, S.H.; Heo, Y.S.; Kang, N.J.; Bode, A.M.; Dong, Z.; et al. Myricetin suppresses UVB-induced wrinkle formation and MMP-9 expression by inhibiting Raf. *Biochem. Pharmacol.* **2010**, *79*, 1455–1461. [CrossRef]
107. Jung, S.K.; Lee, K.W.; Byun, S.; Lee, E.J.; Kim, J.E.; Bode, A.M.; Dong, Z.; Lee, H.J. Myricetin inhibits UVB-induced angiogenesis by regulating PI-3 kinase in vivo. *Carcinogenesis* **2010**, *31*, 911–917. [CrossRef] [PubMed]
108. Rosas-Martínez, M.; Gutiérrez-Venegas, G. Myricetin inhibition of peptidoglycan-induced COX-2 expression in H9c2 cardiomyocytes. *Prev. Nutr. Food Sci.* **2019**, *24*, 202. [CrossRef] [PubMed]
109. Cui, J.; Li, G.; Yin, J.; Li, L.; Tan, Y.; Wei, H.; Liu, B.; Deng, L.; Tang, J.; Chen, Y.; et al. GSTP1 and cancer: Expression, methylation, polymorphisms and signaling (review). *Int. J. Oncol.* **2020**, *56*, 867–878. [CrossRef] [PubMed]
110. Nobuoka, A.; Takayama, T.; Miyanishi, K.; Sato, T.; Takanashi, K.; Hayashi, T.; Kukitsu, T.; Sato, Y.; Takahashi, M.; Okamoto, T.; et al. Glutathione-S-transferase P1-1 protects aberrant crypt foci from apoptosis induced by deoxycholic acid. *Gastroenterology* **2004**, *127*, 428–443. [CrossRef]
111. Van Zanden, J.J.; Geraets, L.; Wortelboer, H.M.; Van Bladeren, P.J.; Rietjens, I.M.C.M.; Cnubben, N.H.P. Structural requirements for the flavonoid-mediated modulation of glutathione S-transferase P1-1 and GS-X pump activity in MCF7 breast cancer cells. *Biochem. Pharmacol.* **2004**, *67*, 1607–1617. [CrossRef]
112. Saeed, M.E.M.; Yücer, R.; Dawood, M.; Hegazy, M.E.F.; Drif, A.; Ooko, E.; Kadioglu, O.; Seo, E.J.; Kamounah, F.S.; Titinchi, S.J.; et al. In silico and in vitro screening of 50 curcumin compounds as EGFR and NF-KB inhibitors. *Int. J. Mol. Sci.* **2022**, *23*, 3966. [CrossRef]
113. Romano, A.; Khalid, S.A.; Dawood, M.; Boulos, J.C.; Wasfi, M.; Drif, A.; Bahramimehr, F.; Shahhamzehei, N.; Shan, L.; Efferth, T. Molecules identification of gedunin from a phytochemical depository as a novel multidrug resistance-bypassing tubulin inhibitor of cancer cells. *Molecules* **2022**, *27*, 5858. [CrossRef]
114. Saeed, M.E.M.; Drif, A.I.; Efferth, T. Biomarker Profiling Revealed Carcinoembryonic Antigen as a Target of Artesunate in a Ductal Breast Cancer Patient. *Anticancer Res.* **2022**, *42*, 3483–3494. [CrossRef]
115. Yue, G.G.L.; Gomes, A.J.; Saeed, M.E.M.; Tsui, K.Y.; Dawood, M.; Drif, A.I.; Wong, E.C.W.; Lee, W.F.; Liu, W.; Chiu, P.W.Y.; et al. Identification of Active Components in Andrographis Paniculata Targeting on CD81 in Esophageal Cancer in Vitro and in Vivo. *Phytomedicine* **2022**, *102*, 154183. [CrossRef]
116. Ong, K.C.; Khoo, H.-E. *Biological Effects of Myricetin*; Elsevier Science Inc.: Amsterdam, The Netherlands, 1997; Volume 29.
117. Xie, Y.; Wang, Y.; Xiang, W.; Wang, Q.; Cao, Y. Mini-Reviews in Medicinal Chemistry Send Orders for Reprints to Reprints@benthamscience. *Net Mini-Rev. Med. Chem.* **2020**, *20*, 123–133. [CrossRef]
118. Devi, K.P.; Rajavel, T.; Habtemariam, S.; Fazel Nabavi, S.; Nabavi, S.M. Molecular Mechanisms Underlying Anticancer Effects of Myricetin. *Life Sci.* **2015**, *142*, 19–25. [CrossRef] [PubMed]
119. Semwal, D.K.; Semwal, R.B.; Combrinck, S.; Viljoen, A. Myricetin: A Dietary Molecule with Diverse Biological Activities. *Nutrients* **2016**, *8*, 90. [CrossRef] [PubMed]
120. Song, X.; Tan, L.; Wang, M.; Ren, C.; Guo, C.; Yang, B.; Ren, Y.; Cao, Z.; Li, Y.; Pei, J. Myricetin: A Review of the Most Recent Research. *Biomed. Pharmacother.* **2021**, *134*, 111017. [CrossRef]
121. Van Zanden, J.J.; De Mul, A.; Wortelboer, H.M.; Usta, M.; Van Bladeren, P.J.; Rietjens, I.M.C.M.; Cnubben, N.H.P. Reversal of in Vitro Cellular MRP1 and MRP2 Mediated Vincristine Resistance by the Flavonoid Myricetin. *Biochem. Pharmacol.* **2005**, *69*, 1657–1665. [CrossRef] [PubMed]
122. López-Lázaro, M.; Willmore, E.; Austin, C.A. The Dietary Flavonoids Myricetin and Fisetin Act as Dual Inhibitors of DNA Topoisomerases I and II in Cells. *Mutat. Res. Genet. Toxicol. Environ. Mutagen.* **2010**, *696*, 41–47. [CrossRef]

123. Kondo, S.; Carr, B.I.; Takagi, K.; Huang, T.H.; Chou, Y.-M.; Yokoyama, K.; Itakura, K. Expression of Rat Microsomal Epoxide Hydrolase Gene during Liver Chemical Carcinogenesis. *Cancer Res.* **1990**, *50*, 6222–6228.
124. Carr, B.I.; Laishes, B.A. Carcinogen-Induced Drug Resistance in Rat Hepatocytes. *Cancer Res.* **1981**, *41*, 1715–1719.
125. Carr, B.I. Pleiotropic Drug Resistance in Hepatocytes Induced by Carcinogens Administered to Rats. *Cancer Res.* **1987**, *47*, 5577–5583.
126. Solt, D.B.; Shklar, G. Rapid Induction of γ-Glutamyl Transpeptidase-Rich Intraepithelial Clones in 7,12-Dimethylbenz(a)Anthracene-Treated Hamster Buccal Pouch. *Cancer Res.* **1982**, *42*, 285–291.
127. Nakai, Y.; Nonomura, N. Inflammation and Prostate Carcinogenesis. *Int. J. Urol.* **2013**, *20*, 150–160. [CrossRef]
128. Ohshima, H.; Tatemichi, M.; Sawa, T. Chemical Basis of Inflammation-Induced Carcinogenesis. *Arch. Biochem. Biophys.* **2003**, *417*, 3–11. [CrossRef] [PubMed]
129. Ohnishi, S.; Ma, N.; Thanan, R.; Pinlaor, S.; Hammam, O.; Murata, M.; Kawanishi, S. DNA Damage in Inflammation-Related Carcinogenesis and Cancer Stem Cells. *Oxid. Med. Cell. Longev.* **2013**, *2013*, 387014. [CrossRef] [PubMed]
130. Kawanishi, S.; Ohnishi, S.; Ma, N.; Hiraku, Y.; Murata, M. Crosstalk between DNA Damage and Inflammation in the Multiple Steps of Carcinogenesis. *Int. J. Mol. Sci.* **2017**, *18*, 1808. [CrossRef] [PubMed]
131. Feagins, L.A.; Souza, R.F.; Spechler, S.J. Carcinogenesis in IBD: Potential Targets for the Prevention of Colorectal Cancer. *Nat. Rev. Gastroenterol. Hepatol.* **2009**, *6*, 297–305. [CrossRef]
132. Malongane, F.; McGaw, L.J.; Mudau, F.N. The Synergistic Potential of Various Teas, Herbs and Therapeutic Drugs in Health Improvement: A Review. *J. Sci. Food Agric.* **2017**, *97*, 4679–4689. [CrossRef]
133. Ma, J.; Shen, H.; Kapesa, L.; Zeng, S. Lauren Classification and Individualized Chemotherapy in Gastric Cancer (Review). *Oncol. Lett.* **2016**, *11*, 2959–2964. [CrossRef]
134. Efferth, T.; Volm, M. Pharmacogenetics for Individualized Cancer Chemotherapy. *Pharmacol. Ther.* **2005**, *107*, 155–176. [CrossRef]
135. Zhou, M.; Varol, A.; Efferth, T. Multi-Omics Approaches to Improve Malaria Therapy. *Pharmacol. Res.* **2021**, *167*, 105570. [CrossRef]
136. Efferth, T.; Saeed, M.E.M.; Mirghani, E.; Alim, A.; Yassin, Z.; Saeed, E.; Khalid, H.E.; Daak, S. Integration of Phytochemicals and Phytotherapy into Cancer Precision Medicine. *Oncotarget* **2017**, *8*, 50284. [CrossRef]
137. Poornima, P.; Kumar, J.D.; Zhao, Q.; Blunder, M.; Efferth, T. Network Pharmacology of Cancer: From Understanding of Complex Interactomes to the Design of Multi-Target Specific Therapeutics from Nature. *Pharmacol. Res.* **2016**, *111*, 290–302. [CrossRef]
138. Kadioglu, O.; Saeed, M.; Mahmoud, N.; Azawi, S.; Mrasek, K.; Liehr, T.; Efferth, T. Identification of Potential Novel Drug Resistance Mechanisms by Genomic and Transcriptomic Profiling of Colon Cancer Cells with P53 Deletion. *Arch. Toxicol.* **2021**, *95*, 959–974. [CrossRef] [PubMed]
139. Saeed, M.; Kuete, V.; Kadioglu, O.; Börtzler, J.; Khalid, H.; Greten, H.J.; Efferth, T. Cytotoxicity of the Bisphenolic Honokiol from Magnolia Officinalis against Multiple Drug-Resistant Tumor Cells as Determined by Pharmacogenomics and Molecular Docking. *Phytomedicine* **2014**, *21*, 1525–1533. [CrossRef] [PubMed]
140. Lu, X.; Yan, G.; Dawood, M.; Klauck, S.M.; Sugimoto, Y.; Klinger, A.; Fleischer, E.; Shan, L.; Efferth, T. A Novel Moniliformin Derivative as Pan-Inhibitor of Histone Deacetylases Triggering Apoptosis of Leukemia Cells. *Biochem. Pharmacol.* **2021**, *194*, 114677. [CrossRef] [PubMed]
141. Dawood, M.; Fleischer, E.; Klinger, A.; Bringmann, G.; Shan, L.; Efferth, T. Inhibition of Cell Migration and Induction of Apoptosis by a Novel Class II Histone Deacetylase Inhibitor, MCC2344. *Pharmacol. Res.* **2020**, *160*, 105076. [CrossRef] [PubMed]
142. Kadioglu, O.; Saeed, M.E.M.; Mahmoud, N.; Hussein Azawi, S.S.; Rincic, M.; Liehr, T.; Efferth, T. Identification of Metastasis-Related Genes by Genomic and Transcriptomic Studies in Murine Melanoma. *Life Sci.* **2021**, *267*, 118922. [CrossRef]
143. Dawood, M.; Ooko, E.; Efferth, T. Collateral Sensitivity of Parthenolide via NF-KB and HIF-α Inhibition and Epigenetic Changes in Drug-Resistant Cancer Cell Lines. *Front. Pharmacol.* **2019**, *10*, 542. [CrossRef]
144. Magalhães, M.; Manadas, B.; Efferth, T.; Cabral, C. Chemoprevention and Therapeutic Role of Essential Oils and Phenolic Compounds: Modeling Tumor Microenvironment in Glioblastoma. *Pharmacol. Res.* **2021**, *169*, 105638. [CrossRef]
145. Polier, G.; Ding, J.; Konkimalla, B.V.; Eick, D.; Ribeiro, N.; Köhler, R.; Giaisi, M.; Efferth, T.; Desaubry, L.; Krammer, P. H.; et al. Wogonin and Related Natural Flavones Are Inhibitors of CDK9 That Induce Apoptosis in Cancer Cells by Transcriptional Suppression of Mcl-1. *Cell Death Dis.* **2011**, *2*, e182. [CrossRef]
146. Gao, Y.; Zhao, J.; Zu, Y.; Fu, Y.; Liang, L.; Luo, M.; Wang, W.; Efferth, T. Antioxidant Properties, Superoxide Dismutase and Glutathione Reductase Activities in HepG2 Cells with a Fungal Endophyte Producing Apigenin from Pigeon Pea [*Cajanus cajan* (L.) Millsp.]. *Food Res. Int.* **2012**, *49*, 147–152. [CrossRef]

biomedicines

MDPI

Article

Anti-Inflammatory and Cancer-Preventive Potential of Chamomile (*Matricaria chamomilla* L.): A Comprehensive In Silico and In Vitro Study

Assia I. Drif [1], Rümeysa Yücer [1], Roxana Damiescu [1], Nadeen T. Ali [1], Tobias H. Abu Hagar [1], Bharati Avula [2], Ikhlas A. Khan [2] and Thomas Efferth [1,*]

[1] Department of Pharmaceutical Biology, Institute of Pharmaceutical and Biomedical Sciences, Johannes Gutenberg University, Staudinger Weg 5, 55128 Mainz, Germany; adrif@uni-mainz.de (A.I.D.); ryuecer@students.uni-mainz.de (R.Y.); r.damiescu@uni-mainz.de (R.D.); neltayeb@unimainz.de (N.T.A.); habuhaga@students.uni-mainz.de (T.H.A.H.)

[2] National Center for Natural Products Research (NCNPR), School of Pharmacy, University of Mississippi, Oxford, MS 38677, USA; bavula@olemiss.edu (B.A.); ikhan@olemiss.edu (I.A.K.)

* Correspondence: efferth@uni-mainz.de; Tel.: +49-6131-3925751

Abstract: Background and aim: Chamomile tea, renowned for its exquisite taste, has been appreciated for centuries not only for its flavor but also for its myriad health benefits. In this study, we investigated the preventive potential of chamomile (*Matricaria chamomilla* L.) towards cancer by focusing on its anti-inflammatory activity. Methods and results: A virtual drug screening of 212 phytochemicals from chamomile revealed β-amyrin, β-eudesmol, β-sitosterol, apigenin, daucosterol, and myricetin as potent NF-κB inhibitors. The in silico results were verified through microscale thermophoresis, reporter cell line experiments, and flow cytometric determination of reactive oxygen species and mitochondrial membrane potential. An oncobiogram generated through comparison of 91 anticancer agents with known modes of action using the NCI tumor cell line panel revealed significant relationships of cytotoxic chamomile compounds, lupeol, and quercetin to microtubule inhibitors. This hypothesis was verified by confocal microscopy using α-tubulin-GFP-transfected U2OS cells and molecular docking of lupeol and quercetin to tubulins. Both compounds induced G2/M cell cycle arrest and necrosis rather than apoptosis. Interestingly, lupeol and quercetin were not involved in major mechanisms of resistance to established anticancer drugs (ABC transporters, *TP53*, or *EGFR*). Performing hierarchical cluster analyses of proteomic expression data of the NCI cell line panel identified two sets of 40 proteins determining sensitivity and resistance to lupeol and quercetin, further pointing to the multi-specific nature of chamomile compounds. Furthermore, lupeol, quercetin, and β-amyrin inhibited the mRNA expression of the proinflammatory cytokines *IL-1β* and *IL6* in NF-κB reporter cells (HEK-Blue Null1). Moreover, Kaplan–Meier-based survival analyses with NF-κB as the target protein of these compounds were performed by mining the TCGA-based KM-Plotter repository with 7489 cancer patients. Renal clear cell carcinomas (grade 3, low mutational rate, low neoantigen load) were significantly associated with shorter survival of patients, indicating that these subgroups of tumors might benefit from NF-κB inhibition by chamomile compounds. Conclusion: This study revealed the potential of chamomile, positioning it as a promising preventive agent against inflammation and cancer. Further research and clinical studies are recommended.

Keywords: anti-inflammatory; carcinogenesis; cytokines; flavonoids; natural products; prevention; proteomics; Kaplan–Meier survival analysis; microscale thermophoresis

Citation: Drif, A.I.; Yücer, R.; Damiescu, R.; Ali, N.T.; Abu Hagar, T.H.; Avula, B.; Khan, I.A.; Efferth, T. Anti-Inflammatory and Cancer-Preventive Potential of Chamomile (*Matricaria chamomilla* L.): A Comprehensive In Silico and In Vitro Study. *Biomedicines* **2024**, *12*, 1484. https://doi.org/10.3390/biomedicines12071484

Academic Editor: Seungho Baek

Received: 1 March 2024
Revised: 14 June 2024
Accepted: 26 June 2024
Published: 5 July 2024

1. Introduction

It is well-known that inflammation can promote tumorigenesis [1]. Numerous clinical investigations have unraveled that precancerous disorders resulting from inflammation can be prevented from malignant progression by inhibiting inflammation [2]. Therefore, the

quest for novel, effective options to prevent inflammation-related carcinogenesis represents a major focus in oncological research.

In recent years, natural products have gained considerable interest because of their diverse chemical composition, good tolerability, and beneficial pharmacological properties. It has been repeatedly reported that a majority of the current anticancer drugs established in the clinic are of natural origin or derived from natural products [3–5]. Furthermore, advancements in analytical tools and bioinformatics (e.g., "-omics" technologies) have made it easier to harness the potential of natural compounds [3,6–8]. One of the most renowned examples is paclitaxel, extracted from the bark of the Pacific yew, *Taxus brevifolia* [9]. Another notable example is artemisinin, obtained from *Artemisia annua,* which exerts not only antimalarial but also anti-inflammatory and anticancer activities [10]. Similarly, chamomile represents another example of a valuable medicinal plant. It is not just a well-known and widely consumed beverage, as it also possesses pharmacological properties due to its rich content of phenols and flavonoids, which confer antioxidant, antiproliferative, anti-inflammatory, and potential anticancer effects [11–13]. Given the established connection between inflammation and the development of cancer, we focused on the anti-inflammatory properties of *Matricaria chamomilla.*

Previously, we analyzed the inhibitory effects of chamomile on cyclooxygenase-2 (COX2) [12]. Because COX2 expression is regulated by nuclear factor kappa B cells (NF-κB), we then shifted our focus to this transcription factor. COX2 and NF-κB are both well-known players in the inflammatory process. COX2 is an enzyme responsible for producing prostaglandins during inflammation [14]. Nuclear factor-kB is crucial for various cellular processes including inflammation, immunity, cell growth, differentiation, and apoptosis [15]. The NF-κB pathway is generally a proinflammatory signaling pathway by promoting the expression of proinflammatory genes, such as cytokines, chemokines, and adhesion molecules [16]. It is activated through the conversion of the IKB kinase complex (IKK) into a catalytic active form, leading to the degradation of the IKB–NF-κB complex, which releases NF-κB into the nucleus [17]. In chronic inflammation and cancer, NF-κB is persistently dysregulated and active, and it has been implicated in the promotion of cell growth, angiogenesis, and cell proliferation [18]. This underscores the importance of the discovery and development of drugs targeting NF-κB and its pathways.

Thus, our aim in this study was to investigate the inhibitory activity of the secondary metabolites of chamomile (*Matricaria chamomilla* L.) against NF-κB. Through in silico screening, we have determined 6 out of 212 chamomile compounds based on their binding energy (kcal/mol) by using bioinformatical compound screening with PyRx and molecular docking with AutoDock4.2.6. Given our prior research on apigenin [19,20], we now directed our focus towards β-amyrin. The inhibitory activity against NF-κB was evaluated using microscale thermophoresis, an NF-κB reporter cell assay, as well as flow cytometric measurements of reactive oxygen species and mitochondrial membrane potential.

In the second part of our analyses, we selected the cytotoxic compounds lupeol and quercetin from *M. chamomilla*. Using oncobiogram analyses with the NCI panel of tumor cell lines and subsequent verification through confocal microscopy with α-tubulin-GF- transfected U2OS cells, we found that both compounds inhibited microtubules and induced G2/M cell cycle arrest. To perform hierarchical cluster analyses of the proteomes of 60 NCI cell lines, we generated a bioactivity oncobiogram. As lupeol and quercetin were not involved in classical drug resistance mechanisms (e.g., ABC transporters, *TP53*, *EGFR*), hierarchical cluster analyses using proteomic expression data of 3171 proteins in the NCI tumor cell line panel identified candidate proteins predicting sensitivity or resistance to these two compounds.

Moreover, Kaplan–Meier-based survival analyses with NF-κB as the target protein of these compounds were performed by mining the TCGA-based KM-Plotter repository with 7489 cancer patients to envision which tumor types and subtypes might benefit from chamomile treatment.

2. Materials and Methods

2.1. Phytochemical Analysis, Virtual Drug Screening, and Molecular Docking

Phytochemical analysis through liquid chromatography–diode array detector–quadrupole time-of-flight mass spectrometry (LC-DAD-QToF) was previously reported by us [12]. Virtual drug screening of more than 1000 chamomile compounds to COX2 has been also reported by us [12]. This repository of compounds was used for virtual screening and molecular docking to NF-κB in the present investigation.

The crystal structure of NF-κB was taken from the Protein Data Bank (PDB: 1NFI) [21,22], and only the homodimer structure of NF-κB p65-RelA was prepared for virtual drug screening using the software ChimeraXV5 (University of California in San Francisco, San Francisco, CA, USA) (accessed on 30 March 2023) [23]. The water molecules were deleted, polar hydrogen atoms were added and merged, the missing atoms and bonds were repaired, and Kollman charges were added. More than 1000 chamomile compounds were then screened for binding to NF-κB p65-RelA using PyRx version 0.8 [24,25]. Afterwards, 212 out of the 1000 ligands were selected based on their lowest binding energy (LBE, kcal/mol) and subjected to molecular docking against NF-κB using AutoDock 4.2.6 [26–28]. The DNA active site situated in the Rel homology domain (RHD) of NF-κB was defined for the grid box [17,21,29]. Its dimensions were 38 × 58 × 82 Å spacing, 0.622 Å at the grid-center, x = −4.515 Å, y = 72.657 Å, and z = 100.06 Å. The Lamarckian Genetic Algorithm (LGA) was applied to seek the lowest binding energies (LBE, kcal/mol) and predicted inhibition constants (pKi, μM) with docking parameters set to 250 runs and 2,500,000 energy evaluations for each cycle. The data from the histogram were organized in an Excel table (Microsoft Excel 2021 (Version 2306, Build 16.0.16529.20164)). The mean values ± SD were calculated from each of the three independent dockings. BIOVIA Discovery Studio Visualizer 2021 was used to generate the 3D visualization of interactions between the ligand and the amino acid residues of the crystal structure 1NFI [30].

2.2. Microscale Thermophoresis

The microscale thermophoresis (MST) technique was performed to validate the interaction between NF-κB (12054-H09E, Sino Biological Europe GmbH, Eschborn, Germany) and β-amyrin. The recombinant NF-κB protein was labeled using the Monolith Protein Labeling Kit RED-NHS 2nd Generation (MO-L011, NanoTemper Technologies GmbH, Munich, Germany) in accordance with the protocol provided by the manufacturer. Various concentrations (starting from 300 μM to 30 nM) of β-amyrin were incubated with labeled NF-κB (at a concentration of 200 nM) (1:1) for 30 min at room temperature in the dark. The analysis was performed using standard capillaries in the Monolith NT.115 system (NanoTemper Technologies GmbH, Munich, Germany). The MST experiment was conducted with an LED power of 40% and an MST power of 10% for the labeled NF-κB. For the data analysis, the NanoTemper Analysis Software was utilized.

2.3. Cell Culture

The HEK-Blue Null1 cells are a subtype of human embryonic kidney cells (HEK 293) that express secreted embryonic alkaline phosphatase (SEAP) under the control of an NF-κB promoter. The cells were obtained from Invivogen (Toulouse, France) (https://www.invivogen.com/hek-blue-null1v, accessed on 5 December 2019). The cells were maintained in DMEM medium supplied with 2 mM of L-glutamine, 10% fetal bovine serum (FBS), 1% penicillin–streptomycin (Invitrogen, Darmstadt, Germany), and 1 mL of normocin (100 μg/mL). After the second passage, Zeocin (100 μg/mL) was then added to the media (Invivogen, Toulouse, France). The cells were cultured at 37 °C in a humidified environment with 5% CO_2 [31].

The drug-sensitive CCRF-CEM and multidrug-resistant P-glycoprotein-overexpressing CEM-ADR5000 leukemia cells were cultured in RPMI medium mixed with 1% penicillin/streptomycin and 10% FBS. Doxorubicin was added to CEM/ADR5000 every two weeks. The HCT116 $p53^{+/+}$ human wild-type colon cancer cells and their knockout $p53^{-/-}$,

alongside the wild-type human glioblastoma U87.MG cells and their transfected cells with ΔEGFR (U87.MGΔEGFR), were all nurtured in DMEM medium mixed with 1% penicillin/streptomycin and 10% FBS. U87.MGΔEGFR and HCT116 $p53^{-/-}$ were treated every two weeks with geneticin (400 µg/mL).

2.4. NF-κB Reporter Assay

The assay was performed according to the instructions of Invivogen (Toulouse, France). The HEK-Blue Null1 (HKBN1) cells were seeded in a 96-well plate at 100 µL/well and 50,000 cells/well overnight. Then, cells were treated for 24 h with 0.1 µM, 1 µM, and 10 µM of β-amyrin, β-sitosterol, β-eudesmol, daucosterol, myricetin, and apigenin. Triptolide was used as the positive control at concentrations of 0.1 µM and 1 µM. DMSO served as a negative control. TNF-α (100 ng/mL) was added for 24 h to induce the activity of NF-κB. The incubation was at 37 °C in 5% CO_2. QUANTI-Blue™ (QB) solution was used for the detection and quantification of NF-κB (Invivogen, Toulouse, France), and 180 µL of QB was mixed with 20 µL of the supernatant and then incubated for 15 min at 37 °C in 5% CO_2 [32]. The measurement was at 620–655 nm using a microplate reader (Tecan, Crailsheim, Germany). The experiment was independently repeated three times.

2.5. Mitochondrial Membrane Potential Assay

The JC-1 mitochondrial membrane potential assay kit was purchased from Cayman Chemical (Distributor Biomol GmbH, Hamburg, Germany) [33] and used following their instructions [34]. Aliquots of 125,000 HBN1 cells/well and 2 mL/well were seeded in a 6-well plate and left overnight. β-Amyrin (10 µM) and vinblastine as the positive control were added to the cells along with DMSO as the negative control for 24 h. The next day, 100 ng/mL of TNF-α were added for 3 h to induce the activation of NF-κB. The cells were then stained with prediluted JC-1 (1 µL of JC-1 in 9 µL of culture medium) and incubated at 37 °C for 15 min in the dark. Next, the cells were washed with cell-based assay buffer and centrifuged twice at 400 × *g* for 5 min. Finally, the samples were directly measured with a flow cytometer (Novocyte Quanteon, Agilent Technologies, Frankfurt, Germany). Samples of 20,000 cells were analyzed and separated depending on the fluorescence intensity. The JC-1 dye was activated using a 488 nm argon laser. The JC-1 aggregates and monomers both emit green fluorescence (measured at 527 nm), which is detected in the FL1 channel (set at 530 nm). However, JC-1 aggregates representing the healthy cells also emit red fluorescence (measured at 595 nm), detected in the FL2 channel (set at 590 nm) [35]. All experiments were performed three times. The FSC files were analyzed using FlowJo_V10 Software (FLOWJO.LLC 1997–2018).

2.6. ROS Detection

The HEK-Blue null1 cells were seeded in a 6-well plate and incubated for 24 h, allowing attachment. The treatment was for 24 h with varying concentrations of β-amyrin (0.1 µM, 1 µM, and 10 µM). The 3rd day, 100 ng/mL of TNFα was added and left for 24 h. The 4th day, the cells were harvested, washed, and suspended with 1 mL of PBS. 2'7-Dichlorodihydrofluorescein diacetate (H_2DCFH-DA, 10 µM; Sigma-Aldrich, Taufkirchen, Germany) was added and incubated for 30 min at 37 °C. Cells were treated with H_2O_2 (10 µL of the stock concentration; Sigma-Aldrich) for 15 min to activate the ROS generation. DMSO plus H_2O_2 plus TNF-α, cells plus H_2O_2, as well as cells without any treatment were used as controls. Lastly, the samples were directly assessed using a Novocyte Quanteon flow cytometer (Agilent Technologies). The analysis was performed with FlowJo Software (FLOWJO.LLC, 1997–2018). The procedure was independently conducted in triplicate, as described by us [36,37].

2.7. Growth Inhibition Assays

The β-amyrin cytotoxicity was measured through the resazurin reduction assay at 7 different concentrations. Human CCRF-CEM leukemia cells were seeded at a density of

1×10^4 cells/well and 100 µL/well of RPMI 1640 medium in 96-well plates. The cytotoxicity of lupeol and quercetin (Sigma–Aldrich) was tested at 10 µM, 25 µM, 50 µM, and 100 µM on six different cell lines: CCRF-CEM, CEM/ADR5000, U87.MG, U87.MG/ΔEGFR, HCT116 $p53^{+/+}$, HCT116 $p53^{-/-}$, and U2OS.

After 72 h of treatment with β-amyrin, lupeol, and quercetin, 20 µL of 0.01% resazurin solution from Promega (Mannheim, Germany) was added to each well and incubated for over 4 h. The fluorescence signal was subsequently detected using an Infinite M2000 Pro-plate reader (Tecan) with an excitation wavelength of 544 nm and an emission wavelength of 590 nm. The experiment was performed independently in triplicate, and the concentrations were tested in sextuplicate. The results were interpreted as a percentage of cell viability and graphed as a dose–response curve. The IC_{50} value was calculated using Microsoft Excel 2021 (Version 2306, Build 16.0.16529.20164).

A range of human tumor cell lines with diverse origins, including leukemia, melanoma, brain tumors, and carcinoma of the lung, colon, kidney, ovary, breast, or prostate were employed by The National Cancer Institute's Developmental Therapeutics Program (Bethesda, MA, USA) [38,39] to conduct drug screening. The $Log_{10}IC_{50}$ values, obtained through a sulforhodamine 123 assay, along with transcriptomic and proteomic expression data, were deposited on the NCI website [40]. Statistical correlation analyses were performed using Pearson's correlation test (WinStat, Kalmia Inc., Cambridge, MA, USA; accessed on 19 November 2023).

2.8. Immunofluorescence Microscopy of α-Tubulin

U2OS osteosarcoma cells were cultured in µ-slide 8-well plates (ibidi, Gräfelfing, Germany) at a density of 30,000 cells per well and allowed to adhere for 24 h. Subsequently, the cells were treated with concentrations of 0.1, 1, and 10 µM of β-amyrin, quercetin, and lupeol. As positive controls, paclitaxel (1 µM) and vincristine (1 µM) were used (obtained from the University Hospital Pharmacy, Mainz, Germany), while DMSO served as the negative control. After 24 h of treatment, the cells were rinsed with PBS, fixed with 4% paraformaldehyde, and stained with 1 µg/mL of 4'6-diamidino-2-phenylindole (DAPI, Sigma Aldrich). Mounting medium (ibidi, Gräfelfing, Germany) was applied before imaging. Widefield imaging was conducted using a THUNDER Imager Live Cell (Leica Microsystems, Wetzlar, Germany) mounted on a Leica DMi8 microscope stand with a 63×/1.40 NA objective (HC PL APO CS2 63×/1.40 OIL UV). Fluorescence excitation was achieved using LED light sources at 395 nm for DAPI and 488 nm for tubulin–GFP. The camera (Leica DFC9000 GTC) operated in 2 × 2 binning mode, resulting in a pixel size of 206 nm. Image analysis was performed using ImageJ 1.54f software (National Institute of Health, Bethesda, MD, USA). The experimental methodology and microscopy techniques have been previously described [12].

2.9. Molecular Interaction with α- and β-Tubulins

In order to study the affinity of lupeol and quercetin with tubulins, molecular docking in the defined mode was performed with αIB, βI, and βIVb microtubules (PDB ID: 5N5N). The C and H chains of 5N5N were selected for docking, and three grid boxes in three different binding sites of vincristine, paclitaxel, and colchicine were used to compare the binding affinity of the two compounds with their receptor. Their grid box dimensions were 76 × 70 × 60 Å spacing, 0.375 Å at the grid-center, x = 48.907 Å, y = 37.217 Å, and z = 199.886 Å, 54 × 68 × 42 Å spacing, 0.375 Å at the grid-center, x = 49.973 Å, y = 32.388 Å, and z = 177.504 Å, and 126 × 100 × 124 Å spacing, 0.242 Å at the grid-center, x = 52.555 Å, y = 44.736 Å, and z = 169.256 Å, respectively. The molecular docking was performed with AutoDock 4.2.6, and the 3D and 2D pictures showing the interaction of the amino acids with the protein tubulin 5N5N were made using BIOVIA Discovery Studio Visualizer 2021. The mean and SD values were calculated with Microsoft Excel 2021 (Version 2306, Build 16.0.16529.20164) from three independent dockings.

2.10. Cell Cycle Analysis

U2OS cells (250×10^3 cells/well) were seeded and treated for 72 h with a concentration of 1 × IC_{50} and 4 × IC_{50} of lupeol and quercetin, DMSO (negative control), and vincristine (positive control, 1 × IC_{50}) (obtained from the University Hospital Pharmacy, Mainz, Germany). The cells were harvested and centrifuged with cold PBS twice (1500 rpm for 5 min). Cold ethanol (80%) was used for fixation. Samples were kept at −20 °C for 72 h. Before measurement, the cells were suspended with RNAs (Roche Diagnostics, Mannheim, Germany) and then incubated for 30 min. Lastly, 50 µg/mL of propidium iodide (PI) (Sigma-Aldrich) was added before the measurement. The DNA histogram was generated using FL2-A/histogram properties. All experiments were repeated three times independently. The cell cycle distributions were analyzed using FlowJo software (version 10.8.1) (Celeza, Olten, Switzerland) [41,42].

2.11. Cell Death Detection

CCRF-CEM cells (1×10^6 cells/well) and U2OS cells (250×10^3 cells/well) were seeded and treated for 72 h with varying concentrations of lupeol and quercetin. The treatment concentrations for CCRF-CEM cells included 1/4 × IC_{50}, 1/2 × IC_{50}, 1 × IC_{50}, 2 × IC_{50}, and 4 × IC_{50}. For U2OS cells, the treatment concentrations were 1/2 × IC_{50}, 1 × IC_{50}, 2 × IC_{50}, and 4 × IC_{50}. DMSO was used as a negative control. A fluorescein isothiocyanate (FITC)-conjugated annexin V/propidium iodide (PI) assay kit (Bio version Biocat, Heidelberg, Germany) was used to detect apoptosis. The cells were washed with cold PBS and then with 1× binding buffer (Bio Version). Thereafter, 52.5 µL of annexin V master mix (2.5 µL of annexin V, 50 µL of 1 × binding buffer) was added to the cells and incubated at 4 °C in the dark for 15 min. Finally, 403 µL of PI master mix (3 µL of PI, 400 µL of 1 × binding buffer) was added to the cells. The experiments were performed three times independently [41,42].

2.12. Western Blotting

The HEK-Blue null1 cells were seeded for 24 h at a density of 500,000/well in 6-well plates and then treated for 24 h with 10 µM or 50 µM of β-amyrin, quercetin, and lupeol. DMSO served as a negative control. The next day, 100 ng/mL of TNFα was added and left for another 24 h. The cells were harvested on the 4th day, washed, and suspended with 1 mL of PBS × 2. The total protein was extracted using Mammalian Protein Extraction Reagent (M-PER) containing 1% protease inhibitor and phosphatase inhibitor (Thermo Fisher Scientifc, Darmstadt, Germany). The protein amounts were quantified using a microvolume spectrophotometer (NanoDrop, Thermo Fisher Scientific). Afterwards, 30 µg of protein extracts was loaded into each channel of 10% SDS-PAGE gel. After the separation and transfer steps, the polyvinylidene difluoride membrane was blocked in a TBST buffer consisting of 5% bovine serum albumin for 2 h. The membrane was incubated in 1:1000 primary antibodies rabbit mAb NF-κB p65 and GAPDH overnight and in secondary antibody 1:2000 anti-rabbit IgG HRP-linked for 1 h 30 (Cell Signaling Technology, Leiden, The Netherlands). All experiments were repeated three times. The mean and SD values were calculated with Microsoft Excel 2021 (Version 2306, Build 16.0.16529.20164) from three independent dockings. The significance level p value was calculated using t-test tails 2, type2.

2.13. Quantitative Real-Time RT-PCR

The RNA was extracted from the HEK-Blue Null 1 cells treated with 10 µM or 50 µM of β-amyrin, quercetin, and lupeol (Sigma–Aldrich) for 24 h and 100 ng/mL of TNF-α for 24 h. The extraction was performed with the RNeasy Kit from Qiagen (Hilden, Germany). The extracted RNA was converted to cDNA using Luna Script™ RT SuperMix Kit (E3010) following the instructions of the manufacturer (New England Biolabs GmbH, Frankfurt, Germany).

The primers for the *IL1B* and *IL6* genes (interleukin-1β and interleukin-6) were retrieved from the literature [43]. *GAPDH* primers were designed following the protocol previously reported by our team [44]. The primers were procured from Eurofins Genomics Germany GmbH (Ebersberg, Germany).

The real-time quantitative polymerase chain reaction (RT-qPCR) was carried out using 5× Hot Start Taq EvaGreen® qPCR Mix (Axon-Labortechnik, Kaiserslautern, Germany) in a CFX384™ Real Time PCR Detection System (Bio-Rad Laboratories GmbH, Feldkirchen, Germany). The expression of the genes was normalized to *GAPDH*, and the fold of change was calculated with the $2^{\Delta\Delta Ct}$ method [45]. The experiments were independently repeated three times. The mean and SD values were calculated with Microsoft Excel 2021 (Version 2306, Build 16.0.16529.20164). The degree of significance was determined using the *t*-test tails 2 type 2 calculation method.

2.14. Statistical Analysis

For hierarchical cluster analysis of proteomic expression data, we used the method of Ward implemented in the WINStat program (Kalmia, CA, USA).

For survival analysis, we applied Kaplan–Meier statistics. The KM-Plotter database contains data from over 7000 samples across 21 different tumor types [46]. To assess the prognostic significance of *NFKB2* mRNA expression for cancer patient survival, we employed Kaplan–Meier statistics. We utilized false discovery rate (FDR) calculations to mitigate type I errors in multiple comparisons [47,48]. Specifically, we considered only Kaplan–Meier statistics with FDR rates of 5% or lower [49].

3. Results

3.1. Molecular Docking In Silico

Recently, we reported a chemical library of chamomile compounds [12]. In the present investigation, 212 chamomile compounds were utilized for molecular docking with the homodimer structure of NF-κB p65-RelA (PDB: 1NFI) by means of the AutoDock 4.2.6 program (Supplementary Table S1). Out of these 212 molecules, the top 28 were selected for further analysis. Table 1 shows their lowest binding energies (LBE, kcal/mol) as well as their predicted inhibition constants (pKi, μM).

The LBE and pKi values of these 28 compounds significantly correlated with each other using the Pearson correlation test ($p = 2.61 \times 10^{-6}$; $r = 0.76$; Figure 1A). Fifteen LBE values were below −6 kcal/mol, with a range between −8.70 ± <0.01 kcal/mol for β-amyrin and −6.01 ± 0.12 kcal/mol for chlorogenic acid. Their pKi values ranged between 0.42 ± <0.01 μM and 39.73 ± 7.82 μM, respectively (Table 1).

Table 1. Molecular docking of 28 chamomile compounds bound to NF-κB p65-RelA homodimer (PDB ID: 1NFI). The lowest binding energies (LBE, kcal/mol) predicted inhibition constants (μM), and the pharmacophores with the amino acid residues involved in binding of the compounds are represented.

Compounds	LBE (kcal/mol)	pKi (μM)	Pharmacophores
β-Amyrin	−8.70 ± <0.01	0.42 ± <0.01	GLU222, **ASP223**, **ILE224**, GLU225, **PHE239,** PRO275
Lupeol	−7.59 ± 0.01	2.72 ± 0.05	LYS28, GLU222, ASP223, ILE224, GLU225, PHE239, GLN241, PRO275
β-Sitosterol	−7.53 ± 0.10	3.06 ± 0.47	LYS28, GLU222, ASP223, ILE224, GLU225, PHE239, GLN241, PRO275
Luteolin-7-O-glucoside	−6.95 ± 0.03	8.05 ± 0.53	LYs28, ARG30, GLU222, ASP223, ILE224, GLU225, GLY237, **SER238**, **PHE239**, GLN241, PRO275, SER276
Daucosterol	−6.90 ± 0.11	8.79 ± 1.70	HIS181, GLN220, LYS221, GLU222, ALA242, **VAL244**, **ARG246**, GLN247
β-Eudesmol	−6.70 ± 0.01	12.23 ± 0.15	LYS221, GLU222, ILE224, GLU225, VAL226, ARG236, GLY237, SER238, **PHE239**, GLN241, PRO275

Table 1. *Cont.*

Compounds	LBE (kcal/mol)	pKi (μM)	Pharmacophores
(−)-Epicatechin	−6.41 ± 0.04	20.01 ± 1.40	GLU222, ASP223, **ILE224**, GLU225, **PHE239**, PRO275
Myricetin	−6.32 ± 0.17	23.87 ± 7.32	THR71, ARG73, **GLU101**, **ASN139**, **PRO140**, **GLN142**, GLN162, VAL163, **THR164**, PRO177
(+)-Catechin	−6.28 ± 0.02	25.16 ± 0.95	**GLN29**, VAL219, **GLN220**, **LYS221**, VAL224, ARG246, GLN247
Quercetin hydrate	−6.15 ± 0.01	31.17 ± 0.19	**VAL219**, GLN220, LYS221, VAL244, ARG246, **GLN247**
Luteolin	−6.14 ± 0.02	32.14 ± 0.15	HIS181, GLN220, **LYS221**, **GLU222**, HIS245, **ARG246**
Kaempferol	−6.10 ± 0.01	34.24 ± 0.70	VAL219, GLN220, **LYS221**, **VAL244**, ARG246, **GLN247**
Bisabelol oxide B	−6.03 ± 0.01	38.18 ± 0.21	GLN220, LYS221, **VAL244**, HIS245, **ARG246**, GLN247
Chlorogenic acid	−6.01 ± 0.12	39.73 ± 7.82	**GLN29**, PHE184, **LYS218**, VAL219, GLN220, **LYS221**, VAL244, **GLN247**
Apigenin	−5.91 ± 0.00	46.78 ± 0.12	**GLN29**, **GLN220**, LYS221, GLU222, **VAL244**, HIS245, **ARG246**, **GLN247**
A-Bisabolol	−5.85 ± 0.03	51.77 ± 2.68	GLU222, ASP223, ILE224, GLU225, VAL226, ARG236, GLY237, SER238, **PHE239**, GLN241, PRO275
Guaiazulene	−5.75 ± <0.01	61.15 ± 0.10	GLU222, ILE224, GLU225, VAL226, ARG236, GLY237, PHE239, SER240, GLN241, PRO275
Quercitrin	−5.66 ± 0.06	70.71 ± 7.19	**VAL219**, **GLN220**, **LYS221**, **GLU222**, **VAL244**, ARG246, GLN247
Caffeic acid	−5.64 ± 0.05	73.56 ± 5.42	**VAL219**, GLN220, **LYS221**, **GLU222**, VAL244, **ARG246**, GLN247
Bisabolol oxide A	−5.37 ± <0.01	116.55 ± 0.01	VAL219, GLN220, LYS221, ALA242, **VAL244**, HIS245, **ARG246**, GLN247
Chamazulene	−5.32 ± <0.01	126.69 ± 0.26	GLU222, ASP223, ILE224, ARG236, PHE239, SER240, GLN241, PRO275
Bisabolone oxide A	−5.12 ± 0.01	175.23 ± 0.16	GLU222, ASP223, ILE224, GLU225, VAL226, ARG236, GLY237, SER238, **PHE239**, PRO275
Syringic acid	−4.96 ± 0.01	232.16 ± 2.85	**ILE23**, ILE24, GLU25, **GLN26**, GLU49, **ARG50**, **LYS221**, GLU222
Farnesol	−4.68 ± 0.02	374.02 ± 10.22	**GLN29**, **GL220**, LYS221, GLU222, ALA242, VAL244, ARG246, GLN247
Gentisic acid	−4.48 ± 0.01	518.79 ± 9.09	ILE24, GLU25, **GLN26**, **ARG50**, **LYS221**, GLU222
(+)-Terpinen-4-ol	−4.14 ± 0.01	925.85 ± 10.48	VAL219, GLN220, **LYS221**, **GLU222**, VAL244, GLN247
P-Cymene	−4.14 ± <0.01	929.21 ± 0.34	LYS221, ILE224, GLU225, ARG236, GLY237, PHE239, GLN241
Citronellol	−4.10 ± <0.01	990.93 ± 1.02	LYS221, GLU222, ILE224, GLU225, VAL226, ARG236, GLY237, SER238, **PHE239**, GLN241

The top 6 of the 212 compounds were selected for further detailed studies. They were bound to three different pockets within two domains (Figure 1B). In the dimerization domain, daucosterol and apigenin shared the same pocket. On the other hand, β-amyrin, β-sitosterol, β-eudesmol, and triptolide were also bound to the same site, while myricetin was bound to the head of the N-terminal domain. Their interaction and binding with the protein were displayed as two- and three-dimensional figures (Figure 1C–H). Triptolide, as an established inhibitor of NF-κB, was used as a positive control [50]. Its interaction with NF-κB p65 RelA is visualized in Figure 1I.

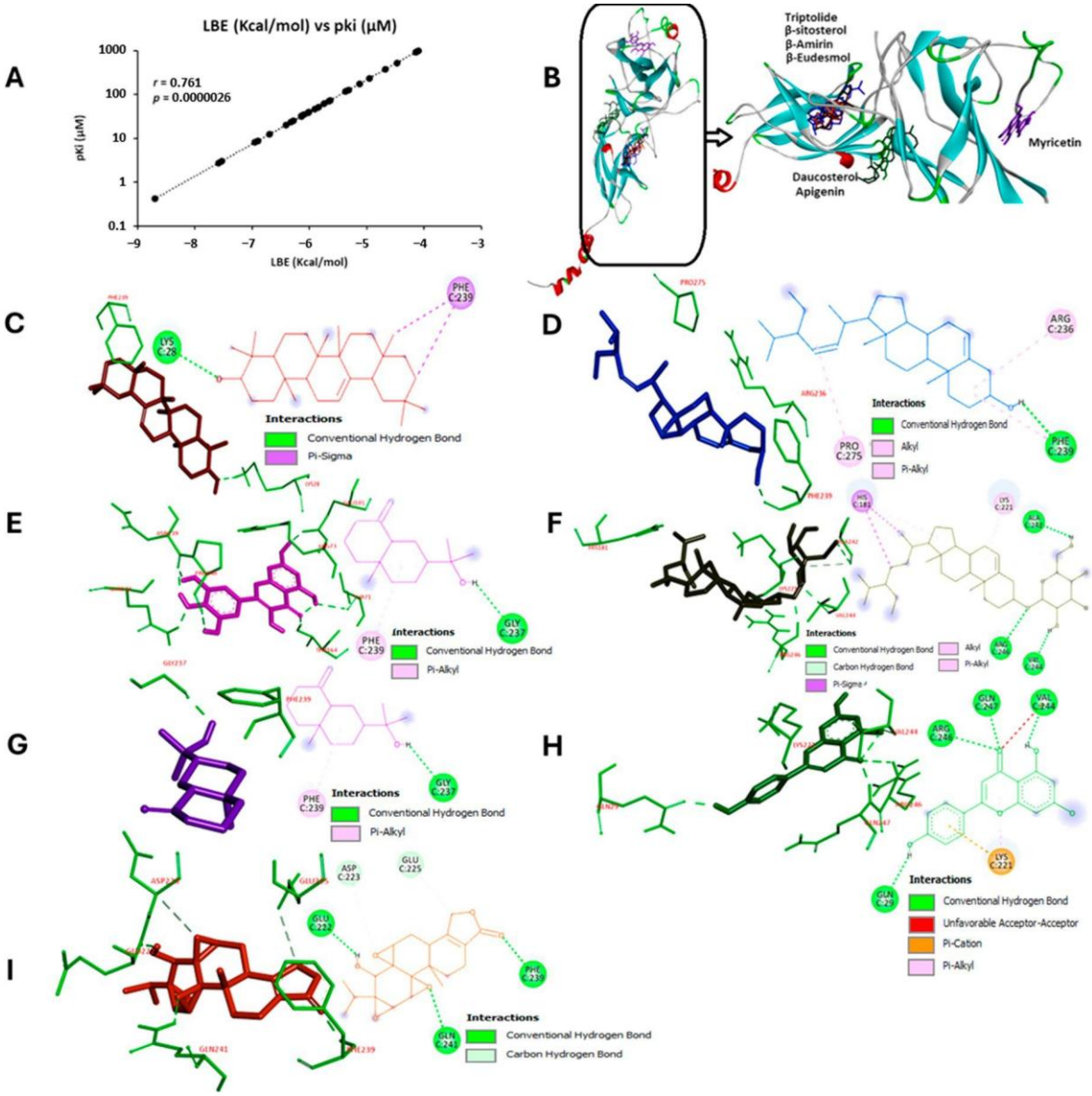

Figure 1. In silico binding of selected phytochemicals extracted from chamomile (*Matricaria chamomilla*) and triptolide (positive control) to NF-κB. Molecular docking analyses have been performed with NF-κB -RelA (PDB ID: 1NFI). (**A**) The lowest binding energies (LBE, kcal/mol) of the top 28/212 compounds (=10.4%) significantly correlated with the predicted inhibition constants (pKi, μM) ($p = 2.61 \times 10^{-6}$; $r = 0.76$). (**B**) The top 6/212 compounds were bound to different pockets within two domains. The interactions of these six compounds with the amino acids of NF-κB are displayed as 2D and 3D figures: (**C**) β-amyrin, (**D**) β-sitosterol, (**E**) myricetin, (**F**) daucosterol, (**G**) β-eudesmol, (**H**) apigenin, and (**I**) triptolide (positive control).

3.2. Microscale Thermophoresis

To exemplarily verify the molecular docking results, we performed microscale thermophoresis (MST) with β-amyrin and NF-κB. Decreasing concentrations of β-amyrin were titrated against the human recombinant NF-κB. The working solutions of β-amyrin were obtained by diluting the stock solution in DMSO with working buffer (MST buffer). The equilibrium constants K_D confirmed that β-amyrin was indeed bound to NF-κB. By using the law of mass action, a K_D value of 943 ± 113 nM was determined (Figure 2A).

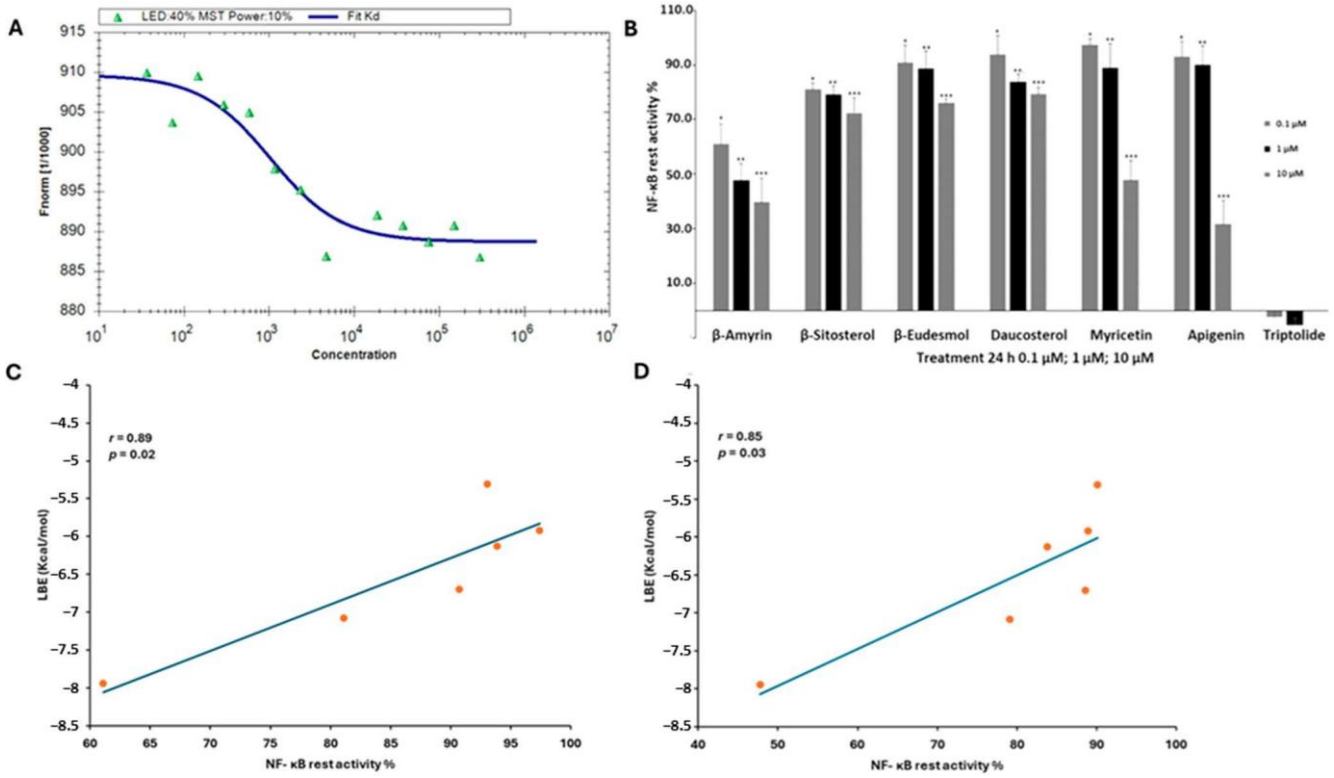

Figure 2. In vitro binding to and inhibition of NF-κB for selected phytochemicals extracted from chamomile (*Matricaria chamomilla*) and triptolide (positive control). (**A**) Binding of β-amyrin to NF-κB as determined through microscale thermophoresis (MST). The resulting binding kinetics is shown as normalized fluorescence (LED power: 40%; MST power: 10%). (**B**) Inhibition of NF-κB activity using an NF-κB reporter assay. The percentages of the NF-κB rest activity are shown after 24 h treatment with β-amyrin, β-sitosterol, β-eudesmol, daucosterol, myricetin, and apigenin at concentrations of 0.1 µM, 1 µM, and 10 µM followed by 100 ng/mL of TNF-α for 24 h (* $p < 0.05$). (**C**,**D**) Pearson correlation of NF-κB rest activity (%) vs. lowest binding energy (kcal/mol) of the six selected compounds at concentrations of (**C**) 0.1 µM and (**D**) 1 µM. The correlation using a concentration of 10 µM was statistically not significant. The mean values ± SD of three independent experiments are shown. (* $p < 0.05$, ** $p < 0.01$, *** $p < 0.001$).

3.3. NF-κB Reporter Assay

To verify the results predicted in silico, these six phytochemicals were subjected to an NF-κB reporter cell assay. We measured the remaining NF-κB activity upon treatment with these compounds at concentrations of 0.1 µM, 1 µM, and 10 µM (Figure 2B). β-Amyrin was the most effective inhibitor of NF-κB activity, with remaining activity values of 38.9% ± 7.3, 52.2% ± 6.2, and 60.3% ± 8.7, respectively. Daucosterol had the lowest inhibitory activity with activity percentages of 6.1% ± 7 (0.1 µM), 16.2% ± 2.9 (1 µM), and 20.8% ± 2.7 (10 µM). Triptolide as a positive control strongly inhibited the NF-κB activity.

To see whether the rest activity measured in vitro may correlate with the LBE values determined in silico, we performed correlation analyses. The NF-κB rest activity (%) significantly correlated with the LBE values (kcal/mol) at 0.1 µM ($p = 0.02$; $r = 0.89$) and 1 µM ($p = 0.03$; $r = 0.85$). The treatment at 10 µM did not correlate with the LBE values $r = -0.15$ (Figure 2B–D).

3.4. Assessment of Oxidative Stress

It is well-known that high levels of reactive oxygen species (ROS) activate NF-κB and foster the inflammation process. In addition, NF-κB increases ROS generation during inflammation [51,52]. Therefore, we measured the ROS levels as a parameter of oxidative

stress. Untreated HEK-Blue Null 1 (HBN1) cells exhibited very low ROS levels (0.68%). However, if the cells were exposed to hydrogen peroxide (H_2O_2) as the positive control, the ROS generation significantly increased by 11.63% (p = 0.02, compared with untreated cells as the negative control). The combination of H_2O_2 and tumor necrosis factor α (TNF-α) as a proinflammatory cytokine further increased the ROS generation up to 14.13% (p = 0.005, compared with the negative control). In contrast, β-amyrin treatment significantly decreased the H_2O_2- and TNF-α-induced ROS generation by 12.30% (p = 0.1), 10.83% (p = 0.05), and 8.80% (p = 0.01) at 0.1 µM, 1 µM, and 10 µM, respectively (Figure 3).

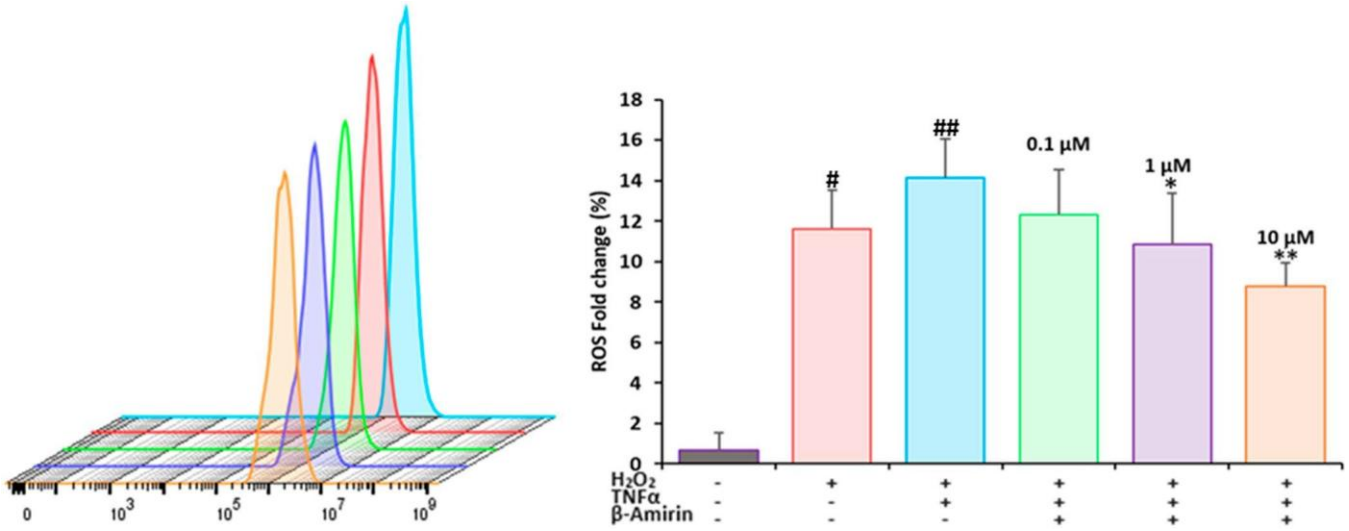

Figure 3. Effect of β-amyrin on the generation of reactive oxygen species (ROS) in HEK-Blue Null 1 (HBN1). The cells were treated with 100 µM of H_2O_2 (15 min) and 100 ng/mL of TNF-α (3 h) with and without β-amyrin at concentrations of 0.1 µM, 1 mM, and 10 µM (24 h). The statistical analysis was performed by using the paired student's *t*-test. * p = 0.05 (1 µM) and ** p = 0.01 (10 µM) compared with TNF-α- and H_2O_2-treated control cells, $^{\#}$ p = 0.02 (cells treated with H_2O_2), and $^{\#\#}$ p = 0.005 (cells treated with TNF-α and H_2O_2) compared with untreated cells. β-amyrin significantly reduced ROS generation. DMSO treatment served as the solvent control. The mean values ± SD of three independent experiments are shown.

3.5. Measurement of the Mitochondrial Membrane Potential

Mitochondria are not only essential for ATP generation and programmed cell death but also play a key role in inflammation [53]. We investigated whether the inhibition of NF-κB after TNF-α induction affected the mitochondrial membrane potential and whether β-amyrin reversed this effect. HEK-Blue Null1 cells were treated with 10 µM of β-amyrin for 24 h and with TNF-α for 3 h. As a positive control, cells were treated with 10 µM of vinblastine (Figure 4). Using flow cytometry and JC-1, we measured a considerable breakdown of the mitochondrial membrane potential (MMP) upon treatment with β-amyrin or vinblastine compared to the untreated control (Figure 4A). β-Amyrin led to a 52.6% increase in the population of cells with disrupted mitochondrial membrane potential (indicative of apoptotic or dead cells), while only 47.6% of cells maintained their MMP (and their viability). In comparison, vinblastine had an effect of 73.6% living cells and 26.6% dead cells (Figure 4B).

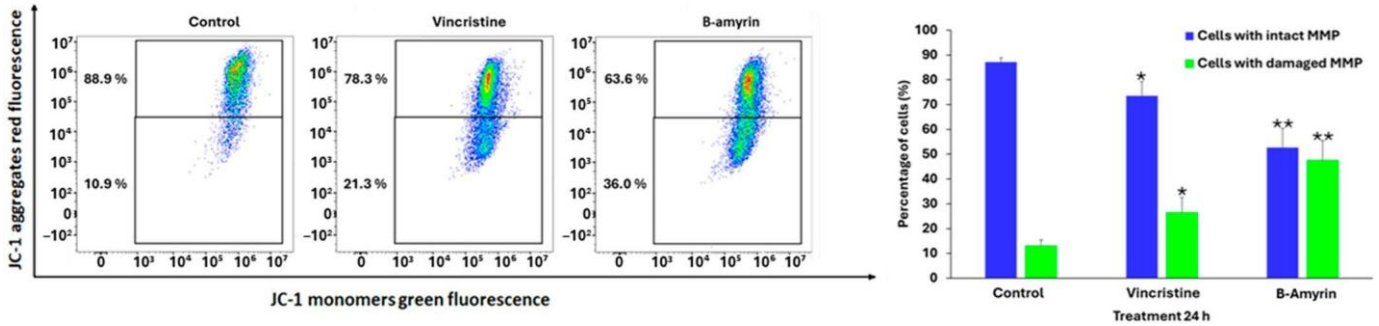

Figure 4. Flow cytometric determination of mitochondrial membrane potential (MMP) in HEK-Blue Null 1 Cells through JC–1 staining. Cells were left untreated (control) or treated with 10 µM of β-amyrin or vinblastine for 24 h, followed by 100 ng/mL of TNF-α for 3 h. (**A**) Representative histograms; (**B**) statistical analysis cells with disrupted MMP (dead cells) or intact MMP (healthy cells). Mean values ± SD of three independent experiments are shown. The results are significant at ** $p < 0.01$ for death cells and * $p < 0.05$ for living cells if compared to the control DMSO untreated cells (paired two-tailed *t*-test).

3.6. Cytotoxicity and Oncobiogram Analyses

The link between inflammation and carcinogenesis is well-established [54]. Accordingly, the first part of the analysis was to compare the effect of the multiple chamomile compounds on the cell viability of 60 cell lines originating from different tumor types. While (+)-catechin, β-sitosterol, daucosterol, caffeic acid, and β-eudesmol were inactive or only minimally active, the strongest inhibition was observed with apigenin and farnesol. Lupeol and quercetin showed intermediate cytotoxicity (Figure 5A–C). Because apigenin and farnesol as the most cytotoxic compounds in this panel were already the subjects of previous investigations by us [19,20,55–57], we chose quercetin and lupeol for further analyses.

As β-amyrin was not included in the NCI database, we performed a growth inhibition assay, which revealed that β-amyrin did not exert any cytotoxic effect on the sensible leukemia cells. The highest inhibition was observed at a concentration of 100 µM (26.2% ± 9.6) (Supplementary Figure S1).

Then, we compiled the sensitivity of the NCI tumor cell lines towards lupeol and quercetin according to their origin, i.e., leukemia, melanoma, and brain tumors as well as carcinoma of the colon, ovary, breast, kidney, lung, and prostate. The mean $\log_{10}IC_{50}$ (M) values for quercetin and lupeol were compared with those for chlorambucil as an established anticancer drug (control). It is evident from the data shown in Figure 5D that all three compounds exhibited the greatest growth-inhibitory efficacy in leukemia cells compared to the cell lines of other tumor types. Melanoma cells were most resistant to quercetin. With some variations, the cytotoxicity of both lupeol and quercetin was approximately comparable to that of chlorambucil.

While natural products are bioactive through multiple mechanisms [58,59], the exact modes of action of lupeol and quercetin are unknown. Therefore, we correlated the $\log_{10}IC_{50}$ values of lupeol and quercetin with those of 91 standard agents with known modes of action (Figure 5E). Both lupeol and quercetin were most frequently correlated with microtubule inhibitors and mTOR inhibitors. Therefore, we subjected both compounds to oncobiogram analysis by compiling the correlation coefficients (*r*-values) of lupeol and quercetin to those of 10 known microtubule inhibitors (Figure 5F). The analysis favored the hypothesis that lupeol and quercetin might also act as tubulin inhibitors.

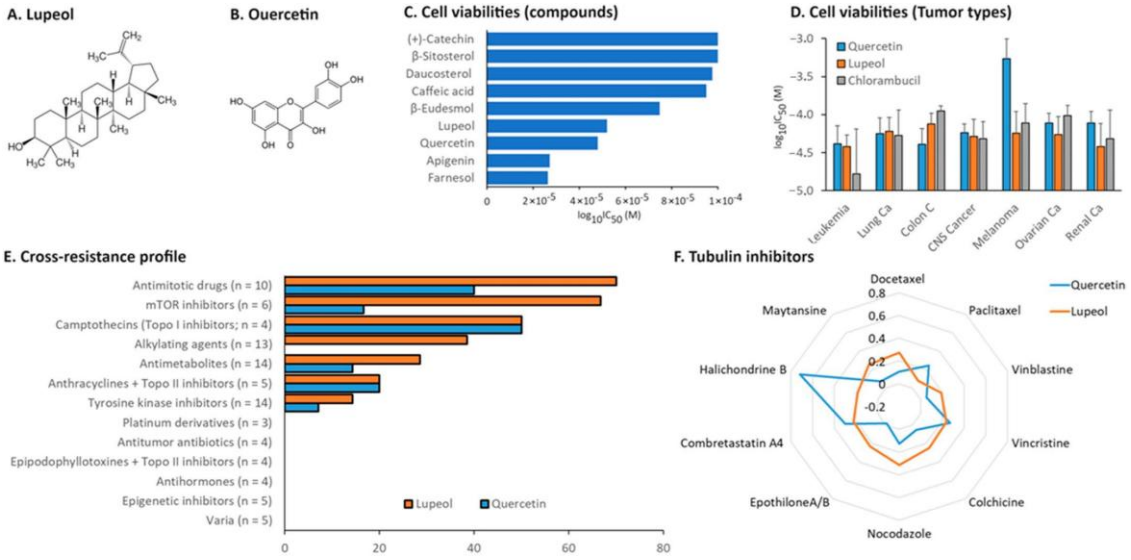

Figure 5. Cytotoxicity and oncobiogram analyses. Chemical structures of (**A**) lupeol and (**B**) quercetin. (**C**) Cytotoxicity of six selected phytochemicals from chamomile to the NCI tumor cell line panel plotted as a mean $\log_{10}IC_{50}$ for each tumor type. (**D**) The cytotoxicity of lupeol and quercetin in cell lines of different tumor types compared with the established anticancer drug chlorambucil as the positive control. (**E**) Cross-resistance profiling of lupeol and quercetin to 91 standard drugs with known modes of action against tumor cells. (**F**) Oncobiogram for lupeol and quercetin. The correlation coefficients for lupeol and quercetin to 10 known tubulin inhibitors are plotted.

3.7. Inhibition of α-Tubulin by Lupeol and Quercetin as Detected through Confocal Immunofluorescence Microscopy

The oncobiogram analysis showed that both lupeol and quercetin might act as microtubule inhibitors. To validate this hypothesis, we treated the U2OS cells transfected with GFP-α-tubulin with lupeol and quercetin (0.1 µM, 1 µM, and 10 µM). Vincristine (1 µM) was used as the control drug to monitor the inhibition of microtubule polymerization, and paclitaxel (1 µM) was used as the control drug to monitor the inhibition of microtubule depolymerization. As can be seen in Figure 6, both lupeol and quercetin affected α-tubulin in a comparable manner to vincristine, indicating that they may have inhibited microtubule polymerization rather than depolymerization.

3.8. Binding of Lupeol and Quercetin to α-Tubulin as Detected through Molecular Docking

To further investigate the possible interactions of lupeol and quercetin to α-tubulin, we performed molecular docking. For quality control of the results obtained in this series of molecular dockings, we first correlated the LBE and pKi values. The Pearson correlation test showed that all LBE values (kcal/mol) correlated significantly with their respective pKi (µM) values at $p = 0.004$ and $r = 0.85$ (Figure 7A).

The in silico analysis demonstrated that lupeol and quercetin had higher binding affinities to α-tubulin at the vincristine binding site compared to the binding sites of paclitaxel and colchicine (Figure 7A). Specifically, the calculation of low binding energy (LBE) for lupeol interacting with α-tubulin at the vincristine's binding site was lower than its LBE value at paclitaxel's binding site, with values of -8.62 ± 0.04 kcal/mol and -7.12 ± 0.01 kcal/mol, respectively. Similarly, quercetin had an LBE with the protein at vincristine's binding site compared to paclitaxel's binding site, with values of -6.77 ± 0.06 kcal/mol and -5.99 ± 0.29 kcal/mol, respectively. In contrast, both compounds had less affinity with the α-tubulin if docked at the colchicine's binding site, with calculated LBE values of -4.48 ± 0.08 kcal/mol for lupeol and -4.72 ± 0.15 kcal/mol for quercetin (Table 2). Figure 7C–E show the 3D and 2D docking poses of vincristine, quercetin, and lupeol, highlighting the amino acid residues involved in the binding of each molecule to α-tubulin at the vincristine binding site.

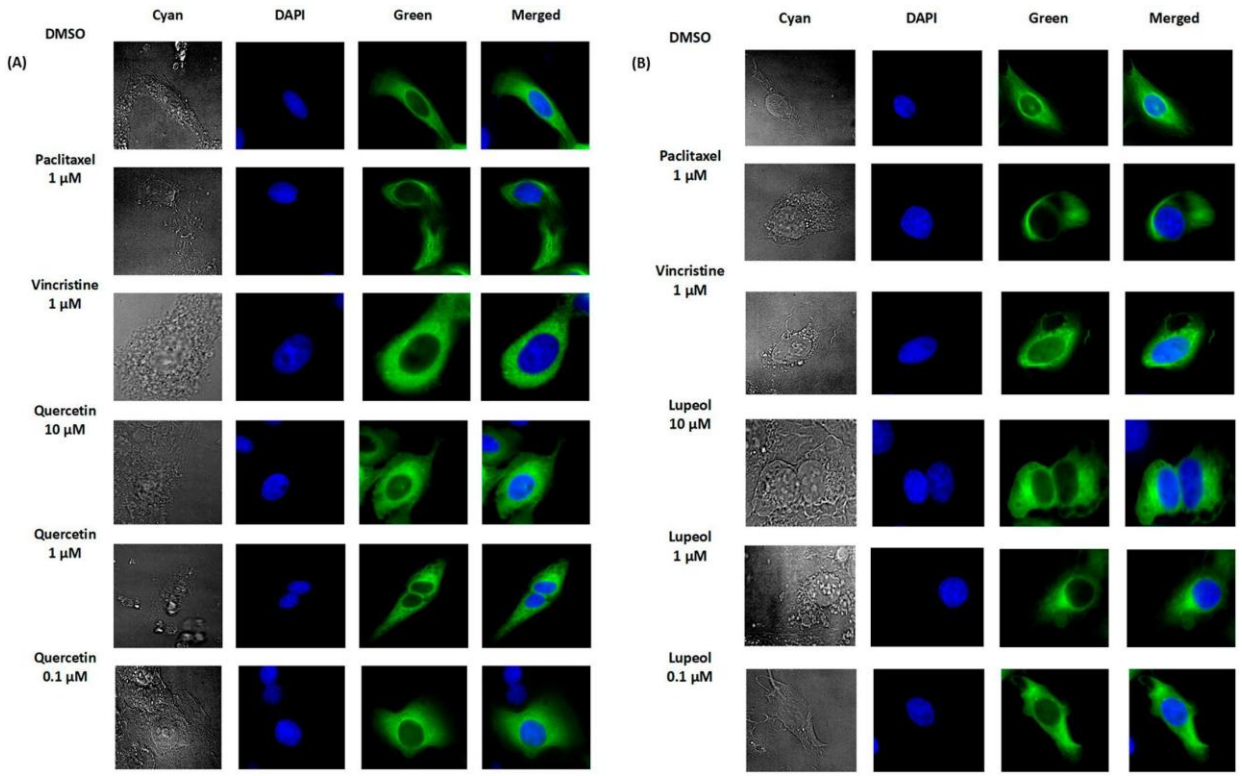

Figure 6. Confocal immunofluorescence microscopy of the microtubule network in U2OS cells upon treatment with (**A**) quercetin and (**B**) lupeol at concentrations of 0.1 µM, 1 µM, and 10 µM for 24 h. Vincristine (1 µM) and paclitaxel (1 µM) served as positive controls and DMSO as the negative control. The cells were imaged using a Thunder Imager Live Cell microscope with a 63×/1.40 NA objective lens (HC PL APO CS2 63×/1.40 OIL UV). The microtubules were visualized using green fluorescence for GFP (green), and the images were merged with DAPI (blue) to highlight the nucleus.

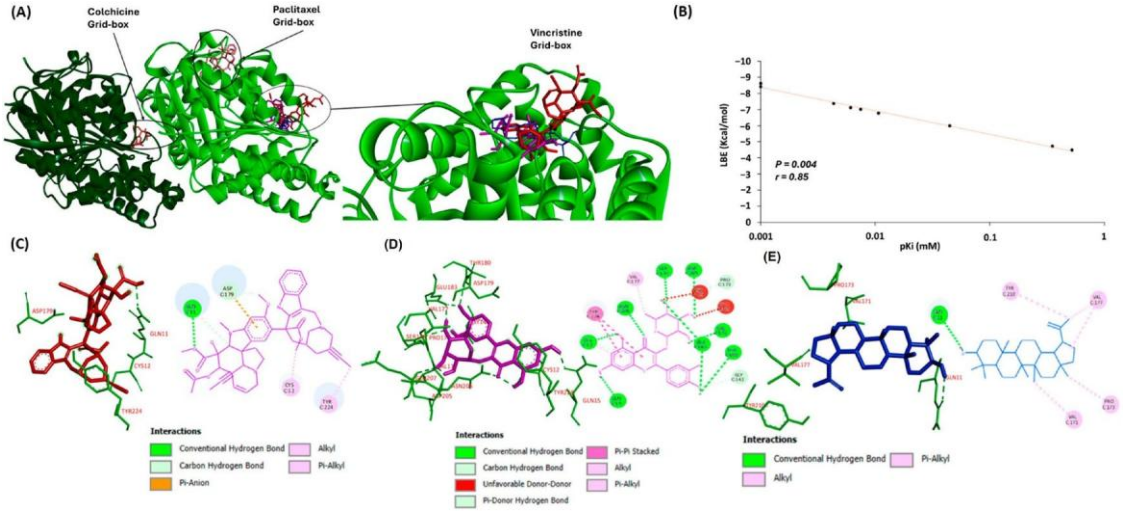

Figure 7. Molecular docking analysis of lupeol and quercetin to tubulin (5N5N). (**A**) Illustrates the binding sites of vincristine, paclitaxel, and colchicine to α- and β-tubulin. On the right, a zoomed-in view shows lupeol and quercetin binding to the same pocket as vincristine. (**B**) The correlation of the predicted inhibition constants (pKi, mM) vs. the lowest binding energies (LBE, kcal/mol) (p = 0.004, r = 0.85). (**C**,**D**) Presents 3D and 2D illustrations of the interaction of lupeol, quercetin, and vincristine with the amino acids of α-tubulin docked at vincristine's binding site. (**C**) Vincristine, (**D**) quercetin, and (**E**) lupeol.

Table 2. Molecular docking of lupeol and quercetin bound to α- and β-tubulin (PDB ID: 5N5N). The lowest binding energies (LBE, kcal/mol), the predicted inhibition constants (μM), and the pharmacophores are represented.

Grid Box	Compounds	LBE (kcal/mol)	pKi (mM)	Pharmacophores
Colchicine grid box	Colchicine	−7.01 ± 0.14	0.007 ± <0.01	α: LEU248, **LYS254**, LYS352 β: GLN11, ASN101, GLY142, GLY143, GLY144, THR145, GLU183, ASN206, TYR224
	Lupeol	−4.48 ± 0.08	0.520 ± 0.07	α: LEU248, LYS254, LYS352 β: GLN11, GLU71, ASP98, ALA99, ALA100, ASN101, GLY142, GLY143, GLY144, THR145, THR179, GLU183
	Quercetin	−4.72 ± 0.15	0.352 ± 0.08	α: GLN247, LEU248, LYS254, LYS352 β: GLN11, ALA12, ASP69, GLU71, ALA99, ALA100, ASN101, GLY144, THR145, THR179, ALA180
Paclitaxel grid box	Paclitaxel	−7.37 ± 0.25	0.004 ± <0.01	α: LEU217, HIS229, LEU230, ALA233, SER236, PHE272, ALA273, PRO274, LEU275, THR276, SER277, ARG278, ARG320, PRO360, **ARG369**, LEU371
	Lupeol	−7.12 ± 0.01	0.006 ± <0.01	α: THR276, GLN281, ARG284, LEU286, LEU371, LYS372
	Quercetin	−5.99 ± 0.29	0.045 ± 0.02	α: LEU217, PRO274, LEU275, THR276, SER277, ARG278, GLN281, LEU286, LEU371, **LYS372**
Vincristine grid box	Vincristine	−8.42 ± 0.15	0.001 ± <0.01	α: **GLN11**, CYS12, GLN15, ASN101, **SER140**, GLY142, GLY143, VAL172, PRO173, SER174, ASP179, THR180, ASN206, TYR224, ASN228
	Lupeol	−8.62 ± 0.04	0.001 ± <0.01	α: GLY10, GLY11, SER140, GLY142, GLY143, VAL171, VAL172, PRO173, SER174, VAL177, ASP179, GLU183, ASN206, TYR210, TYR224
	Quercetin	−6.77 ± 0.06	0.011 ± <0.01	α: CYS12, GLN15, GLY142, VAL172, PRO173, SER174, VAL177, ASP179, GLU183, **ASN206**, GLU207

3.9. Cell Cycle Analysis

Both quercetin and lupeol significantly induced G2/M phase arrest in U2OS cells at 4 × IC_{50}) after 72 h compared to the negative control (DMSO) (Figure 8). Quercetin induced cell cycle arrest with 86.6% of the cells in the G2/M phase (p = 0.0001) and 4.9% in the S phase (p = 0.4). Interestingly, a small but significant portion of cells (7.9%) was also increased in the G0/G1 phase (p = 0.0001), indicating that arresting the cells in the G2/M phase was not the only consequence of treatment. As expected, the positive control vincristine (1 × IC_{50}) induced cell cycle arrest, with 83.6% of cells in the G2/M phase (p = 0.001), 5.9% in the S phase (p = 0.2), and 9.3% in the G0/G1 phase (p = 0.001).

Similarly, lupeol also induced cell cycle arrest in U2OS cells, with 90.9% of the cells in the G2/M phase (p = 0.0002), 5.3% in the S phase (p = 0.05), and 3.8% in the G0/G1 phase (p = 0.0001). Vincristine was used in parallel as the positive control in this experiment, too. A concentration of 1 × IC_{50} induced cell cycle arrest, with 82.3% of cells in the G2/M phase (p = 0.002), 6.0% in the S phase (p = 0.02), and 12.3% in the G0/G1 phase (p = 0.001).

3.10. Drug Resistance Profiling of Lupeol and Quercetin

The question arises as to whether lupeol and quercetin are recognized by classical drug resistance mechanisms and, therefore, whether their activity is hampered by these drug resistance mechanisms. Utilizing the NCI database [40], we correlated the $\log_{10}IC_{50}$ values of lupeol and quercetin with various mechanisms of multidrug resistance in the NCI panel of tumor cell lines (Table 3). Notably, we did not observe an involvement of the two compounds in any drug resistance phenotype, except for one correlation between quercetin and *ABCB5* mRNA expression analyzed through qPCR. This correlation was not significant if mRNA expression was analyzed through microarray hybridization. These findings indicate that these two compounds from chamomile might be useful in inhibiting tumor cells that are otherwise resistant to drugs.

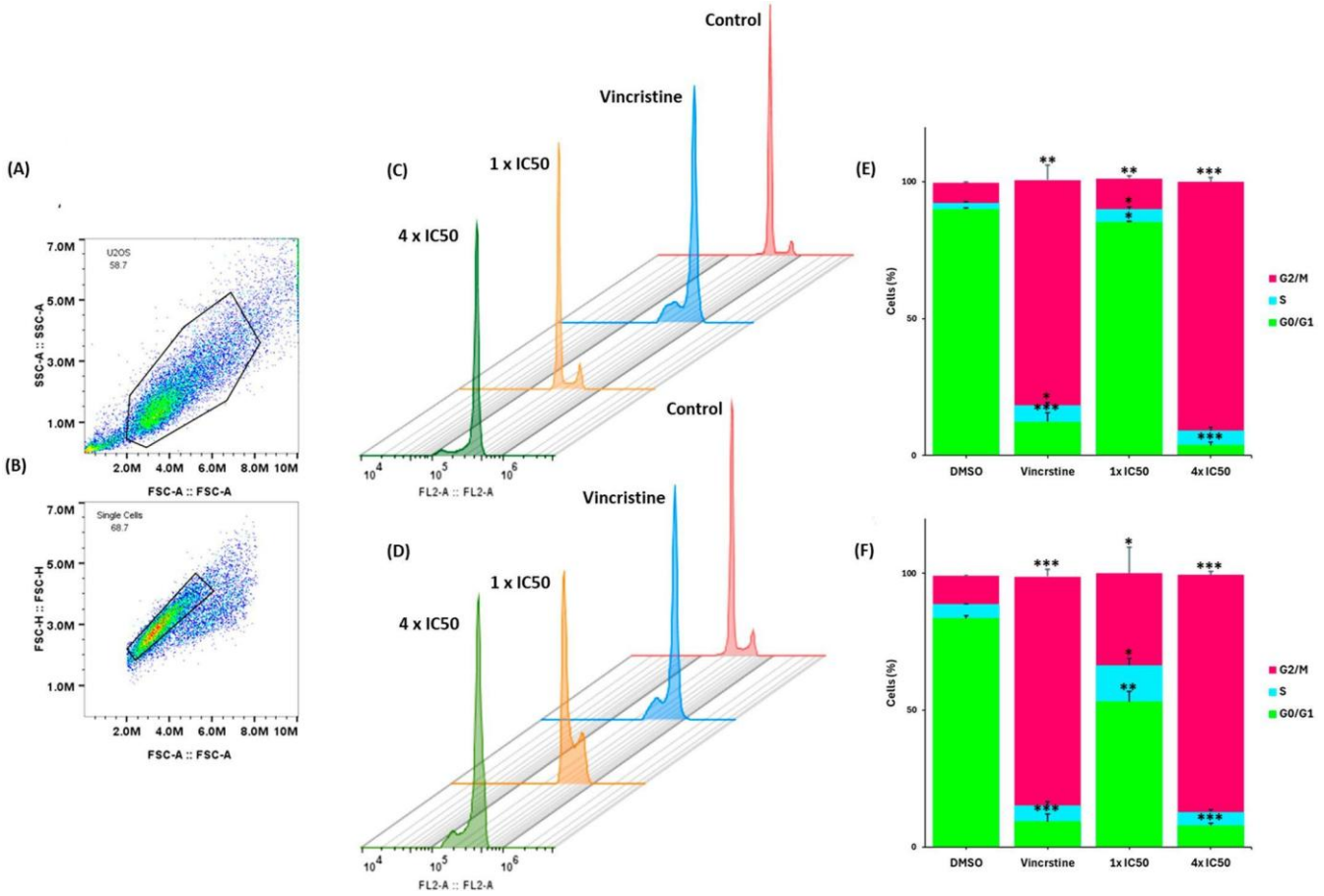

Figure 8. Cell cycle arrest of U2OS cells by quercetin and lupeol. (**A**) Debris was gated out (SSC-A vs. FSC-A) with the first gate. (**B**) With the second gate (FSC-H vs. FSC-A), only single cells of normal morphology were gated. Duplets were gated out. (**C**,**D**) Three-dimensional representation of DNA histograms of U2OS cells exposed to 1 × IC_{50} and 4 × IC_{50} quercetin and lupeol for 72 h. DMSO was used as the negative control, and 1 × IC_{50} vincristine was used as the positive control. (**C**) Cells treated with lupeol and (**D**) cells treated with quercetin. The histograms were obtained through flow cytometry using an excitation of 488 nm and an emission wavelength of 530 nm. (**E**,**F**) Bar diagrams showing the distinct phases of cell cycle upon treatment with quercetin and lupeol for 72 h. (**E**) Cells treated with lupeol and (**F**) cells treated with quercetin. The bar diagrams were created through the calculation of the mean values ± SD of three independent experiments. *** $p < 0.001$, ** $p < 0.01$, and * $p < 0.05$ compared to the negative control using paired two-tailed *t*-test.

Table 3. Correlation between the $\log_{10}IC_{50}$ values for quercetin and lupeol and classical drug resistance mechanisms in the NCI tumor cell line panel.

		Lupeol	Quercetin	Control Drug
		($\log_{10}IC_{50}$, M)	($\log_{10}IC_{50}$, M)	($\log_{10}IC_{50}$, M)
ABCB1 Expression 7q21 (Chromosomal Locus of *ABCB1* Gene)	*r*-value	0.160	0.128	Epirubicin * 0.447
	p-value	0.121	0.203	* 3.55×10^{-4}
ABCB1 Expression (Microarray)	*r*-value	−0.132	−0.631	* 0.533
	p-value	0.159	0.339	* 6.82×10^{-6}
ABCB1 Expression (RT-PCR)	*r*-value	0.027	−0.033	* 0.410
	p-value	0.425	0.413	* 1.54×10^{-3}

Table 3. *Cont.*

		Lupeol	Quercetin	Control Drug
		($log_{10}IC_{50}$, M)	**($log_{10}IC_{50}$, M)**	**($log_{10}IC_{50}$, M)**
ABCB5 Expression				Maytansine
ABCB5 Expression	*r*-value	−0.050	0.207	* 0.454
(Microarray)	*p*-value	0.353	0.086	$*\ 6.67 \times 10^{-4}$
ABCB5 Expression	*r*-value	−0.027	*0.306	* 0.402
(RT-PCR)	*p*-value	0.420	*0.021	* 0.0026
ABCC1 Expression				Vinblastine
DNA Gene	*r*-value	0.059	−0.067	* 0.429
Copy Number	*p*-value	0.329	0.331	* 0.001
ABCC1 Expression	*r*-value	0.040	−0.213	* 0.398
(Microarray)	*p*-value	0.383	0.082	* 0.003
ABCC1 Expression	*r*-value	−0.023	−0.118	0.299
(RT-PCR)	*p*-value	0.436	0.207	* 0.036
ABCG2 Expression				Pancratistatin
ABCG2 Expression	*r*-value	0.105	−0.038	* 0.329
(Microarray)	*p*-value	0.219	0.402	* 0.006
ABCG2 Expression	*r*-value	0.010	−0.040	* 0.346
(Western Blotting)	*p*-value	0.229	0.3982	* 0.004
EGFR Expression				Erlotinib
EGFR Gene	*r*-value	0.049	−0.037	−0.245
Copy Number	*p*-value	0.357	0.404	* 0.029
EGFR Expression	*r*-value	−0.034	−0.068	* −0.458
(Microarray)	*p*-value	0.399	0.328	$*\ 1.15 \times 10^{-4}$
EGFR Expression	*r*-value	−0.101	0.049	* −0.379
(PCR Slot Blot)	*p*-value	0.227	0.358	* 0.002
EGFR Expression	*r*-value	−0.190	0.015	* −0.376
(Protein Array)	*p*-value	0.077	0.461	* 0.001
N-/K-/H-RAS Mutations				Melphalan
TP53 Mutation	*r*-value	−0.034	0.134	* 0.367
(cDNA Sequencing)	*p*-value	0.399	0.190	* 0002
TP53 Mutation				5-Fluorouracil
TP53 Mutation	*r*-value	−0.036	0.395	* −0.502
(cDNA Sequencing)	*p*-value	−0.015	0.277	$*\ 3.50 \times 10^{-5}$
TP53 Function	*r*-value	0.050	−0.079	* −0.436
(Yeast Functional Assay)	*p*-value	0.360	0.311	$*\ 5.49 \times 10^{-4}$
WT1 Expression				Ifosfamide
WT1 Expression	*r*-value	−0.046	−0.103	* −0.316
(Microarray)	*p*-value	0.365	0.250	* 0.007
GSTP1 Expression				Etoposide
GSTP1 Expression	*r*-value	−0.012	−0.012	0.399
(Microarray)	*p*-value	0.468	0.468	$*\ 9.58 \times 10^{-4}$
GST Expression	*r*-value	*0.302	0.028	0.509
(Northern Blot)	*p*-value	*0.010	0.427	$*\ 2.24 \times 10^{-5}$
HSP90 Expression				Geldanamycin
HSP90 Expression	*r*-value	−0.055	−0.045	* −0.392
(Microarray)	*p*-value	0.342	0.384	* 0.001
Proliferation				5-Fluorouracil
(Cell Doubling)	*r*-value	−0.185	0.076	* 0.627
	p-value	0.084	0.313	$*\ 7.14 \times 10^{-6}$

(* indicate $p < 0.05$ and $r > 0.30$ or $r < -0.30$).

3.11. Cytotoxicity Assays for Lupeol and Quercetin

Because the analysis of the NCI cell line panel indicated the activity of both lupeol and quercetin against classical drug resistance mechanisms, we performed resazurin assays to investigate whether these results obtained through correlation analyses could be verified by independent in vitro experimentation.

The dose–response curves in Figure 9 show that multidrug-resistant P-glycoprotein-overexpressing CEM/ADR5000 leukemia cells were cross-resistant to quercetin (degree of resistance: >7.3-fold) and lupeol (degree of resistance: 3.2-fold). The glioblastoma transfected cells with ΔEGFR (U87.MG/ΔEGFR) were 2.3-fold resistant to quercetin and 7.4-fold resistant to lupeol compared to wild-type U87.MG cells. Colorectal *TP53* knockout cells (HCT116 $p53^{-/-}$) were only weakly resistant to quercetin and lupeol (1.4-fold and 1.8-fold, respectively) compared to their corresponding wild-type cells (HCT116 $p53^{+/+}$). All degrees of resistance were, thus, rather low, indicating no or only very low levels of resistance to lupeol and quercetin. These results fit the data obtained from the NCI tumor cell line panel, showing no correlations between the $\log_{10}IC_{50}$ values and the classical resistance mechanisms. The IC_{50} values of U2OS for quercetin and lupeol were higher than those found for most other cell lines tested, indicating that these osteosarcoma cells were more resistant to these two compounds.

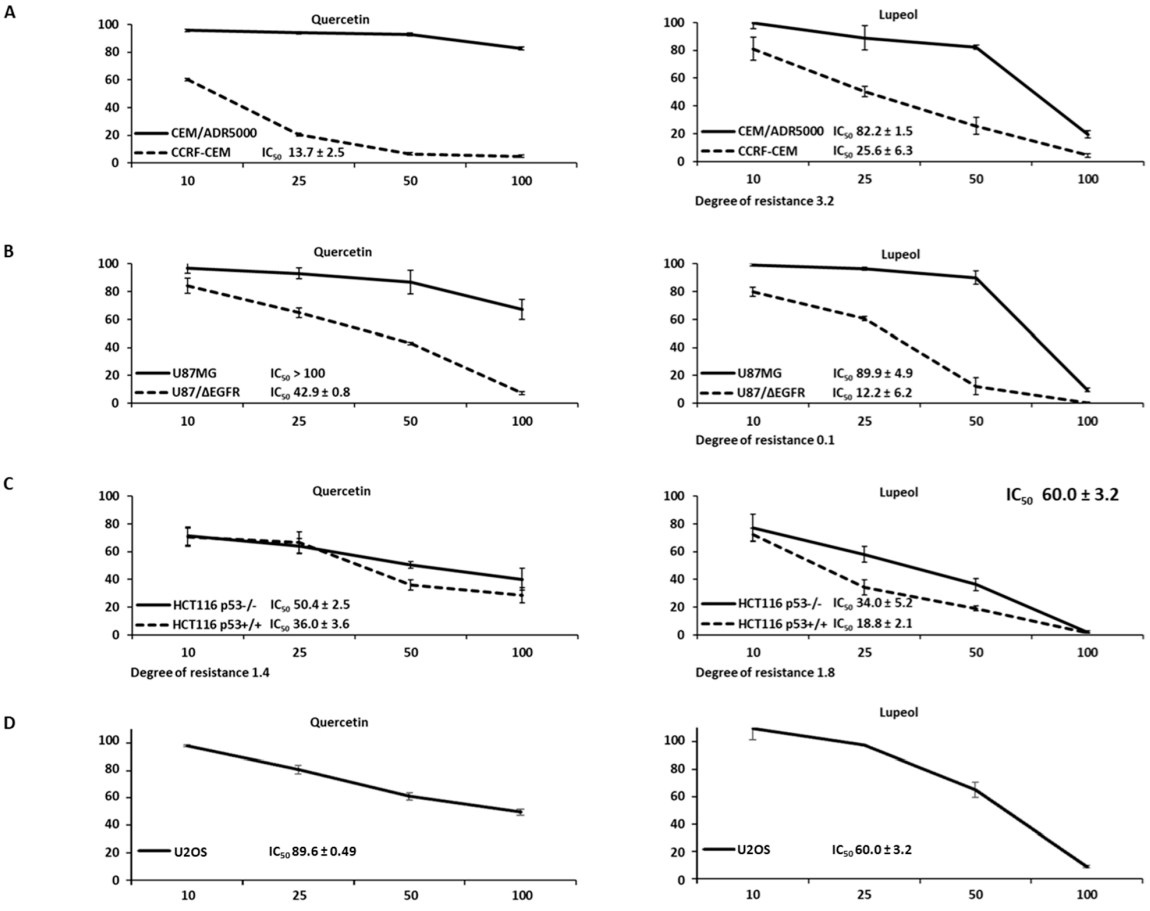

Figure 9. Dose–response curves of quercetin and lupeol as determined through resazurin assay. The mean values and standard deviation values are from three independent experiments. The tumor cells were subjected to treatment with each compound at concentrations of 10 µM, 25 µM, 50 µM, and 100 µM for 72 h. (**A**) Sensitive CCRF-CEM and the drug-resistant P-glycoprotein overexpressing CEM/ADR5000 leukemia cells. (**B**) U87/ΔEGFR transfected with a deletion-activated cDNA of EGFR and its wild-type U87MG glioblastoma cells. (**C**) HCT116 $p53^{+/+}$ and knockout HCT116 $p53^{-/-}$ colorectal cancer cells. (**D**) U2OS osteosarcoma cells.

3.12. Cell Death Detection

We investigated the mode of cell death in CCRF-CEM cells upon treatment with lupeol and quercetin for 72 h. The FITC-conjugated annexin V/PI assay was used to distinguish between living, early apoptotic, late apoptotic, and necrotic cells. Annexin V staining is usually detected in early and late apoptosis, while PI staining indicates late apoptosis and necrosis. Figures 10 and 11 show that both compounds significantly induced necrosis compared to the negative control. Quercetin induced necrosis in 56.40% of CCRF-CEM cells (p = 0.001), while lupeol induced necrosis in 74.33% of cells (p = 0.006). In contrast, early or late apoptosis was detected at low or negligible percentages.

Similarly, the FITC-conjugated annexin V/PI assay was conducted in U2OS cells after treatment with quercetin and lupeol for 72 h. As shown in Figure 11, the cells were rather resistant towards the two compounds, which did not significantly impact the onset of apoptosis but rather necrosis.

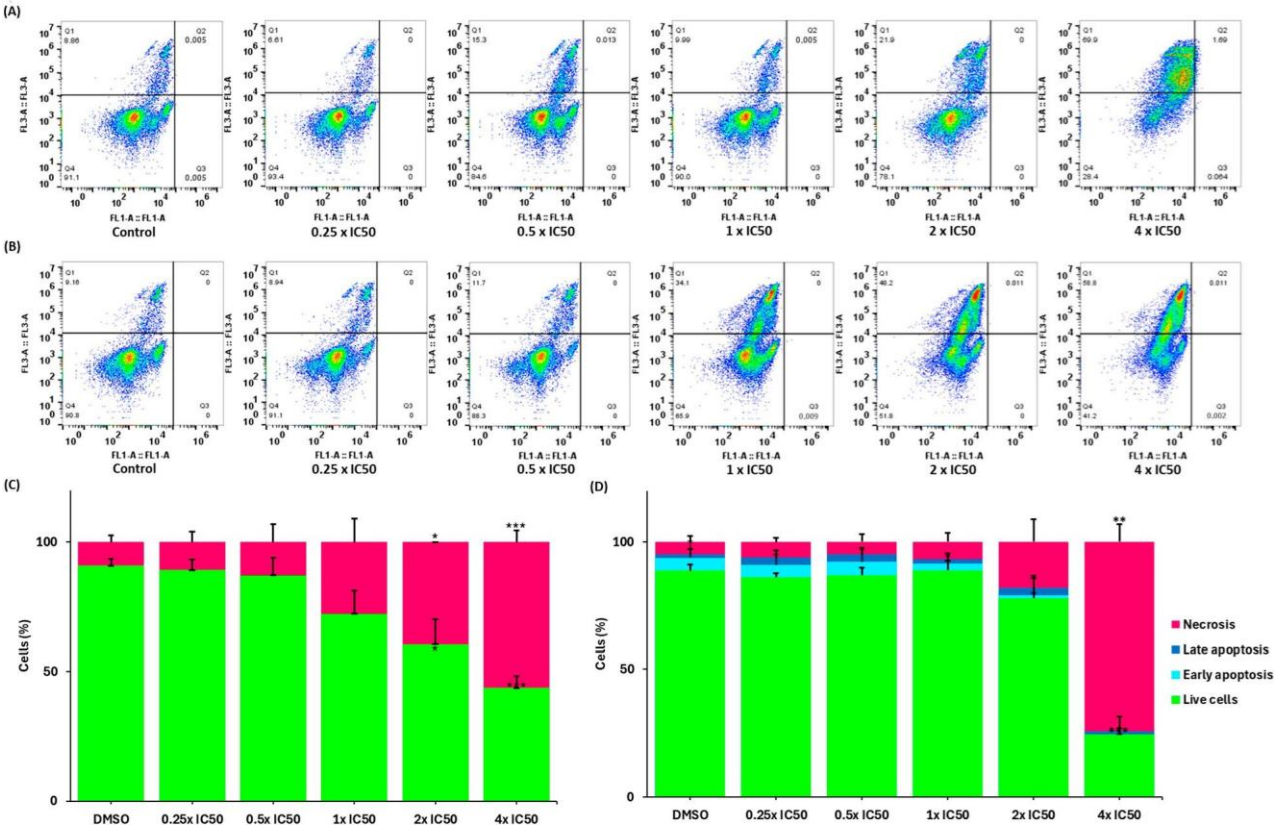

Figure 10. Detection of cell death in CCRF-CEM cells using flow cytometry and annexin-V/PI staining using a flow cytometer. (**A**,**B**) Cells treated for 72 h with 0.25 × IC_{50}, 0.5 × IC_{50}, 1 × IC_{50}, 2 × IC_{50}, and 4 × IC_{50} of quercetin and lupeol, respectively. DMSO was used as the negative control. (**A**) Cells treated with quercetin and (**B**) cells treated with lupeol. Q1 represents necrotic cells (−) annexin V/(+) PI; Q2 represents late apoptotic cells exhibiting annexin V (+)/PI (+); Q3 represents early apoptotic cells (+) annexin V/(−) PI; Q4 represents viable cells (−) annexin V/(−) PI. (**C**,**D**) Bar diagrams representing the percentages of cells in the different quadrants. (**C**) Effects of quercetin and (**D**) effects of lupeol. The treatment of both compounds at increasing concentrations significantly enhanced the percentage of necrotic cells. *** $p < 0.001$, ** $p < 0.01$, and * $p < 0.05$ compared to the negative control using paired two-tailed t-test. The bar diagrams were created through the calculation of the mean values ± SD of three independent experiments.

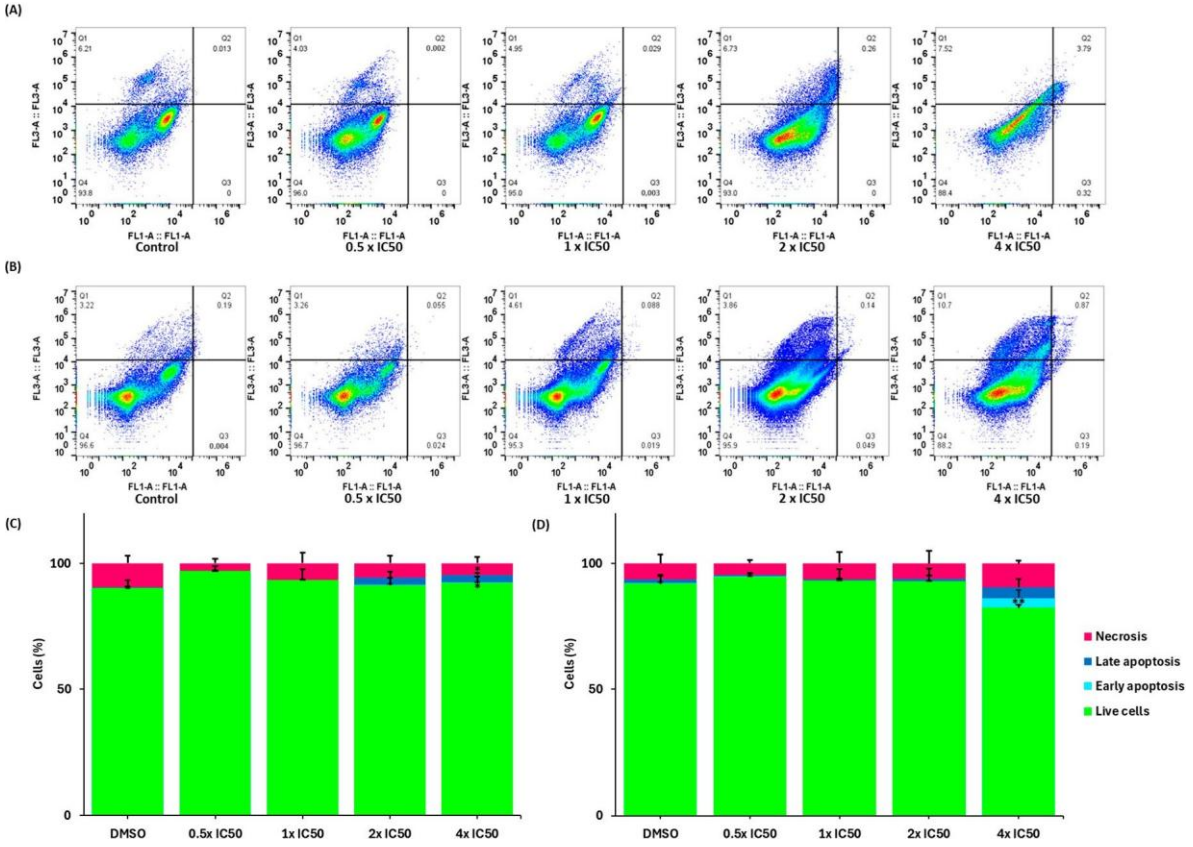

Figure 11. Detection of cell death in U2OS cells using flow cytometry and annexin-V/PI staining using a flow cytometer. (**A**,**B**) Cells treated for 72 h with 0.5 × IC_{50}, 1 × IC_{50}, 2 × IC_{50}, and 4 × IC_{50} of lupeol and quercetin, respectively. (**C**,**D**) represent bar diagrams of the percentage of cells in quadrium treated with lupeol (**C**) and quercetin (**D**). For details, see Figure 10. Treatment with both compounds at 4 × IC_{50} showed a tendency for increased necrosis, which was, however, not statistically significant compared to the negative control.

3.13. Western Blotting

The NF-κB reporter assay in Figure 2 indicated that the selected chamomile compounds inhibited the activity of the NF-κB promoter in the context of anti-inflammatory NF-κB activity. As NF-κB inhibition also plays a role in the apoptosis of cancer cells, we performed a Western blotting experiment to examine the effect of three chamomile compounds (β-amyrin, lupeol, and quercetin) on the protein expression level of NF-κB 65. β-Amyrin and quercetin (50 µM) increased cytoplasmic NF-κB expression, while lupeol displayed non-significant tendencies (Figure 12A).

3.14. Quantitative Real-Time RT-PCR

IL-1β and *IL-6* are known downstream cytokines regulated by NF-κB that are important for mediating proinflammatory and cell-proliferative signals. All three compounds significantly downregulated the expression of the genes encoding *IL-1β* and *IL-6*, particularly at 50 µM (Figure 12C). Notably, quercetin was significantly more effective in downregulating the two genes compared to the other two compounds, with a fold-change in $\log_2$ of −1.11 for *IL-6* ($p = 0.01$) and −0.71 for *IL-1β* ($p = 0.01$). Conversely, β-amyrin displayed the lowest downregulatory activity for IL-6, with fold-changes of $\log_2$ −0.29 for *IL-6* and −0.56 for *IL-1β* ($p = 0.01$). Furthermore, lupeol decreased the genes with $\log_2$ values of −0.54 for *IL-6* ($p = 0.01$) and −0.65 for *IL-1β* ($p = 0.02$).

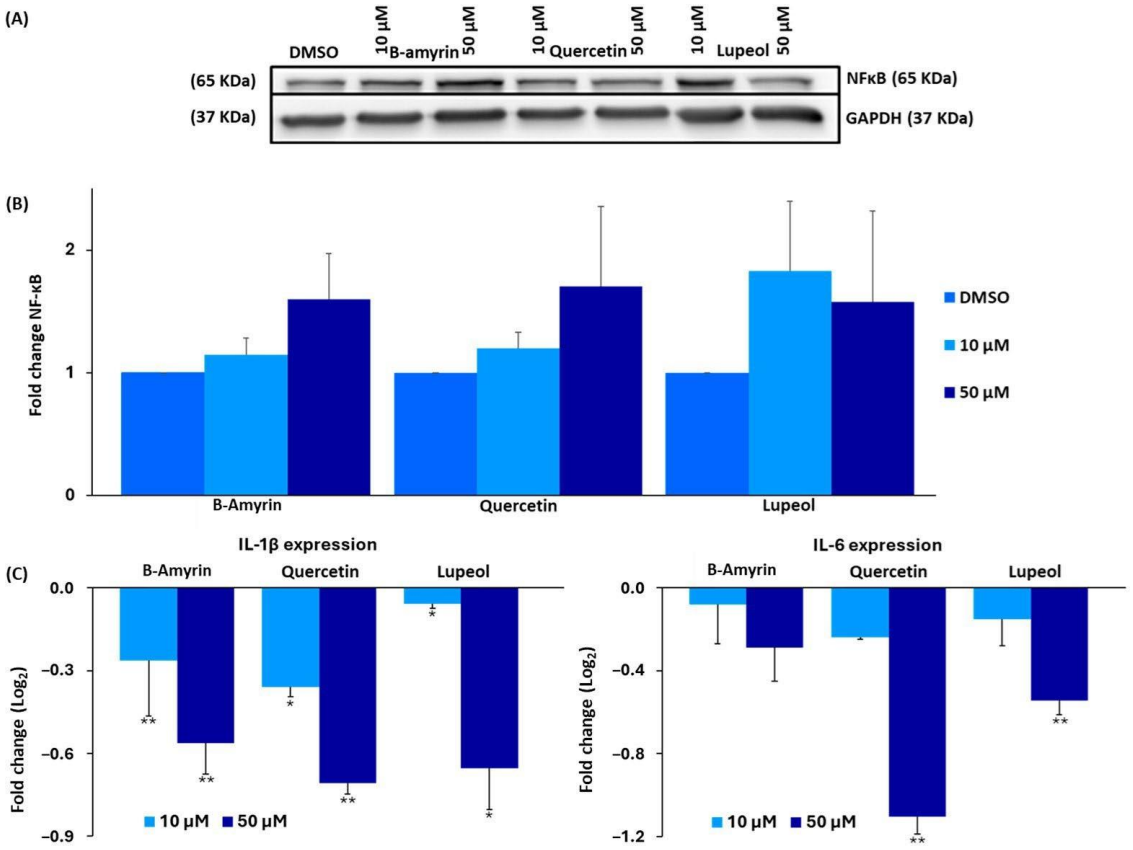

Figure 12. Expression of NF-κB and downstream genes. (**A**) Western blotting analysis of NF-κB in HEK-Blue Null1 cells treated with 10 µM or 50 µM of β-amyrin, quercetin, and lupeol for 24 h, followed by 24 h of TNF-α at 100 ng/mol. (**B**) The percentages of NF-κB expression in the cell. (**C**) qRT-PCR analysis of *IL-1β* and *IL-6* gene expression in HEK-Blue Null 1 cells treated with 10 µM or 50 µM of β-amyrin, quercetin, and lupeol for 24 h with TNF-α 100 ng/mL for another 24 h. The statistical analysis was performed through the paired one-tailed *t*-test (** $p \leq 0.01$) (* $p \leq 0.05$) from three independent trials.

3.15. Proteome Analysis

If all or most of the classical drug resistance mechanisms are not operative for lupeol and quercetin, the question arises as to which factors do determine sensitivity and resistance to these two drugs. Therefore, we conducted a COMPARE analysis by correlating the expression levels of 3171 proteins in the 60 tumor cell lines from the NCI database [40] with the $\log_{10}IC_{50}$ values of both lupeol and quercetin. Subsequently, the top 40 proteins were assembled, and 20 were directly correlated with the two compounds and 20 were reversely correlated. Finally, we generated a two-dimensional clustering and color-coded heat map using a hierarchical Ward cluster method, where, in one dimension, the expression profiles of the 40 proteins appear and, in a second dimension, the different cell lines appear (Figures 13 and 14). The $\log_{10}IC_{50}$ values for lupeol and quercetin, which were not included in the cluster calculations, are shown on the right side of the heat maps for illustration. The cellular responsiveness to both lupeol and quercetin was determined by comparing individual $\log_{10}IC_{50}$ values to the median value across all cell lines. If the $\log_{10}IC_{50}$ value was lower than the median, the cell lines were categorized as sensitive; if it was above the median, the cells were defined as resistant.

	Sensitive	Resistant
Partition (M)	≤−4.270	≥−4.270
Cluster 1	3	14
Cluster 2	12	15
Cluster 3	13	1
χ^2-test:	$p = 1.44 \times 10^{-4}$	

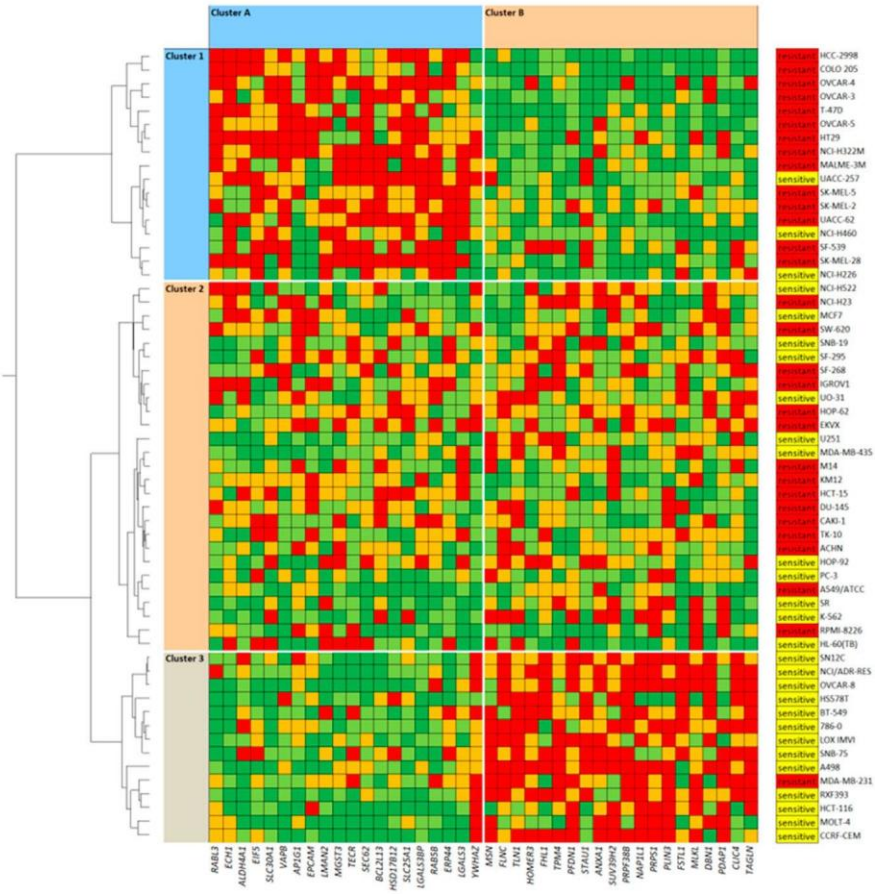

Figure 13. Cluster analysis in a 2D colored heat map of proteins' expression in NCI tumor cell lines responding to lupeol. Clusters A and B represent the top 40 proteins, and clusters 1–3 show the tumor cell lines. The cell lines were clustered according to their degrees of relatedness to each other based on their protein expression included in the analysis. Color code: red, 0–25% quartile; orange, 26–50% quartile; grey, median value; light green, 50–75% quartile; and dark green, 76–100% quartile. Depending on individual $\log_{10}IC_{50}$ values, the responsiveness of the cell lines to lupeol was classified as sensitive if their $\log_{10}IC_{50}$ values were lower than the median value of all cell lines (marked in yellow) and as resistant if their $\log_{10}IC_{50}$ values were higher than the median value (marked in red). The χ2 test shows a statistical significance ($p = 1.44 \times 10^{-4}$) upon comparing the two clusters of protein expression in the cell lines, where clusters 1 and 2 contained mainly resistant cell lines to both lupeol and quercetin, respectively, and cluster 3 contained mainly sensitive cell lines.

For both lupeol and quercetin, we obtained three clusters (clusters 1–3) showing the individual protein expression. Furthermore, we obtained two clusters of cell lines (clusters A and B) (Figures 13 and 14). These clusters were then correlated with the $\log_{10}IC_{50}$ values (which were not included in the cluster calculation). Interestingly, clusters 1 and 2 predominantly included lupeol/quercetin-resistant cell lines, while cluster 3 predominantly contained sensitive cell lines. Cluster A predominantly contained cell lines with high protein expression in cluster 1 and low expression in cluster 3, while in cluster B, the protein expression was the opposite (low in cluster 1 and high in cluster 3). Afterwards, we calculated the difference between sensitive and resistant cell lines using the χ^2 test. The results showed that the distribution of the three clusters was statistically significant for both lupeol ($p = 1.44 \times 10^{-4)}$ and quercetin ($p = 0.044$) (Figures 13 and 14).

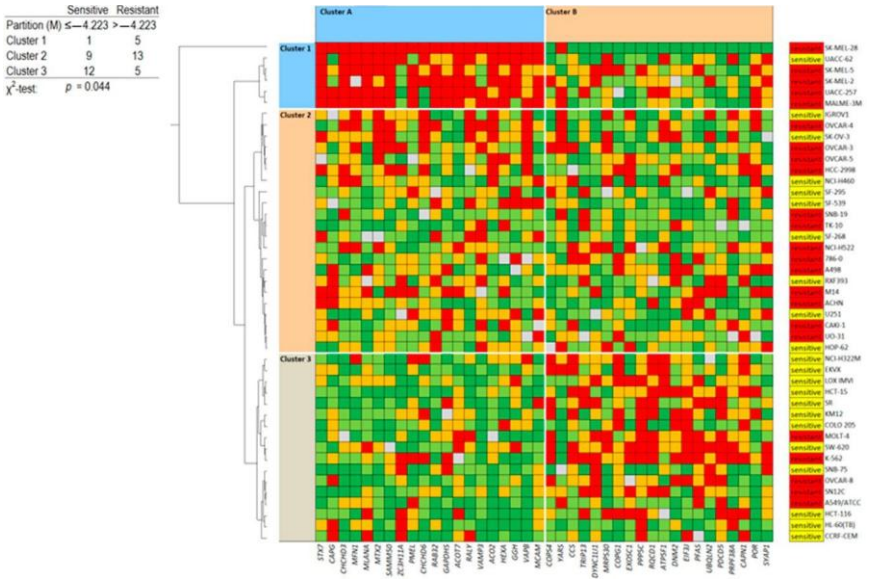

Figure 14. Cluster analysis in a 2D colored heat map of proteins' expression in NCI tumor cell lines responding to quercetin. The χ2 test shows a statistical significance ($p = 0.044$). For further details, see Figure 13.

Each of the 40 proteins was identified through this approach to determine the sensitivity or resistance to lupeol or quercetin. These proteins have been compiled along with their protein symbols, full names, cellular functions, and functional categories in Supplementary Tables S1 and S2. Although these proteins seemed to be unrelated at first sight, it was interesting to observe that they belonged to some common functional categories. These categories are shown in Table 4.

Table 4. Functional categories of proteins identified through the proteomic analyses for lupeol and quercetin, as shown in Figures 13 and 14.

Functional Categories	Protein Symbols (Lupeol Analysis)	Protein Symbols (Quercetin Analysis)
General metabolism	ALDH4A1, ECH1, HSD17B12, TECR	ACO2, ACOT7, GAPDHS, GGH
Protein and vesicle trafficking	AP1G1, LMAN2, PLIN3, RAB5B, SEC62, VAPB	COPG1, DYNC1LI1, STX7, VAPB
DNA/RNA metabolism	EIF5, FHL1, NAP1L1, STAU1, SUV39H2	DYNC1LI1, EIF3J, EXOSC1, PDCD5, PRPF38A, RALY, TRIP13, ZC3H11A
Cell Adhesion	EPCAM, LGALS3, TLN1	MCAM
Chaperones and protein degradation	ERP44, PFDN1	CCS, UBQLN2
Cytoskeleton	FLNC, MSN, STAU1, TPM4	CAPG, DNM2, CAPN1
Immune	ANXA1, FSTL1, LGALS3, LGALS3BP, MGST3, RAB5B, TLN1	YARS
Signal transduction	HOMER2, RABL3, YWHAZ	CAPN1, PPP5C, RQCD1
Cell proliferation and differentiation	DBN1, PDAP1	PDCD5, PPP5C, RQCD1
Cell death	BCL2L13, LGALS3, MLKL	PDCD5, RAB32
Tumor suppressor	TAGLN	
Ion channels and drug transporters	CLIC4, SLC25A1, SLC30A1	
Mitochondrial function		ACO2, ATP5F1, CHCHD3, CHCHD6, MFN1, MRPS30, MTX2, RAB32, SAMM50
Melanosome biogenesis and function		MLANA, PMEL, RAB32
Drug metabolism		POR
Others		CHCHD6, HEXA, VAMP3

(Multiple entries are possible).

3.16. Kaplan–Meier Survival Analysis

Because NF-κB is known for its anti-proliferative, anti-apoptotic, and anti-inflammatory activities in the cell [60], we wanted to survey the role of NF-κB expression for the survival prognosis of cancer patients. We performed Kaplan–Meier survival analysis with the help of the KM-Plotter database. Out of 21 cancer types, the analysis revealed that the higher the *NFKB2* mRNA expressed, the lower the survival time for patients with renal clear cell carcinoma compared with patients with low *NFKB2* expression. Moreover, patients with high *NFKB2* expression in grade 3 renal carcinoma died significantly earlier than those with a low expression. Interestingly, the female patients with renal carcinoma had significantly longer survival times compared with males if *NFKB2* mRNA expression was low. Similarly, patients with low neoantigen load and low *NFKB2* mRNA expression in their renal carcinoma cell type had a better survival prognosis than those with high *NFKB2* expression and a significantly higher survival time than the patients with a low mutational rate (Figure 15). These data indicated that the inhibition of NF-κB could indeed be beneficial in the prevention and treatment of renal carcinoma.

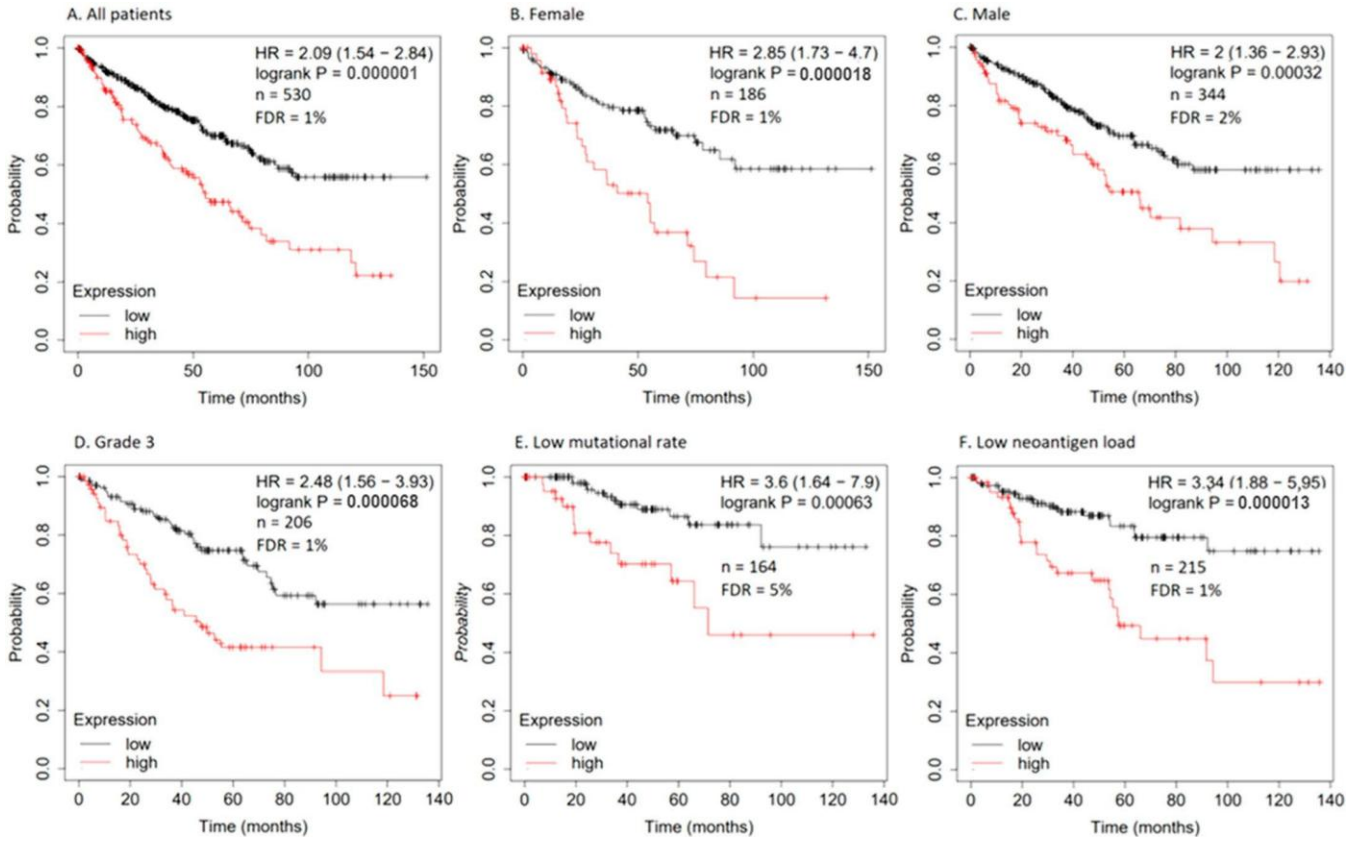

Figure 15. Kaplan–Meier analysis from the KM-Plotter database of overall survival time (months) for renal clear cell carcinoma cells correlating with the expression of *NFKB2* mRNA. (**A–F**) Different patient profiles where NF-κB expression correlated significantly with the overall survival time.

4. Discussion

Chamomile tea is not only used for its exquisite taste but also its numerous health-promoting effects. Renowned for centuries, chamomile contains metabolites that possess anti-inflammatory, antioxidant, and relaxant properties [61,62]. Over decades, many studies have revealed the anti-inflammatory effect of chamomile both in vitro and in vivo [63]. They have demonstrated the inhibitory effect of chamomile extract against markers and pathways at the molecular and cellular levels [64,65]. These findings were complemented by in vivo research, where chamomile compounds exhibited anti-inflammatory effects if tested in animals [66,67]. Adding to this, various clinical studies have shown evidence

of the anti-inflammatory effect of chamomile if tested in patients with different types of inflammatory disease [65,68,69] Moreover, chamomile has garnered attention for its potential in cancer prevention and treatment [70–72]. In vitro results have suggested that chamomile extracts may possess anticancer properties, showing inhibitory effects on the proliferation of cancer cells and in some cases on programed cell death [12,13,73–77]. While there is limited evidence in vivo, some preliminary evidence supports the potential of chamomile as an anticancer and preventive agent [78–80]. The entangled connection between inflammation and carcinogenesis may make a reasonable contribution to this point of view [81,82].

In the same entangled manner, the transcription factor NF-κB was proven to play a role in both inflammation and carcinogenesis [83]. NF-κB not only controls the inflammatory responses with its transcriptional activity on several proinflammatory promoters [84] but also has a crucial role in regulating apoptosis and cell proliferation, mostly by favoring cell survival mechanisms and, therefore, contributing to the initiation and progression of tumors [85,86]. Additionally, NF-κB pathways also play a pivotal role in the development of resistance against anticancer drugs [87,88]. Interestingly, the development of tumors is often driven by similar mechanisms that also cause drug resistance. It is in the nature of the biological system of all organisms to detoxify and excrete harmful substances, such as toxic metabolic products used in chemotherapy, through the activation of pro-survival pathways. This will then annul the induction of cell death and enhance the continuous progression of the tumor in the body [89–91].

These findings and observations prompted the question of whether chamomile or its derivates inhibit NF-κB. NF-κB activation or inhibition plays a key role in cellular processes, such as cell survival, cell growth, cell proliferation, and even cell death in stem cells and different cancer cells, including leukemia [92–95]. To address this, we initiated virtual drug screening to investigate the bindings between 212 chamomile compounds to NF-κB. Subsequently, 28 compounds were further selected for a computational assay in which we calculated the LBE and pKi values. Among these 28 molecules, 15 exhibited LBE values consistently below −6 kcal/mol. Correspondingly, the pKi values demonstrated a diverse range, fluctuating between 0.42 ± <0.01 μM for β-amyrin and 46.78 ± 0.12 μM for apigenin. Six compounds were selected from these results for further in vitro experiments. β-Amyrin, β-sitosterol, β-eudesmol, daucosterol, and myricetin were chosen depending on their binding energy, including a range from the highest to the average and lowest values. Apigenin, with higher binding, was chosen for its popularity and proper comparison with the other compounds. Using an inhibitory NF-κB reporter cell assay where the rest activity of NF-κB was measured, β-amyrin exhibited the highest percentage of inhibition. In contrast, daucosterol demonstrated the lowest inhibitory activity. These experimental results confirm our in silico predictions. Hence, the regression analysis of the data showed that NF-κB rest activity (%) significantly correlated with the LBE values. Additionally, we validated the authenticity of our data using microscale thermophoresis (MST). This result further confirmed the binding of β-amyrin to NF-κB.

It is now evident that activated NF-κB enhances the expression of proinflammatory genes in a positive feedback loop, leading to increased ROS generation in the cell. Elevated ROS levels during chronic inflammatory diseases or cancer can in return further activate NF-κB and upregulate immune responses [96,97]. Accordingly, to validate this relationship, we performed an ROS generation assay using HEK-Blue Null 1 cells treated with β-amyrin and exposed to 100 ng/mL of TNF-α and 10 μM of H_2O_2, thus creating a high oxidative microenvironment within the cell. The results demonstrated that β-amyrin reduced ROS levels significantly. Moreover, it is well-established that both acute and chronic inflammatory diseases are characterized by dysfunction of mitochondria and aggregation of ROS generation. These factors can lead to cell damage or cell death. Alternatively, in other cases, they can trigger the activation of cell survival pathways and cell proliferation [98,99]. In this context, we examined whether the inhibition of NF-κB with β-amyrin might affect the mitochondrial membrane potential (MMP). Employing the MMP-JC1 assay on HEK-Blue

Null 1 treated with β-amyrin and TNF-α (to stimulate NF-κB activation), we observed a significant impact on the breakdown of MMP in the treated samples compared to the control. β-Amyrin treatment increased the population of MMP-disrupted cells by 52.6%. In comparison to vinblastine, 26.6% of the cell population were unhealthy or dead. These results highlight the promising potential of β-amyrin as a potential therapeutic agent for inflammatory diseases and oxidative-stress-related disorders, suggesting its applicability as a cancer-preventive agent or even an adjunctive treatment in cancer therapy.

This leads to the second part of this study, where we studied the therapeutic value of chamomile, particularly focusing on inflammation, cancer prevention, and overcoming drug resistance. We started with cytotoxicity and oncobiogram analyses comparing the effects of multiple chamomile compounds on the cell viability of 60 cell lines originating from various tumor types using the NCI60 database. Notably, quercetin and lupeol exerted significant cytotoxicity, with specific preferences against colon cancer for lupeol and melanoma for quercetin. The oncobiogram analysis further revealed correlations with microtubules and mTOR inhibitors, validating previous studies in which both quercetin and lupeol disturbed the polymerization of microtubules through their binding to tubulin [100,101] and inhibited the mTOR pathway [102,103]. The immunofluorescence microscopy experiment validated these findings, showing clear inhibition of the GFP-α tubulin polarization by lupeol and quercetin (at 10 µM) comparable to the effect of vincristine (at 1 µM). Given the key role of microtubules in cell stabilization and maintenance, the identification of novel tubulin inhibitors for tumor therapy remains essential [104]. Furthermore, the in silico assessment confirmed that both lupeol and quercetin have higher binding affinities with α-tubulin if docked at vincristine's binding site compared to the two other known tubulin inhibitors, paclitaxel and colchicine.

It is well-established that paclitaxel enhances the stability of the microtubules, maintaining them in their polymerized form, which induces the activity of NF-κB through the same pathway as TNF-α. In contrast, colchicine and vincristine are known to destabilize and disturb the microtubule formation, which blocks the translocation of the cytoplasmic NF-κB p65 to the nucleus and reduces the activity of NF-κB through the TNF-α canonical pathway [105–107]. We hypothesize that lupeol and quercetin may act in the same manner as vincristine by inhibiting the microtubules and reducing the activity of NF-κB.

Microtubules are also important for immune reactions and inflammatory processes, as microtubule networks are involved in the migration of immune cells to inflamed tissues [108–110]. Thus, the inhibition of microtubules by anti-inflammatory compounds from chamomile might not only directly inhibit tumor cells but also suppress the activation and migration of inflammatory cells and thereby contribute to the decline of the inflammation process [111].

There is not only a connection between NF-κB and the microtubule but also cytokines. The NF-κB-mediated release of proinflammatory cytokines (e.g., *IL-1β* and *IL-6*) favors not only the activation of immune cells at inflamed sites in the body but also cell survival and cell proliferation. Because receptors for proinflammatory interleukins are expressed at both immune cells and tumor cells, their inhibition by natural products contributes to the suppression of tumor growth [112–114]. We found that β-amyrin, lupeol, and quercetin inhibited the expression of *IL-1β* and *IL-6*, a result that is consistent with the point of view that inhibition of interleukin production also causes the inhibition of tumor cell growth. At the same time, these three substances increased the expression of NF-κB of HEK-Blue Null1 cells. This can be explained by an inhibited translocation of NF-κB from the cytosol to the nucleus, which consequently leads to suppressed interleukin production due to the transcriptional activity of NF-κB in the nucleus. Because microtubules are involved in the translocation of NF-κB from the cytosol to the nucleus [115–117], microtubules inhibited by chamomile compounds may be unable to translocate cytosolic NF-κB to the nucleus, where it can bind to promoters of NF-κB downstream genes. Chamomile compounds may therefore act on multiple intracellular targets and pathways.

Recognizing that chemoresistance represents a major obstacle in cancer treatment, we conducted drug resistance profiling for quercetin and lupeol by correlating their values to classical drug resistance genes, including ABC transporters, oncogenes, tumor suppressors, and other mechanisms. The analysis indicated that the two compounds have no cross-resistance and are not involved in classical drug resistance mechanisms. This is a remarkable result as compounds combatting or bypassing resistance to clinically established drugs are urgently required.

We aimed to verify the correlation analyses with the NCI panel by using specific cell models that showed specifically overexpressed or knocked-out genes conferring drug resistance (P-glycoprotein, *EGFR*, *TP53*). While it is known that established cancer drugs can provoke high levels of resistance in tumors (e.g., CEM/ADR5000 cells were more than 1000-fold resistant to doxorubicin) [118], lupeol and quercetin showed no or only very low degrees of resistance of three or less. These results confirmed our bioinformatic analysis, indicating that both compounds are active against otherwise drug-resistant tumor cells and do not encounter major cross-resistance mechanisms.

It is reasonable to propose that chamomile holds not only the potential to prevent inflammation and cancer but also the ability to overcome drug resistance. This theorizes a dual role for chamomile as a preventive measure but also as an additive to cancer treatment, particularly in cells that exhibit resistance to conventional therapies. These insights open new possibilities for exploring chamomile compounds, such as β-amyrin, lupeol, and quercetin, as valuable assets in addressing the challenges posed by drug-resistant cancer cells. Further research and clinical studies could elucidate the full scope of chamomile's contributions to cancer prevention and treatment.

In this context, it was interesting that the cytotoxicity of both compounds in CCRF-CEM and U2OS cells was not caused by apoptosis as the most common mode of cell death but by necrosis. This might be a cell-type-specific effect as quercetin and lupeol have been reported to induce either apoptosis or necrosis (or necroptosis) in different cell lines [119–124]. Because apoptosis is driven by the balance of pro- and anti-apoptotic proteins in specific signaling cascades, it is known that mutations in specific genes encoding these proteins confer resistance to apoptosis [125–128]. As a consequence, cytotoxic insults may overcome apoptosis resistance by other cell death modes, such as necrosis [129].

Despite the fact that classical drug resistance mechanisms did not affect the responsiveness to lupeol and quercetin, it can be assumed that the different responsiveness of the NCI cell lines may be due to variations in the expression of genes that influence sensitivity and resistance to lupeol and quercetin. Therefore, the question arises as to what are the cellular factors that determine sensitivity or resistance to these two compounds. To explore this further, we analyzed the proteomic expression of the NCI tumor cell lines. In this analysis, we identified 40 proteins whose expression significantly correlated with sensitivity and resistance of the cell lines. Although the two sets of each of the 40 proteins identified through hierarchical cluster analysis for lupeol and quercetin seem to be heterogeneous at first sight, they belong to some common functional categories, i.e., protein and vesicle trafficking, DNA/RNA metabolism, immune function, cytoskeleton, mitochondrial function, cell proliferation and differentiation, cell death, channels and transporters, chaperone functions, signal transduction, and other functions (Table 4). Although these proteins have not been described or only scarcely described so far to determine sensitivity or resistance to lupeol or quercetin and the relationships found in our study are novel, most of the functional protein groups mentioned above are known to influence the response of tumor cells to standard chemotherapy. Therefore, it can be hypothesized that these proteins might also play a role for quercetin and lupeol.

Protein and Vesicle Trafficking: The translocation of proteins and vesicles to their functional sites in tumor cells has received less attention in the context of drug resistance. Impaired distribution of both cellular structures may, however, indeed influence cellular homeostasis and, therefore, contribute to carcinogenesis and differential responses to chemotherapy [130,131]. Our data obtained with lupeol, and quercetin indicate that

there is still an open field for innovative research to uncover the full range of trafficking mechanisms for responses to established cancer drugs as well as cytotoxic natural products.

DNA/RNA Metabolism: This is a huge field spanning many topics, such as transcription and transcription factors [132], translation [133], DNA replication [134], chromatin remodeling [135], chromosome segregation [136,137], etc. These processes are central to the vital functions of tumor cells and play important roles under the selection pressure of anticancer therapies. Understanding these mechanisms in more detail will facilitate the development of novel targeted therapies to address these mechanisms in cancer cells.

Immune Functions: Although tumor immunology has been a thriving field in cancer research, attention has recently focused more on the advent of passive immunotherapies (e.g., therapeutic monoclonal antibodies, immune checkpoint inhibitors) and active immunotherapeutic approaches (e.g., CAR-T). On the other hand, it is also known that the immune system influences the responsiveness of tumors to classical chemotherapy by generating therapy-resistant niches in tumors [138].

Cytoskeleton: Among the cytoskeletal proteins, not only the microtubules as direct targets for Vinca alkaloids, taxanes, and new drug candidates are well-known [139] but also others, such as actin, vimentin, and cytokeratin as well as proteins accompanied by cytoskeletal proteins that contribute to cytoskeletal organization and basic tumor cell features (e.g., cell remodeling during invasion and metastasis, resistance to cisplatin and other drugs, etc.) [140–142].

Mitochondrial Functions: Mitochondria do not only supply cancer cells with energy (in terms of ATP production) but also help them to adapt to cellular stressors, such as nutritional deprivation hypoxia and oxidative stress. Mitochondria provide sufficient biosynthetic flexibility to tumors to survive even under worse conditions [143,144]. Therefore, mitochondrial metabolism is involved in tumor progression and drug resistance [145].

Cell Proliferation and Differentiation: It has been long recognized that slowly growing tumors are more resistant to chemotherapy than fast-growing ones [146]. As a consequence, the cellular differentiation state, e.g., driven by the epidermal growth factor receptor (EGFR), also influences drug response [147,148]. The proteomic analyses in the present study (Table 4) indicate that several proteins involved in cellular differentiation determine sensitivity or resistance to cytotoxic natural products.

Cell Death: Apoptosis as most well-known mode programmed cell death is long known to affect the efficacy of chemotherapy and most other cytotoxic compounds as well [149]. However, in recent years a surprising number of non-apoptotic modes of programmed cell death have been uncovered [150]. Interestingly, these newer forms of cell death also influence the sensitivity and resistance of tumors to chemotherapy [151,152]. In the present investigation, we found that lupeol and quercetin induced necrosis rather than apoptosis. In our proteomic analyses, we also found that several proteins involved in apoptotic and non-apoptotic cell death correlated with these two natural products (Table 4).

Ion Channels and Drug Transporters: The membrane as the first barrier for cytotoxic compounds to enter cells represents an obvious cause of drug resistance. Though transporter molecules from the ATP-binding cassette (ABC) and solute carrier (SLC) families have been intensively studied for their role in cancer drug resistance [153,154], other membrane proteins (e.g., chloride and other ion channels) are associated with cell growth and apoptosis and, thereby, affect the response of tumor cells to chemotherapy [155]. In our own investigations during a period of more than two decades, we found that natural products are a rich source serving either as substrates and inhibitors of drug transporters and even as a new strategy to exploit hypersensitivity (collateral sensitivity) to treat otherwise drug-resistant cells [156]. Our present analysis demonstrated that channels and transporters are also involved in their responsiveness of tumor cells to natural products, such as lupeol and quercetin (Table 4).

Cell Adhesion: It is well known that single-cell tumors, such as leukemia, tend to respond better than solid cancer. One reason may be that solid cancers grow in tissues where the cells are connected to and communicating with each other numerous proteins

including cell adhesion molecules, integrins, adapter proteins, and associated kinases. This set of proteins has been termed "cell adhesion resistome" because these proteins contribute to anticancer drug resistance [157]. The present proteomic analyses revealed a number of proteins also belonging to this cell adhesion resistome (Table 4).

Chaperone Functions: Molecular chaperones are responsible for the correct folding of proteins either in the nascent state if freshly translated amino acid chains are folded to three-dimensional protein structures or if cellular stress causes misfolding and damage of proteins. These quality control mechanisms are crucial for the correct function of proteins. Chaperones, i.e., heat shock proteins, are associated with drug resistance of tumors [158–160]. We found a couple of proteins also belonging to the chaperone system to be linked with response to lupeol and quercetin (Table 4).

Signal Transduction: A quantity of proteins involved in signal transductions that seems to be barely manageable contribute to complex signaling networks that drive cancer cells sensitive or resistant to cancer drugs and cytotoxic natural products [161–163]. Rather than single signaling pathways, sophisticated cross-talks between different signaling routes led to broad networks determining drug response [164,165]. The new discipline of network pharmacology is just beginning to understand these complex mechanisms. This is not also true for established cancer drugs but also for natural products [166]. It will be thriving to further detect single elements in large signaling networks that are responsible for drug response of tumor cells to lupeol and quercetin in the future.

Other Functions: Among the proteins that do not belong to the functional categories mentioned above are DNA repair proteins, tumor suppressors, and others. Because DNA repair mechanisms as well as tumor suppressors (e.g., TP53), are well-known drug resistance mechanisms [167,168], it is also worth speculating that the proteins identified in our analyses contribute to resistance to lupeol and quercetin. It is quite unexpected to find proteins involved in melanosome biogenesis and function among the proteins correlating with quercetin responsiveness. However, because melanosomes generate ROS [169], it is possible that there is a direct or indirect link to the response of anticancer drugs Further experiments are warranted to substantiate these findings.

In the present study, we investigated different mechanisms and targets. It became apparent that inflammation and tumor-killing properties of chamomile compounds are determined by multiple rather than by single mechanisms. The multi-specific action of chamomile and numerous other medicinal plants apparently represents a selection advantage during the evolution of plants on this globe. A large battery of defense mechanisms is superior to combat hostile organisms, such as microbes and herbivores. This principle is also realized in multi-compound pharmacology of medicinal plants. The phytotherapy relies on addressing multiple targets at the same time [58].

In the third part of the present investigation, we therefore focused on the role of NF-κB as prognostic factor for patient survival. Related to this topic the question of NF-κB as potential treatment targets for chamomile compounds addressed in the first two parts of the present study. May chamomile compounds be beneficial to prevent the onset of cancer or bypass drug resistance as additives to standard chemotherapy by inhibition of NF-κB? To clarify the prognostic relevance of NF-κB for survival of cancer patients we took advantage of the transcriptomic analyses of more than 7000 tumor biopsies derived from 21 tumor types of The Cancer Genome Atlas (TCGA) deposited at the KM-Plotter database (https://kmplot.com/analysis/ (accessed on 20 November 2023)). We observed that renal clear cell carcinomas with low NF-κB expression from different patho-clinical categories (gender, grade 3, low mutation status, low neoantigen rate) were significantly correlated with longer patient survival times than tumors with high NF-κB expression using Kaplan-Meier statistics. These results indicate that these subgroups of tumors might benefit from NF-κB inhibition by chamomile compounds.

5. Conclusions

In conclusion, this study highlights the significant therapeutic potential of chamomile compounds, specifically β-amyrin, lupeol, and quercetin, in addressing inflammation and cancer. Through a thorough investigation encompassing virtual screening, experimental assays, and proteomic analyses, we have demonstrated the inhibitory effects of these compounds on NF-κB signaling pathways and cytokine expression. Notably, our findings suggest that chamomile derivatives could serve as promising candidates for both preventive and adjunctive cancer therapies, particularly in overcoming drug resistance mechanisms. Moving forward, further research exploring the activity of the three compounds across all inflammation pathways and conducting clinical trials are essential. This would be beneficial to fully elucidate the clinical implications and therapeutic mechanisms of chamomile compounds, paving the way for the development of novel cancer treatments and personalized medicine approaches.

Supplementary Materials: The following supporting information can be downloaded at: https://www.mdpi.com/article/10.3390/biomedicines12071484/s1, Table S1: Correlation of protein expression identified by COMPARE analysis with $\log_{10}IC_{50}$ values for lupeol in the NCI panel of tumor cell lines; Table S2: Correlation of protein expression identified by COMPARE analysis with $\log_{10}IC_{50}$ values for quercetin in the NCI panel of tumor cell lines.

Author Contributions: A.I.D. performed the experiments and analyses, R.Y. assisted in conducting experiments and the analysis. R.D. performed the microscale thermophoresis experiment, N.T.A. Wrote the methodology for the cell cycle and annexin-v apoptosis experiment in the material and methods section, T.H.A.H. performed the docking analysis of the protein tubulin, B.A. performed the phytochemical analysis, I.A.K. edited the manuscript, and T.E. supervised the project and wrote the manuscript. All authors have read and agreed to the published version of the manuscript.

Funding: This research received no external funding.

Institutional Review Board Statement: Not applicable.

Informed Consent Statement: Not applicable.

Data Availability Statement: Data are available upon reasonable request.

Acknowledgments: We thank the IMB Flow Cytometry Core Facility for usage of Novocyte Quanteon when we performed the ROS assay and the mitochondrial membrane potential JC-1 assay. Special thanks to Stefanie Möckel, Stephanie Nick, and Márton Gelléri and his colleagues from the IMB microscopy core facility. Special thanks to our colleague Xiaohua Lu for her help and support.

Conflicts of Interest: The authors declare no conflicts of interest.

References

1. Piotrowski, I.; Kulcenty, K.; Suchorska, W. Interplay between Inflammation and Cancer. *Rep. Pract. Oncol. Radiother.* **2020**, *25*, 422–427. [CrossRef] [PubMed]
2. Hou, J.; Karin, M.; Sun, B. Targeting Cancer-Promoting Inflammation-Have Anti-Inflammatory Therapies Come of Age? *Nat. Rev. Clin. Oncol.* **2021**, *18*, 261–279. [CrossRef]
3. Newman, D.J.; Cragg, G.M. Natural Products as Sources of New Drugs over the Nearly Four Decades from 01/1981 to 09/2019. *J. Nat. Prod.* **2020**, *83*, 770–803. [CrossRef] [PubMed]
4. Cragg, G.M.; Newman, D.J. Plants as a Source of Anti-Cancer Agents. *J. Ethnopharmacol.* **2005**, *100*, 72–79. [CrossRef]
5. Graham, J.G.; Quinn, M.L.; Fabricant, D.S.; Farnsworth, N.R. Plants Used against Cancer—An Extension of the Work of Jonathan Hartwell. *J. Ethnopharmacol.* **2000**, *73*, 347–377. [CrossRef]
6. Dong, S.; Guo, X.; Han, F.; He, Z.; Wang, Y. Emerging Role of Natural Products in Cancer Immunotherapy. *Acta Pharm. Sin. B* **2021**, *12*, 1163–1185. [CrossRef] [PubMed]
7. Hashem, S.; Ali, T.A.; Akhtar, S.; Nisar, S.; Sageena, G.; Ali, S.; Al-Mannai, S.; Therachiyil, L.; Mir, R.; Elfaki, I.; et al. Targeting Cancer Signaling Pathways by Natural Products: Exploring Promising Anti-Cancer Agents. *Biomed. Pharmacother.* **2022**, *150*, 113054. [CrossRef] [PubMed]
8. Atanasov, A.G.; Zotchev, S.B.; Dirsch, V.M.; Erdogan Orhan, I.; Banach, M.; Rollinger, J.M.; Barreca, D.; Weckwerth, W.; Bauer, R.; Bayer, E.A.; et al. Natural Products in Drug Discovery: Advances and Opportunities. *Nat. Rev. Drug Discov.* **2021**, *20*, 200–216. [CrossRef]

9. Foa, R.; Norton, L.; Seidman, A.D. Taxol (Paclitaxel): A Novel Anti-Microtubule Agent with Remarkable Anti-Neoplastic Activity. *Int. J. Clin. Lab. Res.* **1994**, *24*, 6–14. [CrossRef]
10. Efferth, T.; Oesch, F. The Immunosuppressive Activity of Artemisinin-Type Drugs towards Inflammatory and Autoimmune Diseases. *Med. Res. Rev.* **2021**, *41*, 3023–3061. [CrossRef]
11. Khan, N.; Afsahul Kalam, M.; Tauseef Alam, M.; Anam Ul Haq, S.; Showket, W.; Dar, Z.A.; Rafiq, N.; Mushtaq, W.; Amin Rafeeqi, T.; Yunis Dar, M.; et al. SAMRC Precision Oncology Research Unit (PORU), DSI/NRF SARChI Chair in Precision Oncology and Cancer Prevention (POCP). *Int. Publ. J. Cancer* **2023**, *14*, 490–504. [CrossRef]
12. Drif, A.I.; Avula, B.; Khan, I.A.; Efferth, T. COX2-Inhibitory and Cytotoxic Activities of Phytoconstituents of *Matricaria chamomilla* L. *Appl. Sci.* **2023**, *13*, 8935. [CrossRef]
13. Al-Dabbagh, B.; Elhaty, I.A.; Elhaw, M.; Murali, C.; Al Mansoori, A.; Awad, B.; Amin, A. Antioxidant and Anticancer Activities of Chamomile (*Matricaria recutita* L.). *BMC Res. Notes* **2019**, *12*, 3. [CrossRef] [PubMed]
14. Aoki, T.; Narumiya, S. Prostaglandins and Chronic Inflammation. *Trends Pharmacol. Sci.* **2012**, *33*, 304–311. [CrossRef] [PubMed]
15. Oeckinghaus, A.; Ghosh, S. The NF-KappaB Family of Transcription Factors and Its Regulation. *Cold Spring Harb. Perspect. Biol.* **2009**, *1*, a000034. [CrossRef] [PubMed]
16. Lawrence, T. The Nuclear Factor NF-KappaB Pathway in Inflammation. *Cold Spring Harb. Perspect. Biol.* **2009**, *1*, a001651. [CrossRef] [PubMed]
17. Ghosh, G.; Wang, V.Y.F.; Huang, D.B.; Fusco, A. NF-KB Regulation: Lessons from Structures. *Immunol. Rev.* **2012**, *246*, 36–58. [CrossRef] [PubMed]
18. Miller, S.C.; Huang, R.; Sakamuru, S.; Shukla, S.J.; Attene-Ramos, M.S.; Shinn, P.; Van Leer, D.; Leister, W.; Austin, C.P.; Xia, M. Identification of Known Drugs That Act as Inhibitors of NF-κB Signaling and Their Mechanism of Action. *Biochem. Pharmacol.* **2010**, *79*, 1272–1280. [CrossRef] [PubMed]
19. Saeed, M.; Kadioglu, O.; Khalid, H.; Sugimoto, Y.; Efferth, T. Activity of the Dietary Flavonoid, Apigenin, against Multidrug-Resistant Tumor Cells as Determined by Pharmacogenomics and Molecular Docking. *J. Nutr. Biochem.* **2015**, *26*, 44–56. [CrossRef]
20. Adham, A.N.; Abdelfatah, S.; Naqishbandi, A.M.; Mahmoud, N.; Efferth, T. Cytotoxicity of Apigenin toward Multiple Myeloma Cell Lines and Suppression of INOS and COX-2 Expression in STAT1-Transfected HEK293 Cells. *Phytomedicine* **2021**, *80*, 153371. [CrossRef]
21. Jacobs, M.D.; Harrison, S.C. Structure of an IκBα/NF-KB Complex. *Cell* **1998**, *95*, 749–758. [CrossRef] [PubMed]
22. RCSB PDB—1NFI: I-KAPPA-B-ALPHA/NF-KAPPA-B COMPLEX. Available online: https://www.rcsb.org/structure/1NFI (accessed on 1 October 2023).
23. UCSF Chimera Home Page. Available online: https://www.cgl.ucsf.edu/chimera/ (accessed on 30 March 2023).
24. Supianto, A.A.; Nurdiansyah, R.; Weng, C.W.; Zilvan, V.; Yuwana, R.S.; Arisal, A.; Pardede, H.F.; Lee, M.M.; Huang, C.H.; Ng, K.L. Cluster-Based Text Mining for Extracting Drug Candidates for the Prevention of COVID-19 from the Biomedical Literature. *J. Taibah Univ. Med. Sci.* **2023**, *18*, 787–801. [CrossRef] [PubMed]
25. PyRx (Version 0.8). Available online: https://pyrx.sourceforge.io/ (accessed on 31 March 2023).
26. Search|Scripps Research. Available online: https://www.scripps.edu/search/?s=autodocktools (accessed on 31 March 2023).
27. Morris, G.M.; Goodsell, D.S.; Pique, M.E.; Huey, R.; Forli, S.; Hart, W.E.; Halliday, S.; Belew, R.; Olson, A.J. User Guide AutoDock Version 4.2 Updated for Version 4.2.6 Automated Docking of Flexible Ligands to Flexible Receptors. 1991. Available online: https://autodock.scripps.edu/wp-content/uploads/sites/56/2021/10/AutoDock4.2.6_UserGuide.pdf (accessed on 31 March 2023).
28. AutoDock. Available online: https://autodock.scripps.edu/ (accessed on 31 March 2023).
29. Chen, F.E.; Ghosh, G. Regulation of DNA Binding by Rel/NF-KB Transcription Factors: Structural Views. *Oncogene* **1999**, *18*, 6845–6852. [CrossRef] [PubMed]
30. Free Download: BIOVIA Discovery Studio Visualizer—Dassault Systèmes. Available online: https://discover.3ds.com/discovery-studio-visualizer-download (accessed on 30 March 2023).
31. PRODUCT INFORMATION Contents and Storage. Available online: https://www.invivogen.com/hek-blue-detection (accessed on 1 October 2023).
32. InvivoGen QUANTI-BlueTM Solution|Data Sheet|InvivoGen. Available online: https://www.invivogen.com/reporter-cells (accessed on 1 October 2023).
33. JC-1 Mitochondrial Membrane Potential Assay Kit|Cayman Chemical. Available online: https://www.caymanchem.com/product/10009172/jc-1-mitochondrial-membrane-potential-assay-kit (accessed on 1 October 2023).
34. TABLE OF CONTENTS GENERAL INFORMATION 3 Materials Supplied 3 Safety Data 4 Precautions 4 If You Have Problems 4 Storage and Stability. Available online: https://cdn.caymanchem.com/cdn/insert/10009172.pdf (accessed on 1 October 2023).
35. Sivandzade, F.; Bhalerao, A.; Cucullo, L. Analysis of the Mitochondrial Membrane Potential Using the Cationic JC-1 Dyeas a Sensitive Fluorescent Probe. *Bio-Protocol* **2019**, *9*, e3128. [CrossRef] [PubMed]
36. Wu, C.-F.; Efferth, T. Miltirone Induces G2/M Cell Cycle Arrest and Apoptosis in CCRF-CEM Acute Lymphoblastic Leukemia Cells. *J. Nat. Prod.* **2015**, *78*, 1339–1347. [CrossRef]
37. Zhou, M.; Boulos, J.C.; Klauck, S.M.; Efferth, T.; Zhou, M.; Boulos, J.C.; Efferth, T.; Klauck, S.M. The Cardiac Glycoside ZINC253504760 Induces Parthanatos-Type Cell Death and G2/M Arrest via Downregulation of MEK1/2 Phosphorylation in Leukemia Cells. *Cell Biol. Toxicol.* **2023**, *39*, 2971–2997. [CrossRef]

38. Monga, M.; Sausville, E.A. Developmental Therapeutics Program at the NCI: Molecular Target and Drug Discovery Process. *Leukemia* **2002**, *16*, 520–526. [CrossRef] [PubMed]
39. Shoemaker, R.H. The NCI60 Human Tumour Cell Line Anticancer Drug Screen. *Nat. Rev. Cancer* **2006**, *6*, 813–823. [CrossRef]
40. Developmental Therapeutics Program (DTP). Available online: https://dtp.cancer.gov/ (accessed on 20 November 2023).
41. Zhou, M.; Boulos, J.C.; Omer, E.A.; Klauck, S.M.; Efferth, T. Modes of Action of a Novel C-MYC Inhibiting 1,2,4-Oxadiazole Derivative in Leukemia and Breast Cancer Cells. *Molecules* **2023**, *28*, 5658. [CrossRef]
42. Boulos, J.C.; Chatterjee, M.; Shan, L.; Efferth, T. In Silico, In Vitro, and In Vivo Investigations on Adapalene as Repurposed Third Generation Retinoid against Multiple Myeloma and Leukemia. *Cancers* **2023**, *15*, 4136. [CrossRef]
43. Dennis, R.A.; Trappe, T.A.; Simpson, P.; Carroll, C.; Huang, B.E.; Nagarajan, R.; Bearden, E.; Gurley, C.; Duff, G.W.; Evans, W.J.; et al. *Interleukin-1* Polymorphisms Are Associated with the Inflammatory Response in Human Muscle to Acute Resistance Exercise. *J. Physiol.* **2004**, *560*, 617–626. [CrossRef]
44. Mahmoud, N.; Saeed, M.E.M.; Sugimoto, Y.; Klauck, S.M.; Greten, H.J.; Efferth, T.; Mahmoud, N.; Saeed, M.E.M.; Sugimoto, Y.; Klauck, S.M.; et al. Cytotoxicity of Nimbolide towards Multidrug-Resistant Tumor Cells and Hypersensitivity via Cellular Metabolic Modulation. *Oncotarget* **2018**, *9*, 35762–35779. [CrossRef]
45. Schefe, J.H.; Lehmann, K.E.; Buschmann, I.R.; Unger, T.; Funke-Kaiser, H. Quantitative Real-Time RT-PCR Data Analysis: Current Concepts and the Novel "Gene Expression's C T Difference" Formula. *J. Mol. Med.* **2006**, *84*, 901–910. [CrossRef]
46. Lánczky, A.; Gyo˝rffy, B. Web-Based Survival Analysis Tool Tailored for Medical Research (KMplot): Development and Implementation. *J. Med. Internet Res.* **2021**, *23*, e27633. [CrossRef]
47. Gyo˝ rffy, B. Discovery and Ranking of the Most Robust Prognostic Biomarkers in Serous Ovarian Cancer. *Geroscience* **2023**, *45*, 1889–1898. [CrossRef]
48. Menyhart, O.; Weltz, B.; Gyorffy, B. Multipletesting.Com: A Tool for Life Science Researchers for Multiple Hypothesis Testing Correction. *PLoS ONE* **2021**, *16*, e0245824. [CrossRef]
49. Kaplan-Meier Plotter. Available online: https://kmplot.com/analysis/ (accessed on 20 November 2023).
50. Seo, E.J.; Dawood, M.; Hult, A.K.; Olsson, M.L.; Efferth, T. Network Pharmacology of Triptolide in Cancer Cells: Implications for Transcription Factor Binding. *Investig. New Drugs* **2021**, *39*, 1523–1537. [CrossRef]
51. Ko, E.-Y.; Cho, S.-H.; Kwon, S.-H.; Eom, C.-Y.; Seon Jeong, M.; Lee, W.; Kim, S.-Y.; Heo, S.-J.; Ahn, G.; Pa Lee, K.; et al. The Roles of NF-KB and ROS in Regulation of pro-Inflammatory Mediators of Inflammation Induction in LPS-Stimulated Zebrafish Embryos. *Fish Shellfish Immunol.* **2017**, *68*, 525–529. [CrossRef]
52. Mitochondrial Dysfunction and Inflammatory Responses|Encyclopedia MDPI. Available online: https://encyclopedia.pub/entry/8923 (accessed on 13 October 2023).
53. Albensi, B.C. What Is Nuclear Factor Kappa B (NF-KB) Doing in and to the Mitochondrion? *Front. Cell Dev. Biol.* **2019**, *7*, 470308. [CrossRef]
54. Ohshima, H.; Tatemichi, M.; Sawa, T. Chemical Basis of Inflammation-Induced Carcinogenesis. *Arch. Biochem. Biophys.* **2003**, *417*, 3–11. [CrossRef]
55. Gao, Y.; Zhao, J.; Zu, Y.; Fu, Y.; Liang, L.; Luo, M.; Wang, W.; Efferth, T. Antioxidant Properties, Superoxide Dismutase and Glutathione Reductase Activities in HepG2 Cells with a Fungal Endophyte Producing Apigenin from Pigeon Pea [*Cajanus cajan* (L.) Millsp.]. *Food Res. Int.* **2012**, *49*, 147–152. [CrossRef]
56. Kuete, V.; Efferth, T. Molecular Determinants of Cancer Cell Sensitivity and Resistance towards the Sesquiterpene Farnesol. *Pharmazie* **2013**, *68*, 608–615. [CrossRef] [PubMed]
57. Eichhorn, T.; Greten, H.J.; Efferth, T. Molecular Determinants of the Response of Tumor Cells to Boswellic Acids. *Pharmaceuticals* **2011**, *4*, 1171–1182. [CrossRef]
58. Efferth, T.; Koch, E. Complex Interactions between Phytochemicals. The Multi-Target Therapeutic Concept of Phytotherapy. *Curr. Drug Targets* **2010**, *12*, 122–132. [CrossRef]
59. Muhammad, N.; Usmani, D.; Tarique, M.; Naz, H.; Ashraf, M.; Raliya, R.; Tabrez, S.; Zughaibi, T.A.; Alsaieedi, A.; Hakeem, I.J.; et al. The Role of Natural Products and Their Multitargeted Approach to Treat Solid Cancer. *Cells* **2022**, *11*, 2209. [CrossRef]
60. Dimitrakopoulos, F.I.D.; Kottorou, A.E.; Kalofonou, M.; Kalofonos, H.P. The Fire within: NF-KB Involvement in Non-Small Cell Lung Cancer. *Cancer Res.* **2020**, *80*, 4025–4036. [CrossRef]
61. Gardiner, P. Chamomile (*Matricaria recutita*, *Anthemis nobilis*). In *Longwood Herbal Task Force and the Center for Holistic Pediatric Education and Research*; 1999; pp. 1–21. Available online: https://tratamientocelular.com/papers/cmran.pdf (accessed on 11 October 2022).
62. Dai, Y.L.; Li, Y.; Wang, Q.; Niu, F.J.; Li, K.W.; Wang, Y.Y.; Wang, J.; Zhou, C.Z.; Gao, L.N. Chamomile: A Review of Its Traditional Uses, Chemical Constituents, Pharmacological Activities and Quality Control Studies. *Molecules* **2023**, *28*, 133. [CrossRef]
63. Petronilho, S.; Maraschin, M.; Coimbra, M.A.; Rocha, S.M. In Vitro and in Vivo Studies of Natural Products: A Challenge for Their Valuation. The Case Study of Chamomile (*Matricaria recutita* L.). *Ind. Crop. Prod.* **2012**, *40*, 1–12. [CrossRef]
64. De Cicco, P.; Ercolano, G.; Sirignano, C.; Rubino, V.; Rigano, D.; Ianaro, A.; Formisano, C. Chamomile Essential Oils Exert Anti-Inflammatory Effects Involving Human and Murine Macrophages: Evidence to Support a Therapeutic Action. *J. Ethnopharmacol.* **2023**, *311*, 116391. [CrossRef]

65. Vissiennon, C.; Hammoud, D.; Rodewald, S.; Fester, K.; Goos, K.H.; Nieber, K.; Arnhold, J. Chamomile Flower, Myrrh, and Coffee Charcoal, Components of a Traditional Herbal Medicinal Product, Diminish Proinflammatory Activation in Human Macrophages. *Planta Med.* **2017**, *83*, 846–854. [CrossRef]
66. Zadam, M.H.; Ahmida, M.; Djaber, N.; Ounaceur, L.S.; Sekiou, O.; Taibi, F.; Bencheikh, R.; Chouala, K.; Boudjema, K.; Tichati, L.; et al. In-Vivo Anti-Inflammatory Effects of Roman Chamomile (*Chamaemelum nobile*) Aqueous Extracts Collected from the National Park of El-Kala (North-East, Algeria). *Cell. Mol. Biol.* **2023**, *69*, 245–254. [CrossRef]
67. Martins, M.D.; Marques, M.M.; Bussadori, S.K.; Martins, M.A.T.; Pavesi, V.C.S.; Mesquita-Ferrari, R.A.; Fernandes, K.P.S. Comparative Analysis between Chamomilla Recutita and Corticosteroids on Wound Healing. An in Vitro and in Vivo Study. *Phytother. Res.* **2009**, *23*, 274–278. [CrossRef]
68. Elhadad, M.A.; El-Negoumy, E.; Taalab, M.R.; Ibrahim, R.S.; Elsaka, R.O. The Effect of Topical Chamomile in the Prevention of Chemotherapy-Induced Oral Mucositis: A Randomized Clinical Trial. *Oral Dis.* **2022**, *28*, 164–172. [CrossRef]
69. Shoara, R.; Hashempur, M.H.; Ashraf, A.; Salehi, A.; Dehshahri, S.; Habibagahi, Z. Efficacy and Safety of Topical *Matricaria chamomilla* L. (Chamomile) Oil for Knee Osteoarthritis: A Randomized Controlled Clinical Trial. *Complement. Ther. Clin. Pract.* **2015**, *21*, 181–187. [CrossRef]
70. Srivastava, J.K.; Shankar, E.; Gupta, S. Chamomile: A Herbal Medicine of the Past with a Bright Future (Review). *Mol. Med. Rep.* **2010**, *3*, 895–901.
71. Maleki, M.; Mardani, A.; Manouchehri, M.; Ashghali Farahani, M.; Vaismoradi, M.; Glarcher, M. Effect of Chamomile on the Complications of Cancer: A Systematic Review. *Integr. Cancer Ther.* **2023**, *22*, 15347354231164600. [CrossRef]
72. Thalluri, G.; Srinu, P. Role of Chamomile in Cancer Treat-Ment. *J. Pathol. Clin. Med. Res.* **2018**, *1*, 1.
73. Srivastava, J.K.; Gupta, S. Antiproliferative and Apoptotic Effects of Chamomile Extract in Various Human Cancer Cells. *J. Agric. Food Chem.* **2007**, *55*, 9470–9478. [CrossRef]
74. Sak, K.; Nguyen, T.H.; Ho, D.; Do, T.T.; Raal, A.; Thao, T. Cytotoxic Effect of Chamomile (*Matricaria recutita*) and Marigold (*Calendula officinalis*) Extracts on Human Melanoma SK-MEL-2 and Epidermoid Carcinoma KB Cells. *Cogent. Med.* **2017**, *4*, 1333218. [CrossRef]
75. Shukla, S.; Gupta, S. Apigenin: A Promising Molecule for Cancer Prevention. *Pharm. Res.* **2010**, *27*, 962–978. [CrossRef]
76. Patel, D.; Shukla, S.; Gupta, S. Apigenin and Cancer Chemoprevention: Progress, Potential and Promise (Review). *Int. J. Oncol.* **2007**, *30*, 233–245. [CrossRef]
77. Lefort, É.C.; Blay, J. Apigenin and Its Impact on Gastrointestinal Cancers. *Mol. Nutr. Food Res.* **2013**, *57*, 126–144. [CrossRef]
78. Shwaikh, A.K.; Hassan, A.J.; Rashid, K.H. Synergistic Immunosuppressive Activity of Chamomile Flower (*Matricaria chamomilla* L.) Extracts and Methotrexate in Vivo. *Ann. Rom. Soc. Cell Biol.* **2021**, *25*, 15386–15394.
79. El Joumaa, M.M.; Taleb, R.I.; Rizk, S.; Borjac, J.M. Protective Effect of *Matricaria chamomilla* Extract against 1,2-Dimethylhydrazine-Induced Colorectal Cancer in Mice. *J. Complement. Integr. Med.* **2020**, *17*, 3. [CrossRef]
80. Tousson, E.; El-Atrsh, A.; Elnahas, E.E.; Massoud, A.; Al-Zubaidi, M.; Yan, B. Ameliorative Effects of Spirulina and Chamomile Aqueous Extract against Mice Bearing Ehrlich Solid Tumor Induced Apoptosis. *Asian Oncol. Res. J.* **2019**, *2*, 1–17.
81. Chadwick, D.; Goode, J. Novartis Foundation. In *Cancer and Inflammation*; John Wiley & Sons: Hoboken, NJ, USA, 2004; ISBN 047085510X.
82. Ohnishi, S.; Ma, N.; Thanan, R.; Pinlaor, S.; Hammam, O.; Murata, M.; Kawanishi, S. DNA Damage in Inflammation-Related Carcinogenesis and Cancer Stem Cells. *Oxidative Med. Cell. Longev.* **2013**, *2013*, 387014. [CrossRef]
83. Ben-Neriah, Y.; Karin, M. Inflammation Meets Cancer, with NF-KB as the Matchmaker. *Nat. Immunol.* **2011**, *12*, 715–723. [CrossRef]
84. Neurath, M.F.; Becker, C.; Barbulescu, K. Role of NF-KB in Immune and Inflammatory Responses in the Gut. *Gut* **1998**, *43*, 856–860. [CrossRef]
85. Biswas, D.K.; Shi, Q.; Baily, S.; Strickland, I.; Ghosh, S.; Pardee, A.B.; Iglehart, J.D. NF-κB Activation in Human Breast Cancer Specimens and Its Role in Cell Proliferation and Apoptosis. *Proc. Natl. Acad. Sci. USA* **2004**, *101*, 10137–10142. [CrossRef]
86. Piva, R.; Belardo, G.; Santoro, M.G. NF-κB: A Stress-Regulated Switch for Cell Survival. *Antioxid. Redox Signal.* **2006**, *8*, 478–486. [CrossRef]
87. Olivier, S.; Robe, P.; Bours, V. Can NF-κB Be a Target for Novel and Efficient Anti-Cancer Agents? *Biochem. Pharmacol.* **2006**, *72*, 1054–1068. [CrossRef]
88. Chuang, S.E.; Yeh, P.Y.; Lu, Y.S.; Lai, G.M.; Liao, C.M.; Gao, M.; Cheng, A.L. Basal Levels and Patterns of Anticancer Drug-Induced Activation of Nuclear Factor-KB (NF-KB), and Its Attenuation by Tamoxifen, Dexamethasone, and Curcumin in Carcinoma Cells. *Biochem. Pharmacol.* **2002**, *63*, 1709–1716. [CrossRef]
89. Efferth, T.; Volm, M. Multiple Resistance to Carcinogens and Xenobiotics: P-Glycoproteins as Universal Detoxifiers. *Arch. Toxicol.* **2017**, *91*, 2515–2538. [CrossRef]
90. Aleksakhina, S.N.; Kashyap, A.; Imyanitov, E.N. Mechanisms of Acquired Tumor Drug Resistance. *Biochim. Biophys. Acta (BBA) — Rev. Cancer* **2019**, *1872*, 188310. [CrossRef]
91. Holohan, C.; Van Schaeybroeck, S.; Longley, D.B.; Johnston, P.G. Cancer Drug Resistance: An Evolving Paradigm. *Nat. Rev. Cancer* **2013**, *13*, 714–726. [CrossRef]
92. Xiu, Y.; Dong, Q.; Li, Q.; Boyce, B.; Xue, H.-H.; Zhao, C. Stabilization of NF-κB-inducing kinase suppresses MLL-AF9-induced acute myeloid leukemia. *Cell Rep.* **2018**, *22*, 350–358. [CrossRef] [PubMed]

93. Braun, T.; Carvalho, G.; Fabre, C.; Grosjean, J.; Fenaux, P.; Kroemer, G. Targeting NF-KB in Hematologic Malignancies. *Cell Death Differ.* **2006**, *13*, 748–758. [CrossRef]
94. Zhou, J.; Chooi, J.-Y.; Ching, Y.Q.; Quah, J.Y.; Toh, S.H.-M.; Ng, Y.; Tan, T.Z.; Chng, W.-J. NF-KB Promotes the Stem-like Properties of Leukemia Cells by Activation of LIN28B. *World J. Stem Cells* **2018**, *10*, 34–42. [CrossRef]
95. Dong, Q.M.; Ling, C.; Chen, X.; Zhao, L.I. Inhibition of Tumor Necrosis Factor-α Enhances Apoptosis Induced by Nuclear Factor-KB Inhibition in Leukemia Cells. *Oncol. Lett.* **2015**, *10*, 3793–3798. Available online: https://www.spandidos-publications.com/10.3892/ol.2015.3786# (accessed on 17 March 2024). [CrossRef]
96. Morgan, M.J.; Liu, Z.G. Crosstalk of Reactive Oxygen Species and NF-KB Signaling. *Cell Res.* **2010**, *21*, 103–115. [CrossRef]
97. Sul, O.J.; Ra, S.W. Quercetin Prevents LPS-Induced Oxidative Stress and Inflammation by Modulating NOX2/ROS/NF-KB in Lung Epithelial Cells. *Molecules* **2021**, *26*, 6949. [CrossRef]
98. Plaetzer, K.; Kiesslich, T.; Oberdanner, C.B.; Krammer, B. Apoptosis Following Photodynamic Tumor Therapy: Induction, Mechanisms and Detection. *Curr. Pharm. Des.* **2005**, *11*, 1151–1165. [CrossRef]
99. Yu, W.; Tu, Y.; Long, Z.; Liu, J.; Kong, D.; Peng, J.; Wu, H.; Zheng, G.; Zhao, J.; Chen, Y.; et al. Reactive Oxygen Species Bridge the Gap between Chronic Inflammation and Tumor Development. *Oxidative Med. Cell. Longev.* **2022**, *2022*, 2606928. [CrossRef]
100. Gupta, K.; Panda, D. Perturbation of Microtubule Polymerization by Quercetin through Tubulin Binding: A Novel Mechanism of Its Antiproliferative Activity. *Biochemistry* **2002**, *41*, 13029–13038. [CrossRef]
101. Saleem, M.; Murtaza, I.; Witkowsky, O.; Kohl, A.M.; Maddodi, N. Lupeol Triterpene, a Novel Diet-Based Microtubule Targeting Agent: Disrupts Survivin/CFLIP Activation in Prostate Cancer Cells. *Biochem. Biophys. Res. Commun.* **2009**, *388*, 576–582. [CrossRef]
102. Che, S.; Wu, S.; Yu, P. Lupeol Induces Autophagy and Apoptosis with Reduced Cancer Stem-like Properties in Retinoblastoma via Phosphoinositide 3-Kinase/Protein Kinase B/Mammalian Target of Rapamycin Inhibition. *J. Pharm. Pharmacol.* **2022**, *74*, 208–215. [CrossRef]
103. Xiao, J.; Zhang, B.; Yin, S.; Xie, S.; Huang, K.; Wang, J.; Yang, W.; Liu, H.; Zhang, G.; Liu, X.; et al. Quercetin Induces Autophagy-Associated Death in HL-60 Cells through CaMKKβ/AMPK/MTOR Signal Pathway: Quercetin Induces Autophagic Cell Death in AML. *Acta Biochim. Biophys. Sin.* **2022**, *54*, 1244. [CrossRef]
104. Banerjee, S.; Hwang, D.J.; Li, W.; Miller, D.D. Current Advances of Tubulin Inhibitors in Nanoparticle Drug Delivery and Vascular Disruption/Angiogenesis. *Molecules* **2016**, *21*, 1468. [CrossRef]
105. Jackman, R.W.; Rhoads, M.G.; Cornwell, E.; Kandarian, S.C. Microtubule-Mediated NF-KB Activation in the TNF-α Signaling Pathway. *Exp. Cell Res.* **2009**, *315*, 3242–3249. [CrossRef]
106. Rosette, C.; Karin, M. Cytoskeletal Control of Gene Expression: Depolymerization of Microtubules Activates NF-Kappa B. *J. Cell Biol.* **1995**, *128*, 1111–1119. [CrossRef]
107. Nydam, T.; McIntyre, R.; Moore, E.; Escobar, G.; Hamiel, C.; Gamboni-Robertson, F.; McLaughlin, N.; Banerjee, A. Microtubule disruption inhibits TNFα-induced NF-κB nuclear translocation independent of IκB degradation. *Shock* **2006**, *25*, 18. [CrossRef]
108. Kraus, R.F.; Gruber, M.A. Neutrophils—From Bone Marrow to First-Line Defense of the Innate Immune System. *Front. Immunol.* **2021**, *12*, 767175. [CrossRef] [PubMed]
109. Van Bruggen, S.; Jarrot, P.A.; Thomas, E.; Sheehy, C.E.; Silva, C.M.S.; Hsu, A.Y.; Cunin, P.; Nigrovic, P.A.; Gomes, E.R.; Luo, H.R.; et al. NLRP3 Is Essential for Neutrophil Polarization and Chemotaxis in Response to Leukotriene B4 Gradient. *Proc. Natl. Acad. Sci. USA* **2023**, *120*, e2303814120. [CrossRef] [PubMed]
110. Wang, V.; Pober, J.S.; Manes, T.D. Transendothelial Migration of Human B Cells: Chemokine versus Antigen. *J. Immunol.* **2023**, *211*, 923–931. [CrossRef] [PubMed]
111. Vissenaekens, H.; Criel, H.; Grootaert, C.; Raes, K.; Smagghe, G.; Van Camp, J. Flavonoids and Cellular Stress: A Complex Interplay Affecting Human Health. *Crit. Rev. Food Sci. Nutr.* **2022**, *62*, 8535–8566. [CrossRef] [PubMed]
112. Kurzrock, R. Cytokine Deregulation in Cancer. *Biomed. Pharmacother.* **2001**, *55*, 543–547. [CrossRef] [PubMed]
113. Kamin´ska, K.; Czarnecka, A.M.; Escudier, B.; Lian, F.; Szczylik, C. Interleukin-6 as an Emerging Regulator of Renal Cell Cancer. *Urol. Oncol.* **2015**, *33*, 476–485. [CrossRef] [PubMed]
114. Garon, E.B.; Chih-Hsin Yang, J.; Dubinett, S.M. The Role of Interleukin 1β in the Pathogenesis of Lung Cancer. *JTO Clin. Res. Rep.* **2020**, *1*, 100001. [CrossRef] [PubMed]
115. Mackenzie, G.G.; Keen, C.L.; Oteiza, P.I. Microtubules Are Required for NF-KappaB Nuclear Translocation in Neuroblastoma IMR-32 Cells: Modulation by Zinc. *J. Neurochem.* **2006**, *99*, 402–415. [CrossRef]
116. Shrum, C.K.; Defrancisco, D.; Meffert, M.K. Stimulated Nuclear Translocation of NF-KappaB and Shuttling Differentially Depend on Dynein and the Dynactin Complex. *Proc. Natl. Acad. Sci. USA* **2009**, *106*, 2647–2652. [CrossRef]
117. Rai, A.; Kapoor, S.; Singh, S.; Chatterji, B.P.; Panda, D. Transcription Factor NF-KB Associates with Microtubules and Stimulates Apoptosis in Response to Suppression of Microtubule Dynamics in MCF-7 Cells. *Biochem. Pharmacol.* **2015**, *93*, 277–289. [CrossRef] [PubMed]
118. Efferth, T.; Konkimalla, V.B.; Wang, Y.F.; Sauerbrey, A.; Meinhardt, S.; Zintl, F.; Mattern, J.; Volm, M. Prediction of Broad Spectrum Resistance of Tumors towards Anticancer Drugs. *Clin. Cancer Res.* **2008**, *14*, 2405–2412. [CrossRef] [PubMed]
119. Haghiac, M.; Walle, T. Quercetin Induces Necrosis and Apoptosis in SCC-9 Oral Cancer Cells. *Nutr. Cancer* **2005**, *53*, 220–231. [CrossRef] [PubMed]

120. Khorsandi, L.; Orazizadeh, M.; Niazvand, F.; Abbaspour, M.R.; Mansouri, E.; Khodadadi, A. Quercetin Induces Apoptosis and Necroptosis in MCF-7 Breast Cancer Cells. *Bratisl. Lek. Listy* **2017**, *118*, 123–128. [CrossRef] [PubMed]
121. Min, T.R.; Park, H.J.; Ha, K.T.; Chi, G.Y.; Choi, Y.H.; Park, S.H. Suppression of EGFR/STAT3 Activity by Lupeol Contributes to the Induction of the Apoptosis of Human Non-small Cell Lung Cancer Cells. *Int. J. Oncol.* **2019**, *55*, 320–330. [CrossRef]
122. Khan, K.; Javed, Z.; Sadia, H.; Sharifi-Rad, J.; Cho, W.C.; Luparello, C. Quercetin and MicroRNA Interplay in Apoptosis Regulation in Ovarian Cancer. *Curr. Pharm. Des.* **2021**, *27*, 2328–2336. [CrossRef]
123. Lomphithak, T.; Jaikla, P.; Sae-Fung, A.; Sonkaew, S.; Jitkaew, S. Natural Flavonoids Quercetin and Kaempferol Targeting G2/M Cell Cycle-Related Genes and Synergize with Smac Mimetic LCL-161 to Induce Necroptosis in Cholangiocarcinoma Cells. *Nutrients* **2023**, *15*, 3090. [CrossRef] [PubMed]
124. Seo, S.Y.; Ju, W.S.; Kim, K.; Kim, J.; Yu, J.O.; Ryu, J.-S.; Kim, J.-S.; Lee, H.-A.; Koo, D.-B.; Choo, Y.-K. Quercetin Induces Mitochondrial Apoptosis and Downregulates Ganglioside GD3 Expression in Melanoma Cells. *Int. J. Mol. Sci.* **2024**, *25*, 5146. [CrossRef]
125. Müllauer, L.; Gruber, P.; Sebinger, D.; Buch, J.; Wohlfart, S.; Chott, A. Mutations in Apoptosis Genes: A Pathogenetic Factor for Human Disease. *Mutat. Res. Rev. Mutat. Res.* **2001**, *488*, 211–231. [CrossRef]
126. Ghavami, S.; Hashemi, M.; Ande, S.R.; Yeganeh, B.; Xiao, W.; Eshraghi, M.; Bus, C.J.; Kadkhoda, K.; Wiechec, E.; Halayko, A.J.; et al. Apoptosis and Cancer: Mutations within Caspase Genes. *J. Med. Genet.* **2009**, *46*, 497–510. [CrossRef]
127. Lawrence, M.S.; Stojanov, P.; Mermel, C.H.; Robinson, J.T.; Garraway, L.A.; Golub, T.R.; Meyerson, M.; Gabriel, S.B.; Lander, E.S.; Getz, G. Discovery and Saturation Analysis of Cancer Genes across 21 Tumour Types. *Nature* **2014**, *505*, 495–501. [CrossRef] [PubMed]
128. Bodaar, K.; Yamagata, N.; Barthe, A.; Landrigan, J.; Chonghaile, T.N.; Burns, M.; Stevenson, K.E.; Devidas, M.; Loh, M.L.; Hunger, S.P.; et al. JAK3 Mutations and Mitochondrial Apoptosis Resistance in T-Cell Acute Lymphoblastic Leukemia. *Leukemia* **2022**, *36*, 1499–1507. [CrossRef] [PubMed]
129. Guidicelli, G.; Chaigne-Delalande, B.; Dilhuydy, M.S.; Pinson, B.; Mahfouf, W.; Pasquet, J.M.; Mahon, F.X.; Pourquier, P.; Moreau, J.F.; Legembre, P. The Necrotic Signal Induced by Mycophenolic Acid Overcomes Apoptosis-Resistance in Tumor Cells. *PLoS ONE* **2009**, *4*, e5493. [CrossRef] [PubMed]
130. Wright, P. Targeting Vesicle Trafficking: An Important Approach to Cancer Chemotherapy. *Recent Pat. Anti-Cancer Drug Discov.* **2008**, *3*, 137–147. [CrossRef]
131. Gargalionis, A.N.; Karamouzis, M.V.; Adamopoulos, C.; Papavassiliou, A.G. Protein Trafficking in Colorectal Carcinogenesis-Targeting and Bypassing Resistance to Currently Applied Treatments. *Carcinogenesis* **2015**, *36*, 607–615. [CrossRef]
132. Bushweller, J.H. Targeting Transcription Factors in Cancer—From Undruggable to Reality. *Nat. Rev. Cancer* **2019**, *19*, 611–624. [CrossRef]
133. Fabbri, L.; Chakraborty, A.; Robert, C.; Vagner, S. The Plasticity of MRNA Translation during Cancer Progression and Therapy Resistance. *Nat. Rev. Cancer* **2021**, *21*, 558–577. [CrossRef]
134. da Costa, A.A.B.A.; Chowdhury, D.; Shapiro, G.I.; D'Andrea, A.D.; Konstantinopoulos, P.A. Targeting Replication Stress in Cancer Therapy. *Nat. Rev. Drug Discov.* **2023**, *22*, 38–58. [CrossRef]
135. Zhang, F.L.; Li, D.Q. Targeting Chromatin-Remodeling Factors in Cancer Cells: Promising Molecules in Cancer Therapy. *Int. J. Mol. Sci.* **2022**, *23*, 12815. [CrossRef]
136. Potapova, T.; Gorbsky, G.J. The Consequences of Chromosome Segregation Errors in Mitosis and Meiosis. *Biology* **2017**, *6*, 12. [CrossRef]
137. Sarkar, S.; Sahoo, P.K.; Mahata, S.; Pal, R.; Ghosh, D.; Mistry, T.; Ghosh, S.; Bera, T.; Nasare, V.D. Mitotic Checkpoint Defects: En Route to Cancer and Drug Resistance. *Chromosome Res.* **2021**, *29*, 131–144. [CrossRef] [PubMed]
138. Jinushi, M. Immune Regulation of Therapy-Resistant Niches: Emerging Targets for Improving Anticancer Drug Responses. *Cancer Metastasis Rev.* **2014**, *33*, 737–745. [CrossRef]
139. Liu, Y.M.; Chen, H.L.; Lee, H.Y.; Liou, J.P. Tubulin Inhibitors: A Patent Review. *Expert Opin. Ther. Pat.* **2014**, *24*, 69–88. [CrossRef]
140. Cress, A.E.; Dalton, W.S. Multiple Drug Resistance and Intermediate Filaments. *Cancer Metastasis Rev.* **1996**, *15*, 499–506. [CrossRef]
141. Satelli, A.; Li, S. Vimentin in Cancer and Its Potential as a Molecular Target for Cancer Therapy. *Cell Mol. Life Sci.* **2011**, *68*, 3033–3046. [CrossRef]
142. Shimizu, T.; Fujii, T.; Sakai, H. The Relationship Between Actin Cytoskeleton and Membrane Transporters in Cisplatin Resistance of Cancer Cells. *Front. Cell Dev. Biol.* **2020**, *8*, 597835. [CrossRef]
143. Wallace, D.C. Mitochondria and Cancer. *Nat. Rev. Cancer* **2012**, *12*, 685–698. [CrossRef] [PubMed]
144. O'Malley, J.; Kumar, R.; Inigo, J.; Yadava, N.; Chandra, D. Mitochondrial Stress Response and Cancer. *Trends Cancer* **2020**, *6*, 688–701. [CrossRef]
145. Jin, P.; Jiang, J.; Zhou, L.; Huang, Z.; Nice, E.C.; Huang, C.; Fu, L. Mitochondrial Adaptation in Cancer Drug Resistance: Prevalence, Mechanisms, and Management. *J. Hematol. Oncol.* **2022**, *15*, 97. [CrossRef]
146. Volm, M.; Efferth, T. Prediction of Cancer Drug Resistance and Implications for Personalized Medicine. *Front. Oncol.* **2015**, *5*, 282. [CrossRef]
147. Meyers, M.B.; Shen, W.P.V.; Spengler, B.A.; Ciccarone, V.; O'Brien, J.P.; Donner, D.B.; Furth, M.E.; Biedler, J.L. Increased Epidermal Growth Factor Receptor in Multidrug-Resistant Human Neuroblastoma Cells. *J. Cell Biochem.* **1988**, *38*, 87–97. [CrossRef]

148. Halder, S.; Basu, S.; Lall, S.P.; Ganti, A.K.; Batra, S.K.; Seshacharyulu, P. Targeting the EGFR Signaling Pathway in Cancer Therapy: What's New in 2023? *Expert Opin. Ther. Targets* **2023**, *27*, 305–324. [CrossRef] [PubMed]
149. Mohammad, R.M.; Muqbil, I.; Lowe, L.; Yedjou, C.; Hsu, H.Y.; Lin, L.T.; Siegelin, M.D.; Fimognari, C.; Kumar, N.B.; Dou, Q.P.; et al. Broad Targeting of Resistance to Apoptosis in Cancer. *Semin. Cancer Biol.* **2015**, *35*, S78–S103. [CrossRef]
150. Yan, G.; Elbadawi, M.; Efferth, T. Multiple Cell Death Modalities and Their Key Features. *World Acad. Sci. J.* **2020**, *2*, 39–48. Available online: https://www.spandidos-publications.com//10.3892/wasj.2020.40 (accessed on 7 June 2024). [CrossRef]
151. Li, Y.J.; Lei, Y.H.; Yao, N.; Wang, C.R.; Hu, N.; Ye, W.C.; Zhang, D.M.; Chen, Z.S. Autophagy and Multidrug Resistance in Cancer. *Chin. J. Cancer* **2017**, *36*, 52. [CrossRef]
152. Tong, X.; Tang, R.; Xiao, M.; Xu, J.; Wang, W.; Zhang, B.; Liu, J.; Yu, X.; Shi, S. Targeting Cell Death Pathways for Cancer Therapy: Recent Developments in Necroptosis, Pyroptosis, Ferroptosis, and Cuproptosis Research. *J. Hematol. Oncol.* **2022**, *15*, 174. [CrossRef] [PubMed]
153. Robey, R.W.; Pluchino, K.M.; Hall, M.D.; Fojo, A.T.; Bates, S.E.; Gottesman, M.M. Revisiting the Role of ABC Transporters in Multidrug-Resistant Cancer. *Nat. Rev. Cancer* **2018**, *18*, 452–464. [CrossRef]
154. Puris, E.; Fricker, G.; Gynther, M. The Role of Solute Carrier Transporters in Efficient Anticancer Drug Delivery and Therapy. *Pharmaceutics* **2023**, *15*, 364. [CrossRef]
155. Zhao, J.; Li, M.; Xu, J.; Cheng, W. The Modulation of Ion Channels in Cancer Chemo-Resistance. *Front. Oncol.* **2022**, *12*, 945896. [CrossRef]
156. Efferth, T.; Saeed, M.E.M.; Kadioglu, O.; Seo, E.J.; Shirooie, S.; Mbaveng, A.T.; Nabavi, S.M.; Kuete, V. Collateral Sensitivity of Natural Products in Drug-Resistant Cancer Cells. *Biotechnol. Adv.* **2020**, *38*, 107342. [CrossRef]
157. Dickreuter, E.; Cordes, N. The Cancer Cell Adhesion Resistome: Mechanisms, Targeting and Translational Approaches. *Biol. Chem.* **2017**, *398*, 721–735. [CrossRef] [PubMed]
158. Krawczyk, Z.; Gogler-Pigłowska, A.; Sojka, D.R.; Scieglinska, D. The Role of Heat Shock Proteins in Cisplatin Resistance. *Anti-Cancer Agents Med. Chem.* **2018**, *18*, 2093–2109. [CrossRef]
159. Saini, J.; Sharma, P.K. Clinical, Prognostic and Therapeutic Significance of Heat Shock Proteins in Cancer. *Curr. Drug Targets* **2018**, *19*, 1478–1490. [CrossRef] [PubMed]
160. Basset, C.A.; Conway de Macario, E.; Leone, L.G.; Macario, A.J.L.; Leone, A. The Chaperone System in Cancer Therapies: Hsp90. *J. Mol. Histol.* **2023**, *54*, 105–118. [CrossRef] [PubMed]
161. Wang, X.; Jiang, W.; Du, Y.; Zhu, D.; Zhang, J.; Fang, C.; Yan, F.; Chen, Z.S. Targeting Feedback Activation of Signaling Transduction Pathways to Overcome Drug Resistance in Cancer. *Drug Resist. Updates* **2022**, *65*, 100884. [CrossRef] [PubMed]
162. Bharathiraja, P.; Yadav, P.; Sajid, A.; Ambudkar, S.V.; Prasad, N.R. Natural Medicinal Compounds Target Signal Transduction Pathways to Overcome ABC Drug Efflux Transporter-Mediated Multidrug Resistance in Cancer. *Drug Resist. Updates* **2023**, *71*, 101004. [CrossRef] [PubMed]
163. Bou Antoun, N.; Chioni, A.M. Dysregulated Signalling Pathways Driving Anticancer Drug Resistance. *Int. J. Mol. Sci.* **2023**, *24*, 12222. [CrossRef] [PubMed]
164. Poornima, P.; Kumar, J.D.; Zhao, Q.; Blunder, M.; Efferth, T. Network Pharmacology of Cancer: From Understanding of Complex Interactomes to the Design of Multi-Target Specific Therapeutics from Nature. *Pharmacol. Res.* **2016**, *111*, 290–302. [CrossRef] [PubMed]
165. Lecca, P.; Re, A. Network-Oriented Approaches to Anticancer Drug Response. *Methods Mol. Biol.* **2017**, *1513*, 101–117. [CrossRef]
166. Luo, S.; Huang, M.; Lu, X.; Zhang, M.; Xiong, H.; Tan, X.; Deng, X.; Zhang, W.; Ma, X.; Zeng, J.; et al. Optimized Therapeutic Potential of Yinchenhao Decoction for Cholestatic Hepatitis by Combined Network Meta-Analysis and Network Pharmacology. *Phytomedicine* **2024**, *129*, 155573. [CrossRef]
167. Hientz, K.; Mohr, A.; Bhakta-Guha, D.; Efferth, T. The Role of P53 in Cancer Drug Resistance and Targeted Chemotherapy. *Oncotarget* **2017**, *8*, 8921–8946. [CrossRef] [PubMed]
168. Motegi, A.; Masutani, M.; Yoshioka, K.I.; Bessho, T. Aberrations in DNA Repair Pathways in Cancer and Therapeutic Significances. *Semin. Cancer Biol.* **2019**, *58*, 29–46. [CrossRef] [PubMed]
169. Fruehauf, J.P.; Trapp, V. Reactive Oxygen Species: An Achilles' Heel of Melanoma? *Expert Rev. Anticancer Ther.* **2008**, *8*, 1751–1757. [CrossRef] [PubMed]

biomedicines

MDPI

Correction

Correction: Drif et al. Anti-Inflammatory and Cancer-Preventive Potential of Chamomile (*Matricaria chamomilla* L.): A Comprehensive in Silico and in Vitro Study. Biomedicines 2024, 12(7), 1484

[1] Department of Pharmaceutical Biology, Institute of Pharmaceutical and Biomedical Sciences, Johannes Gutenberg University, Staudinger Weg 5, 55128 Mainz, Germany
[2] National Center for Natural Products Research (NCNPR), School of Pharmacy, University of Mississippi, Oxford, MS 38677, USA
* Correspondence: efferth@uni-mainz.de; Tel.: +49-6131-3925751

Text Correction

There was an error in the original publication [1]. A correction has been made to the **Section Results**, **Sub-section 3.12. Cell Death Detection**, the first two paragraphs of page. The correct terms "late apoptotic/necrotic" and "primary necrosis" have been added. Additionally, the percentage of late apoptotic/necrotic cells treated with 72 h quercetin 4×IC50 and with 72 h lupeol 4×IC50 have been corrected. The corrected paragraph is as follows:

"We investigated the mode of cell death in CCRF-CEM cells upon treatment with lupeol and quercetin for 72 h. The FITC-conjugated annexin V/PI assay was used to distinguish between living, early apoptotic, late apoptotic/necrotic, and primary necrotic cells. Annexin V is usually detected in early and late apoptosis. However, PI staining detects cells in late apoptosis and necrosis. Figure 10 shows that both compounds significantly induced cell death compared to the negative control. Quercetin induced late apoptosis/necrosis in 58.70% of cells at 4×IC50 ($p = 0.002$), while lupeol induced late apoptosis/necrosis in 73.80% of cells ($p = 0.001$)."

A correction has been also made in the **Section Discussion**, **page 27 (paragraph 4)**. The correct term "late apoptosis/necrosis" has been corrected. The corrected paragraph is as follows:

"In this context, it was interesting that the cytotoxicity of both compounds in CCRF-CEM late apoptosis/necrosis. This might be a cell-type-specific effect as quercetin and lupeol have been reported to induce either apoptosis or necrosis (or necroptosis) in different cell lines [119–124]. Because apoptosis is driven by the balance of pro- and anti-apoptotic proteins in specific signaling cascades, it is known that mutations in specific genes encoding these proteins confer resistance to apoptosis [125–128]. As a consequence, cytotoxic insults may overcome apoptosis resistance by other cell death modes [129]."

Figure/Table Legend

In the original publication [1], there was a mistake in the legends for **Figures 10.** The measurement of apoptosis was added and the legends A/C to lupeol and B/D to quercetin have been changed and the correct term "late apoptosis/necrosis" has been added. The was a slight mistake in the gating. The correct legends appear below**.**

As for the **Figure 11** in the original publication, which presented Annexin V/PI staining results on GFP-transfected U2OS cells, is no longer considered valid. It was subsequently recognized that GFP fluorescence interfered with Annexin V-FITC detection, leading to

Citation: Lastname, F.; Lastname, F.; Lastname, F. Title. *Journal Name* **2021**, *x*, Firstpage–Lastpage. https://doi.org/10.3390/xxxxx

Received: 1 March 2024
Revised: 14 June 2024
Accepted: 26 June 2024

Published: 5 July 2024**Publisher's Note:** MDPI stays neutral with regard to jurisdictional claims in published maps and institutional affiliations.

signal overlap and potentially incorrect interpretation of apoptosis data. As a result, Figure 11 is being removed from the article. The corrected version of the paper will no longer include this figure. This correction does not affect the scientific conclusions of the study. The main findings remain unchanged, including: The IC_{50} values for quercetin (89.6 μM) and lupeol (60 μM) in U2OS cells are relatively high, indicating moderate cytotoxicity, the apoptosis assay (Annexin V/PI) was less critical for this cell line. The cell cycle analysis clearly showed G_2/M arrest, further confirming the reliability of the cytotoxicity findings. The authors apologize for any inconvenience caused and appreciate the opportunity to make this correction.

"**Figure 10.** Detection of cell death in CCRF-CEM cells using flow cytometry and annexin-V/PI staining to measure apoptosis by flow cytometer. (**A**, **B**) Cells treated with 0.25 × IC_{50}, 0.5 × IC_{50}, 1 × IC_{50}, 2 × IC_{50}, and 4 × IC_{50} of quercetin and lupeol, for 72 h. DMSO was used as negative control. (**A**) Cells treated lupeol and (**B**) cells treated with quercetin. Q1 represents necrotic cells (−) annexin V/(+) PI; Q2 represents late apoptotic cells exhibiting annexin V (+)/PI (+); Q3 represents early apoptotic cells (+) annexin V/(−) PI; Q4 represents viable cells (−) annexin V/(−) PI. (**C**, **D**) Bar diagrams representing the percentages of cells in the different quadrants. (**C**) Effects of lupeol and (**D**) Effects of quercetin. The treatment of both compounds at increasing concentrations significantly enhanced the percentage of necrotic cells. *** $p < 0.001$, ** $p < 0.01$, and * $p < 0.05$ compared to the negative control using paired two-tailed t-test. The bar diagrams were created the calculation of the mean values ± SD of three independent experiments."

"**Figure 11.** has been removed due to technical issues that rendered the data invalid. This correction does not affect the results or conclusions of the original article."

The authors state that the scientific conclusions are unaffected. This correction was approved by the Academic Editor. The original publication has also been updated.

Error in Figure/Table

In the original publication [1], there was a mistake in **Figures 10 and 11** as published. The gating of the figure 10 has been correctly adjusted and figure 11 has been removed, as it was not critical to the main findings of the study and its removal does not impact the conclusions of the article.

The corrected appears below. The authors state that the scientific conclusions are unaffected. This correction was approved by the Academic Editor. The original publication has also been updated.

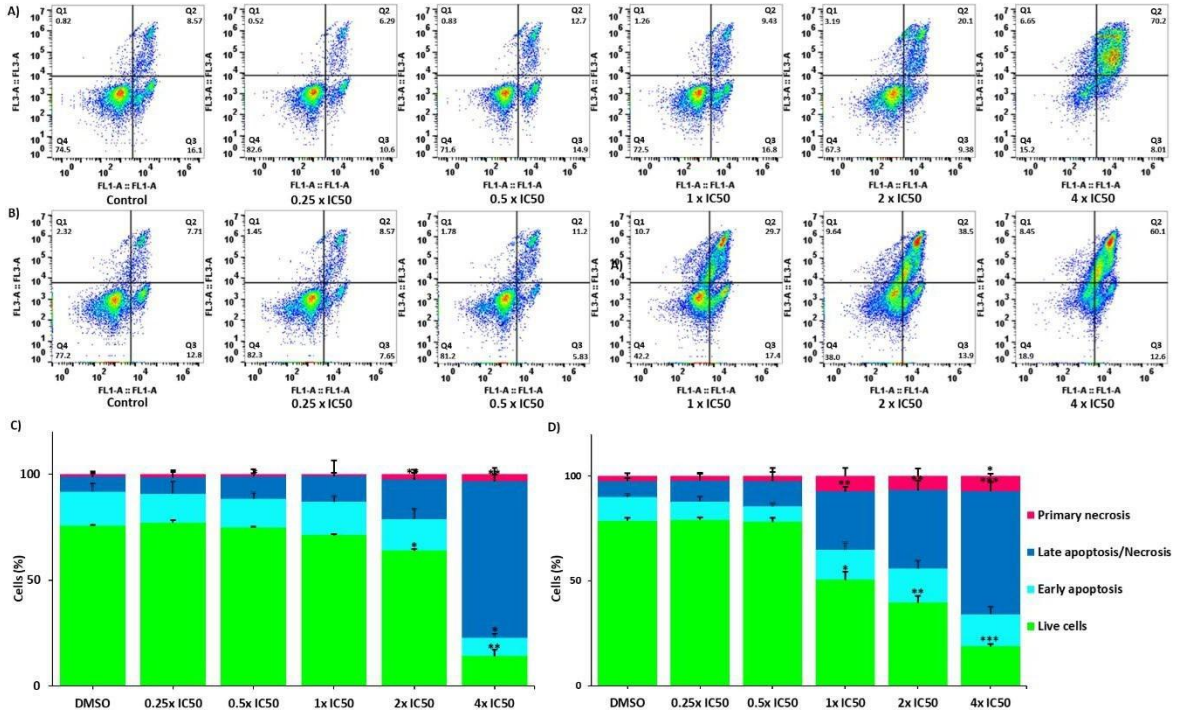

Figure 10. Detection of cell death in CCRF-CEM cells using flow cytometry and annexin-V/PI staining to measure apoptosis by flow cytometer. (**A**, **B**) Cells treated with 0.25 × IC_{50}, 0.5 × IC_{50}, 1 × IC_{50}, 2 × IC_{50}, and 4 × IC_{50} of quercetin and lupeol, for 72 h. DMSO was used as negative control. (**A**) Cells treated lupeol and (**B**) cells treated with quercetin. Q1 represents primary necrotic cells (−) annexin V/(+) PI; Q2 represents late apoptotic/necrotic cells exhibiting annexin V (+)/PI (+); Q3 represents early apoptotic cells (+) annexin V/(−) PI; Q4 represents viable cells (−) annexin V/(−) PI. (**C**, **D**) Bar diagrams representing the percentages of cells in the different quadrants. (**C**) Effects of lupeol and (**D**) Effects of quercetin. The treatment of both compounds at increasing concentrations significantly enhanced the percentage of necrotic cells. *** $p < 0.001$, ** $p < 0.01$, and * $p < 0.05$ compared to the negative control using paired two-tailed t-test. The bar diagrams were created the calculation of the mean values ± SD of three independent experiments.

Figure 11. has been removed due to technical issues. This correction does not affect the results or conclusions of the original article

Reference

1. Drif, A.I.; Yücer, R.; Damiescu, R.; Ali, N.T.; Abu Hagar, T.H.; Avula, B.; Khan, I.A.; Efferth, T. Anti-Inflammatory and Cancer-Preventive Potential of Chamomile (*Matricaria chamomilla* L.): A Comprehensive In Silico and In Vitro Study. *Biomedicines* **2024**, *12*, 1484. https://doi.org/10.3390/biomedicines12071484.

International Journal of
Molecular Sciences

MDPI

Article

In Silico and In Vitro Screening of 50 Curcumin Compounds as EGFR and NF-κB Inhibitors

Mohamed E. M. Saeed [1], Rümeysa Yücer [1,2,3], Mona Dawood [1,4], Mohamed-Elamir F. Hegazy [1,5], Assia Drif [1], Edna Ooko [1], Onat Kadioglu [1], Ean-Jeong Seo [1], Fadhil S. Kamounah [6], Salam J. Titinchi [7], Beatrice Bachmeier [8] and Thomas Efferth [1,*]

[1] Department of Pharmaceutical Biology, Institute of Pharmaceutical and Biomedical Sciences, Johannes Gutenberg University, Staudinger Weg 5, 55128 Mainz, Germany; saeed@uni-mainz.de (M.E.M.S.); ryuecer@students.uni-mainz.de (R.Y.); modawood@uni-mainz.de (M.D.); hegazy@uni-mainz.de (M.-E.F.H.); drif@uni-mainz.de (A.D.); ooko@uni-mainz.de (E.O.); kadioglu@uni-mainz.de (O.K.); seo@uni-mainz.de (E.-J.S.)
[2] Department of Pharmacognosy, Hamidiye Faculty of Pharmacy, University of Health Sciences, Üsküdar, Istanbul 34668, Turkey
[3] Department of Pharmacognosy and Phytochemistry, Faculty of Pharmacy, Bezmialem Vakif University, Istanbul 34093, Turkey
[4] Faculty of Medical Laboratory Sciences, Al-Neelain University, Khartoum 11121, Sudan
[5] Chemistry of Medicinal Plants Department, National Research Centre, 33 El-Bohouth St., Dokki, Giza 12622, Egypt
[6] Department of Chemistry, University of Copenhagen, Universitetsparken 5, 2100 Copenhagen, Denmark; fadil@chem.ku.dk
[7] Department of Chemistry, University of the Western Cape, P/B X17, Bellville, Cape Town 7535, South Africa; titinchi@uni-mainz.de
[8] Institute of Pharmaceutical Biology, Goethe University Frankfurt, 60438 Frankfurt am Main, Germany; b.bachmeier@em.uni-frankfurt.de
* Correspondence: efferth@uni-mainz.de; Tel.: +49-6131-39-25751; Fax: +49-6131-39-23752

Abstract: The improvement of cancer chemotherapy remains a major challenge, and thus new drugs are urgently required to develop new treatment regimes. Curcumin, a polyphenolic antioxidant derived from the rhizome of turmeric (*Curcuma longa* L.), has undergone extensive preclinical investigations and, thereby, displayed remarkable efficacy in vitro and in vivo against cancer and other disorders. However, pharmacological limitations of curcumin stimulated the synthesis of numerous novel curcumin analogs, which need to be evaluated for their therapeutic potential. In the present study, we calculated the binding affinities of 50 curcumin derivatives to known cancer-related target proteins of curcumin, i.e., epidermal growth factor receptor (EGFR) and nuclear factor κB (NF-κB) by using a molecular docking approach. The binding energies for EGFR were in a range of −12.12 (±0.21) to −7.34 (±0.07) kcal/mol and those for NF-κB ranged from −12.97 (±0.47) to −6.24 (±0.06) kcal/mol, indicating similar binding affinities of the curcumin compounds for both target proteins. The predicted receptor-ligand binding constants for EGFR and curcumin derivatives were in a range of 0.00013 (±0.00006) to 3.45 (±0.10) μM and for NF-κB in a range of 0.0004 (±0.0003) to 10.05 (±4.03) μM, indicating that the receptor-ligand binding was more stable for EGFR than for NF-κB. Twenty out of 50 curcumin compounds showed binding energies to NF-κB smaller than −10 kcal/mol, while curcumin as a lead compound revealed free binding energies of >−10 kcal/mol. Comparable data were obtained for EGFR: 15 out of 50 curcumin compounds were bound to EGFR with free binding energies of <−10 kcal/mol, while the binding affinity of curcumin itself was >−10 kcal/mol. This indicates that the derivatization of curcumin may indeed be a promising strategy to improve targe specificity and to obtain more effective anticancer drug candidates. The in silico results have been exemplarily validated using microscale thermophoresis. The bioactivity has been further investigated by using resazurin cell viability assay, lactate dehydrogenase assay, flow cytometric measurement of reactive oxygen species, and annexin V/propidium iodide assay. In conclusion, molecular docking represents a valuable approach to facilitate and speed up the identification of novel targeted curcumin-based drugs to treat cancer.

check for updates

Citation: Saeed, M.E.M.; Yücer, R.; Dawood, M.; Hegazy, M.-E.F.; Drif, A.; Ooko, E.; Kadioglu, O.; Seo, E.-J.; Kamounah, F.S.; Titinchi, S.J.; et al. In Silico and In Vitro Screening of 50 Curcumin Compounds as EGFR and NF-κB Inhibitors. *Int. J. Mol. Sci.* **2022**, *23*, 3966. https://doi.org/10.3390/ijms23073966

Academic Editor: Biji Theyilamannil Kurien

Received: 29 September 2021
Accepted: 29 March 2022
Published: 2 April 2022

Publisher's Note: MDPI stays neutral with regard to jurisdictional claims in published maps and institutional affiliations.

Keywords: bioinformatics; cancer; natural products; phytochemicals; synthetic derivatives; virtual drug screening

1. Introduction

Cancer is currently one of the leading causes of death worldwide. Incidence and death rates are increasing for several types of cancer [1,2]. More than 21 million cancer incidences have been predicted to occur in the year 2025 (https://www.statista.com/statistics/1031316/new-cancer-cases-forecast-worldwide/; accessed on 1 March 2022). Many advances have been made in the early diagnosis and treatment of cancer. However, lowering cancer mortality rates still remains a vital challenge [3]. Cancer chemotherapy involves using natural or synthetic chemicals to prevent or suppress cancer growth. As a matter of fact, more than half of all available anticancer drugs are derivatives of natural products or are compounds that mimic the modes of action of natural products [4]. The advantages of phytochemicals are their lower toxicity profiles and their ability to target multiple signaling pathways that prevent the rapid development of drug resistance [5–7]. A number of phytochemicals are known to address cancer-related target proteins, such as the epidermal growth factor receptor (EGFR) [8–11] or the nuclear factor-kappa B (NF-κB) [12–14] and others.

Curcumin is a naturally occurring compound derived from the rhizomes of *Curcuma longa* L. As a member of the ginger family, it has been commonly used as a spice for food preservation as well as in folk medicine. It possesses a wide array of functional characteristics, including antioxidant and anti-inflammatory [15] as well as antiviral, antibacterial, and antifungal properties [16]. Curcumin has been extensively investigated for its cellular and molecular modes of action against cancer [17,18], diabetes [19], neurological ailments [20], and osteoarthritis [21], and even entered several clinical trials [22,23]. Curcumin inhibits cancer cell proliferation [24,25], DNA repair along the p53-p21/GADD45A-cyclin/CDK-Rb/E2F-DNMT1 axis [26,27], metastasis by the NF-κB/c-JUN/MMP pathway [28], and the CXC-chemokine/NF-κB signaling pathway [29–31] as well as angiogenesis by the protein kinase C/NF-κB/AP-1 pathway [32,33]. EGFR is upregulated in several tumor types, including lung and colorectal tumors making EGFR an exquisite therapeutic target. Curcumin targets EGFR in lung cancer [34,35] and colorectal carcinoma [36,37] types leading to tumor cell killing. The transcription factor NF-κB is targeted by curcumin in a wide range of tumor types, including leukemia and lymphoma [38–42].

In contrast to conventional anticancer drugs that often exert severe side effects such as myelosuppression, mucositis, alopecia, nausea, vomiting, and others, curcumin displays only minimal toxicity [43–45]. However, the poor bioavailability of curcumin represents a major disadvantage for its clinical application [46]. Many efforts have been undertaken to improve its bioavailability using a variety of approaches, including innovative drug delivery systems (nanoparticles, liposomes, phospholipids, etc.) as well as the development of novel synthetic curcumin derivatives [47–51]. By synthesizing chemical libraries of curcumin derivatives and subjecting them to biological scrutiny, compounds with improved pharmacological features may be yielded.

Our study focuses on curcumin and a total of 50 curcumin compounds that were either reported by us [17] or mined in the PubChem database (https://pubchem.ncbi.nlm.nih.gov; accessed on 31 October 2021). We attempted to predict their activity using an in silico molecular docking approach. For this reason, we calculated the binding energies of these derivatives to two cancer-related proteins, i.e., EGFR and NF-κB. These proteins have been previously described as target proteins of curcumin [52].

The epidermal growth factor receptor (EGFR) is a tyrosine kinase in the cell membrane of many tumor types. This transmembrane receptor belongs to a gene family with three other members (HER2-4). The binding of extracellular ligands, i.e., epidermal growth factor (EGF) and transforming growth factor (TGFα), leads to dimerization, autophosphorylation,

and downstream activation of signal transduction pathways. This ultimately leads to carcinogenesis, cell growth, metastasis, and inhibition of apoptosis [53], as well as the development of resistance to cytotoxic chemotherapy and radiotherapy [54]. Targeted therapies with small molecules (e.g., erlotinib, gefitinib, afatinib) or monoclonal antibodies (e.g., cetuximab, panitumumab) have significantly improved the treatment outcome of innumerable patients [55]. However, resistance to these targeted drugs has been emerging [56,57]. Thus, the search for new EGFR inhibitors has to continue [58]. In this context, phytochemicals gained interest as novel lead compounds [59].

The nuclear factor 'kappa-light-chain-enhancer' of activated B-cells (NF-κB) is a transcription factor that binds to specific DNA sequences (the 10 bp long κB motif) and thereby regulates the expression of downstream genes. This primarily involves genes that control the immune response, inflammation, cell proliferation, and apoptosis [60,61]. Since NF-κB activation is important for cancer development and progression [62], this transcription factor has become a target molecule for new drug development [63,64]. Phytochemicals represent an important reservoir for the identification of NF-κB inhibitors in cancer [65–67]. Interestingly, EGFR and NF-κB cooperate in tumor cells, amplifying their oncogenic signals [68]. Therefore, it is particularly useful to investigate inhibitors that inhibit both cancer-related proteins simultaneously to achieve a more effective antitumor effect.

The concept of the present investigation was to identify curcumin derivatives with better binding affinities to EGFR and NF-κB to improve tumor specificity and reduce side effects on normal organs. To validate the molecular docking data, we exemplarily tested the inhibitory effect of curcumin and two of the derivatives investigated by western blot experiments with these four proteins towards EGFR and NF-κB. Our results support the concept that novel synthetic curcumin derivatives with improved specificity to important cancer-related targets could be identified by combined in silico–in vitro drug screening approaches.

2. Results

2.1. Molecular Docking

We first performed molecular docking of 50 curcumin compounds (Figure S1) mined from the PubChem database (https://pubchem.ncbi.nlm.nih.gov/; accessed on 31 October 2021) against EGFR and NF-κB. We intended to predict the potential activity of the synthetic derivatives by calculating their in silico binding activities to these proteins. It is noteworthy that the synthetic curcumin derivatives showed low binding energy values (i.e., higher affinities) to both target proteins.

The binding energies for EGFR were in a range of −12.12 (±0.21) to −7.34 (±0.07) kcal/mol and those for NF-κB ranged from −12.97 (±0.47) to −6.24 (±0.06) kcal/mol, indicating similar binding affinities of the curcumin compounds for both target proteins (Table 1). Molecular dockings of curcumin and two selected curcumin derivatives to EGFR are shown in Figure 1. The three compounds were bound to the same domain but with different amino acids within this pharmacophore.

The predicted receptor-ligand binding constants for EGFR and curcumin derivatives were in a range of 0.00013 (±00.0006) to 3.45 (±0.10) μM and for NF-κB in a range of 0.0004 (±0.0003) to 10.05 (±4.03) μM, indicating that the receptor-ligand binding was more stable for EGFR than for NF-κB (Table 1). Molecular dockings of curcumin and two selected curcumin derivatives to NF-κB are shown in Figure 2. Like EGFR, the three compounds were bound to the same domain of NF-κB.

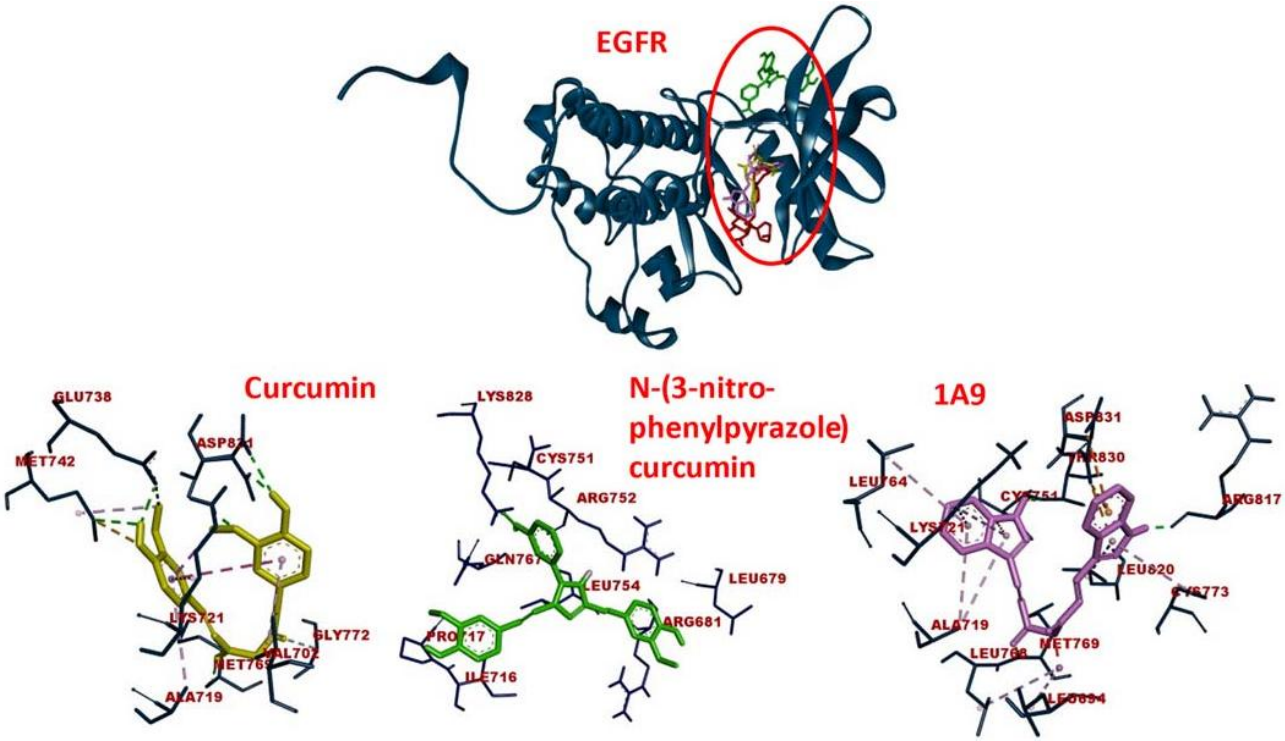

Figure 1. Molecular docking of curcumin-type compounds to EGFR. Top: The compounds were bound to the same domain of EGFR. Bottom: curcumin, *N*-(3-nitrophenylpyrazole) curcumin, and the derivative 1A9 were bound to different amino acids in this domain. The red circle indicates the binding site of the three compounds.

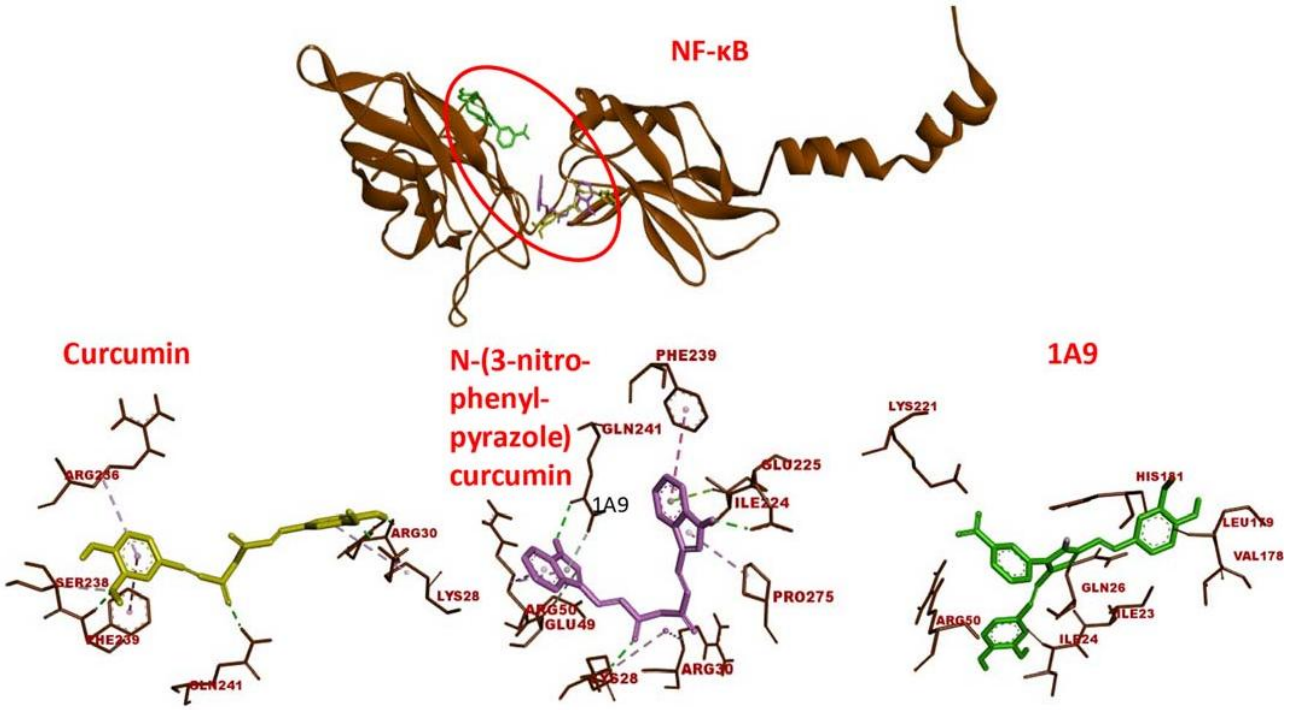

Figure 2. Molecular docking of curcumin-type compounds to NF-κB. Top: The compounds were bound to the same domain of EGFR. Bottom: curcumin, *N*-(3-nitrophenylpyrazole) curcumin, and the derivative 1A9 were bound to different amino acids in this domain. The red circle indicates the binding site of the three compounds.

Table 1. Mean binding energies and predicted binding constants were obtained by molecular docking for 50 curcumin compounds. Dockings were independently carried out three times with every 250,000 runs (mean values ± SD).

	Compounds	EGFR (Mean Binding Energy, kcal/mol)	EGFR (Mean pKi, μM)	NF-κB (Mean Binding Energy, kcal/mol)	NF-κB (Mean pKi, μM)
1	Curcumin	−9.42 ± 0.09	0.13 ± 0.02	−8.38 ± 0.16	0.73 ± 0.21
2	Bisdemethoxycurcumin	−8.51 ± 0.02	0.58 ± 0.02	−7.96 ± 0.05	1.46 ± 0.11
3	Diacetylcurcumin	−10.72 ± 0.49	0.02 ± 0.02	−9.67 ± 0.26	0.09 ± 0.04
4	[^{18}FP]-curcumin	−8.70 ± 0.21	0.43 ± 0.14	−9.01 ± 0.07	0.25 ± 0.03
5	Monodemethoxycurcumin	−9.04 ± 0.06	0.24 ± 0.02	−8.07 ± 0.10	1.23 ± 0.20
6	(E,E)-Bis(2-hydroxybenzylidene)acetone	−7.95 ± 0.01	1.49 ± 0.04	−7.21 ± 0.06	5.19 ± 0.50
7	Curcumin monoglucoside	−9.72 ± 0.76	0.11 ± 0.11	−9.57 ± 0.34	0.11 ± 0.06
8	Di-*O*-(2-thienoyl) curcumin	−11.71 ± 0.26	0.003 ± 0.002	−10.71 ± 0.17	0.01 ± <0.01
9	Cis-curcumin	−9.07 ± 0.30	0.24 ± 0.10	−8.81 ± 0.33	0.39 ± 0.21
10	Curcumin diglucoside	−9.10 ± 0.99	0.39 ± 0.35	−10.35 ± 0.35	0.03 ± 0.02
11	Tetrahydrocurcumin	−9.13 ± 0.17	0.21 ± 0.06	−8.28 ± 0.21	0.90 ± 0.34
12	Allyl curcumin	−10.07 ± 0.07	0.04 ± 0.01	−9.15 ± 0.04	0.20 ± 0.01
13	Monodemethylcurcumin	−9.96 ± 0.10	0.05 ± 0.01	−8.16 ± 0.56	0.59 ± 0.12
14	Didemethylcurcumin	−9.90 ± 0.07	0.06 ± 0.01	−8.71 ± 0.25	0.49 ± 0.18
15	Curcumin-4′-*O*-β-D-gentiotrioside	−7.85 ± 0,59	3.11 ± 0.23	−7.51 ± 0.37	3.47 ± 2.05
16	4-Benzylidene curcumin	−10.62 ± 0.72	0.03 ± 0.03	−9.10 ± 0.10	0.21 ± 0.04
17	Monoglycinoyl curcumin	−12.12 ± 0.21	0.0013 ± 0.0006	−10.07 ± 0.08	0.04 ± 0.01
18	Ethyl curcumin	−10.09 ± 0.11	0.04 ± 0.01	−9.23 ± 0.05	0.17 ± 0.01
19	Curcumin dimer 1	−11.64 ± 0.56	0.004 ± 0.003	−11.11 ± 0.65	0.01 ± 0.01
20	*N*-phenylpyrazole curcumin	−8.63 ± 0.19	0.49 ± 0.14	−8.81 ± 0.01	0.35 ± 0.01
21	Curcumin β-D-glucuronide	−10.36 ± 0.19	0.04 ± 0.02	−10.07 ± 0.36	0.05 ± 0.03
22	3,4-Difluorobenzylidene curcumin	−10.08 ± 0.13	0.04 ± 0.01	−9.30 ± 0.07	0.15 ± 0.02
23	Di-*O*-(2-hydroxyethyl) curcumin	−9.60 ± 0.27	0.10 ± 0.05	−8.97 ± 0.55	0.35 ± 0.27
24	4-(4-hydroxybenzylidene) curcumin	−10.55 ± 0.12	0.02 ± <0.01	−8.98 ± 0.04	0.26 ± 0.02
25	*N*-(3-nitrophenylpyrazole) curcumin	−10.50 ± 0.02	0.02 ± <0.01	−9.57 ± 0.01	0.097 ± <0.01
26	*N*-(4-flurophenylpyrazole) curcumin	−8.46 ± 0.19	0.65 ± 0.19	−8.81 ± 0.09	0.35 ± 0.06
27	*N*-(4-methoxyphenylpyrazole) curcumin	−8.49 ± 0.04	0.60 ± 0.03	−8.95 ± 0.11	0.28 ± 0.05
28	Di-*O*-chloropropionylethyl curcumin	−10.92 ± 0.25	0.01 ± <0.01	−10.36 ± 0.59	0.03 ± 0.02
29	Curcumin tri-adamantylaniniethylcarbonate	−10.75 ± 0.23	0.01 ± 0.01	−12.97 ± 0.47	0.0004 ± 0.0003
30	Curcumin dimer 2	−11.08 ± 0.24	0.01 ± <0.01	−12.05 ± 0.46	0.002 ± 0.001
31	Curcumin tri-trithiadiazolaminoethylcarbonate	−10.35 ± 0.55	0.03 ± 0.02	−10.97 ± 0.53	0.01 ± 0.01
32	4-(4-hydroxy-3-methoxybenzylidene) curcumin	−11.44 ± 0.16	0.004 ± 0.002	−10.97 ± 0.53	0.01 ± 0.01
33	Curcumin-β-D-glucuronide triacetate methyl ester	−10.06 ± 0.79	0.07 ± 0.06	−10.35 ± 0.35	0.03 ± 0.02
34	Curcumin 4′-*O*-β-D-gentiobiosyl 4″-*O*-β-D-glucoside	−9.54 ± 0.25	0.11 ± 0.05	−10.23 ± 0.59	0.04 ± 0.04
35	Tetrahydrocurcumin isoxazole	−9.43 ± 0.20	0.13 ± 0.04	−8.60 ± 0.41	0.57 ± 0.32
36	Hexahydrocurcumin	−9.25 ± 0.11	0.17 ± 0.03	−8.41 ± 0.27	0.73 ± 0.35
37	Bisdemethoxycurcumin isoxazole	−7.45 ± 0.01	3.45 ± 0.10	−7.55 ± 0.10	2.96 ± 0.47
38	Curcumin dimer 3	−10.28 ± 0.22	0.03 ± 0.01	−10.50 ± 0.77	0.01 ± 0.01
39	Curcumin ED	−9.59 ± 0.08	0.10 ± 0.02	−8.69 ± 0.14	0.43 ± 0.10
40	Curcumin PE	−9.24 ± 0.12	0.17 ± 0.03	−8.22 ± 0.22	0.99 ± 0.33
41	Curcumin sulfate	−9.31 ± 0.16	0.15 ± 0.04	−9.84 ± 0.08	0.06 ± 0.01
42	Ferrocenyl curcumin	−8.34 ± 0.22	0.80 ± 0.29	−7.10 ± 0.33	6.87 ± 3.92
43	Di-*O*-deconyl curcumin	−10.57 ± 0.17	0.01 ± <0.01	−11.58 ± 0.85	0.02 ± 0.01
44	GNF-pf-2695 ((2E,5E)-2,5-bis[(3,4,5-trimethoxyphenyl) methylidene]cyclopentan-1-one)	−7.34 ± 0.07	4.22 ± 0.51	−7.56 ± 0.15	2.93 ± 0.78
45	Perfluoro curcumin	−7.55 ± 0.19	3.03 ± 0.86	−6.86 ± 0.28	10.05 ± 4.03
46	Keto-curcumin	−9.89 ± 0.41	0.07 ± 0.04	−8.78 ± 0.15	0.37 ± 0.09
47	Disalicyloyl curcumin	−7.67 ± 0.58	0.02 ± 0.02	−6.24 ± 0.06	26.77 ± 3.36
48	HO-3867 (3E,5E)-3,5-bis[(4-fluorophenyl)methylidene]-1-[(1-hydroxy-2,2,5,5-tetramethylpyrrol-3-yl)methyl]piperidin-4-one)	−9.73 ± 0.03	0.07 ± <0.01	−7.79 ± 0.10	1.96 ± 0.33
49	1A6 ((1E,6E)-4-chloro-1,7-bis(3,4-dimethoxyphenyl)hepta-1,6-diene-3,5-dione)	−8.94 ± 0.06	0.28 ± 0.03	−8.28 ± 0.21	0.90 ± 0.34
50	1A9 ((1E,6E)-4-chloro-1,7-di(1H-indol-3-yl)hepta-1,6-diene-3,5-dione)	−9.57 ± 0.02	0.10 ± 0.03	−8.51 ± 0.11	0.58 ± <0.01

As a next step, we correlated the binding energies of the compounds for EGFR and NF-κB. By using Pearson correlation test, we found statistically significant relationships between binding energies and predicted inhibition constants of EGFR ($p = 2.73 \times 10^{-9}$; $r = 0.715$) and of ($p = 4.39 \times 10^{-7}$; $r = 0.631$) as well as of binding energies between EGFR and NF-κB ($p = 4.32 \times 10^{-5}$; $r = 0.526$) and predicted binding energies between both proteins ($p = 2.53 \times 10^{-8}$; $r = 0.682$). These results indicate that there may be a relationship between the "druggability" of the compounds being EGFR or NF-κB inhibitors. Compounds that were better bound to EGFR also showed a significant relationship to better bind to NF-κB and vice versa (Figure 3).

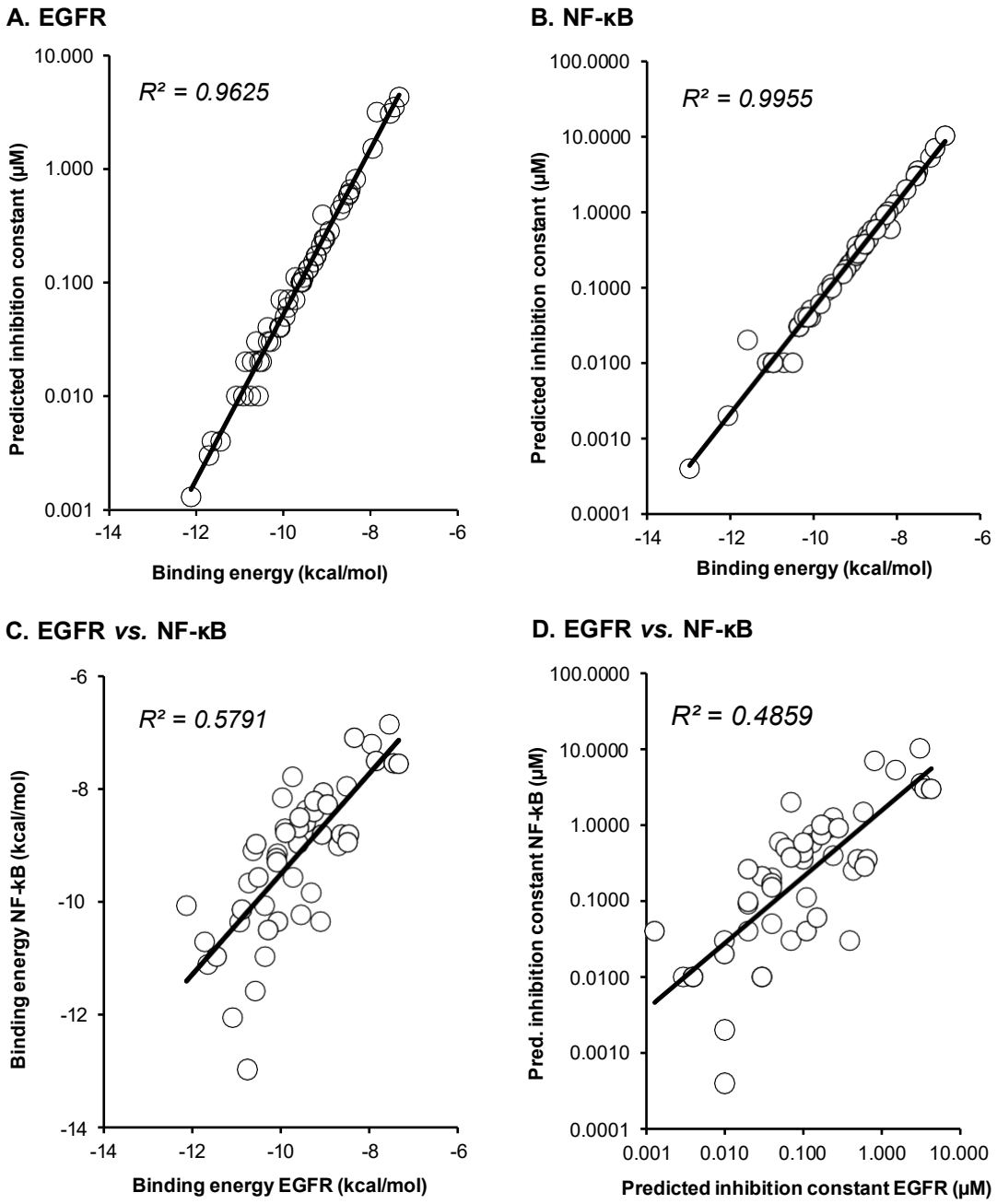

Figure 3. Correlation of binding energies (kcal/mol) and predicted inhibition constants (pKi, μM) of 50 curcumin compounds were calculated using the Pearson correlation test. Correlation of binding energies and pKi values for (**A**) EGFR and (**B**) NF-κB. Correlation of (**C**) binding energies or (**D**) pKi values between EGFR and NF-κB.

2.2. Microscale Thermophoresis

To verify the in silico predictions, we performed microscale thermophoresis. This is a biophysical assay to study the interactions between chemical ligands and their target proteins. For this reason, we used recombinant EGFR and NF-κB and assayed them with curcumin, *N*-(3-nitrophenylpyrazole) curcumin, and curcumin derivative 1A9. The equilibrium constants (K_D) indicate that the three curcumin-type compounds were bound to EGFR and NF-κB (Figure 4).

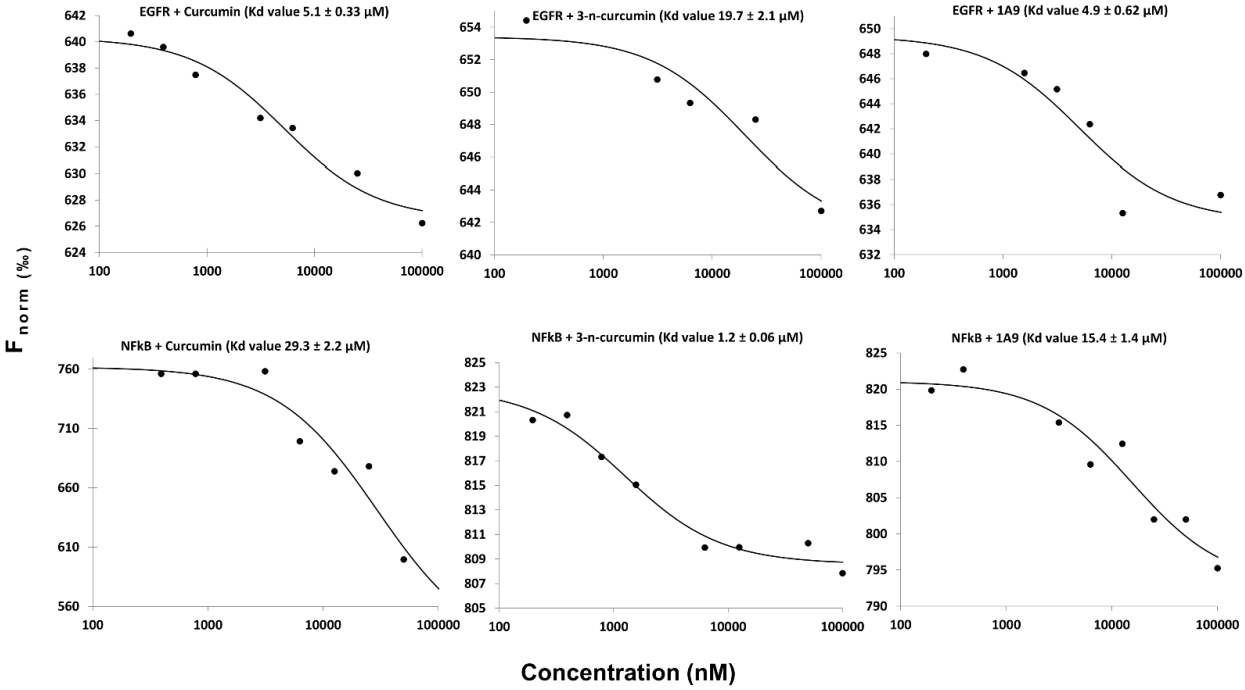

Figure 4. Analysis of the interaction between curcumin derivatives with recombinant EGFR and NF-κB by microscale thermophoresis (MST). The recombinant proteins were used at a concentration of 200 nM, while the concentration of curcumin, *N*-(3-nitrophenylpyrazole) curcumin, and the curcumin derivative 1A9 ranged from 100 to 100,000 nM. The migration of the fluorescent proteins was determined upon local heating using a Monolith NT.115^{Pico} with 40% LED power and 80% MST power for EGFR and with 20% LED power and 20% MST power for NF-κB at room temperature.

2.3. Resazurin Assay

To study the effect of selected compounds on cell viability, we treated human CCRF-CEM leukemia and human A549 lung cancer cells with curcumin, *N*-(3-nitrophenylpyrazole) curcumin, and the curcumin derivative 1A9. CCRF-CEM and A549 cells were chosen as examples of hematopoietic and solid tumor cells. Peripheral blood mononuclear cells (PBMCs) were isolated from a healthy subject to compare the inhibitory effects of the curcumin compounds between tumor and normal cells. As shown in Figure 5, all three compounds inhibited the viability of CCRF-CEM and A549 cells in a dose-dependent manner, while normal PBMCs were not or only minimally inhibited. The dose-response curves were taken to calculate the 50% inhibition concentrations (IC_{50}). CCRF-CEM leukemia cells were about one order of magnitude more sensitive to the compounds than A549 cells and *N*-(3-nitrophenylpyrazole) curcumin revealed a higher inhibitory activity than the other two compounds (Table 2).

Table 2. IC_{50} values of CCRF-CEM leukemia and A549 lung carcinoma cells treated with curcumin, 1A9, and *N*-(3-nitrophenylpyrazole) curcumin as determined by the resazurin assay. The IC_{50} values (µM) were calculated from the dose-response curves shown in Figure 5. DMSO was used as vehicle control. Mean ± SD of three independent measurements.

Cells	Compounds		
	Curcumin	***N*-(3-Nitrophenylpyrazole) Curcumin**	**1A9**
CCRF-CEM	3.0 ± 0.4	1.9 ± 0.4	2.6 ± 0.3
A549	29.4 ± 1.9	18.9 ± 1.4	23.3 ± 1.2
PBMC	>100	>100	>100

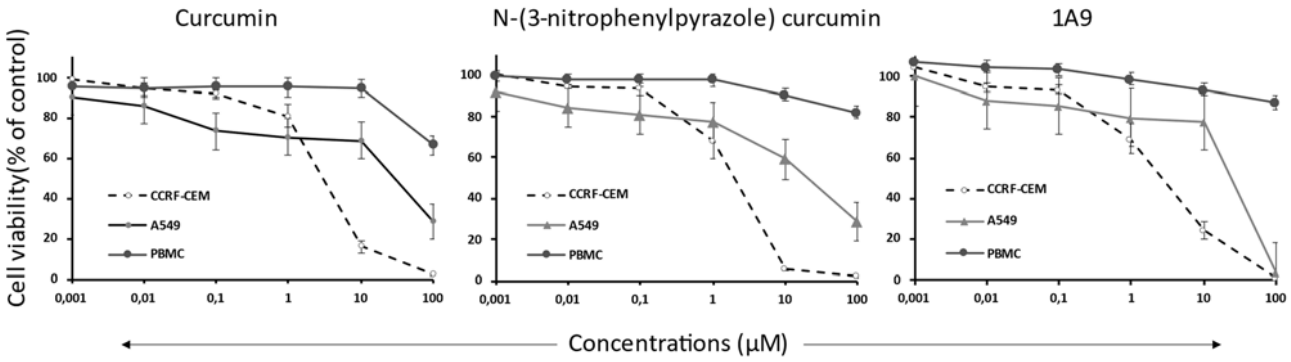

Figure 5. Cell viability dose-response curves of CCRF-CEM leukemia cells, A549 lung carcinoma cells, and healthy peripheral blood mononuclear cells treated with curcumin, 1A9, and *N*-(3-nitrophenylpyrazole) curcumin as determined by the resazurin assay. Cells were incubated with concentrations from 10^{-3} to 100 µM and incubated at 37 °C for 72 h. DMSO was used as vehicle control. Mean ± SD of three independent measurements.

2.4. LDH Assay

To assess the cytotoxicity, the LDH cell death assay was performed that measures the release of LDH from cells due to membrane damage. As shown in Figure 6, all three curcumin-type compounds led to a dose-dependent LDH release in a concentration range of 0.01 to 10 µM in CCRF-CEM leukemia cells. Only negligible LDH release was found in healthy peripheral blood mononuclear cells, indicating tumor-specific cytotoxic effects of the three curcumin compounds.

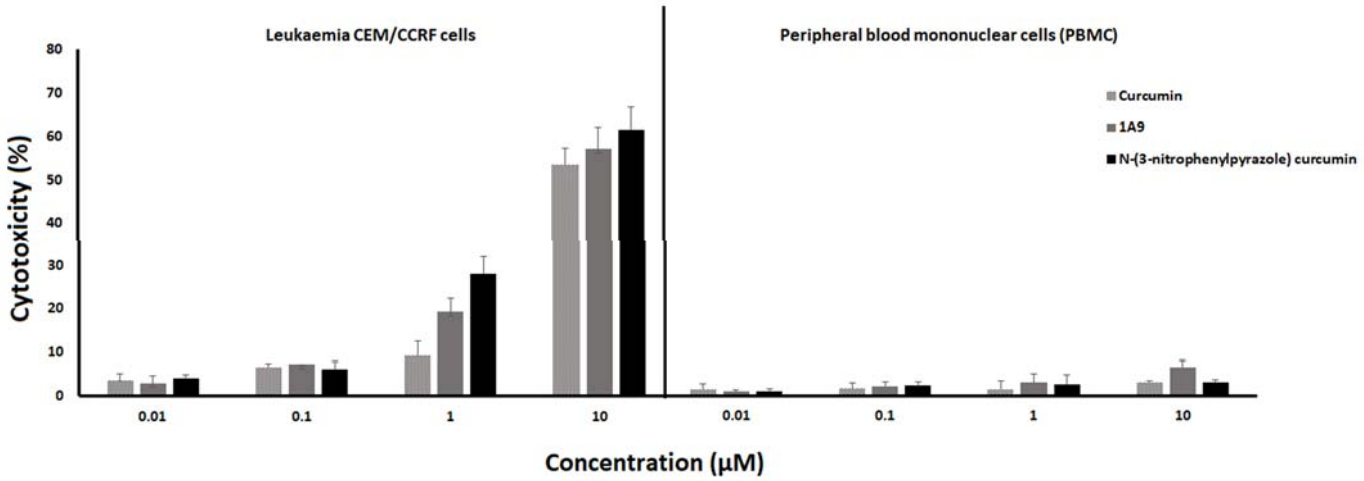

Figure 6. Cytotoxicity in CCRF-CEM leukemia cells (left) and peripheral blood mononuclear cells (PBMCs) of a healthy donor (right) by curcumin, 1A9, and *N*-(3-nitrophenylpyrazole) curcumin as determined by the release of lactate dehydrogenase. Cells were incubated with concentrations from 0.01 to 10 µM and incubated at 37 °C for 48 h. DMSO was used as vehicle control. Mean ± SD of three independent measurements.

2.5. ROS Assay

The generation of reactive oxygen species (ROS) upon exposure of CCRF-CEM cells with *N*-(3-nitrophenylpyrazole) curcumin or 1A9 was compared with the ROS generation by curcumin. As shown in Figure 7, dose-dependent effects were observed with 0.5×, 1×, and 2× IC_{50} concentrations of these three compounds. The strongest ROS generation was measured with 1A9, the lowest one with *N*-(3-nitrophenylpyrazole) curcumin. Curcumin produced intermediate ROS amounts.

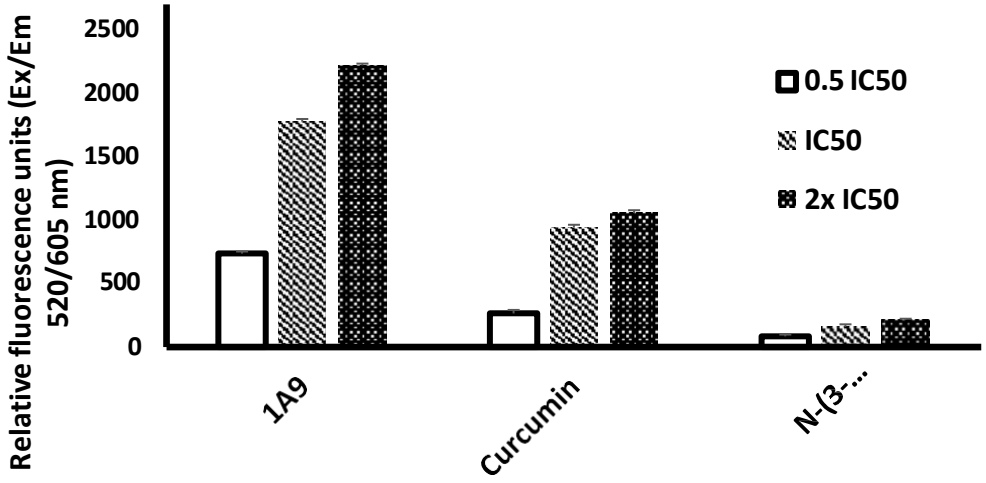

Figure 7. Generation of reactive oxygen species in CCRF-CEM cells by curcumin, *N*-(3-nitrophenylpyrazole) curcumin, and 1A9. Cells were incubated with 0.5×, 1×, 2×, or 4× IC_{50} and incubated at 37 °C for 24 h. DMSO was used as vehicle control. Mean ± SD of three independent measurements.

2.6. Annexin/PI Assay

The induction of early and late apoptosis by the three curcumin compounds was determined by the annexin V/propidium iodide assay and flow cytometry. Incubation of CCRF-CEM cells at 37 °C for 24 h showed clear dose-dependent induction either of early or late apoptosis in a concentration range from 0.5× to 4× IC_{50} (Figure 8). The effects of 1A9 were even stronger: the highest fraction of apoptotic cells was observed already at the lowest concentration of 0.5× IC_{50}. Higher concentrations led to a decrease in early apoptotic cells and an increase in late apoptotic cells, indicating a concentration-dependent switch from early to late apoptosis upon exposure with 1A9 at 37 °C for 24 h (Figure 8). Although *N*-(3-nitrophenylpyrazole) curcumin was cytotoxic in the LDH assay and inhibited viability in the resazurin assay, it did not induce early or late apoptosis after 24 h incubation (Figure 8). Even after prolonged incubation at 37 °C for 48 or 72 h, *N*-(3-nitrophenylpyrazole) curcumin did not induce apoptosis (Figure 9). The low percentages of apoptosis cells did not exceed the low rates of spontaneous apoptosis in DMSO-treated control cells.

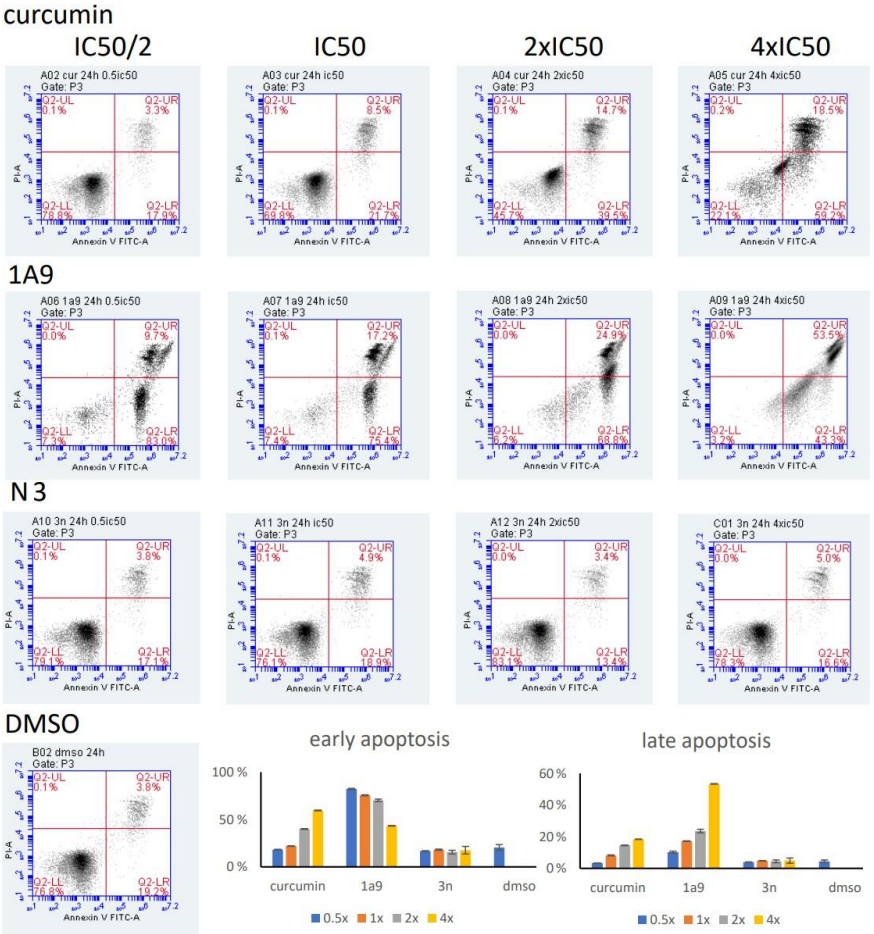

Figure 8. Induction of apoptosis in CCRF-CEM cells upon exposure at 37 °C for 24 h with curcumin, *N*-(3-nitrophenylpyrazole) curcumin, and 1A9 as determined by the annexin V/propidium iodide assay and flow cytometry. Cells were incubated with 0.5 ×, 1 ×, 2 ×, or 4 × IC_{50}. DMSO was used as vehicle control. Mean ± SD of three independent measurements.

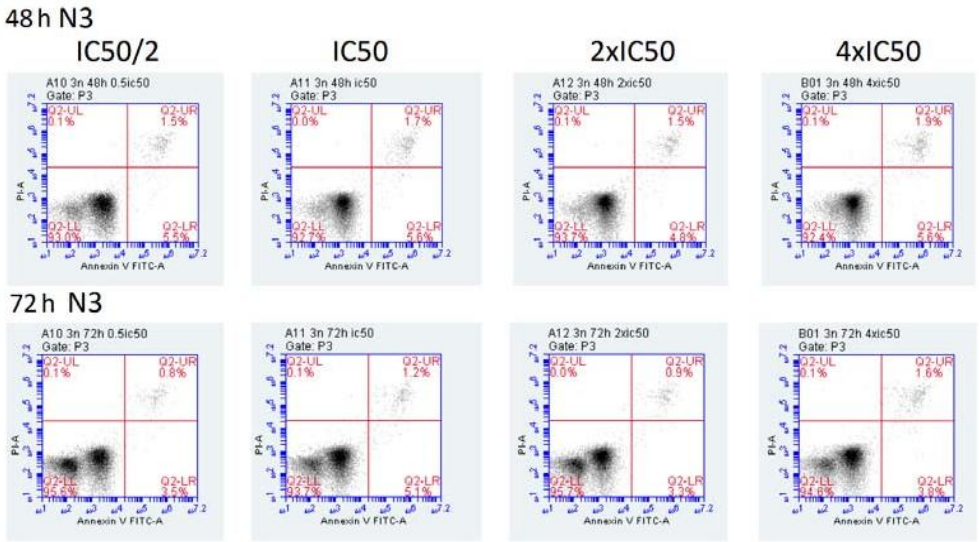

Figure 9. *Cont.*

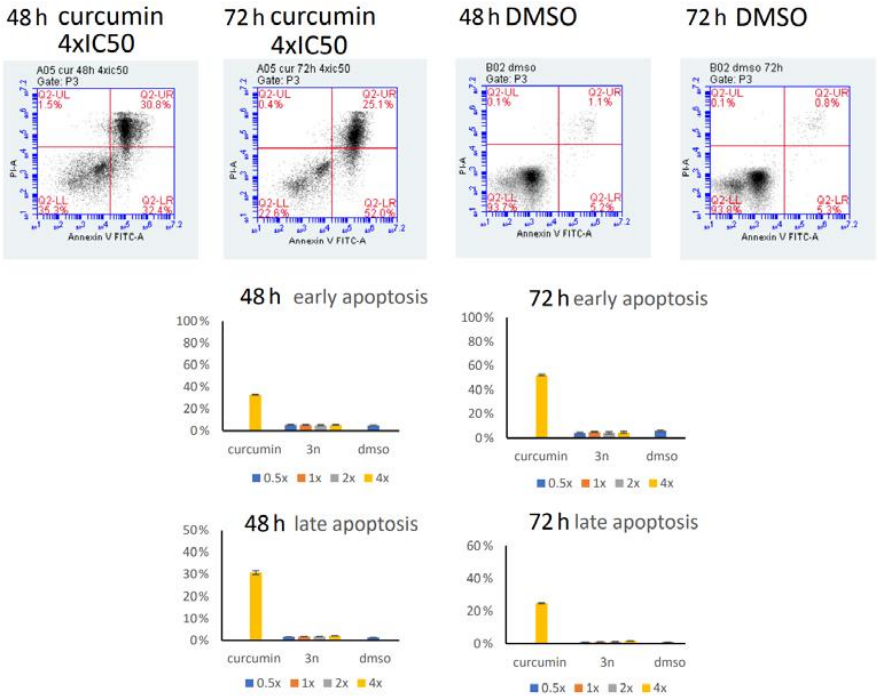

Figure 9. Induction of apoptosis in CCRF-CEM cells upon exposure at 37 °C for 48 or 72 h with *N*-(3-nitrophenylpyrazole) curcumin as determined by the annexin V/propidium iodide assay and flow cytometry. Cells were incubated with 0.5×, 1×, 2×, or 4× IC_{50} *N*-(3-nitrophenylpyrazole) curcumin. Positive control: curcumin (4× IC_{50}); negative control: DMSO. Mean ± SD of three independent measurements.

3. Discussion

In the present study, we investigated the in silico binding affinities of a total of 50 curcumin compounds to EGFR and NF-κB. The aim was to find novel derivatives with improved binding properties to these two cancer-related proteins as a starting point to develop curcumin-based drugs with improved pharmacological features.

EGFR plays a central role in the pathogenesis and progression of different carcinoma types. EGFR is overexpressed in many human carcinomas and is also involved in developing resistance to chemotherapy [54,56]. On average, 50–70% of lung, colon, and breast carcinoma express EGFR [69]. Inhibition of EGFR phosphorylation is caused by directly inhibitor effects of curcumin on the tyrosine kinase activity of EGFR as well as by curcumin-induced alterations of the physical plasma membrane properties influencing receptor dimerization [70]. Additionally, curcumin downregulated EGFR protein expression [36].

From previous investigations on the activity of curcumin derivatives towards EGFR [71], it is known that substitutions on the phenyl rings affected the extent of EGFR down-regulation. Moreover, methoxy or hydroxy substituents increased the compounds' activity, while other alkyloxy groups did not. The activity was, in general, not influenced by methoxy, hydroxy, or halogen groups. Remarkably, *N*-(3-nitrophenylpyrazole) curcumin was bound better to EGFR than the halogenated curcumin derivatives investigated in this study, including difluorinated curcumin that is frequently described in the literature as a promising drug candidate for further drug development [72].

NF-κB regulates the expression of genes involved in many processes that play a key role in cancer biology, such as proliferation, migration, and apoptosis. NF-κB influences the expression of genes that are involved in a large number of physiological processes, including immune response, cell survival, differentiation, and proliferation. Curcumin has been described as a potent inhibitor of NF-κB activation [73]. Twenty out of 50 curcumin compounds showed binding energies to NF-κB smaller than −10 kcal/mol, while curcumin as a lead compound revealed free binding energies of > −10 kcal/mol. Comparable data

were obtained for EGFR: 15 out of 50 curcumin compounds were bound to EGFR with free binding energies of <-10 kcal/mol, while the binding affinity of curcumin itself was >-10 kcal/mol. This indicates that the derivatization of curcumin may indeed be a promising strategy to improve targe specificity and to obtain more effective anticancer drug candidates.

Even though *N*-(3-nitrophenylpyrazole) curcumin was bound to EGFR and NF- κB, it inhibited cell viability (as shown by the resazurin assay) and was cytotoxic (as shown by the LDH assay) in a comparable manner as curcumin and 1A9, *N*-(3-nitrophenylpyrazole) curcumin did not induce ROS generation and did not induce apoptosis. This indicates that different curcumin derivatives may activate different downstream mechanisms despite identical upstream targets (EGFR, NF-κB). *N*-(3-nitrophenylpyrazole) curcumin apparently induced a ROS-independent non-apoptotic pathway of cell death. This is a novel finding that may have important therapeutic implications. It is well-known that tumor cells with defective apoptotic regulation exert resistance to the induction of cell death, resulting in tumor progression and resistance to anticancer drugs [74,75]. Having cytotoxic drugs at hand, such as *N*-(3-nitrophenylpyrazole) curcumin, may allow one to bypass apoptosis resistance and kill otherwise apoptosis-resistant tumors. It is now well-known that a plethora of different cell death mechanisms can be operative in tumor cells [76,77]. It is beyond the scope of the present investigation to clarify which alternative mechanisms of cell death are responsible for the cytotoxic activity of *N*-(3-nitrophenylpyrazole) curcumin. We will address this issue in the future.

4. Materials and Methods

4.1. Chemicals

Chemical structures for in silico analyses were downloaded from PubChem (https://pubchem.ncbi.nlm.nih.gov/; accessed on 31 October 2021). Curcumin and DMSO were of analytical grade and purchased from Sigma-Aldrich (Taufkirchen, Germany). The curcumin derivative 1A9 was synthesized as recently reported [17]. *N*-(3-nitrophenylpyrazole) curcumin was provided by Dr. Fadhil S. Kamounah (Department of Chemistry, University of Copenhagen, Denmark). Stock solutions (50 mM) were prepared in DMSO, stored at -20 °C, and diluted to the final concentration in fresh media before each experiment. The chemical structures of 50 curcumin compounds are shown in Supplementary Figure S1.

4.2. Docking

The X-ray crystallography-based three-dimensional protein structures of EGFR and NF-κB (PDB codes 1M17 and IVKX, respectively) were obtained from the RCSB Protein Data Bank (http://www.rcsb.org/pdb/home/home.do; accessed on 31 October 2021) and used as docking templates throughout the calculations. Two-dimensional structures of curcumin and its derivatives were energy-minimized and converted to 3D structures compatible for docking operation using the Chem 3D program. Molecular docking was then carried out with the AutoDock program 4.2.6 (The Scripps Research Institute, La Jolla, CA, USA) following a previously reported protocol [78,79]. Docking parameters were set to 250 runs and 250,000 energy evaluations for each cycle. Three independent cycles were performed, resulting in a total number of 750,000 calculations per compound and target protein. VMD (Visual Molecular Dynamics, Visual Molecular Dynamics, http://www.ks.uiuc.edu/Research/vmd/; accessed on 31 October 2021) was used as a visualization tool to illustrate further the binding modes obtained from docking.

4.3. Microscale Thermophoresis

In vitro protein binding assays were performed to validate the in silico interaction between EGFR and NF-κB). The recombinant proteins were obtained from commercial sources (EGFR cat. No. 10001-H08H, NF-κB cat. No. 12054-H09E, Sino Biological Europe GmbH, Eschborn, Germany). The proteins were labeled according to the Monolith™ NT.115 Protein Labeling Kit RED-NHS (NanoTemper Technologies GmbH, Munich, Ger-

many). Varying concentrations of curcumin, *N*-(3-phenylpyrazole) curcumin, and the curcumin derivative 1A9 ranging from 100 to 100,000 nM were titrated with labeled EGFR or NF-κB. As previously described, the experiments were carried out using standard capillaries in the NanoTemper Monolith™ NT (NanoTemper Technologies GmbH, Munich, Germany) [80,81]. Microscale thermophoresis (MST) was performed with 40% LED power and 80% MST power for the labeled EGFR and with 20% LED power and 20% MST power for the labeled NF-κB.

4.4. Cell Culture

The A549 lung cancer cell line was obtained from the German Cancer Research Center (DKFZ, Heidelberg, Germany). The original source of the cell lines is the American Type Culture Collection (ATCC, Manassas, VA, USA). The cells were cultivated in a completed DMEM culture medium with GlutaMAX (Invitrogen, Germany) supplemented with 10% fetal bovine serum, l-glutamine (2 mM), and 1% of a 10,000 U/mL penicillin G and 10 mg/mL streptomycin at 37 °C in a humidified air incubator (95%) containing 5% CO_2. All experiments were performed on cells in the logarithmic growth phase. CCRF-CEM cells were a gift from Dr. Axel Sauerbrey (University Hospital for Pediatrics, Univerity of Jena, Germany) and maintained in an RPMI medium supplemented with fetal bovine serum, glutamine, and penicillin as described above.

Peripheral blood from healthy donors was obtained from Transfusion Center (University Medical Center, Johannes Gutenberg University Mainz, Mainz, Germany). Human peripheral blood mononuclear cells (PBMCs) were isolated by density gradient centrifugation using Histopaque-1077® (Sigma-Aldrich Co. LLC, Darmstadt, Germany), strictly following the manufacturer's instructions. Isolated PBMCs were resuspended in warm Panserin 413 medium (PAN-Biotech, Aidenbach, Germany) supplemented with 2% phytohemagglutinin M (PHA-M, Life Technologies, Darmstadt, Germany) and then immediately used for experimentation.

4.5. Resazurin Cell Viability Assay

Viable cells reduce the non-fluorescent resazurin to the strongly-fluorescent resorufin. Suspension cells (1×10^4 cells/well) or adherent cells (5×10^3 cells/well, incubated overnight to allow attachment) were seeded in 96-well plates at a volume of 100 µL. Varying concentrations of curcumin, 1A9, or *N*-(3-nitrophenylpyrazole) curcumin were added to reach a total volume of 200 µL. After 72 h, 20 µL of 0.01% *w*/*v* resazurin (Sigma-Aldrich) was added to each well, and cells were incubated for another 4 h at 37 °C. The fluorescence of resorufin was measured at 544 nm (excitation) and 590 nm (emission) using an Infinite M2000 Pro™ plate reader (Tecan, Crailsheim, Germany). Each experiment was independently performed three times with six parallel measurements each. The effects on cell viability were assessed according to the percentage of untreated control and 50% inhibition concentrations (IC_{50}) were calculated from dose-response curves using GraphPad Prism® v6.0 software (GraphPad Software Inc., San Diego, CA, USA).

4.6. Lactate Dehydrogenase (LDH) Assay

The LDH release from the cells was determined using an LDH-cytotoxicity assay kit (catalog no. ab65393, Abcam, Berlin, Germany). CEM/CCRF leukemia cells and peripheral blood mononuclear cells (PBMCs) were seeded in 96-well plates at a density of 4×10^4 cells/well. Varying concentrations ranging from 0.01 to 10 µM of curcumin, *N*-(3-nitrophenylpyrazole) curcumin, or 1A9 were added to the cells and incubated for 48 h. At the end of the incubation period, the plates were gently shaken to ensure LDH was evenly distributed in the culture medium. Afterward, cells were precipitated at 600 × *g* for 10 min and 10 µL/well of the clear supernatant medium were transferred to optically clear 96-well plates. The LDH reaction mix (100 µL/well) was added and incubated for 30 min at room temperature. The absorbance of LDH was measured with an Infinite M2000 Pro™ plate reader (Tecan, Crailsheim, Germany) using a 450 (440–490) nm filter.

4.7. Reactive Oxygen Species (ROS) Detection Assay

Intracellular reactive oxygen species (ROS) were determined using the cellular reactive oxygen species detection assay kit (catalog No. ab186027, Abcam, Berlin, Germany). Briefly, 4×10^4 CEM/CCRF leukemia cells/well were seeded in 96-well plates and incubated with 100 µL/well of ROS red working solution for 1 h in an incubator at 37 °C in a 5% CO_2 atmosphere. Afterward, cells were treated with curcumin, *N*-(3-nitrophenylpyrazole) curcumin, or 1A9. For each compound, varying concentrations (0.5× IC_{50}, IC_{50}, 2× IC_{50}) were used. After incubation for 24 h, the ROS induction was monitored at Ex/Em = 520/605 nm using an Infinite M2000 Pro™ plate reader (Tecan, Crailsheim, Germany).

4.8. Annexin V/Propidium Iodide (PI) Assay

CCRF-CEM cells (1×10^6 cells/mL) were seeded in 6-well plates and different concentrations of curcumin, 1A9, or *N*-(3-nitrophenylpyrazole) curcumin (0.5×, 1×, 2×, 4× IC_{50}) were applied at 37 °C for 24 h. The cells were washed and re-suspended in 1 mL cold PBS and 500 µL 1× binding buffer, respectively, followed by incubation with 5 µL annexin V/PI and 10 µL of PE (50 mg/mL) (Thermo Fisher Scientific, Dreieich, Germany) in the dark for 15 min. The histograms were measured using an Accuri C6 flow cytometer (Becton Dickinson, Heidelberg, Germany). Four different cell populations were determined: viable cells, annexin V positive/PI negative cells (cells that are in early apoptosis), annexin V negative/PI-positive cells (cells that are necrotic), and annexin V positive/PI-positive cells (cells that are in late apoptosis or already dead).

5. Conclusions

In conclusion, we speculated that synthetic derivatives bear potential for cancer treatment, especially as EGFR inhibitors. Some synthetic derivatives are bound to and inhibit their target proteins in a comparable or even better manner than their parent lead compound, curcumin. The chemistry of curcumins is a fascinating area of research. It should be kept in mind that curcumin is not only active against cancer but also against many diseases such as metabolic syndrome, ulcerative colitis and inflammatory diseases in general, neurodegenerative diseases, infectious diseases, etc. [82–86]. It is well in the scope of expectations that some of the curcumin derivatives described in the present study may also be valuable drug candidates for other diseases than cancer. We believe they may be valuable candidates in the further drug discovery process.

Supplementary Materials: Supplementary materials can be found at https://www.mdpi.com/article/10.3390/ijms23073966/s1.

Author Contributions: T.E. and B.B. designed the study. R.Y., A.D. and M.D. performed molecular docking experiments and calculations. M.E.M.S., E.O., R.Y., E.-J.S., A.D., M.D. and O.K. carried out the experiments. S.J.T. and F.S.K. synthesized the compounds. M.-E.F.H. optimized the compounds and revised the structures for molecular docking. T.E. supervised the work and provided the facilities for the study. M.E.M.S. and T.E. wrote the manuscript. All authors have read and agreed to the published version of the manuscript.

Funding: M.-E.F.H. gratefully acknowledges the financial support from the Alexander von Humboldt Foundation "Georg Foster Research Fellowship for Experienced Researchers". M.E.M.S., O.K. and E.J.S. are funded by intramural funds at the Johannes Gutenberg University Mainz, Germany. We are grateful for a Ph.D. stipend from the German Academic Exchange Service (DAAD) to E.O.

Institutional Review Board Statement: Not applicable.

Informed Consent Statement: Not applicable.

Data Availability Statement: Data available on request.

Acknowledgments: M.-E.F.H. gratefully acknowledges the financial support from the Alexander von Humboldt Foundation "Georg Foster Research Fellowship for Experienced Researchers". R.Y. is funded by the Theophrastus Foundation, Germany. M.E.M.S., O.K. and E.-J.S. are funded by intramural funds at the Johannes Gutenberg University Mainz, Germany. We are grateful for a Ph.D. stipend from the German Academic Exchange Service (DAAD) to E.O.

Conflicts of Interest: The authors declare that there is no conflict of interest.

References

1. Siegel, R.L.; Miller, K.D.; Jemal, A. Cancer statistics 2018. *CA Cancer J. Clin.* **2018**, *68*, 7–30. [CrossRef] [PubMed]
2. Toyoda, Y.; Tabuchi, T.; Nakayama, T.; Hojo, S.; Yoshioka, S.; Maeura, Y. Past trends and future estimation of annual breast cancer incidence in Osaka, Japan. *Asian Pac. J. Cancer Prev.* **2016**, *17*, 52.
3. Mattiuzzi, C.; Lippi, G. Current cancer epidemiology. *J. Epidemiol. Glob. Health* **2019**, *9*, 217–222. [CrossRef] [PubMed]
4. Newman, D.J.; Cragg, G.M. Natural products as sources of new drugs over the last 25 years. *J. Nat. Prod.* **2007**, *70*, 461–477. [CrossRef] [PubMed]
5. Kuete, V.; Efferth, T. African flora has the potential to fight multidrug resistance of cancer. *BioMed Res. Int.* **2015**, *2015*, 914813. [CrossRef]
6. Efferth, T.; Saeed, M.E.M.; Kadioglu, O.; Seo, E.J.; Shirooie, S.; Mbaveng, A.T.; Nabavi, S.M.; Kuete, V. Collateral sensitivity of natural products in drug-resistant cancer cells. *Biotechnol. Adv.* **2020**, *38*, 107342. [CrossRef]
7. Efferth, T.; Kadioglu, O.; Saeed, M.E.M.; Seo, E.-J.; Mbaveng, A.T.; Kuete, V. Medicinal plants and phytochemicals against multidrug-resistant tumor cells expressing ABCB1, ABCG2, or ABCB5: A synopsis of 2 decades. *Phytochem. Rev.* **2021**, *20*, 7–53. [CrossRef]
8. Sertel, S.; Plinkert, P.K.; Efferth, T. Natural products derived from traditional Chinese medicine as novel inhibitors of the epidermal growth factor receptor. *Comb. Chem. High Throughput Screen.* **2010**, *13*, 849–854. [CrossRef]
9. Zhao, Q.; Kretschmer, N.; Bauer, R.; Efferth, T. Shikonin and its derivatives inhibit the epidermal growth factor receptor signaling and synergistically kill glioblastoma cells in combination with erlotinib. *Int. J. Cancer* **2015**, *137*, 1446–1456. [CrossRef]
10. Saeed, M.E.M.; Rahama, M.; Kuete, V.; Dawood, M.; Elbadawi, M.; Sugimoto, Y.; Efferth, T. Collateral sensitivity of drug-resistant ABCB5- and mutation-activated EGFR overexpressing cells towards resveratrol due to modulation of SIRT1 expression. *Phytomedicine* **2019**, *59*, 152890. [CrossRef]
11. Lee, H.Y.J.; Meng, M.; Liu, Y.; Su, T.; Kwan, H.Y. Medicinal herbs and bioactive compounds overcome the drug resistance to epidermal growth factor receptor inhibitors in non-small cell lung cancer. *Oncol. Lett.* **2021**, *22*, 646. [CrossRef] [PubMed]
12. Hamdoun, S.; Efferth, T. Ginkgolic acids inhibit migration in breast cancer cells by inhibition of NEMO sumoylation and NF-κB activity. *Oncotarget* **2017**, *8*, 35103–35115. [CrossRef] [PubMed]
13. Chen, H.; Liu, R.H. Potential mechanisms of action of dietary phytochemicals for cancer prevention by targeting cellular signaling transduction pathways. *J. Agric. Food. Chem.* **2018**, *66*, 3260–3276. [CrossRef] [PubMed]
14. Dawood, M.; Ooko, E.; Efferth, T. Collateral sensitivity of parthenolide via NF-κB and HIF-α inhibition and epigenetic changes in drug-resistant cancer cell lines. *Front. Pharmacol.* **2019**, *10*, 542. [CrossRef]
15. Menon, V.P.; Sudheer, A.R. Antioxidant and anti-inflammatory properties of curcumin. *Adv. Exp. Med. Biol.* **2007**, *595*, 105–125.
16. Moghadamtousi, S.Z.; Kadir, H.A.; Hassandarvish, P.; Tajik, H.; Abubakar, S.; Zandi, K. A review on antibacterial, antiviral, and antifungal activity of curcumin. *BioMed Res. Int.* **2014**, *2014*, 186864.
17. Ooko, E.; Alsalim, T.; Saeed, B.; Saeed, M.E.; Kadioglu, O.; Abbo, H.S.; Titinchi, S.J.; Efferth, T. Modulation of P-glycoprotein activity by novel synthetic curcumin derivatives in sensitive and multidrug-resistant T-cell acute lymphoblastic leukemia cell lines. *Tox. Appl. Pharmacol.* **2016**, *305*, 216–233. [CrossRef]
18. Liu, L.; Fu, Y.; Zheng, Y.; Ma, M.; Wang, C. Curcumin inhibits proteasome activity in triple-negative breast cancer cells through regulating p300/miR-142-3p/PSMB5 axis. *Phytomedicine* **2020**, *78*, 153312. [CrossRef]
19. Heshmati, J.; Moini, A.; Sepidarkish, M.; Morvaridzadeh, M.; Salehi, M.; Palmowski, A.; Mojtahedi, M.F.; Shidfar, F. Effects of curcumin supplementation on blood glucose, insulin resistance and androgens in patients with polycystic ovary syndrome: A randomized double-blind placebo-controlled clinical trial. *Phytomedicine* **2021**, *80*, 153395. [CrossRef]
20. Seo, E.J.; Efferth, T.; Panossian, A. Curcumin downregulates expression of opioid-related nociceptin receptor gene (OPRL1) in isolated neuroglia cells. *Phytomedicine* **2018**, *50*, 285–299. [CrossRef]
21. Hsiao, A.F.; Lien, Y.C.; Tzeng, I.S.; Liu, C.T.; Chou, S.H.; Horng, Y.S. The efficacy of high- and low-dose curcumin in knee osteoarthritis: A systematic review and meta-analysis. *Complement. Ther. Med.* **2021**, *63*, 102775. [CrossRef] [PubMed]
22. Saghatelyan, T.; Tananyan, A.; Janoyan, N.; Tadevosyan, A.; Petrosyan, H.; Hovhannisyan, A.; Hayrapetyan, L.; Arustamyan, M.; Arnhold, J.; Rotmann, A.R.; et al. Efficacy and safety of curcumin in combination with paclitaxel in patients with advanced, metastatic breast cancer: A comparative, randomized, double-blind, placebo-controlled clinical trial. *Phytomedicine* **2020**, *70*, 153218. [CrossRef] [PubMed]
23. Zhang, T.; He, Q.; Liu, Y.; Chen, Z.; Hu, H. Efficacy and safety of curcumin supplement on improvement of insulin resistance in people with type 2 diabetes mellitus: A systematic review and meta-analysis of randomized controlled trials. *Evid.-Based Complement. Altern. Med.* **2021**, *2021*, 4471944. [CrossRef]

24. Sertel, S.; Eichhorn, T.; Bauer, J.; Hock, K.; Plinkert, P.K.; Efferth, T. Pharmacogenomic determination of genes associated with sensitivity or resistance of tumor cells to curcumin and curcumin derivatives. *J. Nutr. Biochem.* **2012**, *23*, 875–884. [CrossRef] [PubMed]
25. Ye, M.X.; Li, Y.; Yin, H.; Zhang, J. Curcumin: Updated molecular mechanisms and intervention targets in human lung cancer. *Int. J. Mol. Sci.* **2012**, *13*, 3959–3978. [CrossRef] [PubMed]
26. Kong, Y.; Ma, W.; Liu, X.; Zu, Y.; Fu, Y.; Wu, N.; Liang, L.; Yao, L.; Efferth, T. Cytotoxic activity of curcumin towards CCRF-CEM leukemia cells and its effect on DNA damage. *Molecules* **2009**, *14*, 5328–5338. [CrossRef] [PubMed]
27. Tong, R.; Wu, X.; Liu, Y.; Liu, Y.; Zhou, J.; Jiang, X.; Zhang, L.; He, X.; Ma, L. Curcumin-induced DNA demethylation in human gastric cancer cells is mediated by the DNA-damage response pathway. *Oxid. Med. Cell. Longev.* **2020**, *2020*, 2543504. [CrossRef] [PubMed]
28. Bachmeier, B.; Nerlich, A.G.; Iancu, C.M.; Cilli, M.; Schleicher, E.; Vené, R.; Dell'Eva, R.; Jochum, M.; Albini, A.; Pfeffer, U. The chemopreventive polyphenol Curcumin prevents hematogenous breast cancer metastases in immunodeficient mice. *Cell Physiol. Biochem.* **2007**, *19*, 137–152. [CrossRef]
29. Killian, P.H.; Kronski, E.; Michalik, K.M.; Barbieri, O.; Astigiano, S.; Sommerhoff, C.P.; Pfeffer, U.; Nerlich, A.G.; Bachmeier, B.E. Curcumin inhibits prostate cancer metastasis in vivo by targeting the inflammatory cytokines CXCL1 and -2. *Carcinogenesis* **2012**, *33*, 2507–2519. [CrossRef]
30. Kronski, E.; Fiori, M.E.; Barbieri, O.; Astigiano, S.; Mirisola, V.; Killian, P.H.; Bruno, A.; Pagani, A.; Rovera, F.; Pfeffer, U.; et al. miR181b is induced by the chemopreventive polyphenol curcumin and inhibits breast cancer metastasis via down-regulation of the inflammatory cytokines CXCL-1 and -2. *Mol. Oncol.* **2014**, *8*, 581–595. [CrossRef]
31. Ruiz de Porras, V.; Bystrup, S.; Martínez-Cardús, A.; Pluvinet, R.; Sumoy, L.; Howells, L.; James, M.I.; Iwuji, C.; Manzano, J.L.; Layos, L.; et al. Curcumin mediates oxaliplatin-acquired resistance reversion in colorectal cancer cell lines through modulation of CXC-Chemokine/NF-κB signalling pathway. *Sci. Rep.* **2016**, *6*, 24675. [CrossRef] [PubMed]
32. Norooznezhad, F.; Rodriguez-Merchan, E.C.; Asadi, S.; Norooznezhad, A.H. Curcumin: Hopeful treatment of hemophilic arthropathy via inhibition of inflammation and angiogenesis. *Expert Rev. Hematol.* **2020**, *13*, 5–11. [CrossRef] [PubMed]
33. Bhandarkar, S.S.; Arbiser, J.L. Curcumin as an inhibitor of angiogenesis. *Adv. Exp. Med. Biol.* **2007**, *595*, 185–195. [PubMed]
34. Shafiee, M.; Mohamadzade, E.; Shahid Sales, S.; Khakpouri, S.; Maftouh, M.; Parizadeh, S.A.; Hasanian, S.M.; Avan, A. Current status and perspectives regarding the therapeutic potential of targeting EGFR pathway by curcumin in lung cancer. *Curr. Pharm. Des.* **2017**, *23*, 2002–2008. [CrossRef] [PubMed]
35. Wan Mohd Tajuddin, W.N.B.; Lajis, N.H.; Abas, F.; Othman, I.; Naidu, R. Mechanistic understanding of curcumin's therapeutic effects in lung cancer. *Nutrients* **2019**, *11*, 2989. [CrossRef]
36. Pabla, B.; Bissonnette, M.; Konda, V.J. Colon cancer and the epidermal growth factor receptor: Current treatment paradigms, the importance of diet, and the role of chemoprevention. *World J. Clin. Oncol.* **2015**, *6*, 133–141. [CrossRef]
37. Ruiz de Porras, V.; Layos, L.; Martínez-Balibrea, E. Curcumin: A therapeutic strategy for colorectal cancer? *Semin. Cancer Biol.* **2021**, *73*, 321–330. [CrossRef]
38. Thomas, R.K.; Sos, M.L.; Zander, T.; Mani, O.; Popov, A.; Berenbrinker, D.; Smola-Hess, S.; Schultze, J.L.; Wolf, J. Inhibition of nuclear translocation of nuclear factor-kappaB despite lack of functional IkappaBalpha protein overcomes multiple defects in apoptosis signaling in human B-cell malignancies. *Clin. Cancer Res.* **2005**, *11*, 8186–8194. [CrossRef]
39. Zambre, A.P.; Kulkarni, V.M.; Padhye, S.; Sandur, S.K.; Aggarwal, B.B. Novel curcumin analogs targeting TNF-induced NF-kappaB activation and proliferation in human leukemic KBM-5 cells. *Bioorg. Med. Chem.* **2006**, *14*, 7196–7204. [CrossRef]
40. Mackenzie, G.G.; Queisser, N.; Wolfson, M.L.; Fraga, C.G.; Adamo, A.M.; Oteiza, P.I. Curcumin induces cell-arrest and apoptosis in association with the inhibition of constitutively active NF-kappaB and STAT3 pathways in Hodgkin's lymphoma cells. *Int. J. Cancer* **2008**, *123*, 56–65. [CrossRef]
41. Shehzad, A.; Lee, J.; Lee, Y.S. Curcumin in various cancers. *Biofactors* **2013**, *39*, 56–68. [CrossRef] [PubMed]
42. Zhu, G.; Shen, Q.; Jiang, H.; Ji, O.; Zhu, L.; Zhang, L. Curcumin inhibited the growth and invasion of human monocytic leukaemia SHI-1 cells in vivo by altering MAPK and MMP signalling. *Pharm. Biol.* **2020**, *58*, 25–34. [CrossRef] [PubMed]
43. Song, X.; Zhang, M.; Dai, E.; Luo, Y. Molecular targets of curcumin in breast cancer (Review). *Mol. Med. Rep.* **2019**, *19*, 23–29. [CrossRef]
44. Akbari, S.; Kariznavi, E.; Jannati, M.; Elyasi, S.; Tayarani-Najaran, Z. Curcumin as a preventive or therapeutic measure for chemotherapy and radiotherapy induced adverse reaction: A comprehensive review. *Food Chem. Toxicol.* **2020**, *145*, 111699. [CrossRef] [PubMed]
45. Ashrafizadeh, M.; Zarrabi, A.; Hashemi, F.; Moghadam, E.R.; Hashemi, F.; Entezari, M.; Hushmandi, K.; Mohammadinejad, R.; Najafi, M. Curcumin in cancer therapy: A novel adjunct for combination chemotherapy with paclitaxel and alleviation of its adverse effects. *Life Sci.* **2020**, *256*, 117984. [CrossRef]
46. Liu, W.; Zhai, Y.; Heng, X.; Che, F.Y.; Chen, W.; Sun, D.; Zhai, G. Oral bioavailability of curcumin: Problems and advancements. *J. Drug Target.* **2016**, *24*, 694–702. [CrossRef]
47. Anand, P.; Kunnumakkara, A.B.; Newman, R.A.; Aggarwal, B.B. Bioavailability of curcumin: Problems and promises. *Mol. Pharm.* **2007**, *4*, 807–818. [CrossRef]
48. Vyas, A.; Dandawate, P.; Padhye, S.; Ahmad, A.; Sarkar, F. Perspectives on new synthetic curcumin analogs and their potential anticancer properties. *Curr. Pharm. Des.* **2013**, *19*, 2047–2069.

49. Ooko, E.; Kadioglu, O.; Greten, H.J.; Efferth, T. Pharmacogenomic characterization and isobologram analysis of the combination of ascorbic acid and curcumin-two main metabolites of *Curcuma longa*-in cancer cells. *Front. Pharmacol.* **2017**, *8*, 38. [CrossRef]
50. Karimpour, M.; Feizi, M.A.H.; Mahdavi, M.; Krammer, B.; Verwanger, T.; Najafi, F.; Babaei, E. Development of curcumin-loaded gemini surfactant nanoparticles: Synthesis, characterization and evaluation of anticancer activity against human breast cancer cell lines. *Phytomedicine* **2019**, *57*, 183–190. [CrossRef]
51. Moballegh Nasery, M.; Abadi, B.; Poormoghadam, D.; Zarrabi, A.; Keyhanvar, P.; Khanbabaei, H.; Ashrafizadeh, M.; Mohammadinejad, R.; Tavakol, S.; Sethi, G. Curcumin delivery mediated by bio-based nanoparticles: A review. *Molecules* **2020**, *25*, 689. [CrossRef] [PubMed]
52. Lin, J.K. Molecular targets of curcumin. *Adv. Exp. Med. Biol.* **2007**, *595*, 227–243. [PubMed]
53. Sigismund, S.; Avanzato, D.; Lanzetti, L. Emerging functions of the EGFR in cancer. *Mol. Oncol.* **2018**, *12*, 3–20. [CrossRef] [PubMed]
54. Yan, G.E.; Efferth, T. Broad-spectrum cross-resistance to anticancer drugs mediated by epidermal growth factor receptor. *Anticancer Res.* **2019**, *39*, 3585–3593. [CrossRef] [PubMed]
55. Singh, D.; Attri, B.K.; Gill, R.K.; Bariwal, J. Review on EGFR inhibitors: Critical updates. *Mini Rev. Med. Chem.* **2016**, *16*, 1134–1166. [CrossRef] [PubMed]
56. Yan, G.; Saeed, M.E.M.; Foersch, S.; Schneider, J.; Roth, W.; Efferth, T. Relationship between EGFR expression and subcellular localization with cancer development and clinical outcome. *Oncotarget* **2019**, *10*, 1918–1931. [CrossRef]
57. Kadioglu, O.; Saeed, M.E.M.; Mahmoud, N.; Azawi, S.; Mrasek, K.; Liehr, T.; Efferth, T. Identification of novel drug resistance mechanisms by genomic and transcriptomic profiling of glioblastoma cells with mutation-activated EGFR. *Life Sci.* **2021**, *284*, 119601. [CrossRef]
58. Efferth, T. Signal transduction pathways of the epidermal growth factor receptor in colorectal cancer and their inhibition by small molecules. *Curr. Med. Chem.* **2012**, *19*, 5735–5744. [CrossRef]
59. Kadioglu, O.; Cao, J.; Saeed, M.E.; Greten, H.J.; Efferth, T. Targeting epidermal growth factor receptors and downstream signaling pathways in cancer by phytochemicals. *Target. Oncol.* **2015**, *10*, 337–353. [CrossRef]
60. Taniguchi, K.; Karin, M. NF-κB, inflammation, immunity and cancer: Coming of age. *Nat. Rev. Immunol.* **2018**, *18*, 309–324. [CrossRef]
61. Hoesel, B.; Schmid, J.A. The complexity of NF-κB signaling in inflammation and cancer. *Mol. Cancer* **2013**, *12*, 86. [CrossRef] [PubMed]
62. Karin, M. Nuclear factor-kappaB in cancer development and progression. *Nature* **2006**, *441*, 431–436. [CrossRef] [PubMed]
63. Gilmore, T.D.; Herscovitch, M. Inhibitors of NF-kappaB signaling: 785 and counting. *Oncogene* **2006**, *25*, 6887–6899. [CrossRef] [PubMed]
64. Gaptulbarova, K.A.; Tsyganov, M.M.; Pevzner, A.M.; Ibragimova, M.K.; Litviakov, N.V. NF-kB as a potential prognostic marker and a candidate for targeted therapy of cancer. *Exp. Oncol.* **2020**, *42*, 263–269.
65. Ríos, J.L.; Recio, M.C.; Escandell, J.M.; Andújar, I. Inhibition of transcription factors by plant-derived compounds and their implications in inflammation and cancer. *Curr. Pharm. Des.* **2009**, *15*, 1212–1237. [CrossRef]
66. Luqman, S.; Pezzuto, J.M. NFkappaB: A promising target for natural products in cancer chemoprevention. *Phytother. Res.* **2010**, *24*, 949–963. [CrossRef]
67. Soukhtanloo, M.; Mohtashami, E.; Maghrouni, A.; Mollazadeh, H.; Mousavi, S.H.; Roshan, M.K.; Tabatabaeizadeh, S.A.; Hosseini, A.; Vahedi, M.M.; Jalili-Nik, M.; et al. Natural products as promising targets in glioblastoma multiforme: A focus on NF-κB signaling pathway. *Pharmacol. Rep.* **2020**, *72*, 285–295. [CrossRef]
68. Shostak, K.; Chariot, A. EGFR and NF-κB: Partners in cancer. *Trends Mol. Med.* **2015**, *21*, 385–393. [CrossRef]
69. Normanno, N.; De Luca, A.; Bianco, C.; Strizzi, L.; Mancino, M.; Maiello, M.R.; Carotenuto, A.; De Feo, G.; Caponigro, F.; Salomon, D.S. Epidermal growth factor receptor (EGFR) signaling in cancer. *Gene* **2006**, *366*, 2–16. [CrossRef]
70. Starok, M.; Preira, P.; Vayssade, M.; Haupt, K.; Salome, L.; Rossi, C. EGFR Inhibition by curcumin in cancer cells: A dual mode of action. *Biomacromolecules* **2015**, *16*, 1634–1642. [CrossRef]
71. Wada, K.; Lee, J.Y.; Hung, H.Y.; Shi, Q.; Lin, L.; Zhao, Y.; Goto, M.; Yang, P.C.; Kuo, S.C.; Chen, H.W.; et al. Novel curcumin analogs to overcome EGFR-TKI lung adenocarcinoma drug resistance and reduce EGFR-TKI-induced GI adverse effects. *Bioorg. Med. Chem.* **2015**, *23*, 1507–1514. [CrossRef] [PubMed]
72. Momtazi, A.A.; Sahebkar, A. Difluorinated curcumin: A promising curcumin analogue with improved anti-tumor activity and pharmacokinetic profile. *Curr. Pharm. Des.* **2016**, *22*, 4386–4397. [CrossRef] [PubMed]
73. Hackler, L., Jr.; Ozsvari, B.; Gyuris, M.; Sipos, P.; Fabian, G.; Molnar, E.; Marton, A.; Farago, N.; Mihaly, J.; Nagy, L.I.; et al. The curcumin analog C-150, influencing NF-kappaB, UPR and Akt/Notch pathways has potent anticancer activity in vitro and in vivo. *PLoS ONE* **2016**, *11*, e0149832. [CrossRef] [PubMed]
74. Carneiro, B.A.; El-Deiry, W.S. Targeting apoptosis in cancer therapy. *Nat. Rev. Clin. Oncol.* **2020**, *17*, 395–417. [CrossRef] [PubMed]
75. Wong, R.S. Apoptosis in cancer: From pathogenesis to treatment. *J. Exp. Clin. Cancer Res.* **2011**, *30*, 87. [CrossRef]
76. Reed, J.C. Bcl-2: Prevention of apoptosis as a mechanism of drug resistance. *Hematol. Oncol. Clin. N. Am.* **1995**, *9*, 451–473. [CrossRef]
77. Gottesman, M.M. Mechanisms of cancer drug resistance. *Annu. Rev. Med.* **2002**, *53*, 615–627. [CrossRef]

78. Kadioglu, O.; Saeed, M.E.; Valoti, M.; Frosini, M.; Sgaragli, G.; Efferth, T. Interactions of human P-glycoprotein transport substrates and inhibitors at the drug binding domain: Functional and molecular docking analyses. *Biochem. Pharmacol.* **2016**, *104*, 42–51. [CrossRef]
79. Abdelfatah, S.; Böckers, M.; Asensio, M.; Kadioglu, O.; Klinger, A.; Fleischer, E.; Efferth, T. Isopetasin and S-isopetasin as novel P-glycoprotein inhibitors against multidrug-resistant cancer cells. *Phytomedicine* **2021**, *86*, 153196. [CrossRef]
80. Lu, X.; Yan, G.; Dawood, M.; Klauck, S.M.; Sugimoto, Y.; Klinger, A.; Fleischer, E.; Shan, L.; Efferth, T. A novel moniliform in derivative as pan-inhibitor of histone deacetylases triggering apoptosis of leukemia cells. *Biochem. Pharmacol.* **2021**, *194*, 114677. [CrossRef]
81. Naß, J.; Abdelfatah, S.; Efferth, T. The triterpenoid ursolic acid ameliorates stress in *Caenorhabditis elegans* by affecting the depression-associated genes skn-1 and prdx2. *Phytomedicine* **2021**, *88*, 153598. [CrossRef] [PubMed]
82. Kumar, S.; Ahuja, V.; Sankar, M.J.; Kumar, A.; Moss, A.C. Curcumin for maintenance of remission in ulcerative colitis. *Cochrane Database Syst. Rev.* **2012**, *10*, CD008424. [PubMed]
83. Bukhari, S.N.; Franzblau, S.G.; Jantan, I.; Jasamai, M. Current prospects of synthetic curcumin analogs and chalcone derivatives against Mycobacterium tuberculosis. *Med. Chem.* **2013**, *9*, 897–903. [CrossRef] [PubMed]
84. Monroy, A.; Lithgow, G.J.; Alavez, S. Curcumin and neurodegenerative diseases. *BioFactors* **2013**, *39*, 122–132. [CrossRef]
85. Cicero, A.F.; Colletti, A. Role of phytochemicals in the management of metabolic syndrome. *Phytomedicine* **2016**, *23*, 1134–1144. [CrossRef]
86. Hernandez, M.; Wicz, S.; Corral, R.S. Cardioprotective actions of curcumin on the pathogenic NFAT/COX-2/prostaglandin E2 pathway induced during *Trypanosoma cruzi* infection. *Phytomedicine* **2016**, *23*, 1392–1400. [CrossRef]

Mainz, Juni 2025

Assia Hornstein

Biopharmacologist (PhD) in Cancer and Inflammation with hands-on experience in clinical trial documentation, scientific publishing, and laboratory research. Passionate about translating biomedical findings into therapeutic strategies. I'm driven by the wish to make people's lives easier through meaningful work and knowledge.

PERSÖNLICHE DATEN

+491622420656

hornstein.ass.i@outlook.de

Klasse B

Arbeitserlaubnis Verfügbar

SKILLS

Office-Programme (Excel, Access, Word, PowerPoint), MicroMeasure, Python, Pyrex, Autodocktool, BIOVIA Discovery Studio Visualizer, Tecanreader, Nanotemper, Flowcytometer, Spectrophotometer, ImageJ, AMDock, Elektronische Mikroskope, ChimeraX, Pymol statistical analysis, clinical documentation, scientific writing, ICH-GCP guidelines, cancer research, in-vitro research, data management, strong communication, project management, collaboration.

SPRACHEN

Englisch ★★★★★

German ★★★★★

Französisch ★★★★★

Arabisch ★★★★★

Japanisch ★☆☆☆☆

BERUFSERFAHRUNG

Doktorandin
09/2018 - vsl. 2025

Johannes Gutenberg-Universität Mainz, Mainz

Erfahrung in Zellkultur, Zytotoxizitätstests, Funktionsassays, Western Blot, qRT- PCR, Immunhistochemie, Immunofluoreszenz, Durchflusszytometrie, Molekulardocking, Virtual Drug Screening, Microscale Thermophoresis; Projekt Management und Team Arbeit; zudem Leitung und Betreuung von Praktikanten, Koordination von Praktikumsaktivitäten und Betreuung der Studierenden bei Projekten sowie deren Weiterentwicklung. Co-Autorin in einem klinischen Forschungsprojekt mit Verantwortung für die Datenkuratierung und Dokumentation von Patienten*

Managing Editor
01/2022 - 12/2024

Phytomedicine, Elsevier GmbH

Verwaltung des Redaktionsprozesses wissenschaftlicher Veröffentlichungen, Koordination von Manuskriptüberprüfungen, Sicherstellung der Einhaltung von Verlagsstandards sowie Aufrechterhaltung der Kommunikation mit Autoren

Studentische Hilfskraft
10/2019 - 03/2020

Deutsches Kinderkrebsregister (DKKR) Universitätsmedizin Mainz, Deutschland

Unterstützung bei der Eingabe von Informationen in Datenbanken, Übersetzung von Korrespondenz und Materialien (Deutsch- Englisch) sowie Übernahme organisatorischer Aufgaben im Rahmen eines Symposiums

Praktikum im Bereich Kundenberatung
04/2019 - 07/2019

LimitSport, Mainz

Kundenberatung. Kontakt und Koordination mit französischen Kunden.

Zertifizierung

- Zertifikat von ICH-GCP NIDA clinical trials network
- Zertifikat von Projekt Management Institute und Linkedin

PUBLIKATIONEN

ANTI-INFLAMMATORY AND CANCER PREVENTIVE POTENTIAL OF CHAMO-MILE (MATRICARIA CHAMOMILLA L.): A COMPREHENSIVE IN SILICO AND IN VITRO STUDY
Biomedecines Journal, mdpi, 2024

COX2-INHIBITORY AND CYTOTOXIC ACTIVITIES OF PHYTOCONSTITUENTS OF MATRICARIA CHAMOMILLA L.
Applied Sciences Journal, mdpi, 2023

IN SILICO AND IN VITRO SCREENING OF 50 CURCUMIN COMPOUNDS AS EGFR AND NF- KB INHIBITORS
International Journal of Molecular Sciences, 2022

BIOMARKER PROFILING REVEALED CARCINOEMBRYONIC ANTIGEN AS A TARGET OF ARTESUNATE IN A DUCTAL BREAST CANCER PATIENT*
Anticancer research, 2022

IDENTIFICATION OF ACTIVE COMPONENTS IN ANDROGRAPHIS PANICULATA TARGETING ON CD81 IN ESOPHAGEAL CANCER IN VITRO AND IN VIVO
Phytomedicine Journal, 2022

IDENTIFICATION OF GEDUNIN FROM A PHYTOCHEMICAL DEPOSITORY AS A NOVEL MULTIDRUG RESISTANCE-BYPASSING TUBULIN INHIBITOR OF CANCER CELLS
Molecules Journal, 2022

Konferenzen/Präsentationen

Young Presenter
09/2020
World Cancer Congress (Lisbon, Portugal)
Präsentation zum Thema COX2-Inhibitory and Cytotoxic Activities of Phytoconstituents of Matricaria chamomilla L.

Praktikantin
07/2014 - 08/2014
CHU Mustapha Alger, Algier
Abteilung Onkologie: Vorbereitung von Blutproben zur Analyse und Assistenz der Laborbiologen während des Analyseprozesses

Praktikantin
07/2013 - 07/2013
CHU Mustapha Alger, Algier
Abteilung Onkologie: Vorbereitung von Blutproben zur Analyse und Assistenz der Laborbiologen während des Analyseprozesses

BILDUNGSWEG

Ph.D. Pharmazie und Biomedizin
11/2018 - vsl. 2025
Johannes Gutenberg University Mainz am Institut für Pharmazie und Biomedizin. Abteilung für Pharmazeutische Biologie
Schwerpunkte: Entzündungshemmung und Krebsprävention mit Naturstoffen; Doktorarbeit zum Thema ‚The Effect of Chamomile and Curcumin Compounds Against Inflammation and Cancer'

M.Sc. Biotechnologie und Pflanzenwissenschaft
09/2014 - 06/2016
Université des Sciences et de la Technologie Houari (Algier)
Schwerpunkte: Biotechnologie und Pflanzenwissenschaften; Masterarbeit zum Thema ‚Biosystematische Untersuchung der Gattung Bellevalia der Hyacinthaceae'

B.Sc. Biologie, Physiologie und Pflanzengenetik
09/2011 - 06/2014
Université des Sciences et de la Technologie Houari (Algier)
Schwerpunkte: Biologie, Physiologie und Pflanzengenetik; Bachelorarbeit zum Thema ‚Wirkung von Salicylsäure und Stress auf Bohnenp anzen (Phaseolus vulgaris)'

Abitur (Baccalaureat)
09/2010 - 06/2011
Saint-Elizabeth-Gymnasium (Algier)
Schwerpunkt: Naturwissenschaft

WEITERBILDUNG

Deutsche Sprachschulung von Level A1 bis C1
01/2017 - 04/2018
Sprachschulen (Berlin) A1-B1: F&U Sprachschule, B2-C1: Die Deutschschule und Hartnack Schule in Berlin. TestDAF-Vorbereitungskurs: Die Languagekult Schule in Mainz.